



Faculdade de Medicina de São José do Rio Preto
Programa de Pós-graduação em Ciências da Saúde

Giovana Mussi Polachini

**PROTEÔMICA DO CARCINOMA
EPIDERMÓIDE DE CABEÇA E PESCOÇO:
IDENTIFICAÇÃO E VALIDAÇÃO DE
BIOMARCADORES POTENCIAIS**

Tese apresentada à Faculdade de Medicina de São José do Rio Preto para obtenção do Título de Doutor no Curso de Pós-Graduação em Ciências da Saúde, Eixo Temático: Medicina e Ciências Correlatas.

São José do Rio Preto - SP
2010

Giovana Mussi Polachini

**PROTEÔMICA DO CARCINOMA
EPIDERMÓIDE DE CABEÇA E PESCOÇO:
IDENTIFICAÇÃO E VALIDAÇÃO DE
BIOMARCADORES POTENCIAIS**

**Tese apresentada à Faculdade
de Medicina de São José do Rio
Preto para obtenção do Título
de Doutor no Curso de Pós-
Graduação em Ciências da
Saúde, Eixo Temático: Medicina
e Ciências Correlatas.**

Orientadora: Profa. Dra. Eloiza Helena Tajara da Silva

**São José do Rio Preto - SP
2010**

Polachini, Giovana Mussi.

Proteômica do carcinoma epidermóide de cabeça e pescoço: identificação e validação de biomarcadores potenciais / Giovana Mussi Polachini

São José do Rio Preto, 2010

165 p.

Tese (Doutorado) – Faculdade de Medicina de São José do Rio Preto – FAMERP

Eixo Temático: Medicina e Ciências Correlatas

Orientadora: Profa. Dra. Eloiza Helena Tajara da Silva

1. Câncer de cabeça e pescoço; 2. Tumores; 3. Margens cirúrgicas normais; 4. Proteômica; 5. Eletroforese bidimensional; 6. Eletroforese unidimensional; 7. Espectrometria de massas; 8. *Western blot*; 9. Imunohistoquímica; 10. Marcadores moleculares.

Giovana Mussi Polachini

**PROTEÔMICA DO CARCINOMA
EPIDERMÓIDE DE CABEÇA E PESCOÇO:
IDENTIFICAÇÃO E VALIDAÇÃO DE
BIOMARCADORES POTENCIAIS**

**BANCA EXAMINADORA
TESE PARA OBTENÇÃO DO TÍTULO DE DOUTOR**

Presidente e Orientador: Profa. Dra. Eloiza Helena Tajara da Silva

2º Examinador: Prof. Dr. Hamilton Cabral

3º Examinador: Prof. Dr. Carlos Alberto Labate

4º Examinador: Prof. Dr. Fernando Drimel Molina

5º Examinador: Prof. Dr. Luiz Carlos de Mattos

Suplentes: Prof. Dr. José Victor Maniglia, Prof. Dr. Cleslei Fernando Zanelli,
Profa. Dra. Agnes Cristina Fett Conte, Prof. Dr. Fábio Cesar Gozzo, Prof. Dr. Ricardo
Luiz Dantas Machado.

São José do Rio Preto, 22/06/2010.

SUMÁRIO

Dedicatória	i
Agradecimentos	ii
Epígrafe	vi
Lista de Figuras	vii
Lista de Tabelas	xii
Lista de Abreviaturas e Símbolos	xv
Resumo	xix
Abstract	xxi
1. Introdução	1
1.1. Objetivos	5
2. Artigos Científicos	6
<i>Artigo I. Solubilization of proteins from human lymph node tissue and two-dimensional gel storage</i>	7
<i>Artigo II. Annexin A1 subcellular expression in laryngeal squamous cell carcinoma</i>	15
<i>Artigo III. Genomics and proteomics approaches to the study of cancer-stroma interactions</i>	29
<i>Artigo IV. Protein profiles of polar TNM groups in oral carcinomas: non-aggressive large tumors and their small aggressive opponents</i>	45
3. Conclusões	131
4. Referências Bibliográficas	134

Dedico este trabalho:

Aos meus pais Oswaldo (in memoriam) e Marylene.

Às minhas tias Aracy (in memoriam) e Mary Isabel.

À minha madrinha Elvira.

À minha sobrinha Gabriela.

Aos meus primos Maria José, Sombra e Juliana.

À minha orientadora Eloiza.

“Certa vez conheci um homem. Um homem diferente dos de sua época. Evoluído. Um homem com sua história de felicidade e sofrimento. Um homem de sentimento! Um homem consciente. Que se dava... Que se envolvia... (...) Um homem no qual a justiça, a bondade, o amor transbordavam do seu interior com um brilho tão intenso, que se refletiam num espaço imenso. Um homem que se foi, mas deixou uma herança do tamanho da esperança, o seu exemplo. Este homem, a quem eu tanto devo, está presente em todos os meus momentos. Este homem, que conheci tão de perto e que partiu sem adeus, (...) era simplesmente meu pai.” (Carmen Vervloet)

*“(...) sou dos que acreditam que a felicidade é possível, que o amor é possível, que não existe só desencontro e traição, mas ternura, amizade, compaixão, ética e delicadeza.”
(Lya Luft)*

“O valor das coisas não está no tempo em que elas duram, mas na intensidade com que acontecem. Por isso existem momentos inesquecíveis, coisas inexplicáveis e pessoas incomparáveis.” (Fernando Pessoa)

AGRADECIMENTOS

A realização deste trabalho contou com a colaboração de várias pessoas e instituições. Em especial, agradeço:

À minha orientadora Profa. Dra. Eloiza Helena Tajara da Silva, por sua orientação dedicada e muito competente. Ela é uma profissional exemplar, honesta, obstinada e sempre preocupada com a excelência do trabalho. O amor e a devoção que ela tem pela pesquisa me estimulam a trabalhar e a gostar, cada dia mais, desta carreira. Além de ser diretamente responsável por minha formação acadêmico-científica, também contribuiu (e ainda contribui) para o meu crescimento pessoal, me transmitindo valores e conselhos valiosos e me ajudando a “enxergar a vida com outros olhos”. Nestes mais de dez anos de convívio, ela sempre foi compreensiva e generosa comigo. Sinto muito orgulho de ser sua aluna, e é um prazer continuar a ser sua orientanda. Obrigada por mais este voto de confiança, esta oportunidade; enfim, por tudo!

Aos pesquisadores do grupo GENCAPO (*Head and Neck Genome Project*), por terem me disponibilizado as amostras biológicas utilizadas neste estudo e os seus respectivos dados; além de terem colaborado, de outras maneiras, para o desenvolvimento do presente trabalho. Em especial, me refiro à Dra. Eloiza H. Tajara (coordenadora da equipe, FAMERP, S. J. do Rio Preto, SP), aos Drs. Pedro Michaluart Junior (Faculdade de Medicina, USP, SP), Victor Wünsch Filho (Faculdade de Saúde Pública, USP, SP), Marcos Brasilino de Carvalho (Hospital Heliópolis, SP), Fabio Daumas Nunes (Faculdade de Odontologia, USP, SP), Patrícia Maluf Cury (FAMERP), José Francisco de Góis Filho e Erica Erina Fukuyama (Instituto do Câncer Arnaldo

Vieira de Carvalho, SP), e às Dras. Adriana Madeira (UFES, Universidade Federal do Espírito Santo, Alegre, ES) e Ana Maria Mercante (Hospital Heliópolis, SP).

A todos os Pacientes, que, voluntariamente, doaram as suas amostras, sem as quais este trabalho seria impossível.

Aos Drs. Jorge Kalil e Edecio Cunha Neto, e à bióloga Msc. Andréia Kuramoto (Instituto do Coração/INCOR, USP, SP), pela colaboração valiosa nos experimentos de 2D-DIGE (*Fluorescent two-dimensional differential in-gel electrophoresis*).

À Faculdade de Medicina de São José do Rio Preto/FAMERP, sua direção e vice-direção, pela infra-estrutura de pesquisa e ensino.

Ao Programa de Pós-Graduação em Ciências da Saúde da FAMERP, em especial aos seus coordenadores (Drs. Domingo Marcolino Braile, Reinaldo Azoubel, Emmanuel de Almeida Burdmann e Dra. Dorotéia Rossi Silva Souza) e funcionários (especialmente, José Antônio, Fabiana e Rosimeire), pelo constante incentivo e preocupação com a qualidade deste trabalho e com a minha formação científica.

Aos Professores do Programa de Pós-Graduação em Ciências da Saúde (FAMERP), que compartilharam os seus conhecimentos, contribuindo para o meu aprimoramento intelectual e acadêmico.

A todos os Funcionários da FAMERP, da FUNFARME e do Hospital de Base de S. J. do Rio Preto, pela eficiência e simpatia com que sempre me atenderam.

Ao Laboratório Nacional de Luz Síncrotron/LNLS (Campinas, SP), em especial aos Profs. Drs. Fabio Cesar Gozzo (atualmente na Universidade de Campinas/UNICAMP, Campinas), Nilson I. T. Zanchin e à Profa. Dra. Adriana Paes Leme, por colaborarem na obtenção e análise dos dados de espectrometria de massas, e por me auxiliarem na solução de dúvidas.

Aos alunos do Prof. Dr. Fabio C. Gozzo, Msc. Luiz Fernando A. Santos e Dr. Amadeu H. Iglesias (UNICAMP), e às funcionárias Msc. Margareth S. Navarro e Dras. Bianca Alves Pauletti e Thais Caroline D. Dombroski (Centro de Biologia Molecular e Estrutural/CeBiME, LNLS, Campinas), pelo auxílio nos experimentos de espectrometria de massas, no processamento dos dados e no esclarecimento de dúvidas.

Às professoras Dras. Sônia Maria Oliani (IBILCE, UNESP, S. J. do Rio Preto) e Dorotéia Rossi S. Souza (FAMERP), constituintes da Banca de meu Exame de Qualificação, que contribuíram com sugestões pertinentes para o presente trabalho.

À Profa. Dra. Andréia Machado Leopoldino (USP, Ribeirão Preto, SP), por ter contribuído ativamente neste estudo, por seus conselhos e sugestões valiosos e, também, por sua amizade.

Ao amigo Tiago Henrique (mestrando, FAMERP), pelo auxílio fundamental na análise de imagens dos géis 2-DE; enfim, por toda a ajuda.

À *GE Healthcare Life Sciences do Brasil*, especialmente ao Dr. Maurício Ribeiro Marques, pelo excelente e competente atendimento, além do esclarecimento de dúvidas relativas à Proteômica.

À FAPESP (Fundação de Amparo à Pesquisa do Estado de São Paulo), à CAPES (Coordenação de Aperfeiçoamento de Pessoal de Nível Superior), ao CNPq (Conselho Nacional de Desenvolvimento Científico e Tecnológico), à FINEP (Financiadora de Estudos e Projetos) e ao LNLS, financiadores deste trabalho.

Aos amigos do Laboratório de Marcadores Moleculares e Bioinformática Médica/LMMBM (FAMERP), Ulises, Tiago, Rodrigo, Fernanda, Jackeline, Caíque, Flávio, Bianca, Flávia, Natália, Alessandra, Evelise e Juliana, pela colaboração, apoio, companheirismo e amizade sempre demonstrados.

À Profa. Dra. Flávia Cristina Rodrigues Lisoni (UNESP, Ilha Solteira, SP), por ter me ensinado tantas coisas quando realizei o estágio básico e a iniciação científica no laboratório da Profa. Eloiza Tajara.

À amiga Rose (INCOR, USP, SP), por seu apoio e compreensão fundamentais quando mais precisei.

Às queridas amigas Carmen, Jucimara, Mariângela, Alessandra Laranja, Ana Paula Balbino, Ana Paula Marcovecchio, Alessandra Trovó, Simone, Josefa, Maria Luíza, Elizete, Maria, Shirley, Marlene, Leila e Nice, pela grande e eterna amizade, carinho e apoio sempre demonstrados.

Aos amigos Danielle, Karin, André e Rodrigo Teixeira, pela amizade e apoio essenciais durante as minhas estadas em Londres e Amsterdam.

Às minhas queridas tias Aracy (*in memoriam*), Mary Isabel, Elvira (minha madrinha) e Evanil, pelo incentivo e amor com que sempre me acompanharam e auxiliaram.

Aos estimados primos José Sombra e Maria José, meus grandes amigos e incentivadores. Muito obrigada por tudo!

À amada prima Juliana, por sua amizade, amor, carinho e companheirismo.

Aos meus amados pais Oswaldo (*in memoriam*) e Marylene, pelo imenso e incondicional amor, desprendimento e dedicação com que sempre cuidaram de mim. Amo muito vocês! Saudades infinitas de você, meu querido Pai!

Aos meus irmãos Gustavo e Adriano, pela amizade.

À amada sobrinha Gabriela, por seu amor, carinho e consideração.

E a Deus pela vida... por tudo!

“E ainda que tivesse o dom de profecia, e conhecesse todos os mistérios e toda a ciência, e ainda que tivesse toda a fé, de maneira tal que transportasse os montes, e não tivesse Amor, nada seria.”

(São Paulo, I Coríntios 13:2)

“Para ser grande, sê inteiro: nada teu exagera ou exclui. Sê todo em cada coisa. Põe quanto és no mínimo que fazes. Assim em cada lago a lua toda brilha, porque alta vive.”

(Fernando Pessoa)

"Bom mesmo é ir à luta com determinação, abraçar a vida e viver com paixão, perder com classe e vencer com ousadia, pois o triunfo pertence a quem mais se atreve. E a vida é muito para ser insignificante.”

(Charles Chaplin)

LISTA DE FIGURAS

Artigo I

Figure 1. Comparison of solubilization conditions. Lysis and solubilization from human lymph node tissue proteins were performed using six different buffers (1-6): (A) Buffer 1 (285 spots); (B) Buffer 2 (281 spots); (C) Buffer 3 (113 spots); (D) Buffer 4 (283 spots); (E) Buffer 5 and (F) Buffer 6. Composition of buffers as in Table 1. Proteins were separated on a 13 cm pH 3-10 IPG, 12.5% SDS-PAGE and stained with Coomassie Blue.....11

Figure 2. A one-year-old archived SDS-PAGE and mass spectrum of tryptic peptides derived from hemoglobin. (A) A one-year-old archived SDS-PAGE of a sample from a patient with head and neck squamous cell carcinoma. Highlighted in circle is the spot excised from the gel. (B) Mass spectrum corresponding to a spot with apparent pI and MW of 7.1 and 14.5 kDa, respectively.....12

Artigo II

Figure 1. Validation of ANXA1 gene by real-time polymerase chain reaction (PCR). Quantitative PCR was carried out on 15 squamous cell carcinoma and eight tumour margin samples. Gene expression is shown as $\log 2^{-\Delta\Delta Ct}$ ($\Delta\Delta Ct$ ranged from 0.04053 to 0.70222). Differences between tumour and normal samples were significant ($P < 0.001$).....20

Figure 2. Immunohistochemical features of laryngeal squamous cells. Non-tumoural areas (A,B) strongly express ANXA1 in nuclei, cytoplasm and membrane. ANXA1 expression is lower in dysplastic areas (C,D), tumoural samples (E,F) and in metastatic

areas (G,H), especially in nuclei and in cytoplasm (A,C,E,G, H&E; B,D,F,H, annexin A1, LSAB).....21

Figure 3. Analysis of ANXA1 protein. Representative Western blots illustrating ANXA1 expression in a subset of (A,B) eight laryngeal squamous cell carcinomas and eight matched non-neoplastic surgical margins by using anti-annexin A1. A, Surgical margins (lanes 1, 3, 5, 7) and tumour samples (lanes 2, 4, 6, 8) from patients 105, 102, 96 and 136, respectively. B, Surgical margins (lanes 1, 3, 5, 7) and tumour samples (lanes 2, 4, 6, 8) from patients 35, 31, 19 and 18, respectively. MW, molecular weight marker. Uncleaved ANXA1 (unANXA1): 37 kDa; cleaved fragment (clANXA1): 33 kDa. β -actin was used as an internal control.....24

Artigo III

Figure 1. Immunofluorescence analysis of cytokeratin and vimentin in stromal fibroblasts and Hep-2 cell line. (A and D) Absence of immunoreactivity in sections incubated with control nonimmune mouse serum. Stromal fibroblasts (B and E) and Hep-2 cell line (C and F) were positive for vimentin and cytokeratin, respectively. (G): Densitometric analysis of immunofluorescence reaction to vimentin and cytokeratin in stromal fibroblasts and Hep-2 cell line. Scale bar, 20 μ m.....35

Figure 2. Growth curve of Hep-2 cell line. Hep-2 cells were cultured in complete medium, treated with self-conditioned medium (HCM) or with conditioned medium from fibroblast cultures (FCM) and collected 1, 3, 5 and 7 days after medium replacement. Data are means \pm s.d. of two independent experiments in duplicates. * $P < 0.05$. Error bars indicate S.D.....36

Figure 3. Immunohistochemistry reaction with AnxA5 antibody showed the presence of gold particles on the cytoplasm of apoptotic cells. Hep-2 cells (A) without treatment and (B) treated with conditioned medium from fibroblast culture (FCM) show AnxA5

immunoreactivity. Apoptotic cells immunolabeling for AnxA5 can be seen in Hep-2 cells treated with FCM (arrows). Staining with haematoxylin. Scale bar, 20µm.....36

Figure 4. Real-time PCR gene expression in a conditioned medium-treated neoplastic cell line and in primary tumors. (A) Expression of *ARID4A*, *CALR*, *DAP3*, *GNB2L1*, *PRDX1*, *RNF10*, *SQSTM1* and *USP9X* genes in Hep-2 cells treated with conditioned medium from fibroblast cultures. (B). *ARID4A* gene expression in 47 laryngeal and oral tongue carcinomas. Relative quantitation of target gene expression for each sample was calculated according to Pfaffl [50]; *GAPDH* was used as the internal reference and control sample as the calibrator. Values were Log₂ transformed (y-axis) so that all values below -1 indicate down-regulation in gene expression while values above 1 represent up-regulation in tumor samples compared to normal samples.....38

Figure 5. Enlarged 2-DE gels of proteins from conditioned medium-treated Hep-2 cells and stromal fibroblasts. Five proteins (arrows), tubulin beta (A-B), alpha enolase (C-D), aldolase A (E-F), glyceraldehyde-3-phosphate dehydrogenase (G-H) and heterogeneous nuclear ribonucleoprotein C (I-J) were down-regulated in Hep-2 cell line treated with fibroblast conditioned medium (A, C, E, G and I) and two proteins (K-L), vimentin (arrow on left) and actin (arrow on right), were underexpressed in fibroblasts treated with Hep-2 cell line conditioned medium (K).....39

Artigo IV

Figure 1. Detailed alteration patterns of proteins in OSCC tumors identified by 2-DE and mass spectrometry: annexin A1 (ANXA1), beta-globin (HBB), creatine kinase M-type (M-CK), myoglobin (MB), cofilin-1 (CFL1), galectin-7 (Gal-7), glutathione S-transferase P (GSTP1-1), heat shock 27 kDa (HSP 27), calgranulin-B (S100-A9), superoxide dismutase (SOD1), tropomyosin 4 (TPM4). Tumor samples from tongue (C02) and floor of mouth (C04). T1-2N+ = “more-aggressive” tumors; T2-3N0 = “less-aggressive” tumors; N+ = metastatic tumors; N0 = non-metastatic tumors.....81

Figure 2. Analysis of CK-4 protein. Representative Western blots illustrating CK-4 expression in a subset of (A,B) eight oral squamous cell carcinomas and five non-neoplastic surgical margins by using anti-CK-4. A, Tumour samples (lanes 1, 3, 5, 7) and matched margins (lanes 2, 4, 6, 8) from patients with T1N0, T4N2, T4N1 and T4N1 carcinomas, respectively. B, Surgical margin (lane 1) and tumour samples (lanes 2, 3, 4, 5) from patients with T4N2, T4N2, T4N2, T1N0 and T2N2, respectively. β -actin was used as an internal control. MW, PageRuler™ Prestained Protein Ladder.....82

Figure 3. Immunohistochemical analysis of CK-4 expression in OSCC. In panels (A,B), complete absence of CK-4 expression is observed in tumor tissues, whereas in clear contrast, in panels (C,D), CK-4 is significantly overexpressed in normal surgical margins. Slides were photographed at 400X (A, B, D) and 100X (C) magnifications.....83

Supporting Figure 1. 2-DE maps of tumor pools from OSCC patients. Pools of N+ (A), N0 (B), T1-2N+ (C), and T2-3N0 (D) tumors. Differentially expressed proteins between A and B and between C and D are highlighted by arrows.....84

Supporting Figure 2. Detailed alteration patterns of proteins in OSCC tumors and surgical margins identified by 2-DE and mass spectrometry: myosin light chain 1/3, skeletal muscle isoform (MLC1/MLC3); beta-globin (HBB); carbonic anhydrase 3 (CA-III); creatine kinase M-type (M-CK); cytokeratin-4 (CK-4); gamma-actin (ACTG); myoglobin (MB); myosin light chain 3 (MYL3); myosin regulatory light chain 2, skeletal muscle isoform (MLC2B); myosin regulatory light chain 2, ventricular/cardiac muscle isoform (MLC-2v); tropomyosin-1 (TPM1); tropomyosin-2 (TPM2); tropomyosin-3 (TPM3); alpha-enolase (ENO1); cofilin-1 (CFL1); cyclophilin A (PPIase A); cytokeratin-19 (CK-19); glutathione S-transferase P (GSTP1-1); heat shock 27 kDa (HSP 27); calgranulin-B (S100-A9); serum albumin (ALB); stratifin (SFN); superoxide dismutase [Cu-Zn] (SOD1); tropomyosin-4 (TPM4); vimentin (VIM). T1-2N+ (“more-aggressive”) tumors and matched surgical margins from tongue (C02) and floor of mouth (C04).....85

Supporting Figure 3. Detailed alteration patterns of proteins in OSCC tumors and surgical margins identified by 2-DE and mass spectrometry: myosin light chain 1/3, skeletal muscle isoform (MLC1/MLC3); annexin A1 (ANXA1); carbonic anhydrase 3 (CA-III); creatine kinase M-type (M-CK); gamma-actin (ACTG); myoglobin (MB); myosin light chain 3 (MYL3); myosin regulatory light chain 2, skeletal muscle isoform (MLC2B); myosin regulatory light chain 2, ventricular/cardiac muscle isoform (MLC-2v); tropomyosin-1 (TPM1); tropomyosin-2 (TPM2); tropomyosin-3 (TPM3); troponin T, slow skeletal muscle (TnTs); alpha-enolase (ENO1); cofilin-1 (CFL1); cyclophilin A (PPIase A); cytokeratin-19 (CK-19); galectin-7 (Gal-7); heat shock 27 kDa (HSP 27); serum albumin (ALB); stratifin (SFN); tropomyosin-4 (TPM4). T2-3N0 tumors and matched surgical margins from tongue (C02) and floor of mouth (C04).....86

LISTA DE TABELAS**Artigo I**

Table 1. Lysis buffer composition. Composition of six lysis buffers tested for protein solubilization efficiency.....	9
---	---

Artigo II

Table 1. List of the 20 most abundant tags in laryngeal tumour serial analysis of gene expression (SAGE) libraries and 20 most abundant tags in non-neoplastic SAGE library.....	19
--	----

Table 2. Frequency of nuclear, cytoplasmic and membranous immunoreactivity of ANXA1 in normal, dysplastic, primary tumour and metastatic cells from 95 patients with laryngeal squamous cell carcinoma.....	22
---	----

Table 3. Results of a 2 X 2 comparison of nuclear, cytoplasmic and membranous ANXA1 expression among normal, dysplastic, primary tumour and metastatic cells from 95 patients with laryngeal squamous cell carcinoma.....	23
---	----

Table 4. Comparison of nuclear, cytoplasmic and membranous ANXA1 immunoexpression among normal, dysplastic, primary tumour and metastatic cells from 95 patients with laryngeal squamous cell carcinoma.....	23
--	----

Table 5. Pathological features of eight patients with laryngeal squamous cell carcinoma as well as the results of Western blot and immunohistochemical analysis.....	25
--	----

Artigo III

Table 1. Information on biological processes based on Gene ontology. Top down- and up-regulated genes selected by RaSH in Hep-2 samples treated with FCM.....37

Table 2. Information on biological processes based on Gene Ontology. Top down regulated genes selected by RaSH in CAF samples treated with HCM.....37

Additional File 1. Clinicopathological features of 24 patients with laryngeal SCC and 23 patients with oral tongue SCC.....41

Additional File 2. Underexpressed proteins in Hep-2 cells and fibroblasts treated with conditioned medium from fibroblasts (FCM) and Hep-2 (HCM), respectively.....41

Artigo IV

Table 1. Experimental design for 2-D DIGE.....77

Table 2. Differentially expressed proteins in oral squamous cell carcinomas identified by 2-DE and MS/MS. Lower (↓) and higher (↑) expression in T1-2N+ tumors versus T2-3N0 tumors (A) and in T2-4N+ tumors versus T2-4N0 tumors (D); lower (↓) and higher (↑) expression in tumors in relation to normal tissues (B, C, E, F, G); lower (↓) and higher (↑) expression in T1-2N+ tumors from C02/C04 sites (H) versus T1-2N+ tumors from C01 site (I). C01=Malignant neoplasm of base of tongue; C02=Malignant neoplasm of other and unspecified parts of tongue; C04=Malignant neoplasm of floor of mouth.....78

Supporting Table 1. Clinicopathological features of patients in this study.....87

Supporting Table 2. Composition of pools used for 1-DE and 2-DE experiments.....	92
Supporting Table 3. Differentially expressed proteins identified by 2-DE and mass spectrometry in oral squamous cell carcinomas.....	94
Supporting Table 4. Proteins expressed in “more-aggressive” (T1-2N+) tumors. Proteins from about 10 to 45kD separated by 1-DE and identified by ESI-Q-TOF-MS/MS analysis	97
Supporting Table 5. Proteins expressed in “less-aggressive” (T2-3N0) tumors. Proteins from about 10 to 45kD separated by 1-DE and identified by ESI-Q-TOF-MS/MS analysis.....	109
Supporting Table 6. Proteins expressed in normal surgical margins. Proteins from about 10 to 45kD separated by 1-DE and identified by ESI-Q-TOF-MS/MS analysis.....	122

LISTA DE ABREVIATURAS E SÍMBOLOS

ACN	Acetonitrila
ANXA1	<i>Annexin A1</i> (anexina A1)
ASB-14	Amidosulfobetaina-14
BSA	Albumina sérica bovina
CCEO	Carcinoma de Células Escamosas Oral
CECP	Carcinoma Epidermóide de Cabeça e Pescoço
CHAPS	3-[(3-colamidopropil) dimetilamônio]-1-propano sulfonato
cm	Centímetro (s)
LC (CL)	<i>Liquid Chromatography</i> (Cromatografia Líquida)
CP (1, 2, 3)	Centro de Coleta de Amostras de Cabeça e Pescoço (1=Hospital do Câncer Arnaldo Vieira de Carvalho, 2=Hospital Heliópolis, 3=Hospital das Clínicas, São Paulo, SP)
Cy2, Cy3, Cy5	Corantes fluorescentes, solúveis em água, reativos e da família de corantes cianina [Cy2: 488 (excitação)/520 nm (emissão); Cy3: 532/580 nm; Cy5: 633/670 nm].
Da	Dalton (s)
1-DE	Eletroforese unidimensional
2-D	Bidimensional
2-DE	Eletroforese bidimensional
2D-DIGE	<i>Two-Dimensional Difference Gel Electrophoresis</i> (Eletroforese Diferencial em Gel Bidimensional ou Eletroforese de Fluorescência Diferencial em Gel Bidimensional)
DTE	Ditioeritritol
DTT	Ditiotreititol

EDTA	Ácido etilenodiaminotetracético
ESI	<i>Electrospray Ionization</i> (Ionização por “Electrospray”)
ESI-QUAD-TOF ou ESI-Q-TOF	Espectrômetro de massas que utiliza ionização por “electrospray” e dois analisadores (dos tipos quadrupolo e tempo-de-vôo) de massas associados (em <i>tandem</i>).
g	Aceleração da gravidade
h	Hora (s)
<i>Hep-2 cell line</i>	Linhagem celular derivada de carcinoma epidermóide de laringe
HNSCC	<i>Head and Neck Squamous Cell Carcinoma</i> (Carcinoma de Células Escamosas de Cabeça e Pescoço)
HPV	<i>Human Papiloma Virus</i> (Vírus do Papiloma Humano ou Papilomavírus Humano)
IEF	Focalização isoeletrica
IPG	Gradiente de pH imobilizado
kDa	Quilodalton (s)
LMW	Marcador de baixo peso molecular
LSCC	<i>Laryngeal Squamous Cell Carcinoma</i> (Carcinoma de Células Escamosas de Laringe)
MALDI	<i>Matrix Assisted Laser Desorption Ionization</i> (Ionização a Laser Assistida por Matriz)
MALDI-QUAD-TOF ou MALDI Q-TOF	Espectrômetro de massas que utiliza dessorção/ionização a laser assistida por matriz e dois analisadores (quadrupolo e tempo-de-vôo) de massas associados (em <i>tandem</i>).
MALDI-TOF-TOF	Espectrômetro de massas que utiliza dessorção/ionização a laser assistida por matriz e dois analisadores (do tipo tempo-de-vôo) de massas associados (em <i>tandem</i>).
M	Molar
M1, M0	Presença (M1) e ausência (M0) de metástase à distância

mA	Miliampere (s)
mg/mL	Miligrama (s) por mililitro
min	Minuto (s)
mM	Milimolar (s)
mm	Milímetro (s)
MW	Peso molecular
N+, N0	Linfonodos comprometidos (N+: 1, 2, 3) e não comprometidos (N0) por células neoplásicas
NCBI	<i>National Center for Biotechnology Information</i> (Centro Nacional de Informação para Biotecnologia)
nm	Nanômetro
NP	Código de referência da proteína no NCBI
NP-40	Nonidet P-40
OSCC	<i>Oral Squamous Cells Carcinoma</i> (Carcinoma de Células Escamosas Oral)
P	Número de acesso da proteína no <i>Swiss-Prot</i>
pH	Potencial hidrogeniônico
pI	Ponto isoelétrico
Q ou QUAD	Analisador de massas do tipo quadropolo
rpm	Rotação (s) por minuto
SAGE	<i>Serial Analysis of Gene Expression</i> (Análise Seriada da Expressão Gênica)
SB 3-10	N-decil-N, N-dimetil-3-amônio-1-propanosulfonato
SDS	Dodecil sulfato de sódio
SDS-PAGE	Eletroforese em gel de poliacrilamida com SDS
T1, T2, T3, T4	Tamanhos dos tumores (T1 < T2 < T3 < T4)

TBP	Tributilfosfina
TFA	Ácido trifluoroacético
TNM	Classificação dos tumores malignos (T=tamanho do tumor, N=comprometimento ou não de linfonodos regionais por células neoplásicas, M=presença ou não de metástase à distância) segundo a União Internacional Contra o Câncer (<i>International Union Against Cancer/UICC</i>).
TOF	<i>Time-of-Flight</i> (analisador de massas do tipo tempo-de-vôo)
V	Volt (s)
v/v	Volume por volume
Vh	Volt-hora (s)
W	Watt (s)
w/v	Massa por volume
μA	Microampere (s)
μg	Micrograma (s)
μL	Microlitro (s)
μM	Micromolar (s)
μm	Micrômetro (s)
$^{\circ}\text{C}$	Grau (s) Celsius
%	Porcentagem
α	Alfa
β	Beta
Δ	Delta

RESUMO

Introdução: Os tumores epidermóides de cavidade oral, laringe e faringe, coletivamente conhecidos como carcinomas de células escamosas de cabeça e pescoço, estão fortemente relacionados ao consumo de tabaco e álcool e ainda resultam em taxas elevadas de mortalidade. O desenvolvimento de um tumor primário representa um risco maior de tumores secundários surgirem no epitélio contíguo, uma provável consequência da resposta anormal do microambiente à exposição do trato aerodigestivo superior a carcinógenos. A previsão do comportamento tumoral ainda representa um desafio para clínicos e pesquisadores. A presença de metástase em linfonodos regionais é o fator prognóstico mais importante, porém é limitado quanto à predição de recidiva local ou de sobrevivência. Além disso, a doença metastática precoce não é frequentemente detectada pelas análises clínica, histológica e radiológica. Este fato enfatiza a necessidade de identificação de biomarcadores que possam efetivamente contribuir para o diagnóstico precoce e para a previsão da progressão tumoral.

Objetivos: No presente estudo, analisamos carcinomas de células escamosas orais de diferentes subsítios anatômicos e suas mucosas adjacentes normais correspondentes com o objetivo de comparar os perfis de expressão protéica no contexto de um prognosticador conhecido, ou seja, a presença de células neoplásicas em linfonodos regionais, e de uma classificação refinada em relação a prognóstico, reunindo em dois grupos os tumores pequenos, mas já metastáticos, e os grandes não-metastáticos. Também investigamos o proteoma do microambiente do tumor para identificar marcadores de agressividade que possam ser relevantes para prognóstico e terapia.

Materiais e Métodos: Para atingir tais objetivos, realizamos eletroforeses uni e

bidimensional (1-DE e 2-DE), eletroforese de fluorescência diferencial em gel bidimensional (2-D DIGE), espectrometria de massas, *Western blot* e imunohistoquímica. **Resultados e Discussão:** Uma variedade de fatores influenciam na preparação de amostras protéicas e a otimização da solubilização de proteínas e de protocolos de 2-DE foi fundamental para a aquisição de resultados consistentes. Foram observadas muitas diferenças entre tumores metastáticos e não-metastáticos e entre tumores e células normais, incluindo expressões alteradas de anexina A1, calgranulina-B, cofilina-1, galectina-7, glutationa S-transferase P, citoqueratina-4 e creatina quinase. Estas proteínas estão envolvidas em sinalização, resposta inflamatória, apoptose, desenvolvimento, processos metabólicos, e adesão, motilidade, diferenciação e proliferação celulares, e podem estar relacionadas ao fenótipo agressivo. O microambiente tumoral também pode contribuir para o processo neoplásico. Os nossos resultados de fatores parácrinos sintetizados *in vitro* por células estromais mostraram expressão gênica e protéica alterada nas células neoplásicas após tratamento com meio condicionado de fibroblastos associados a tumor, e vice-versa. **Conclusões:** Os dados aqui obtidos podem ajudar a compreender os mecanismos da agressividade do carcinoma epidermóide oral no nível molecular e a influência do microambiente tumoral no processo carcinogênico. Tais genes e proteínas podem representar novos biomarcadores de prognóstico para este tipo de câncer.

Palavras-chave: 1. Câncer de cabeça e pescoço; 2. Tumores; 3. Margens cirúrgicas normais; 4. Interação estroma-tumor; 5. Proteômica; 6. Eletroforese bidimensional; 7. Eletroforese unidimensional; 8. Espectrometria de massas; 9. *Western blot*; 10. Imunohistoquímica; 11. Marcadores moleculares.

ABSTRACT

Introduction: Epidermoid tumors of the oral cavity, larynx and pharynx, collectively known as head and neck squamous cell carcinomas, are strongly related to tobacco and alcohol consumption and still result in high mortality rates. The development of a primary tumor anticipates a greater risk of second cancers occurring in the contiguous epithelium, which can be a consequence of the abnormal response of the microenvironment to the carcinogen exposure in the upper aerodigestive tract. The prediction of tumor behavior for patients with these carcinomas still represents a challenge for clinicians and researchers. The presence of regional lymph node metastasis is their most important prognostic factor but is limited in predicting local recidive or survival. In addition, early metastatic disease is often missed by clinical, histological and radiological analysis. This emphasizes the need for identifying biomarkers which may effectively contribute to early diagnosis and prediction of tumor progression. **Objectives:** In this study, we analyzed oral squamous cell carcinomas (OSCCs) from different anatomic subsites and their matched adjacent normal mucosa aiming to compare the protein expression profiles in the context of a known prognosticator, namely, the presence of neoplastic cells in regional lymph nodes and of a refined classification in regard to prognosis, grouping into two groups small but already metastatic and large non-metastatic tumors. We also aimed to investigate the proteome of the tumor microenvironment to identify markers of aggressiveness that may be relevant for prognosis and therapy. **Materials and Methods:** To reach these objectives, we performed one- and two-dimensional electrophoresis (1-DE and 2-DE), fluorescent two-dimensional differential in-gel electrophoresis (2-D DIGE), mass spectrometry, Western blot and immunohistochemistry to analyze the protein

expression in OSCCs. **Results and Discussion:** A variety of factors influence the protein sample preparation and the optimization of protein solubilization and 2-DE protocols was fundamental for the acquisition of consistent results. Many protein differences between metastatic and non-metastatic tumors and between tumor and normal cells including abnormal expression of annexin A1, calgranulin-B, cofilin-1, galectin-7, glutathione S-transferase P, cytokeratin-4 and creatine kinase were observed. These proteins are involved in cell signaling, inflammatory response, apoptosis, cell motility and adhesion, development, cell differentiation and proliferation and metabolic process, and may be related to the aggressive phenotype. Tumor microenvironment may also contribute to the neoplastic process. Our results on paracrine factors synthesized in vitro by stromal cells showed altered gene and protein levels in neoplastic cells after treatment with conditioned medium from tumor-associated fibroblasts, and vice-versa. **Conclusions:** The data may help to understand the mechanisms governing aggressiveness in OSCCs at the molecular level and the contributions of the tumor microenvironment to carcinogenic process, providing new insights into signaling and metabolic pathway abnormalities that could be useful to prognosis.

Keywords: 1. Head and neck cancer; 2. Tumors; 3. Normal surgical margins; 4. Stroma-tumor interaction; 5. Proteomics; 6. Two-dimensional electrophoresis; 7. One-dimensional electrophoresis; 8. Mass spectrometry; 9. *Western blot*; 10. Immunohistochemistry; 11. Molecular markers.

1. INTRODUÇÃO

1. INTRODUÇÃO

Muitos avanços recentes na biologia do câncer resultaram de abordagens tecnológicas de alta eficiência. A análise em larga escala de transcritos e proteínas esclareceu diferentes aspectos da tumorigênese e proporcionou oportunidades excepcionais para a identificação de novos alvos terapêuticos. Neste contexto, não há dúvidas de que os microarranjos de DNA, a análise seriada da expressão gênica (SAGE) e, mais recentemente, técnicas de sequenciamento de amplo alcance têm contribuído com uma grande quantidade de dados de expressão gênica em câncer. Entretanto, a análise do perfil transcricional sofre influência da susceptibilidade do RNA à degradação e da baixa correspondência entre RNA e proteínas.⁽¹⁾ Na verdade, para obtenção de conclusões válidas sobre o significado funcional de um conjunto de transcritos, dados sobre os níveis de expressão das proteínas correspondentes são geralmente decisivos. Além disso, modificações pós-traducionais, interações entre proteínas, transporte e degradação, que modulam as atividades e as funções das proteínas, são informações importantes perdidas pela análise da expressão do RNA mensageiro.⁽²⁾

O estudo do conteúdo protéico das células tumorais é, portanto, crucial para a definição do perfil molecular do câncer. Duas técnicas principais são bastante utilizadas na análise proteômica, a eletroforese em gel bidimensional (2-DE) e a espectrometria de massas (MS), que permitem a separação e a identificação de proteínas, respectivamente. Nos últimos anos, vários progressos tecnológicos foram incorporados a essas metodologias, aumentando a sua eficiência e precisão. A eletroforese diferencial em gel bidimensional (2-D DIGE), por exemplo, é uma versão recente mais eficiente da 2-DE e

permite a análise de duas amostras protéicas no mesmo gel, reduzindo possíveis variações entre géis.⁽³⁾ A espectrometria de massas também evoluiu,⁽²⁾ empregando o fracionamento multidimensional de proteínas para aumentar a cobertura,⁽⁴⁾ novas ferramentas para estudar modificações pós-traducionais,⁽⁵⁾ a purificação por afinidade seguida por espectrometria de massas para avaliar interações entre proteínas,⁽⁶⁾ ou combinando a separação por cromatografia líquida (LC) e a espectrometria de massas em *tandem* (MS/MS) com métodos semi-quantitativos e quantitativos para medir as concentrações absoluta e relativa de proteínas.^(7, 8) Além disso, imunoenaios do tipo *multiplex* têm sido desenvolvidos para o rastreamento simultâneo de múltiplos biomarcadores de proteínas.⁽⁹⁾

Apesar das limitações quanto à cobertura do proteoma e ao número elevado de horas que os experimentos consomem, a proteômica tem sido utilizada para estudar uma ampla variedade de tumores (ou fluídos corporais), tais como os de mama,⁽¹⁰⁻¹³⁾ bexiga,⁽¹⁴⁻¹⁷⁾ rim,⁽¹⁸⁻²¹⁾ fígado,⁽²²⁻²⁵⁾ pulmão,⁽²⁶⁻²⁹⁾ próstata,⁽³⁰⁻³³⁾ esôfago,⁽³⁴⁻³⁶⁾ e os de cabeça e pescoço.⁽³⁷⁻⁴⁶⁾

Em câncer de cabeça e pescoço, diversos dados de proteômica sugerem que o perfil protéico pode ter valor diagnóstico e preditivo,^(43, 47-49) inclusive nas fases iniciais da doença.^(46, 50, 51) Marcadores de diagnóstico precoce e de prognóstico são particularmente importantes para esses tumores, pois os pacientes apresentam poucos sintomas nas fases iniciais da doença. Este fato, somado à falta de métodos de rastreio eficazes, resulta no diagnóstico tardio e em altas taxas de mortalidade.

Os carcinomas de cabeça e pescoço são heterogêneos quanto aos sítios anatômicos que acometem e às suas apresentações e desfechos clínicos.^(52, 53) Entre eles, o carcinoma de células escamosas oral (CCEO) é um dos tipos mais comuns com cerca

de 270.000 novos casos no mundo por ano,^(54, 55) a maioria dos quais relacionados ao consumo de tabaco e álcool.⁽⁵⁶⁻⁵⁸⁾ O papilomavírus humano (HPV) também tem sido identificado como um fator causal e esta associação é especialmente forte para os tumores de orofaringe e para os não-fumantes e não-etilistas, porém mais fraca para os carcinomas de cavidade oral e laringe.^(59, 60)

O desenvolvimento de um tumor primário representa um risco maior de tumores secundários surgirem no epitélio contíguo, uma provável consequência da resposta anormal do microambiente à exposição do trato aerodigestivo superior a carcinógenos.

A presença de metástase em linfonodos regionais ainda é o mais importante fator prognóstico em câncer oral, similarmente a outros tumores de cabeça e pescoço.⁽⁶¹⁾ No entanto, a doença metastática precoce não é frequentemente detectada pelas avaliações clínica, histológica e radiológica.^(62, 63) Este fato enfatiza a necessidade de identificação de biomarcadores de detecção precoce, que possam ajudar a compreender o comportamento do tumor e a aumentar as taxas de sobrevivência.

No presente estudo, foram utilizadas as eletroforeses 1-D, 2-D e 2-D DIGE, além de espectrometria de massas para analisar a expressão de proteínas em CCEOs de diferentes subsítios anatômicos e nas mucosas adjacentes normais correspondentes. Inicialmente, nós investigamos o perfil de expressão protéico no contexto de um prognosticador conhecido, ou seja, a presença de células neoplásicas nos linfonodos regionais, independentemente do tamanho do tumor, como usualmente é feito para os carcinomas de cabeça e pescoço. Em seguida, utilizando um refinamento para classificar os carcinomas orais em relação ao prognóstico, nós separamos em dois grupos os tumores pequenos, mas já metastáticos e os grandes não-metastáticos. A justificativa para esta classificação exploratória é o fato de que os critérios padrões,

conforme discutido por Patel e Shah,⁽⁶⁴⁾ são limitados em prever recidiva local ou sobrevida.

1.1. OBJETIVOS

O objetivo geral do presente trabalho foi a pesquisa de marcadores proteicos de diagnóstico, prognóstico e classificação do câncer de cabeça e pescoço. Os seus objetivos específicos compreenderam:

1. Otimizar protocolos de extração de proteínas e de eletroforese bidimensional para uso no Laboratório de Marcadores Moleculares e Bioinformática Médica/LMMBM (FAMERP);
2. Investigar diferenças entre o perfil proteico do carcinoma epidermóide de cavidade oral com fenótipo invasivo e o do carcinoma oral não-invasivo, independentemente do tamanho do tumor, bem como as diferenças entre os tumores e as mucosas normais correspondentes. Além disso, o presente trabalho teve como objetivo analisar diferenças proteicas entre os tumores pequenos metastáticos e os grandes não-metastáticos;
3. Validar, por imuno-histoquímica e *Western blotting*, biomarcadores potenciais identificados por técnicas de proteômica em tumores de cabeça e pescoço;
4. Avaliar a influência do microambiente tumoral no desenvolvimento do câncer de cabeça e pescoço.

Short communication

Solubilization of Proteins from Human Lymph Node Tissue and Two-Dimensional Gel Storage

Alessandra Bernadete Trovó de Marqui^{1, #}, Alessandra Vidotto^{2, #}, Giovana Mussi Polachini^{2, #},
Cláudia de Mattos Bellato³, Hamilton Cabral⁴, Andréia Machado Leopoldino², José Francisco de Góis Filho⁵,
Érica Erina Fukuyama⁵, Flávio Aurélio Parente Settanni⁵, Patrícia Maluf Cury²,
Gustavo Orlando Bonilla-Rodriguez⁴, Mario Sergio Palma⁶ and Eloiza Helena Tajara^{2, *}

¹UNESP-Universidade Estadual Paulista, Instituto de Biociências, Letras e Ciências Exatas-IBILCE,
Departamento de Biologia, São José do Rio Preto, SP, Brazil

²FAMERP-Faculdade de Medicina de São José do Rio Preto, Departamento de Biologia Molecular, São José do Rio Preto, SP, Brazil

³USP- Universidade de São Paulo, Centro de Energia Nuclear para Agricultura/CENA, Piracicaba, SP, Brazil

⁴UNESP-Universidade Estadual Paulista, Instituto de Biociências, Letras e Ciências Exatas-IBILCE, Departamento de Física,
São José do Rio Preto, SP, Brazil

⁵Hospital do Câncer Arnaldo Vieira de Carvalho, SP, Brazil

⁶UNESP-Universidade Estadual Paulista, Instituto de Biociências de Rio Claro, Centro de Estudos em Insetos Sociais,
Departamento de Biologia, Rio Claro, SP, Brazil

Received 9 August 2005, Accepted 13 October 2005

In the present study, we compared six different solubilization buffers and optimized two-dimensional electrophoresis (2-DE) conditions for human lymph node proteins. In addition, we developed a simple protocol for 2-D gel storage. Efficient solubilization was obtained with lysis buffers containing (a) 8 M urea, 4% CHAPS (3-[(3-cholamidopropyl)dimethylammonio]-1-propanesulfonate), 40 mM Tris base, 65 mM DTT(dithiothreitol) and 0.2% carrier ampholytes; (b) 5 M urea, 2 M thiourea, 2% CHAPS, 2% SB 3-10 (N-decyl-N, N-dimethyl-3-ammonio-1-propanesulfonate), 40 mM Tris base, 65 mM DTT and 0.2% carrier ampholytes or (c) 7 M urea, 2 M thiourea, 4% CHAPS, 65 mM DTT and 0.2% carrier ampholytes. The optimal protocol for isoelectric focusing (IEF) was accumulated voltage of 16,500 Vh and 0.6% DTT in the rehydration solution. In the experiments conducted for the sodium dodecyl sulfate-polyacrylamide gel electrophoresis (SDS-PAGE), best results were obtained with a doubled concentration (50 mM Tris, 384 mM glycine, 0.2% SDS) of the SDS electrophoresis buffer in the cathodic reservoir as compared to the concentration in the anodic reservoir (25 mM Tris, 192 mM glycine, 0.1% SDS). Among the five protocols tested for gel storing,

success was attained when the gels were stored in plastic bags with 50% glycerol. This is the first report describing the successful solubilization and 2D-electrophoresis of proteins from human lymph node tissue and a 2-D gel storage protocol for easy gel handling before mass spectrometry (MS) analysis.

Keywords: Gel storage, Human lymph node tissue, Protein solubilization, Two-dimensional gel electrophoresis

Introduction

The analytical potential of 2-DE is dependent on good sample preparation, in order to obtain reproducibility, good resolution and a great spot number of proteomic maps. In many cases, the proteins of the sample need to be solubilized, disaggregated, denatured and reduced (Shaw and Riederer, 2003). For this purpose, mixtures of chaotropic compounds, detergents or surfactants, reducing agents and carrier ampholytes are employed (Molloy, 2000; Garfin, 2003).

The role of chaotropes, such as urea and thiourea, is to disrupt hydrogen bonding, leading to protein unfolding and denaturation. Surfactants such as CHAPS, SB 3-10, ASB-14 (amidofolbetaine-14) and SDS act synergistically with chaotropes. Reducing agents, such as DTT and TBP (tributyl phosphine), are used to break intramolecular and intermolecular

[#]The authors contributed equally to this work.

*To whom correspondence should be addressed.
Tel 55 17 3201 5737, Fax 55 17 3234 6407
E-mail: tajara@famerp.br

disulfide bonds. Carrier ampholytes enhance protein solubility by minimizing protein aggregation due to charge-charge interactions (Herbert, 1999; Molloy, 2000; Berkelman and Stenstedt, 2002; Shaw and Riederer, 2003).

Due to variable protein expression from one tissue to another, conditions of protein solubilization that are optimal for one particular tissue type may not hold for others. In addition, several 2-DE steps must be optimized for each tissue in order to obtain good results. In the present study, a comparison was made of six previously described solubilization methods for obtaining proteomic maps of human lymph node tissue. We also describe a simple 2-D gel storage protocol for easy gel handling prior to MS analysis.

Materials and Methods

Thirty-one lymph nodes were collected from head and neck squamous cell carcinoma patients at the Cancer Hospital "Arnaldo Vieira de Carvalho", São Paulo, Brazil. Tissue samples were obtained immediately after the removal of the surgical specimen, snap-frozen and stored in liquid nitrogen. The Ethics Committee approved the research, and written informed consent was obtained from all patients.

One lymph node sample was cut into six pieces of about 5 mm³. 500 µL of one out of six different lysis buffers were added to each piece (Table 1). The specimens were disrupted by sonication 12 times at intervals of 10 s at 10°C and vortexed for 2 min. The lysates were centrifuged at 10,000 rpm for 3 min at 4°C. The supernatants were transferred to other tubes, the insoluble pellets were washed with 200 µL lysis buffers and the second supernatants were collected. The protein concentration of the supernatants was determined by the Bradford method (Bradford, 1976). The protein samples were stored at -70°C.

2-DE was performed using IPGphor and SE 600 Ruby (GE Healthcare). For IEF, 500 µg protein were diluted with rehydration

solution (8 M urea, 2% CHAPS, 0.6% DTT, 0.5% IPG buffer, bromophenol blue trace) to a total volume of 250 µL. IPG strips (pH 3-10 L, 13 cm) were rehydrated in this solution for 12 h under mineral oil. IEF was performed at 20°C, with the following parameters: 500 V (1 h), 1,000 V (1 h), 8,000 V (2 h or 3 : 30 h or 5 h), 500 V (0 h or 1 h), until 16,500 Vh, 26,500 Vh or 41,500 Vh were attained. The current was limited to 50 µA/strip. After IEF, the IPG strip was stored at -70°C until analysis by SDS-PAGE.

The individual strips were incubated, at room temperature, in the equilibrium solution A (2% SDS, 50 mM Tris-HCl pH 8.8, 6 M urea, 30% glycerol, bromophenol blue trace and 1% DTT), followed by solution B (solution A except that DTT was replaced by 2.5% iodoacetamide), for 15 min each. When the proteins were solubilized using solutions containing TBP, the strips were only incubated in solution C (solution A except that DTT was replaced by 5 mM TBP) for 30 min. The IPG strips were washed in SDS electrophoresis buffer (25 mM Tris base, 192 mM glycine, 0.1% SDS), placed on top of 12.5% SDS-PAGE and sealed in place with sealing solution (0.5% low-melting agarose in SDS electrophoresis buffer). The electrophoresis conditions were 15 mA/gel for 30 min, followed by 30 mA/gel for 5 h at room temperature.

Proteins were detected by Coomassie Blue staining. Briefly, gels were incubated overnight in fixing solution (50% ethanol, 10% acetic acid), followed by a destaining solution (50% ethanol, 5% acetic acid) for 3 min, and incubated for 90 min with 0.05% Coomassie Brilliant Blue R-250 solution (0.125 g Coomassie Brilliant Blue R-250, 40% methanol, 10% acetic acid). Subsequently, the gels were washed four times with destaining solution, for 15, 45, 120 and 120 min, respectively, and incubated in preserving solution (5% acetic acid) for approximately 72 h.

For gel storing, five protocols were tested.

- Protocol 1. The gel was washed twice in solution D (30% ethanol) for 30 min, followed by solution E (30% ethanol, 3.5% glycerol) for 60 min.
- Protocol 2. The gel was incubated in 4.3% glycerol for 5 min.
- Protocol 3. The gel was washed four times in water for 4 h.
- Protocol 4. The gel was incubated in 8.7% glycerol for 60 min.

Table 1. Lysis buffer composition. Composition of six lysis buffers tested for protein solubilization efficiency

	Buffer 1	Buffer 2	Buffer 3	Buffer 4	Buffer 5	Buffer 6
Chaotropes	8 M Urea	5 M Urea 2 M Thiourea	5 M Urea 2 M Thiourea	7 M Urea 2 M Thiourea	5 M Urea 2 M Thiourea	7 M Urea 2 M Thiourea
Detergents	4% CHAPS	2% CHAPS 2% SB 3-10	2% CHAPS 2% SB 3-10	4% CHAPS	2% CHAPS 1% SB 3-10 1% ASB -14	2% CHAPS 0.5% ASB -14
Salts	40 mM Tris base	40 mM Tris base	40 mM Tris base			
Reducing agents	65 mM DTT	65 mM DTT	2 mM TBP	65 mM DTT	2 mM TBP	65 mM DTT
Carrier ampholytes	0.2% (pH 3-10)	0.2% (pH 3-10)	0.2% (pH 3-10)	0.2% (pH 3-10)	0.2% (pH 3-10)	0.2% (pH 3-10)
References	(Herbert, 1999; Molloy <i>et al.</i> , 1998)	(Rabilloud <i>et al.</i> , 1997)	(Rabilloud <i>et al.</i> , 1997; Molloy <i>et al.</i> , 1998; Tachibana <i>et al.</i> , 2003)	(Molloy, 2000; Berkelman and Stenstedt, 2002; Rabilloud <i>et al.</i> , 1997; Görg <i>et al.</i> , 2000)	(Garfin, 2003)	(Castellanos-Serra and Paz-Lago, 2002)

• Protocol 5. The gel was incubated in 10% methanol for 48 h. The gels were placed between two cellophane sheets PT (CooperCell) previously embedded in solution E (protocol 1), in water (protocol 2), in 8.7% glycerol (protocol 3 and 4) or stored in a clear plastic bag with 2 ml of 50% glycerol solution applied over both surfaces of the gel. The bag was sealed.

No gel drying equipment was used. Stained and stored gels were scanned with an ImageScanner (GE-Healthcare), and spot detection was manually performed with the Melanie 3.0 software (GeneBio).

One protein spot from 2-DE gel was selected, excised, digested with trypsin and submitted to MALDI-TOF-TOF (Matrix Assisted Laser Desorption - Time of Flight - Time of Flight) 4700 Proteomics Analyser (Applied Biosystems) operated in positive ion reflectron mode to identify the peptides. Such spot was manually cut out from the gel in a clean-air cabinet, to prevent contamination. The protein spot was placed into 0.5 mL tube previously washed with 50% methanol and deionized water. The gel pieces were destained in 250 μ L of 50% acetonitrile (ACN)/50 mM ammonium bicarbonate under constant agitation to complete colourlessness. The gel pieces were then dehydrated with 200 μ L of ACN for 15 min; acetonitrile was discarded and the gel pieces dried in Speed Vac for 30 min. For rehydration and digestion, each gel piece was rehydrated with 20 μ L of a trypsin solution (0.4 μ g modified trypsin in 50 mM acetic acid and 50 mM ammonium bicarbonate). After 30 min incubation at room temperature, a volume of 50 μ L of 50 mM ammonium bicarbonate or the sufficient amount to cover the gel pieces was added, and the sample was incubated for 24 h at 37°C in a water bath, for enzymatic cleavage. Peptides were extracted with 50 μ L 1% trifluoroacetic acid/TFA (first extraction: overnight) and 50 μ L 1% TFA/50% ACN (second extraction: 2 h). The resulting supernatants were mixed and concentrated in a vacuum centrifuge to 10 μ L.

About 1 μ L of this solution was eluted in 1 μ L matrix solution (10 mg/mL α -cyano-4-hydroxycinnamic acid, 0.1% TFA in 50% ACN). Then, 0.5 μ L of the mixture was spotted on a sample plate and introduced into the mass spectrometer after drying. The instrument was calibrated externally using 4700 standard kit (Applied Biosystems).

Proteins were identified by MASCOT MS/MS Ions Search (http://www.matrixscience.com/cgi/search_form.pl?FORMVER=2&SEARCH=MIS). The search parameters were set up as follows: MSDB (Mass Spectrometry Protein Sequence Database); taxonomy *Homo sapiens*; 1 missed cleavage; carbamidomethylation of cysteine and oxidation of methionine as fixed and variable modification, respectively; peptide mass and MS/MS tolerance of 1 and 0.8 Da, respectively; the peptide ion MH^+ and monoisotopic masses.

In the present study, all chemicals used were of highest quality (Merck, Calbiochem, GE Healthcare, Sigma and Bio-Rad).

Results and Discussion

Initial extraction and solubilization is a key factor for proteomic analysis. In the present study, we tested six buffers for solubilization of protein from human lymph node samples, which differed in one or more components, including chaotropes, detergents and reducing agents (Table 1).

Extraction buffer 1 is a standard solution for protein solubilization. About 285 spots were visualized in the gel using this solution (Fig. 1A). Buffers 2 and 3 have similar compositions, except for the reducing agent, and about 281 and 113 spots were visualized in the gels, respectively (Fig. 1B, C). In buffer 4, Tris base was not used for protein solubilization. The results showed 283 spots (Fig. 1D). In lysis buffers 5 and 6, ASB-14 was used as detergent and the gels exhibited poor resolution and streaking (Figs. 1E, F). In conclusion, buffers 1, 2 and 4 were the best solutions for protein solubilization of human lymph node tissue with regard to gel quality. Also, these solutions resulted in high protein concentration (9.8 μ g/ μ L, 8.0 μ g/ μ L and 8.9 μ g/ μ L, respectively), higher than buffer 3 (6.6 μ g/ μ L), but much higher than buffers 5 and 6 (0.3 μ g/ μ L and 1.2 μ g/ μ L). Sharp differences are seen comparing Fig. 1C with 1A, 1B and 1D and reflect the results of the Bradford assay. Although this assay is sensitive to various components of lysis buffers, the reagents of buffers 1-6 probably had no effect on protein quantification, and the gel quality showed to be consequence of the buffer efficiency. Thirty other human lymph node samples were also submitted to buffer 4 and all gels showed excellent quality.

In the buffers tested, urea varied from 5 to 8 M, CHAPS from 2 to 4%, SB 3-10 from 1 to 2%, and ASB-14 from 0.5 to 1%. The carrier ampholytes were used at a low concentration (0.2%), in order to avoid extended running times, because they contribute to the initial conductivity of the sample solution (Garfin, 2003). Tris base was added to three buffers (1, 2 and 3). This compound is used when basic conditions are required for full solubilization or to minimize proteolysis (Rabilloud, 1996). However, addition of ionic compounds in buffers for protein solubilization can result in first-dimension disturbances. Therefore, salts must be removed after the solubilization step or maintained at as low a concentration (lower than 10 mM) in the rehydration solution and IEF (Berkelman and Stenstedt, 2002; Shaw and Riederer, 2003). In our experiments, Tris base was added to the buffers at 40 mM, but the final salt concentration during rehydration was maintained at approximately 10 mM.

Thiourea was introduced in combination with urea, to increase the solubility of proteins, mainly of membrane proteins. The use of this component inhibits the adsorption of protein to the gel matrix, when IEF is conducted in IPG. This efficient chaotrope is poorly soluble in water and requires high concentrations of urea for solubility (optimal condition is 2 M thiourea in 5-7 M urea). This reagent improved the solubility of proteins as compared to urea alone, as already stated by other authors (Rabilloud *et al.*, 1997; Pasquali *et al.*, 1997; Musante *et al.*, 1998; Rabilloud, 1998; Giavalisco *et al.*, 2003; Méchin *et al.*, 2003; Taylor and Pfeiffer, 2003).

We also examined three zwitterionic detergents (CHAPS, SB 3-10, ASB-14). The sulfobetaine CHAPS is the most commonly used detergent for 2-DE, from 2% to 4% in high concentrations of urea. Sulfobetaines with long linear tails (i.e., SB 3-10, ASB-14) have been shown to possess a greater

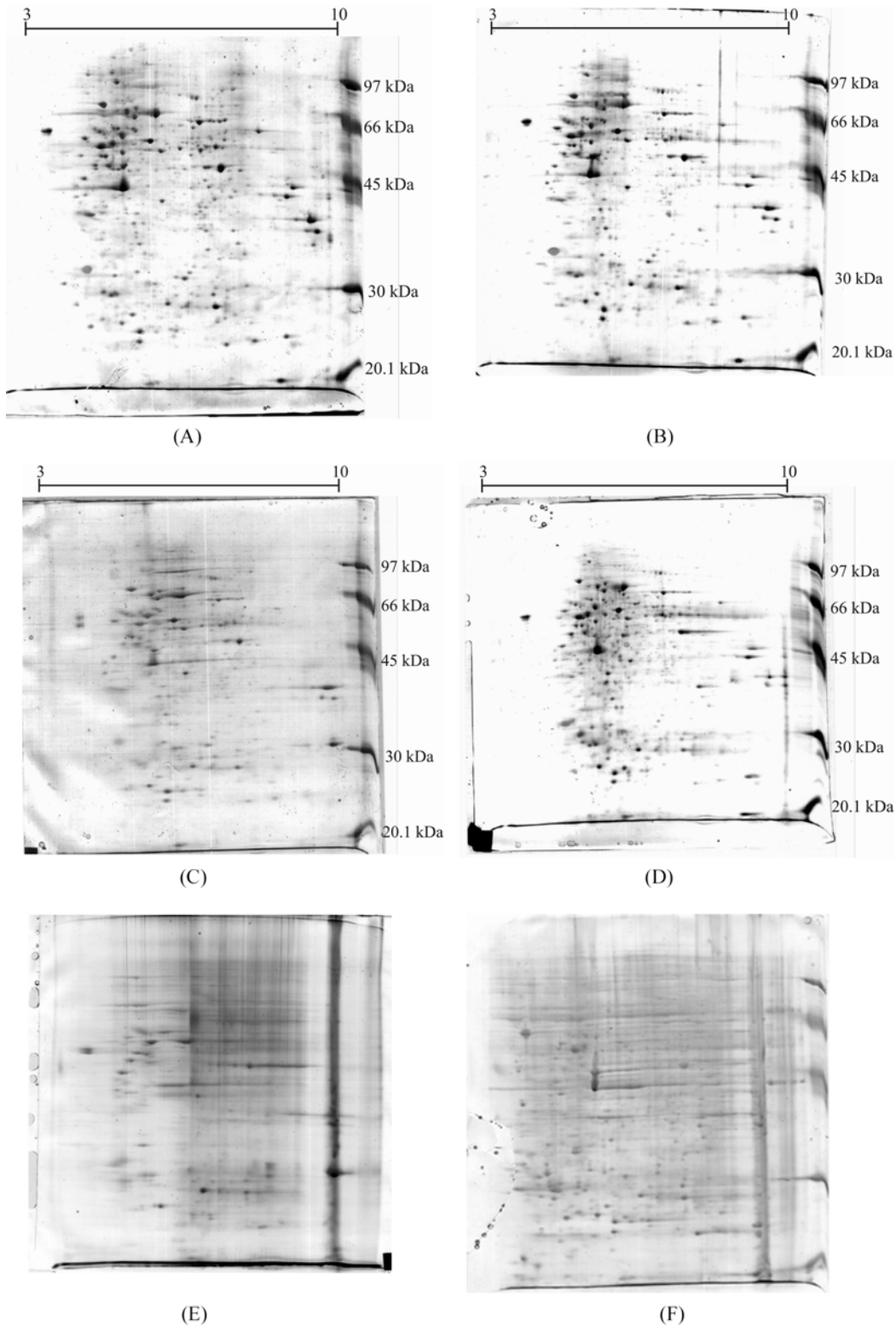


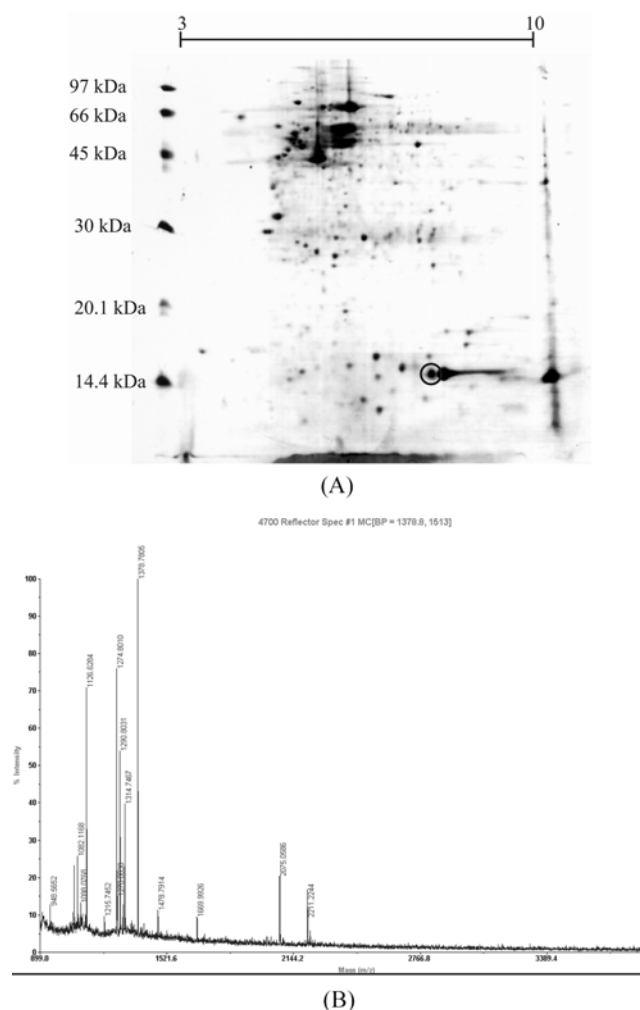
Fig. 1. Comparison of solubilization conditions. Lysis and solubilization from human lymph node tissue proteins were performed using six different buffers (1-6): (A) Buffer 1 (285 spots); (B) Buffer 2 (281 spots); (C) Buffer 3 (113 spots); (D) Buffer 4 (283 spots); (E) Buffer 5 and (F) Buffer 6. Composition of buffers as in Table 1. Proteins were separated on a 13 cm pH 3-10 IPG, 12.5% SDS-PAGE and stained with Coomassie Blue.

ability to solubilize membrane proteins. However, SB 3-10 has poor solubility in high concentrations of urea (Herbert, 1999; Görg and Weiss, 1999). In contrast, ASB-14 is compatible with 9 M urea, but results in large horizontal streaking towards the basic end of the strip. This streaking appears to be an interaction between ASB-14 and the cathode rather than purely an issue with basic proteins, as the effect was independent of the pH range of the IPG strip (pH 3-10 or pH 4-7) (Stanley *et al.*, 2003). Our gels also showed increased streaking in all pH ranges when ASB-14 was used in the extraction solution (Fig. 1E, 1F). Studies using three different detergents (CHAPS, ASB-14 or NP-40) in the solubilization solution also showed more streaking in the second dimension with ASB-14 than with CHAPS (Carboni *et al.*, 2002). The ionic detergent SDS is very effective for protein solubilization, however it is incompatible with IEF (Zuobi-Hasona *et al.*, 2005). For this reason, it was not selected for our optimization experiments.

As for reducing agents, TBP and DTT are commonly used in extraction solutions. When the proteins are solubilized using reagents containing free thiol such as DTT, IPG equilibration requires two steps: reduction (by DTT) and alkylation (by iodoacetamide). DTT has been the standard reducing agent for 2-DE for many years (Molloy, 2000; Görg *et al.*, 2000) and is effective for reducing protein disulfide bonds prior to SDS-PAGE, while iodoacetamide eliminates artifacts of disulfide formation during electrophoresis, for less streaking and better resolution. However, DTT is charged, especially at alkaline pH, and thus migrates out of the pH gradient during IEF, which results in loss of solubility for some proteins. In contrast, TBP lacks a free thiol group, making the second equilibration of the IPG strips unnecessary. In addition, TBP is neutral and does not migrate during IEF, thus, the reducing conditions are maintained over the entire focusing process. On the other hand, TBP has a low solubility, is unstable, volatile and toxic (Rabilloud, 1996; Herbert *et al.*, 1998; Molloy *et al.*, 1998; Berkelman and Stenstedt, 2002). In the present study, the buffers 2 and 3, used for protein solubilization, had similar compositions, except for the reducing agent (DTT in buffer 2 and TBP in buffer 3). Nevertheless, the numbers of spots visualized were very different (281 vs 113 spots), probably due to the reducing agent. Therefore, DTT showed significant improvements in the resolution of proteins by 2-DE. Similar results were reported for myelin proteins (Taylor and Pfeiffer, 2003).

The solubilization of proteins was performed in the absence of protease inhibitors, but using 2 M thiourea, and the sample was processed at 4 to 10°C. According to literature, proteolysis can be inhibited by preparing the sample at such a low temperature, in the presence of Tris base, 2 M thiourea and in strong denaturants such as 8 M urea (Rabilloud, 1996; Carboni *et al.*, 2002; Castellanos-Serra and Paz-Lago, 2002; Berkelman and Stenstedt, 2002).

IEF and SDS-PAGE were also developed using duplicate extracts from buffers 1, 2 and 4. Extracts from other buffers



step tested the SDS electrophoresis buffer at a doubled concentration (50 mM Tris-base, 384 mM glycine, 0.2% SDS) in the cathodic reservoir as compared to the anodic reservoir. This condition resulted in decreased protein smearing in the gel, which is usually caused by buffer depletion during electrophoresis (data not shown). The most important component of the typical second-dimension buffer system must be SDS, which binds protein at a relatively constant ratio, thereby allowing for the size-based separation imparted by the sieving matrix. It was observed that buffer depletion during electrophoresis causes dissociation of the SDS from the protein and, consequently, elongated protein patterns or smearing (Werner, 2003).

Five protocols for gel storing were tested and success was attained when the gels were stored in plastic bags with 50% glycerol solution (Protocol 5). This procedure permitted the easy handling of the gel, without the risk of breakage and without harming the image and MS analysis. The gels were submitted to spot excision and MS analysis up to one year after SDS-PAGE. Figure 2A shows a one-year-old archived SDS-PAGE of a sample from a patient with head and neck squamous cell carcinoma. The MS spectrum corresponding to a spot with apparent pI and MW of 7.1 and 14.5 kDa, respectively, is presented in Figure 2B. This protein spot was identified as hemoglobin. The remaining protocols resulted in cracking gels. Preservation of gels for a long time after electrophoresis is frequently desirable, mainly if their transport to another laboratory is necessary. Several methods for drying polyacrylamide gels have been described. These protocols have been routinely applied in thin gels (0.8 mm). However, cracking gels were observed when these methods were performed in thick 2-D gels (1.5 mm).

Progress in sample preparation methodology for 2-DE has focused on improvements in sample buffer constituents to achieve better representation of the proteome. However, it must be taken into account that a variety of factors influence the sample preparation steps, some of which have been reported in this manuscript. We highlighted that this is the first report describing the successful solubilization and 2-DE of protein from human lymph node tissue and a simple protocol for long time preservation of 2D gels.

Acknowledgments We thank Professor Carlos Roberto Ceron, Keity Souza Santos, Lucilene Delazari dos Santos and Ana Maria Galvan Custódio for useful suggestions. We also thank Nicole S. L. Grosso for critically reading the English manuscript and Celso Pereira Reis Filho for technical support. This work has been supported by the Brazilian Synchrotron Light Laboratory (LNLS) under proposal MAS 3159 and also by grants from Fundação de Amparo à Pesquisa do Estado de São Paulo/FAPESP (Grant 01/14473-0), Conselho Nacional de Desenvolvimento Científico e Tecnológico/CNPq and Coordenação de Aperfeiçoamento de Pessoal de Nível Superior/CAPES.

References

- Berkelman, T. and Stenstedt, T. (2002) *2-D Electrophoresis using immobilized pH gradients. Principles and Methods*. Amersham Biosciences, Uppsala, Sweden.
- Bradford, M. M. (1976) A rapid and sensitive method for the quantitation of microgram quantities of protein utilizing the principle of protein-dye binding. *Anal. Biochem.* **72**, 248-254.
- Carboni, L., Piubelli, C., Righetti, P. G., Jansson, B. and Domenici, E. (2002) Proteomic analysis of rat brain tissue: Comparison of protocols for two-dimensional gel electrophoresis analysis based on different solubilizing agents. *Electrophoresis* **23**, 4132-4141.
- Castellanos-Serra, L. and Paz-Lago, D. (2002) Inhibition of unwanted proteolysis during sample preparation: Evaluation of its efficiency in challenge experiments. *Electrophoresis* **23**, 1745-1753.
- Garfin, D. E. (2003) Two-dimensional gel electrophoresis: an overview. *Trends Analyt. Chem.* **22**, 263-272.
- Giavalisco, P., Nordhoff, E., Lehrach, H., Gobom, J. and Klose, J. (2003) Extraction of proteins from plant tissues for two-dimensional electrophoresis analysis. *Electrophoresis* **24**, 207-216.
- Görg, A. and Weiss, W. (1999) Analytical IPG-Dalt. *Methods Mol. Biol.* **112**, 189-195.
- Görg, A., Obermaier, C., Boguth, G., Harder, A., Scheibe, B., Wildgruber, R. and Weiss, W. (2000) The current state of two-dimensional electrophoresis with immobilized pH gradients. *Electrophoresis* **21**, 1037-1053.
- Herbert, B. (1999) Advances in protein solubilisation for two-dimensional electrophoresis. *Electrophoresis* **20**, 660-663.
- Herbert, B. R., Molloy, M. P., Gooley, A. A., Walsh, B. J., Bryson, W. G. and Williams, K. L. (1998) Improved protein solubility in two-dimensional electrophoresis using tributyl phosphine as reducing agent. *Electrophoresis* **19**, 845-851.
- Hoving, S., Gerrits, B., Voshol, H., Muler, D., Roberts, R. C. and Oostrum, J. (2002) Preparative two-dimensional gel electrophoresis at alkaline pH using narrow range immobilized pH gradients. *Proteomics* **2**, 127-134.
- Méchin, V., Consoli, L., Guilloux, M. L. and Damerval, C. (2003) An efficient solubilization buffer for plant proteins focused in immobilized pH gradients. *Proteomics* **3**, 1299-1302.
- Molloy, M. P. (2000) Two-dimensional electrophoresis of membrane proteins using immobilized pH gradients. *Anal. Biochem.* **280**, 1-10.
- Molloy, M. P., Herbert, B. R., Walsh, B. J., Tyler, M. I., Traini, M., Sanchez, J., Hochstrasser, D. F., Williams, K. L. and Gooley, A. A. (1998) Extraction of membrane proteins by differential solubilization for separation using two-dimensional gel electrophoresis. *Electrophoresis* **19**, 837-844.
- Musante, L., Candiano, G. and Ghiggeri, G. M. (1998) Resolution of fibronectin and other uncharacterized proteins by two-dimensional polyacrylamide electrophoresis with thiourea. *J. Chromatogr. B. Biomed. Sci. Appl.* **705**, 351-356.
- Pasquali, C., Fialka, I. and Huber, L.A. (1997) Preparative two-dimensional gel electrophoresis of membrane proteins. *Electrophoresis* **18**, 2573-2581.
- Rabilloud, T. (1996) Solubilization of proteins for electrophoretic

- analysis. *Electrophoresis* **17**, 813-829.
- Rabilloud, T. (1998) Use of thiourea to increase the solubility of membrane proteins in two-dimensional electrophoresis. *Electrophoresis* **19**, 758-760.
- Rabilloud, T., Adessi, C., Giraudel, A. and Lunardi, J. (1997) Improvement of the solubilization of proteins in two-dimensional electrophoresis with immobilized pH gradients. *Electrophoresis* **18**, 307-316.
- Shaw, M. M. and Riederer, B. M. (2003) Sample preparation for two-dimensional gel electrophoresis. *Proteomics* **3**, 1408-1417.
- Stanley, B. A., Neverova, I., Brown, H. A. and Van Eyk, J. E. (2003) Optimizing protein solubility for two-dimensional gel electrophoresis analysis of human myocardium. *Proteomics* **3**, 815-820.
- Tachibana, M., Ohkura, Y., Kobayashi, Y., Sakamoto, H., Tanaka, Y., Watanabe, J., Amikura, K., Nishimura, Y., Akagi, K. (2003) Expression of apolipoprotein A1 in colonic adenocarcinoma. *Anticancer Res.* **23**, 4161-4167.
- Taylor, C. M. and Pfeiffer, S. E. (2003) Enhanced resolution of glycosylphosphatidylinositol-anchored and transmembrane proteins from the lipid-rich myelin membrane by two-dimensional gel electrophoresis. *Proteomics* **3**, 1303-1312.
- Werner, W. E. (2003) Run parameters affecting protein patterns from second dimension electrophoresis gels. *Anal. Biochem.* **317**, 280-283.
- Zuobi-Hasona, K., Crowley, P. J., Hasona, A., Bleiweis, A. S., Brady, L. J. (2005) Solubilization of cellular membrane proteins from *Streptococcus mutans* for two-dimensional gel electrophoresis. *Electrophoresis* **26**, 1200-1205.

Annexin A1 subcellular expression in laryngeal squamous cell carcinoma

V A F Alves, S Nonogaki,¹ P M Cury,² V Wünsch-Filho,³ M B de Carvalho,⁴ P Michaluart-Júnior,⁵ R A Moyses,⁵ O A Curioni,⁴ D L A Figueiredo,⁶ C Scapulatempo-Neto, E R Parra, G M Polachini,¹¹ R Silistino-Souza,⁷ S M Oliani,⁷ W A Silva-Júnior,⁸ F G Nobrega,⁹ Head and Neck Genome Project/GENCAPO,¹⁰ E H Tajara^{11,12} & M A Zago¹³

Department of Pathology, School of Medicine, USP and ¹Pathology Division, Adolfo Lutz Institute, São Paulo, ²Department of Pathology, School of Medicine/FAMERP, São José do Rio Preto, ³Department of Epidemiology, School of Public Health, USP, ⁴Head and Neck Surgery Department, Heliópolis Hospital and ⁵Division of Head and Neck Surgery, Department of Surgery, School of Medicine, USP, São Paulo, ⁶Department of Ophthalmology, Otorhinolaryngology and Head and Neck Surgery, School of Medicine of Ribeirão Preto, USP, ⁷Department of Biology, Instituto de Biociências, Letras e Ciências Exatas/IBILCE, São Paulo State University/UNESP, São José do Rio Preto, ⁸Department of Genetics, School of Medicine of Ribeirão Preto, USP, ⁹Department of Biosciences and Oral Diagnosis, São José dos Campos Dental School, São Paulo State University/UNESP, São José dos Campos, ¹⁰<http://ctc.fmrp.usp.br/clinicalgenomics/cp/group.asp> (complete author list and addresses presented in the Appendix), ¹¹Department of Molecular Biology, School of Medicine/FAMERP, São José do Rio Preto, ¹²Department of Genetics and Evolutionary Biology, Institute of Biosciences, USP, and ¹³Department of Clinical Medicine, School of Medicine of Ribeirão Preto, USP, SP, Brazil

Date of submission 27 December 2007
Accepted for publication 1 July 2008

Alves V A F, Nonogaki S, Cury P M, Wünsch-Filho V, de Carvalho M B, Michaluart-Júnior P, Moyses R A, Curioni O A, Figueiredo D L A, Scapulatempo-Neto C, Parra E R, Polachini G M, Silistino-Souza R, Oliani S M, Silva-Júnior W A, Nobrega F G, Head and Neck Genome Project/GENCAPO, Tajara E H & Zago M A

(2008) *Histopathology* 53, 715–727

Annexin A1 subcellular expression in laryngeal squamous cell carcinoma

Aims: Annexin A1 (ANXA1) is a soluble cytoplasmic protein, moving to membranes when calcium levels are elevated. ANXA1 has also been shown to move to the nucleus or outside the cells, depending on tyrosine-kinase signalling, thus interfering in cytoskeletal organization and cell differentiation, mostly in inflammatory and neoplastic processes. The aim was to investigate subcellular patterns of immunohistochemical expression of ANXA1 in neoplastic and non-neoplastic samples from patients with laryngeal squamous cell carcinomas (LSCC), to elucidate the role of ANXA1 in laryngeal carcinogenesis.

Methods and results: Serial analysis of gene expression experiments detected reduced expression of ANXA1 gene in LSCC compared with the corresponding non-

neoplastic margins. Quantitative polymerase chain reaction confirmed ANXA1 low expression in 15 LSCC and eight matched normal samples. Thus, we investigated subcellular patterns of immunohistochemical expression of ANXA1 in 241 paraffin-embedded samples from 95 patients with LSCC. The results showed ANXA1 down-regulation in dysplastic, tumourous and metastatic lesions and provided evidence for the progressive migration of ANXA1 from the nucleus towards the membrane during laryngeal tumorigenesis.

Conclusions: ANXA1 dysregulation was observed early in laryngeal carcinogenesis, in intra-epithelial neoplasms; it was not found related to prognostic parameters, such as nodal metastases.

Keywords: annexin A1, head and neck neoplasm, immunohistochemistry, laryngeal neoplasm

Address for correspondence: Eloiza Helena Tajara, PhD, Department of Molecular Biology, School of Medicine/FAMERP, São José do Rio Preto, CEP 15090-000, SP, Brazil. e-mail: tajara@famerp.br

Abbreviations: ANX, annexin; CI, confidence interval; EGFR, epidermal growth factor receptor; H2G, Hyper and Hypo-expressed Genes; HNSCC, head and neck squamous cell carcinoma; OR, odds ratio; PVDF, polyvinylidene-fluoride; qPCR, quantitative polymerase chain reaction; SAGE, serial analysis of gene expression; SCC, squamous cell carcinoma; SDS, sodium dodecyl sulphate

Introduction

Annexins (ANX) are a family of proteins present in many organisms, from mould to humans, regulated by fluctuations in cellular calcium levels and implicated in multiple molecular and cellular processes. The unique calcium- and lipid-binding properties enable them to associate with negatively charged membrane phospholipids in a calcium-dependent and reversible manner. This property links annexins to membrane-related events such as cytoskeletal organization, transport, ion fluxes and, consequently, to cell differentiation and migration.¹

ANX is composed of a conserved COOH-terminal with repetitive homologous domains responsible for calcium and phospholipid binding properties. The variable N-terminal region, which is unique in length and sequence, interacts with many cytosolic ligands and is subject to post-translational modification such as myristoylation and phosphorylation. N-terminal tyrosine phosphorylation of some annexins is catalysed by the epidermal growth factor receptor (EGFR) and Src-family tyrosine kinases, which alter their proteolytic sensitivity and calcium affinities (for review, see).²

Annexins are soluble and localized in the cytoplasm of cells, moving to membranes when calcium levels are elevated. Different studies have shown that some annexins move from cytoplasm to nucleus or outside the cells, both processes apparently dependent on tyrosine-kinase signalling.^{3,4} Interestingly, nuclear retention of ANX by site-directed mutagenesis in the nuclear export signal sequence of the N-terminus results in reduced cell proliferation and increased doubling time of cells.⁵ Under conditions of inflammation following their induction by glucocorticoids, human ANX are exported outside of cells and may bind membrane receptors, inhibiting the accumulation of inflammatory cells at sites of injury.¹

The mammalian subfamily A of annexins encompasses human ANX represented by 12 members and classified from A1 to A13.⁶ To date, there is no evidence that loss, mutation, translocation or amplification of human ANX genes play a causative role in any disease, although abnormal expression levels or localization might contribute to pathological conditions

such as inflammatory processes, cardiovascular disease and cancer.

In fact, different members of the ANX family have been reported to be involved in the neoplastic process with a potential tumour suppressor role. For example, ANX7 has been implicated as a tumour-suppressor gene in prostatic tumours.⁷ Furthermore, overexpression of ANXA2,⁸ ANXA4⁹ and ANXA8¹⁰ is observed in various tumours.

Annexin A1 (ANXA1), a 37-kDa protein, is claimed to participate in cell transformation as well as in inflammation, signal transduction, keratinocyte differentiation, apoptosis and gene expression modulation.^{11–16} The relationship between ANXA1 and the neoplastic process may be derived from the fact that it is a substrate of EGFR and other kinases involved in tumour development.²

ANXA1 has been shown to be up-regulated in pancreatic carcinoma,¹⁷ hairy cell leukaemia¹⁸ and skin tumours¹⁹ and down-regulated in prostatic,²⁰ oesophageal,²¹ breast²² and head and neck neoplasms.^{23–26}

Head and neck squamous cell carcinomas (HNSCCs) account for a significant proportion of all new cancer diagnoses worldwide, and their incidence, in particular of those arising from the larynx and oral cavity, is increasing in developed countries. Laryngeal SCC is estimated to have affected 11 295 patients in the USA in 2007.²⁷ In the early stages, these carcinomas frequently cause few symptoms, resulting in a delay in diagnosis, with a significant impact on patient management and overall survival rates. In this context, molecular markers potentially related to multistep carcinogenesis are urgently needed to assess HNSCC, to further our understanding of the mechanisms of disease formation and for screening for potential therapeutic targets.

In the present study, by using serial analysis of gene expression (SAGE) and real-time quantitative polymerase chain reaction (qPCR), we identified and validated reduced expression of ANXA1 gene (gene ID 301) in laryngeal SCCs. In addition, we investigated subcellular patterns of immunohistochemical expression of ANXA1 in normal and dysplastic areas, primary neoplasia and lymph node metastasis, searching for

evidence for the role of ANX in laryngeal carcinogenesis.

Materials and methods

CASE SELECTION

For SAGE experiments, two fresh samples of primary laryngeal cancer, one with lymph node metastasis (N+ status) and one without lymph node metastasis (N- status), and the corresponding non-neoplastic margins were obtained from patients with surgically resected carcinoma at Hospital do Câncer Arnaldo Vieira de Carvalho, São Paulo, SP.

Immunohistochemical analysis was performed on 241 formalin-fixed paraffin-embedded tissue sections from non-neoplastic mucosa, dysplastic epithelium, primary carcinomas and their lymph node metastases. The samples were obtained from 95 patients with surgically resected laryngeal SCC at Hospital das Clínicas and Hospital Heliópolis, São Paulo, SP, Hospital das Clínicas, Ribeirão Preto, SP and Universidade do Vale do Paraíba, São José dos Campos, SP, between 2002 and 2004. The average age of patients was 58.1 years (SD 10.8, range 27–83 years), and the male/female ratio was 7.7:1. Most patients were smokers or former smokers (72.6%) and had a history of chronic alcohol abuse (66.3%). A small subset of 16 samples (eight laryngeal SCCs and eight matched non-neoplastic surgical margins) from the same group of 95 patients was analysed by Western blot.

The expression of *ANXA1* transcripts was validated by qPCR in fresh samples from a different set of 15 laryngeal SCCs and eight non-neoplastic surgical margins.

The study protocol was approved by the ethics committees of enrolled institutions and by the National Committee of Ethics in Research (CONEP 1763/05, 18/05/2005). Tissue samples were taken after obtaining written informed consent from each patient and processed anonymously. Pathological procedures were performed according to protocols approved by the Brazilian Society of Pathology.²⁸ All histopathological reports and slides were reviewed by senior pathologists (V.A.F.A., P.M.C., E.R.P., C.S-N.), thus confirming the diagnosis and selecting the most representative areas for immunohistochemistry.

RNA AND PROTEIN EXTRACTION AND REVERSE TRANSCRIPTION

Fresh samples of primary laryngeal cancer were frozen in liquid nitrogen and stored at -80°C . Total RNA was

extracted using TRIzol[®] LS Reagent (Invitrogen Corp., Carlsbad, CA, USA) and treated with RQ1 RNase-Free DNase (Promega Corp., Madison, WI, USA). cDNA synthesis was performed using the High Capacity cDNA Archive kit (Applied Biosystems, Foster City, CA, USA) as described by the manufacturer. Total protein was extracted by 100% isopropyl alcohol, 0.3 M guanidine hydrochloride in 95% ethanol, 100% ethanol and 1% sodium dodecyl sulphate (SDS).

SERIAL ANALYSIS OF GENE EXPRESSION

SAGE was carried out using the I-SAGE[™] Kit (Invitrogen). Clones were checked and sequenced with forward M13 primer in a MegaBACE[™]1000 sequencer (Amersham Biosciences, Piscataway, NJ, USA) or PRISM[®] 377 DNA Sequencer (Applied Biosystems) using DYE-dynamic ET Dye Terminator Sequencing Kit (Amersham Biosciences), or ABI PRISM[®] BigDye[™] Primer Cycle Sequencing Kit (Applied Biosystems), respectively.

For each SAGE library, 6000 sequencing reactions were performed and the SAGE tags were obtained with SAGE[™] Analysis 2000 Software 4.0, with minimum tag count set to 1 and maximum ditag length set to 28 bp, whereas other parameters were set as default. The results were analysed with the help of the tools developed by Hyper and Hypo-expressed Genes (H2G) software (http://gdm.fmrp.usp.br/tools_bit.php) and short tags that exhibited at least a twofold change were selected (<http://cgap.nci.nih.gov/SAGE/AnatomicViewer>). H2G is a bioinformatics tool designed to select over- and down-regulated genes from SAGE datasets and to evaluate differences in gene expression.

QUANTITATIVE REAL-TIME POLYMERASE CHAIN REACTION

Real-time quantification was performed in duplicate using a Primer Express designed TaqMan assay for *ANXA1*. To normalize sample loading, the differences of threshold cycles (ΔCt) were derived by subtracting the Ct value for the internal reference (*GAPDH*) from the Ct values of the evaluated genes. The relative fold value was obtained by the formula $2^{-\Delta\Delta\text{Ct}}$ using the median ΔCt value of surgical margin samples as a reference, and $\Delta\Delta\text{Ct}$ was calculated by subtracting the reference ΔCt from the ΔCt values of the tumour samples. Expression of all samples was measured in a single plate for each gene evaluated. Kruskal–Wallis with Dunn's post test was performed using Prism 4 (GraphPad Software, Inc., San Diego, CA, USA; <http://www.graphpad.com>).

IMMUNOHISTOCHEMISTRY

Immunohistochemical analyses were performed using the conventional protocol. Sections from representative formalin-fixed paraffin-embedded samples were immunostained with a monoclonal antibody to ANXA1, with amplification by the streptavidin-peroxidase method. Briefly, after deparaffinization in xylene and rehydration in graded ethanol, antigen epitope retrieval was performed using 10 mM citric acid solution, pH 6.0 in a pressure cooker. Endogenous peroxidase activity was blocked with 6% hydrogen peroxide for 20 min.

Primary mouse anti-annexin 1 monoclonal antibody (clone 29, code no. 610067, BD Transduction Labora-

tories, San Diego, CA, USA), diluted 1:4000, was incubated for 30 min at 37°C followed by overnight incubation at 4°C, and then by addition of biotinylated antimouse secondary antibody and streptavidin-horse-radish peroxidase (LSAB+, code no. k0690; Dako, Carpinteria, CA, USA).

The reaction product was developed by 3,3'-diaminobenzidine and H₂O₂ and counterstaining was performed with Harris haematoxylin. The primary antibody was omitted for negative controls and endothelial cells of tonsil were used as positive control. Immunoexpression of ANXA1 was assessed independently in the nucleus, cytoplasm and membrane and graded subjectively as 0 (no evidence of immunoreac-

Table 1. List of the 20 most abundant tags in laryngeal tumour serial analysis of gene expression (SAGE) libraries and 20 most abundant tags in non-neoplastic SAGE library

Most abundant tags in laryngeal tumour				Most abundant tags in non-neoplastic laryngeal tissue			
Tags	No.	Unigene	Gene symbol	Tags	No.	Unigene	Gene symbol
TACCTGCAGA	3907	Hs.416073	<i>S100A8</i>	TACCTGCAGA	3948	Hs.416073	<i>S100A8</i>
GAAATAAAGC	2124	Hs.413826	<i>IGHG3</i>	GTGGCCACGG	3758	Hs.112405	<i>S100A9</i>
GTGGCCACGG	1515	Hs.112405	<i>S100A9</i>	TTTCCTGCTC	1845	Hs.139322	<i>SPRR3</i>
GTTGTGGTTA	1278	Hs.48516	<i>B2M</i>	AGAAAGATGT	1337	Hs.78225	<i>ANXA1</i>
TAAACCAAAT	1063	Hs.105924	<i>DEFB4</i>	AAAGCGGGGC	823	Hs.74070	<i>KRT13</i>
CTTCCTTGCC	915	Hs.2785	<i>KRT17</i>	GGGCTGGGGT	729	Hs.430207	<i>RPL29</i>
CCCATCGTCC	792	Hs.193989	<i>TARDBP</i>	ATCCTTGCTG	728	Hs.412999	<i>CSTA</i>
TTTCCTGCTC	706	Hs.139322	<i>SPRR3</i>	GCATAATAGG	596	Hs.458236	<i>LOC352870</i>
CTGGGTTAAT	647	Hs.298262	<i>RPS19</i>	CCCATCGTCC	559	Hs.193989	<i>TARDBP</i>
GATCTCTTGG	621	Hs.38991	<i>S100A2</i>	GAGGGAGTTT	556	Hs.76064	<i>RPL27A</i>
GAGATAAATG	593	Hs.3185	<i>LY6D</i>	GGCAGAGAAG	531	Hs.3235	<i>KRT4</i>
GGGCTGGGGT	575	Hs.430207	<i>RPL29</i>	GGATTTGGCC	527	Hs.302588	<i>EST</i>
CGCCGACGAT	552	Hs.265827	<i>IFI6</i>	GAAATAAAGC	499	Hs.413826	<i>IGHG3</i>
CCTAGCTGGA	509	Hs.401787	<i>PPIA</i>	GATCTCTTGG	498	Hs.38991	<i>S100A2</i>
TAGGTTGTCT	476	Hs.401448	<i>TPT1</i>	TAGGTTGTCT	483	Hs.401448	<i>TPT1</i>
AAAAAAAAAA	466	Hs.0	No unigene cluster	GTGGAAGACG	468	Hs.80395	<i>MAL</i>
GGATTTGGCC	454	Hs.302588	<i>EST</i>	GGCAAGCCCC	368	Hs.425293	<i>RPL10A</i>
AAAGCACAAG	446	Hs.367762	<i>KRT6A</i>	TGGGGAGAGG	347	Hs.288998	<i>S100A14</i>
GAGGGAGTTT	399	Hs.76064	<i>RPL27A</i>	CTCCCCAAG	341	Hs.366	<i>MGC27165</i>
GCATAATAGG	361	Hs.458236	<i>LOC352870</i>	TGCACGTTTT	323	Hs.169793	<i>RPL32</i>

tivity), grades 1 (5–25% of positive cells), 2 (26–50%), 3 (51–75%) and 4 (>75% of positive cells). Expression differences were evaluated between cases showing (a) negative or grade 1 and (b) grades 2, 3 and 4.

WESTERN BLOT

For Western blot analysis, the antibodies used were polyclonal anti-ANXA1 diluted 1:1000 (Zymed Laboratories, Cambridge, UK), and monoclonal anti- β -actin antibody diluted 1:5000 (Sigma-Aldrich, St Louis, MO, USA). In brief, protein samples (9 μ g) were loaded onto 12% resolving gel with 5% stacking gel (SDS–polyacrylamide gel electrophoresis) in denaturing conditions at 130 V for 90 min. The molecular weight ladder was the PageRuler™ Prestained Protein Ladder (Fermentas Life Sciences, Glen Burnie, MD, USA).

The proteins were then transferred electrophoretically (325 mA per blot 70 min; Mini Protean 3 Cell, BioRad, Hercules, CA, USA) to polyvinylidene difluoride (PVDF) paper (Immobilon, Millipore, Billerica, MA, USA) soaked in transfer buffer (25 mM Tris, 0.2 M glycine) and 20% methanol v/v. The PVDF membranes were submitted to chromogenic staining using the Western Breeze kit (Invitrogen). The blots were then scanned and analysed (Gel Logic HP 2200; Carestream Health, Rochester, NY, USA).

STATISTICAL ANALYSIS

To evaluate if the subcellular ANXA1 expression pattern was similar in sections from dysplasia, tumour and metastases from the same individual, different immunohistochemical results were analysed using non-parametric unbalanced repeated measures ANOVA.²⁹ Differences in immunohistochemical results were also analysed using χ^2 test and Fisher's exact test with Bonferroni correction. The association of ANX immun-expression with presence or absence of node metastasis was analysed by χ^2 and Fisher's exact test. Statistical significance was set at $P < 0.05$.

Results

SAGE

Approximately 100 000 tags were obtained by sequencing three SAGE libraries, obtained from two samples of SCC of the larynx and from a pool of the corresponding non-neoplastic margins. Excluding redundancy, this approach identified about 17 000 non-redundant tags in each library. The annotation

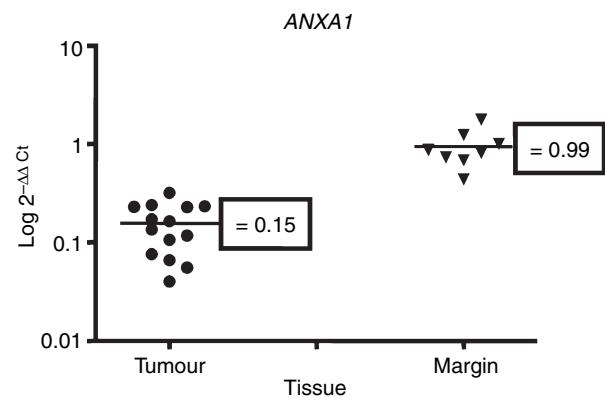


Figure 1. Validation of ANXA1 gene by real-time polymerase chain reaction (PCR). Quantitative PCR was carried out on 15 squamous cell carcinoma and eight tumour margin samples. Gene expression is shown as $\log 2^{-\Delta\Delta C_t}$ ($\Delta\Delta C_t$ ranged from 0.04053 to 0.70222). Differences between tumour and normal samples were significant ($P < 0.001$).

was based on two specific tools, SAGEmap (<http://www.ncbi.nlm.nih.gov/SAGE/>) and CGAP SAGE Genie (<http://cgap.nci.nih.gov/SAGE>). The 20 most abundant transcripts for each library are listed in Table 1.

QUANTITATIVE REAL-TIME PCR

Based on the normalized tag ratios of tumour/non-neoplastic tissues, a set of genes was selected to be validated by real-time PCR, using the H2G tool. The results obtained for ANXA1 transcripts in 15 laryngeal SCCs and eight non-neoplastic margins are shown in Figure 1. A significant reduction ($P < 0.001$) of ANXA1 transcript levels in tumour samples was observed.

IMMUNOLOGICAL ANALYSIS

Immunohistochemical analysis was performed in 241 samples from 95 patients with laryngeal SCC. Of these, 90 patients had cervical lymph node resection and, thus, had valid pathological information about node metastasis. The immunohistochemistry for ANXA1 in nuclei, cytoplasm and membrane of non-tumour, dysplastic, tumour and metastatic areas of these laryngeal SCCs is presented in Figure 2.

As depicted in Table 2, ANXA1 was detected in nuclei of 88.5% of non-neoplastic squamous epithelial samples, contrasting with only 69.0% of dysplastic samples, 67.0% of primary carcinomas and 62.5% of lymph node metastases. Cytoplasmic ANXA1 immunoreactivity was detected in 98.7% of normal tissues and in 93.1, 86.4 and 87.5% of dysplastic, tumour and

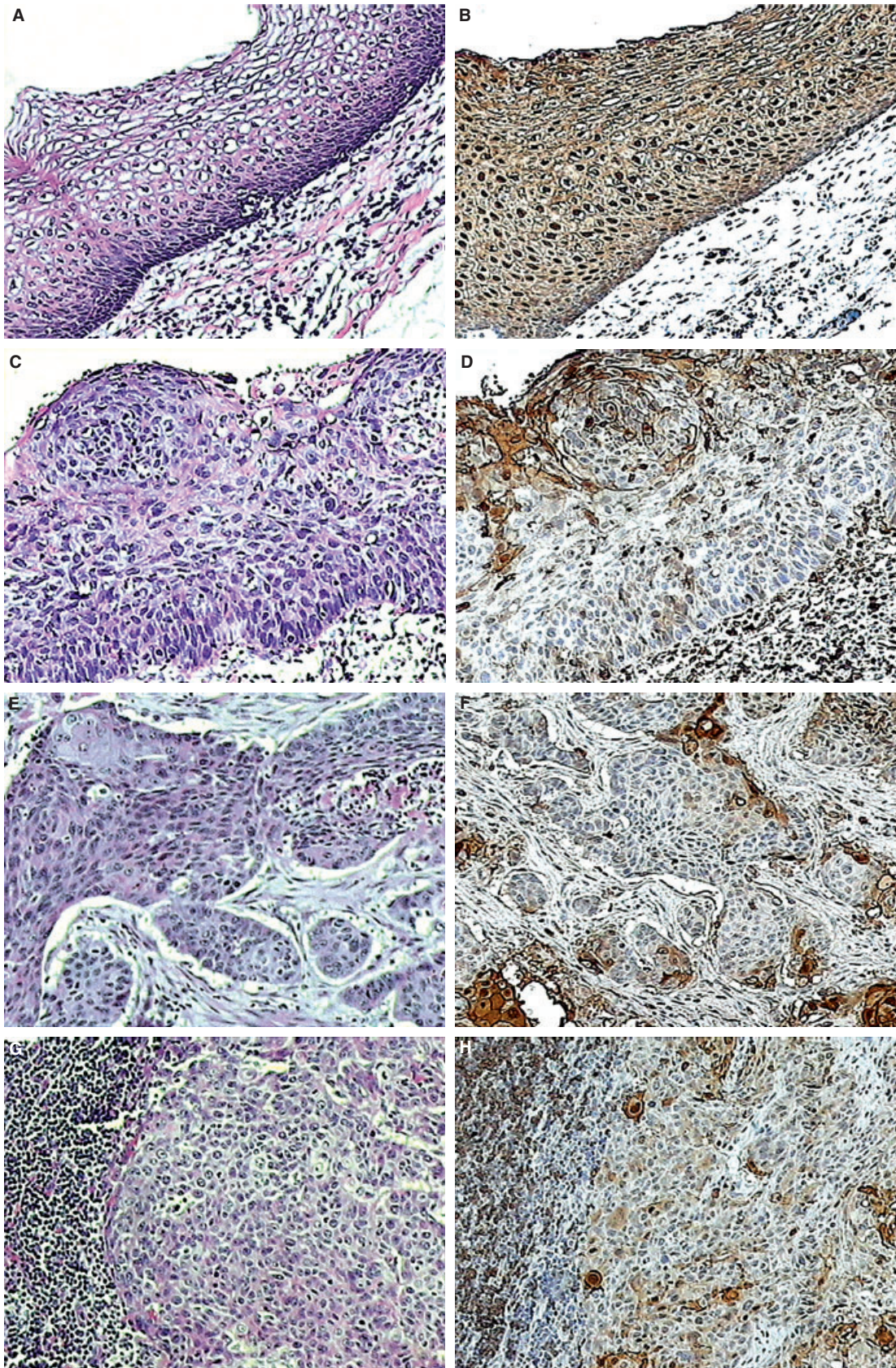


Table 2. Frequency of nuclear, cytoplasmic and membranous immunoreactivity of ANXA1 in normal, dysplastic, primary tumour and metastatic cells from 95 patients with laryngeal squamous cell carcinoma

Immunohistochemical reactivity	Normal tissue		Dysplastic cells		Tumour		Metastasis	
	<i>n</i>	%	<i>n</i>	%	<i>n</i>	%	<i>n</i>	%
Nucleus								
Negative	9	11.5	9	31.0	29	33.0	9	37.5
Positive <i>P</i> < 0.001	69	88.5	20	69.0	59	67.0	15	62.5
Cytoplasm								
Negative	1	1.3	2	6.9	12	13.6	3	12.5
Positive <i>P</i> < 0.001	77	98.7	27	93.1	76	86.4	21	87.5
Membrane								
Negative	36	46.2	14	48.3	28	31.8	11	45.8
Positive <i>P</i> < 0.001	42	53.8	15	51.7	60	68.2	13	54.2
Total	78	100.0	29	100.0	88	100.0	24	100.0

metastatic areas, respectively. Neoplastic areas exhibited the highest frequency of membranous immunoreactivity.

Using χ^2 test and Fisher's exact test with Bonferroni correction ($\alpha = 0.05/6 = 0.0083$), we performed a 2×2 comparison (six different comparisons) of nuclear, cytoplasmic and membranous ANXA1 expression among normal, dysplastic, primary tumour and metastatic areas (Table 3). The results showed significantly lower expression in the nucleus and cytoplasm of tumour compared with normal tissues, as well as higher expression in the membrane of tumour versus normal samples. Furthermore, differences in expression were found in the cytoplasm and membrane when comparing dysplasia with tumour and tumour with metastasis.

Statistical analysis of cytoplasmic ANXA1 expression in normal tissue showed significant differences ($P < 0.05$) in relation to dysplastic, tumour and metastatic tissues considering the dependence measurements for each patient (Table 4). Significant differences in cytoplasmic immunoreactivity were also observed between dysplasia and tumour or metastasis and between tumour and metastasis. Membranous and nuclear reactivity were similar between normal and tumour areas and between dysplasia and metastasis, but significantly different in dysplasia or metastasis compared with normal or tumour tissues.

The loss of immunoreactivity of ANXA1 was not predictive for the presence of lymph node metastasis.

The odds ratios (OR) of having node metastasis in the group showing ANXA1 loss in any subcellular localization relative to the OR of having no metastasis were 0.549 [$P = 0.196$; confidence interval (CI) 0.22, 1.37], 0.44 ($P = 0.309$; CI 0.11, 1.69) and 0.63 ($P = 0.329$; CI 0.25, 1.60) for nuclear, cytoplasmic and membranous ANXA1 immunoreactivity, respectively.

The results of Western blot for ANXA1 expression in 16 samples were quantified and normalized against β -actin. The data were consistent with the immunohistochemical study and showed higher levels of ANX in most surgical margins than in tumours (Figure 3). In all samples, the uncleaved protein (37 kDa) and two cleaved fragments (approximately 33 and 35 kDa) were observed. Pathological features as well as Western blot and immunohistochemistry results are summarized in Table 5.

Discussion

By using SAGE, we observed a significant reduction in gene expression of ANXA1 in laryngeal SCC. In addition, by immunohistochemistry on a different set of samples, we also detected decreased immunoreactivity of ANXA1 in the nucleus and cytoplasm of dysplastic, primary tumour and metastatic lymph node cells of larynx compared with normal tissue. The decreased expression of the protein was observed not in all, but in a significant proportion of cases.

Figure 2. Immunohistochemical features of laryngeal squamous cells. Non-tumoural areas (A,B) strongly express ANXA1 in nuclei, cytoplasm and membrane. ANXA1 expression is lower in dysplastic areas (C,D), tumoural samples (E,F) and in metastatic areas (G,H), especially in nuclei and in cytoplasm (A,C,E,G, H&E; B,D,F,H, annexin A1, LSAB).

Table 3. Results of a 2 × 2 comparison of nuclear, cytoplasmic and membranous ANXA1 expression among normal, dysplastic, primary tumour and metastatic cells from 95 patients with laryngeal squamous cell carcinoma

Areas	P-value		
	Nucleus	Cytoplasm	Membrane
Normal × dysplasia	0.038**	0.178**	0.845*
Normal × tumour	0.002*	<0.001*	<0.001*
Normal × metastasis	0.011**	0.040**	0.978
Dysplasia × tumour	0.937*	0.006*	<0.001*
Dysplasia × metastasis	0.621*	0.649**	0.859*
Tumour × metastasis	0.600*	0.049*	0.001**

* χ^2 test. ** χ^2 and Fisher's exact test with Bonferroni correction ($\alpha = 0.05/6 = 0.0083$).

Table 4. Comparison of nuclear, cytoplasmic and membranous ANXA1 immunorexpression among normal, dysplastic, primary tumour and metastatic cells from 95 patients with laryngeal squamous cell carcinoma

Areas	P-value*		
	Nucleus	Cytoplasm	Membrane
Normal × dysplasia	<0.0001	<0.0001	<0.0001
Normal × tumour	0.0589	0.0035	0.1105
Normal × metastasis	<0.0001	<0.0001	<0.0001
Dysplasia × tumour	<0.0001	<0.0001	<0.0001
Dysplasia × metastasis	0.1554	0.0216	0.1784
Tumour × metastasis	<0.0001	<0.0001	<0.0001

P-values were calculated considering non-parametric unbalanced repeated measures ANOVA.

SAGE is a high-throughput technique that allows measurement of expression levels of a large number of transcripts. Although SAGE is a very powerful method for detecting both known and unknown transcripts, it usually requires independent confirmation at protein level. For this reason, we used Western blot and immunohistochemistry to validate changes in ANXA1 expression. Similar to SAGE, Western blot requires unfixed tissue, but in contrast to immunohistochemistry, reveals no details of topography or subcellular expression. Therefore, immunohistochemistry was a good choice for visualizing pathological features,

semiquantitatively measuring expression of ANX and evaluating its localization.

The loss of ANXA1 protein immunorexpression was found herein as an early event in head and neck oncogenesis, detected in the pre-invasive stages. This important finding confirms and extends previous studies of Garcia Pedrero and collaborators,²³ who observed down-regulation of ANXA1 in 11 out of 16 laryngeal carcinomas. Those authors also reported lower immunorexpression of ANXA1 in eight dysplastic lesions of the head and neck, although no information was provided regarding the sites of these lesions. Vishwanatha and collaborators³⁰ found loss of anti-inflammatory activity of ANXA1 and up-regulation of proinflammatory cyclooxygenase-2 in oral cells exposed to smokeless tobacco, thus proposing that the dual effect of these regulatory events might lead the cells down the carcinogenic pathway. Silistino-Souza and collaborators²⁶ have also shown down-regulation of ANXA1 expression in the nucleus and cytoplasm of surgical tissue specimens from 20 patients with laryngeal cancer and a significant increase of the protein in the cytoplasmic granules and nuclei of tumour and peritumoral mast cells. These authors suggested that tumour cells could recruit and activate mast cells to release biological mediators, which may alter the microenvironment and promote or inhibit tumour growth. Taken together, these findings may provide an important link between inflammatory mediators and carcinogenesis in HNSCCs, since tobacco consumption is the commonest aetiological risk factor for the development of these tumours³¹ and hyperproliferation of head and neck squamous cells is nearly always found in the context of chronic inflammation.

An important discrepancy between our findings and those of Garcia Pedrero and collaborators²³ is that, in the present study, down-regulation of ANXA1 was not predictive for lymph node metastases. In keeping with the fact that ANX down-regulation is an early event and possibly not strictly related to progression, this result might be site-dependent, since our study was focused specifically on laryngeal SCCs.

The reduced ANX expression in HNSCC as well as in other tumours may be explained by DNA mutations, post-transcriptional/post-translational events or by regulatory mechanisms. Loss of heterozygosity in the 9q12-q21.2 region has been described in HNSCC³² and may affect the promoter or the coding sequence of the ANXA1 gene. Otherwise, alterations at RNA level or epigenetic mechanisms are probably uncommon and have not been described. Post-translational events such as ANXA1 phosphorylation are of interest, especially

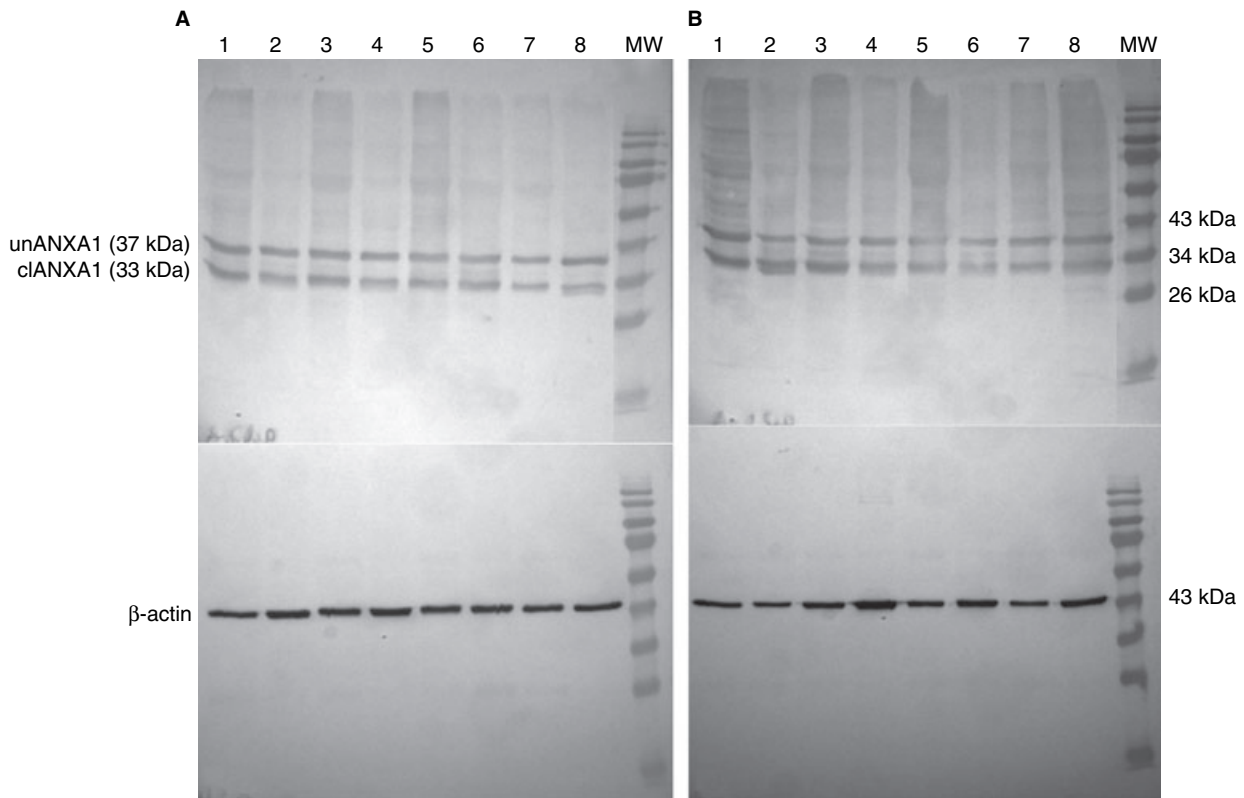


Figure 3. Analysis of ANXA1 protein. Representative Western blots illustrating ANXA1 expression in a subset of (A,B) eight laryngeal squamous cell carcinomas and eight matched non-neoplastic surgical margins by using anti-annexin A1. A, Surgical margins (lanes 1, 3, 5, 7) and tumour samples (lanes 2, 4, 6, 8) from patients 105, 102, 96 and 136, respectively. B, Surgical margins (lanes 1, 3, 5, 7) and tumour samples (lanes 2, 4, 6, 8) from patients 35, 31, 19 and 18, respectively. MW, molecular weight marker. Uncleaved ANXA1 (unANXA1): 37 kDa; cleaved fragment (cANXA1): 33 kDa. β -actin was used as an internal control.

because annexin is a substrate of EGFR,² which is overexpressed and serves as a tumour growth marker in HNSCC.³³ Phosphorylated ANXA1 is apparently prone to tryptic cleavage at the N-terminal region and may be involved, for example, in controlling and limiting leucocyte emigration into inflamed tissue through ANXA1 N-terminal peptides.³⁴

By Western blot, we could observe three ANXA1 fragments at almost the same molecular weight, supporting the fact that ANXA1 has three cleavable sites. Since the annexin N-terminal domain is susceptible to cleavage, tissue storage conditions or protein extraction procedures may influence the levels of peptides. However, the fresh samples of primary laryngeal cancer analysed in the present study, once collected, were immediately snap-frozen and stored at -80°C until protein isolation. Our Western blot results also indicate, in most cases, a satisfactory correlation with ANXA1 expression data obtained by immunohistochemical analysis. Differences can be explained by the use of different antibodies with distinctive binding properties.

Recently, Sakaguchi and collaborators³⁵ have observed EGF-induced ANXA1 cleavage in normal human keratinocytes and have shown that phosphorylation of ANXA1 occurs before the cleavage event by lysosomal enzymes. The authors also showed that this pathway is constitutively activated in squamous cancer cells.

Garcia Pedrero,²³ Rodrigo²⁵ and collaborators have detected low ANXA1 expression significantly associated with parameters of aggressiveness in HNSCCs. Since immunohistochemical analysis showed strong positive signals in differentiated areas, whereas poorly differentiated tumours were commonly found to be negative; those authors suggested that ANXA1 expression is in fact linked to epithelial differentiation.

To the best of our knowledge, this is the first study to assess the intracellular distribution of ANXA1 in a large set of laryngeal carcinomas, except for the 20 cases in the above-mentioned study of Silistino-Souza and collaborators.²⁶ The only other study of such subcompartmentalization that could be found regard-

Table 5. Pathological features of eight patients with laryngeal squamous cell carcinoma as well as the results of Western blot and immunohistochemical analysis

Features	Patients																	
	105		102		96		136		35		31		19		18			
Surgical margins	Tumour free																	
Differentiation	Moderate		Well				Well		Moderate		Moderate		Moderate		Moderate			
TNM	T4N2cM0		T2N1M0		T4N0M0		T4N2bM0		T4N0M0		T4N2cM0		T4N0M0		T4N2bM0			
Neural invasion	+		-		-		-		-		+		-		-			
Depth of infiltration	Invasive		Cartilage		Cartilage		Cartilage		Invasive		Invasive		Invasive		Cartilage			
Lymphatic infiltration	-		-		-		-		-		-		-		-			
Vascular infiltration	-		+		-		-		-		-		-		-			
Inflammatory peritumoral infiltration	Moderate		Weak		Weak		Weak		Moderate		Moderate		Weak		Moderate			
Immunoreactivity	Tu	M																
	Nucleus		3		4		2		4		3		3		1		3	
	Cytoplasm		3		4		2		4		4		4		3		4	
Membrane		3		1		4		4		3		4		4		2		
Western blot*	1.03	1.48	0.87	1.03	1.02	1.26	1.08	0.93	1.82	1.72	1.12	1.41	1.17	1.32	1.39	1.47		

*Relative intensity of the ANXA1 (cleaved and uncleaved protein) signal in Western blot.

ing upper aerodigestive tract tumours was from Liu and collaborators³⁶ in oesophageal carcinomas. Although those authors did not mention the number of cases studied, they reported a reduction of ANXA1 immunoexpression on the cell membrane and nucleoplasm of neoplastic squamous cells, contrasting with an increase in nuclear membranous immunofluorescence, thus suggesting that translocation of ANXA1 from the cellular to nuclear membrane might be related to oesophageal oncogenesis. Because of differences in technique (primary anti-ANXA1 monoclonal antibody: Santa Cruz Biotechnology Inc., Santa Cruz, CA, USA, and indirect immunofluorescence versus clone 29, BD Transduction Labs and streptavidin-biotin LSAB+ Dako) or in the specific organ investigated (larynx versus oesophagus), we were not able to confirm such differences in the intracellular pattern of ANXA1 immunoexpression. In fact, we observed differences in membranous ANXA1 expression (data from Table 4) between normal and dysplasia (or metastasis), but not between normal and invasive tumour from the same individual. Otherwise, applying the χ^2 and Fisher's exact tests, nuclear and cytoplasmic expression were

lower and membranous expression higher in primary carcinoma compared with normal tissues (data from Table 3). However, the latter data should be interpreted with caution since the ANXA1 levels in tissue areas and subcellular compartments are interdependent variables.

To explain why membranous ANXA1 expression does not follow the same pattern as nucleus and cytoplasmic expression in our laryngeal samples, a better understanding of the factors influencing annexin expression dysregulation, translocation and exportation would be necessary. Also, it would be important to know if these factors are related to tumour cell characteristics and activated or inhibited by chronic inflammation in tumours, which is nearly always found in HNSCCs. In this respect, discussion of data on the influence of calcium levels and protein phosphorylation on ANX trafficking may be pertinent.

Different annexins are distributed in a diffuse pattern throughout the cytosol or localized to specific regions or structures in the cell at low free calcium levels. After stimulation, each one assumes a distinct position at

cellular membranes.³⁷ Monastyrskaya and collaborators³⁸ have mapped the calcium-induced translocations of annexins in live cells and observed that upon elevation of calcium, ANXA1 becomes associated with intracellular membranes and the nuclear envelope. Because changes in calcium levels regulate signalling events, different annexins may allow a spatially confined, graded response to extra- or intracellular stimuli.³⁷

Solito and collaborators³⁹ have provided molecular, microscopic and pharmacological evidence supporting the view that the trafficking of ANXA1 from the cytoplasm to the cell surface induced by a proinflammatory stimulus is dependent on serine²⁷ phosphorylation of ANX, and both phosphoinositide-3-kinase and mitogen-activated protein kinase are critical to this event. These kinases are activated in response to different stimuli, including growth factors and environmental stresses, and are involved in various responses such as cell death, survival, cell motility and differentiation. In addition, the authors have suggested that both phosphorylation and lipidation may contribute to ANXA1 export outside the cell. Since ANXA1 is related to cell proliferation and differentiation processes, the analysis of post-translation modifications and subcellular expression may help in understanding the role of this protein in normal and pathological conditions.

In summary, translocation of ANX between cellular compartments in normal cells is affected by calcium levels, and is dependent on phosphorylation or induced by glucocorticoids during inflammation.^{1,39-41} In tumour cells, calcium levels and other factors may be impaired and result in abnormal localization of annexins. The explanation for the dysregulation of expression and translocation of annexins in tumours remains to be established and may be cause or effect, linked to inflammation, signal transduction, differentiation, transport or other cell processes.

The importance of the ANX family is emerging and is likely to contribute to our understanding of the link between inflammation, hyperproliferation of epithelial cells and carcinogenesis. Their role in molecular pathways^{2,16,42,43} as well as their clinical implications,⁴⁴ are just beginning to emerge in the literature. However, much information is still lacking and prospective studies, dealing with diagnosis, prognosis and treatment, are needed.

Acknowledgments

The authors acknowledge the financial support from Fundação de Amparo à Pesquisa do Estado de São

Paulo/FAPESP (Grants 02/01511-4, 02/07304-0, 02/01520-3, 02/01503-1, 04/12054-9), and Associação Beneficente Alzira Denise Hertzog Silva/ABADHS, and the researcher fellowships from Conselho Nacional de Pesquisas (CNPq), Coordenação de Aperfeiçoamento de Pessoal de Nível Superior (CAPES), Instituto Israelita de Ensino e Pesquisa Albert Einstein, and The Ludwig Institute for Cancer Research. The authors also acknowledge Dr Maurício Lacerda Nogueira, Professor Egle Solito and Professor José Antonio Cordeiro for their valuable suggestions.

Appendix

The GENCAPO (Head and Neck Genome) Project members are the following: Cury PM³, de Carvalho MB⁷, Dias-Neto E¹, Figueiredo DLA⁸, Fukuyama EE⁵, Góis-Filho JF⁵, Leopoldino AM¹², Mamede RCM⁸, Michaluart-Junior P¹, Moreira-Filho CA¹, Moyses RA¹, Nóbrega FG⁴, Nóbrega MP⁴, Nunes FD⁶, Ojopi EPB¹, Okamoto OK¹¹, Serafini LN⁸, Severino P², Silva AMA⁷, Silva Jr WA⁸, Silveira NJF¹⁰, Souza SCOM⁶, Tajara EH³, Wünsch-Filho V⁹, Zago MA⁸, Amar A⁷, Arap SS¹, Araújo NSS¹, Araújo-Filho V¹, Barbieri RB⁷, Bandeira CM⁴, Bastos AU⁷, Bogossian AP⁴, Braconi MA⁴, Brandão LG¹, Brandão RM⁸, Canto AL⁴, Carmona-Raphe J³, Carvalho-Neto PB⁷, Casemiro AF⁷, Cerione M⁵, Cernea CR¹, Cicco R⁵, Chagas MJ⁴, Chedid H⁷, Chiappini PBO⁷, Correia LA⁷, Costa A⁹, Costa ACW⁷, Cunha BR³, Curioni OA⁷, Dias THG¹, Durazzo M¹, Ferraz AR¹, Figueiredo RO⁹, Fortes CS⁹, Franzi SA⁷, Frizzera APZ³, Gallo J¹, Gazito D⁷, Guimarães PEM¹, Gutierrez AP⁷, Inamine R⁹, Kaneto CM⁸, Lehn CN⁷, López RVM⁹, Macarencio R⁴, Magalhães RP¹, Martins AE⁷, Meneses C⁴, Mercante AMC⁷, Montenegro FLM¹, Pinheiro DG⁸, Polachini GM³, Porsani AF⁷, Rapoport A⁷, Rodini CO⁶, Rodrigues AN⁹, Rodrigues-Lisoni FC³, Rodrigues RV³, Rossi L⁷, Santos ARD⁸, Santos M⁷, Settani F⁵, Silva FAM¹², Silva IT⁸, Silva-Filho GB¹, Smith RB¹, Souza TB⁷, Stabenow E¹, Takamori JT⁷, Tavares MR¹, Turcano R¹, Valentim PJ⁵, Vidotto A³, Volpi EM¹, Xavier FCA⁶, Yamagushi F⁵, Cominato ML⁵, Correa PMS⁴, Mendes GS⁵, Paiva R⁵, Ramos O¹, Silva C¹, Silva MJ⁵, Tarlá MVC⁸.

Affiliations: ¹School of Medicine, USP, São Paulo, ²The Albert Einstein Jewish Teaching and Research Institute (IIEP), São Paulo, ³School of Medicine of São José do Rio Preto, ⁴São José dos Campos Dental School, UNESP, ⁵Cancer Institute Arnaldo Vieira de Carvalho, São Paulo, ⁶School of Dentistry, USP, São Paulo, ⁷Heliópolis Hospital, São Paulo, ⁸School of Medicine of Ribeirão Preto, USP, ⁹School of Public Health, USP, São Paulo, ¹⁰University of Vale do Paraíba, São José dos

Campos, ¹¹School of Medicine, UNIFESP, São Paulo, ¹²Faculty of Pharmaceutical Sciences of Ribeirão Preto, USP, SP, Brazil.

References

- Gerke V, Creutz CE, Moss SE. Annexins: linking Ca²⁺ signalling to membrane dynamics. *Nat. Rev. Mol. Cell Biol.* 2005; **6**: 449–461.
- Gerke V, Moss SE. Annexins: from structure to function. *Physiol. Rev.* 2002; **82**: 331–371.
- Mohiti J, Caswell AM, Walker JH. The nuclear location of annexin V in the human osteosarcoma cell line MG-63 depends on serum factors and tyrosine kinase signaling pathways. *Exp. Cell Res.* 1997; **234**: 98–104.
- Deora AB, Kreitzer G, Jacovina AT, Hajjar KA. An annexin 2 phosphorylation switch mediates p11-dependent translocation of annexin 2 to the cell surface. *J. Biol. Chem.* 2004; **279**: 43411–43418.
- Liu J, Rothermund CA, Ayala-Sanmartin J, Vishwanatha JK. Nuclear annexin II negatively regulates growth of LNCaP cells and substitution of ser 11 and 25 to glu prevents nucleocytoplasmic shuttling of annexin II. *BMC Biochem.* 2003; **4**: 10.
- Morgan RO, Fernandez MP. Expression profile and structural divergence of novel human annexin 31. *FEBS Lett.* 1998; **434**: 300–304.
- Srivastava M, Bubendorf L, Srikantan V et al. ANX7, a candidate tumor suppressor gene for prostate cancer. *Proc. Natl. Acad. Sci. USA* 2001; **98**: 4575–4580.
- Emoto K, Sawada H, Yamada Y et al. Annexin II overexpression is correlated with poor prognosis in human gastric carcinoma. *Anticancer Res.* 2001; **21**: 1339–1345.
- Shi T, Dong F, Liou LS, Duan ZH, Novick AC, DiDonato JA. Differential protein profiling in renal-cell carcinoma. *Mol. Carcinog.* 2004; **40**: 47–61.
- Chang KS, Wang G, Freireich EJ et al. Specific expression of the annexin VIII gene in acute promyelocytic leukemia. *Blood* 1992; **79**: 1802–1810.
- Violette SM, King I, Browning JL, Pepinsky RB, Wallner BP, Sartorelli AC. Role of lipocortin I in the glucocorticoid induction of the terminal differentiation of a human squamous carcinoma. *J. Cell. Physiol.* 1990; **142**: 70–77.
- Alldrige LC, Harris HJ, Plevin R, Hannon R, Bryant CE. The annexin protein lipocortin I regulates the MAPK/ERK pathway. *J. Biol. Chem.* 1999; **274**: 37620–37628.
- Lee CH, Marekov LN, Kim S, Brahim JS, Park MH, Steinert PM. Small proline-rich protein 1 is the major component of the cell envelope of normal human oral keratinocytes. *FEBS Lett.* 2000; **477**: 268–272.
- Perretti M, Gavins FN. Annexin I: an endogenous anti-inflammatory protein. *News Physiol. Sci.* 2003; **18**: 60–64.
- Solito E, Kamal A, Russo-Marie F, Buckingham JC, Marullo S, Perretti M. A novel calcium-dependent proapoptotic effect of annexin I on human neutrophils. *FASEB J.* 2003; **17**: 1544–1546.
- Rodrigues-Lisoni FC, Mehet DK, Peitl P Jr et al. *In vitro* and *in vivo* studies on CCR10 regulation by Annexin A1. *FEBS Lett.* 2006; **580**: 1431–1438.
- Bai XF, Ni XG, Zhao P et al. Overexpression of annexin I in pancreatic cancer and its clinical significance. *World J. Gastroenterol.* 2004; **10**: 1466–1470.
- Falini B, Tiacchi E, Liso A et al. Simple diagnostic assay for hairy cell leukaemia by immunocytochemical detection of annexin A1 (ANXA1). *Lancet* 2004; **363**: 1869–1870.
- Hummerich L, Muller R, Hess J et al. Identification of novel tumour-associated genes differentially expressed in the process of squamous cell cancer development. *Oncogene* 2006; **25**: 111–121.
- Kang JS, Calvo BF, Maygarden SJ, Caskey LS, Mohler JL, Ornstein DK. Dysregulation of annexin I protein expression in high-grade prostatic intraepithelial neoplasia and prostate cancer. *Clin. Cancer Res.* 2002; **8**: 117–123.
- Xia SH, Hu LP, Hu H et al. Three isoforms of annexin I are preferentially expressed in normal esophageal epithelia but down-regulated in esophageal squamous cell carcinomas. *Oncogene* 2002; **21**: 6641–6648.
- Shen D, Nooraie F, Elshimali Y et al. Decreased expression of annexin A1 is correlated with breast cancer development and progression as determined by a tissue microarray analysis. *Hum. Pathol.* 2006; **37**: 1583–1591.
- Garcia Pedrero JM, Fernandez MP, Morgan RO et al. Annexin A1 down-regulation in head and neck cancer is associated with epithelial differentiation status. *Am. J. Pathol.* 2004; **164**: 73–79.
- Koike H, Uzawa K, Nakashima D et al. Identification of differentially expressed proteins in oral squamous cell carcinoma using a global proteomic approach. *Int. J. Oncol.* 2005; **27**: 59–67.
- Rodrigo JP, Garcia-Pedrero JM, Fernandez MP, Morgan RO, Suarez C, Herrero A. Annexin A1 expression in nasopharyngeal carcinoma correlates with squamous differentiation. *Am. J. Rhinol.* 2005; **19**: 483–487.
- Silistino-Souza R, Rodrigues-Lisoni FC, Cury PM et al. Annexin I: differential expression in tumor and mast cells in human larynx cancer. *Int. J. Cancer* 2007; **120**: 2582–2589.
- Pickle LW, Hao Y, Jemal A et al. A new method of estimating United States and state-level cancer incidence counts for the current calendar year. *CA Cancer J. Clin.* 2007; **57**: 30–42.
- Bacchi CEAP, Franco MF. *Manual de Padronização de Laudos Histopatológicos*. São Paulo: Reichmann & Autores, 2005.
- Akritas MGAS, Brunner E. Nonparametric hypotheses and rank statistics for unbalanced factorial designs. *J. Am. Stat. Assoc.* 1997; **92**: 258–265.
- Vishwanatha JK, Swinney R, Banerjee AG. Modulation of annexin I and cyclooxygenase-2 in smokeless tobacco-induced inflammation and oral cancer. *Mol. Cell. Biochem.* 2003; **248**: 67–75.
- Proia NK, Paszkiewicz GM, Nasca MA, Franke GE, Pauly JL. Smoking and smokeless tobacco-associated human buccal cell mutations and their association with oral cancer—a review. *Cancer Epidemiol. Biomarkers Prev.* 2006; **15**: 1061–1077.
- Tripathi A, Dasgupta S, Roy A et al. Sequential deletions in both arms of chromosome 9 are associated with the development of head and neck squamous cell carcinoma in Indian patients. *J. Exp. Clin. Cancer Res.* 2003; **22**: 289–297.
- Brinkman BM, Wong DT. Disease mechanism and biomarkers of oral squamous cell carcinoma. *Curr. Opin. Oncol.* 2006; **18**: 228–233.
- Rescher U, Goebeler V, Wilbers A, Gerke V. Proteolytic cleavage of annexin I by human leukocyte elastase. *Biochim. Biophys. Acta* 2006; **1763**: 1320–1324.
- Sakaguchi M, Murata H, Sonogawa H et al. Truncation of annexin A1 is a regulatory lever for linking epidermal growth factor signaling with cytosolic phospholipase A2 in normal and

- malignant squamous epithelial cells. *J. Biol. Chem.* 2007; **282**; 35679–35686.
36. Liu Y, Wang HX, Lu N *et al.* Translocation of annexin I from cellular membrane to the nuclear membrane in human esophageal squamous cell carcinoma. *World J. Gastroenterol.* 2003; **9**; 645–649.
37. Draeger A, Wray S, Babychuk EB. Domain architecture of the smooth-muscle plasma membrane: regulation by annexins. *Biochem. J.* 2005; **387**; 309–314.
38. Monastyrskaya K, Babychuk EB, Hostettler A, Rescher U, Draeger A. Annexins as intracellular calcium sensors. *Cell Calcium* 2007; **41**; 207–219.
39. Solito E, Christian HC, Festa M *et al.* Post-translational modification plays an essential role in the translocation of annexin A1 from the cytoplasm to the cell surface. *FASEB J.* 2006; **20**; 1498–1500.
40. Rhee HJ, Kim GY, Huh JW, Kim SW, Na DS. Annexin I is a stress protein induced by heat, oxidative stress and a sulfhydryl-reactive agent. *Eur. J. Biochem.* 2000; **267**; 3220–3225.
41. Morand EF, Hall P, Hutchinson P, Yang YH. Regulation of annexin I in rheumatoid synovial cells by glucocorticoids and interleukin-1. *Mediators Inflamm.* 2006; **2006**; 73835.
42. Chetcuti A, Margan SH, Russell P *et al.* Loss of annexin II heavy and light chains in prostate cancer and its precursors. *Cancer Res.* 2001; **61**; 6331–6334.
43. Steeg PS, Palmieri D, Ouatas T, Salerno M. Histidine kinases and histidine phosphorylated proteins in mammalian cell biology, signal transduction and cancer. *Cancer Lett.* 2003; **190**; 1–12.
44. Boersma HH, Kietselaer BL, Stolk LM *et al.* Past, present, and future of annexin A5: from protein discovery to clinical applications. *J. Nucl. Med.* 2005; **46**; 2035–2050.

RESEARCH ARTICLE

Open Access

Genomics and proteomics approaches to the study of cancer-stroma interactions

Flávia C Rodrigues-Lisoni^{1,8}, Paulo Peitl Jr², Alessandra Vidotto¹, Giovana M Polachini¹, José V Maniglia³, Juliana Carmona-Raphe¹, Bianca R Cunha¹, Tiago Henrique¹, Caique F Souza^{1,4}, Rodrigo AP Teixeira², Erica E Fukuyama⁵, Pedro Michaluart Jr⁶, Marcos B de Carvalho⁷, Sonia M Oliani², Head and Neck Genome Project GENCAPO⁹, Eloiza H Tajara^{1,4*}

Abstract

Background: The development and progression of cancer depend on its genetic characteristics as well as on the interactions with its microenvironment. Understanding these interactions may contribute to diagnostic and prognostic evaluations and to the development of new cancer therapies. Aiming to investigate potential mechanisms by which the tumor microenvironment might contribute to a cancer phenotype, we evaluated soluble paracrine factors produced by stromal and neoplastic cells which may influence proliferation and gene and protein expression.

Methods: The study was carried out on the epithelial cancer cell line (Hep-2) and fibroblasts isolated from a primary oral cancer. We combined a conditioned-medium technique with subtraction hybridization approach, quantitative PCR and proteomics, in order to evaluate gene and protein expression influenced by soluble paracrine factors produced by stromal and neoplastic cells.

Results: We observed that conditioned medium from fibroblast cultures (FCM) inhibited proliferation and induced apoptosis in Hep-2 cells. In neoplastic cells, 41 genes and 5 proteins exhibited changes in expression levels in response to FCM and, in fibroblasts, 17 genes and 2 proteins showed down-regulation in response to conditioned medium from Hep-2 cells (HCM). Nine genes were selected and the expression results of 6 down-regulated genes (*ARID4A*, *CALR*, *GNB2L1*, *RNF10*, *SQSTM1*, *USP9X*) were validated by real time PCR.

Conclusions: A significant and common denominator in the results was the potential induction of signaling changes associated with immune or inflammatory response in the absence of a specific protein.

Background

Solid tumors are characterized by the presence of two major components: neoplastic cells and a specialized nonmalignant stroma in which they are immersed and are essential for their survival and proliferation. In carcinomas, a basement membrane is usually present between these components [1,2].

The tumor stroma is distinguished by an enrichment of microvessel density, abundance of endothelial cells and precursors, inflammatory cells including lymphocytes, neutrophils, macrophages, dendritic and mast cells, and a connective tissue with fibroblasts, myofibroblasts and

histiocytes responsible for remodeling and deposition of extracellular matrix (ECM) components - fibronectin, collagens, elastin, and glycosaminoglycans [2-4]. Although these cells are nonmalignant, they have a unique gene expression pattern, compared to stroma cells in normal tissues [5,6].

Substantial evidence indicates that the development and the progression of cancer not only depend on its genetic characteristics but also on interactions with its microenvironment [4,7,8]. In fact, tumor cells may alter the surrounding stroma through direct cell contact or via the secretion of paracrine soluble factors, inducing cell differentiation or extracellular matrix modifications [9]. In its turn, stromal cells may promote cancer progression and acquisition of invasiveness [10-12]. It is

* Correspondence: tajara@famerp.br

¹Department of Molecular Biology, School of Medicine (FAMERP), São José do Rio Preto, Brazil

possible that such interactions contribute to the neoplastic cell phenotype and behavior as observed during the normal development process and function of organs and tissues [13,14]. As Albini and Sporn (2008) appropriately propose, the microenvironment may be more than a partner but also an essential component of the cancer, and both should be considered as a functional whole [15].

In this context, inflammation and infection have gained special attention. Well known examples connecting infection-related or -unrelated chronic inflammation and increased risk for cancer development are described in the literature [16], and probably more than 15% of cancers are linked to these factors [17]. TNF-alpha and NF- κ B transcription factor should play a central role in this process, modulating transcription of genes encoding angiogenic and growth factors, inflammatory cytokines and anti-apoptotic proteins [16]. In fact, many inflammatory mediators may influence cell proliferation and tumor development, as demonstrated by our recent studies on annexin A1 [18-20].

Macrophages represent one of the main inflammatory regulators in tumor stroma and are responsible for proliferation, invasion and immunosuppressive signaling, with the production of angiogenic and growth factors, chemokines, cytokines and matrix metalloproteinases [21]. The key partners of macrophages in this network are fibroblasts, the so-called carcinoma-associated fibroblasts (CAFs), which significantly increase the growth of neoplastic or normal cells [22,23] and can enhance tumor engraftment and metastasis in animal models [24]. Recently, Hawsawi et al. (2008) [25] observed well-defined differences in gene expression and proteomic profiles between activated CAFs and fibroblasts from normal stroma, emphasizing their importance in the cancer process.

Regardless of the fact that they are easily identified by their morphology, specific cellular markers for fibroblasts remain unknown, presumably because of their large diversity [26]. In tumor stroma, fibroblasts present a phenotype similar to those associated with wound healing, with a large and euchromatic nucleus and prominent rough endoplasmic reticulum [27,28]. These signals mediating the transition of normal to reactive fibroblasts are still not completely defined.

Many studies have analyzed the role of fibroblasts in cancer initiation and progression. To address this issue, several approaches have been used, as co-culture of cancer cells and fibroblasts and cultures with conditioned medium, combined or not with *in vivo* experiments. The data have shown that these cells, similar to macrophages, overexpress chemokines, interleukines, growth factors and matrix metalloproteinases, promoting inflammatory responses and facilitating angiogenesis,

cancer-cell invasion and proliferation [29-31]. In head and neck cancer, for example, *in vitro* experiments have suggested that the presence of fibroblasts is essential for invasive features either because cancer cells express higher levels of matrix metalloproteinases in the presence of fibroblasts [32,33] or because cancer-associated fibroblasts themselves synthesize these proteins [34,35].

Much of the answer to the question of tumor-stroma interactions lies in the identity of ligands, receptors and effectors of signaling patterns expressed by stroma and tumor cells. Numerous growth factors, cytokines, chemokines, hormones, enzymes and cells responsible for their expression have been characterized but the cross-signaling between pathways in this complex network is far from solved [7,36]. Adding complexity to the scenario, the chemomechanical environment of the extracellular matrix may also act in concert with signaling pathways and affect the cancer process [37].

An important perspective in the study of tumor stroma is the potential use of the gene expression pattern of their cells for diagnostic or prognostic evaluation and as a target for therapy. Supporting this idea are the results from studies on outcome prediction and molecular marker analysis of the stroma [6,38], drugs targeting inflammatory cells [39] and mediators of angiogenesis [40,41].

In order to investigate potential mechanisms by which the tumor microenvironment might contribute to cancer phenotype, we asked whether soluble paracrine factors produced by stromal and neoplastic cells *in vitro* may influence proliferation, and gene and protein expression. For these purposes, we exploited purified fibroblasts isolated from a primary oral cancer and an epithelial cancer cell line linked by conditioned medium and genomic and proteomic approaches. Both cells were treated with the conditioned medium of each other and submitted to analysis by rapid subtraction hybridization methodology, two-dimensional electrophoresis and mass spectrometry. Based on the results of the rapid subtraction hybridization (RaSH) approach, a comparative quantitative real-time PCR was performed to validate the expression of several genes, focusing on those involved in tumorigenesis and inflammation. The results pointed to the participation of several inflammatory mechanisms that might have biological significance in epithelial tumors.

Methods

Primary tumor samples

For conditioned medium experiments, a primary epidermoid (squamous cell) carcinoma of the retromolar area was obtained from a 49-year-old male patient, prior to radiation and/or chemotherapy. Twenty-four laryngeal and 23 oral tongue squamous cell carcinoma (SCC) samples from patients undergoing tumor resection were

used for gene expression analysis. All carcinoma samples were reviewed by senior pathologists and exhibited the presence of at least 70% tumor cells; the corresponding surgical margins were classified to be free of tumor cells.

The study protocol was approved by the National Committee of Ethics in Research (CONEP 1763/05, 18/05/2005), and informed consent was obtained from all patients enrolled.

Epithelial cancer cell line and primary tumor cell cultures

The Hep-2 cell line, originally established from an epidermoid carcinoma of the larynx (ATCC, Rockville, Maryland, USA), was seeded at a density of 1×10^6 cells/mL per 75 cm² culture flask (Corning, NY, USA) in medium MEM-Earle (Cultilab, Campinas, SP, Brazil), pH 7.5, supplemented with 20% fetal calf serum (Cultilab), 1% non-essential amino acids, 0.1% antibiotic/antimycotic (Invitrogen Corporation, Carlsbad, CA, USA), and cultured at 37°C in a humid atmosphere of 5% CO₂.

A primary carcinoma of retromolar area sample showing epithelium and adjacent connective tissues was rinsed multiple times with 100× antibiotic and antimycotic solutions (Invitrogen) and minced into 2-4 mm fragments. Single-cell suspensions were obtained by digestion at 37°C for 1 hour with 40 mg/mL collagenase type I (Sigma Chemical, St Louis, USA). After centrifugation, the cells were washed with PBS, resuspended in DMEM medium supplemented with 20% fetal calf serum (Cultilab), 2 mM glutamine (Invitrogen), 1% non-essential amino acids (Invitrogen), and 0.1% antibiotic/antimycotic (Invitrogen). The cells were seeded at a density of 1×10^6 cells/mL per 75 cm² culture flasks (Corning) and cultured at 37°C in a humid atmosphere of 5% CO₂. Cell medium was changed at 72 h intervals until the cells became confluent. Since fibroblasts were mixed with the epithelial tumor cells at the time of initial plating, fibroblasts were selected by plating the cells growing in medium supplemented with 20% serum for at least 3 weeks [42-44].

Preparation of conditioned medium

Conditioned medium (CM) was prepared from Hep-2 cell or tumor stromal fibroblast cultures showing 80% confluence. Twenty-four, 48 and 72 hours after medium replacement, the supernatant or conditioned medium (CM24, CM48 and CM72, respectively) from three replicas was aspirated and filtered through a 0.22 μm membrane (Millipore) to remove any cell debris and stored at -80°C. Before using, the CM was diluted 1:1 in complete medium. The dilution 1:1 and CM72 were chosen to maximize the chance of detecting a cell response to soluble factors. Optimization experiments showed that dilutions lower than 1:1 resulted in higher numbers of dead cells.

Hep-2 cell-conditioned medium is referred to as HCM and fibroblast-conditioned medium is referred to as FCM.

Growth curve

Hep-2 cells were seeded at a density of 5×10^4 cells in plastic 6-well plates in two sets of quadruplicates. Twenty-four hours later, when cells had already adhered, Hep-2 cultures were incubated with FCMs. One replica in each set was treated with self-conditioned medium and one replica was treated with complete medium.

Medium was replaced on day 4 and cell morphology was observed every day. After 1, 3, 5 and 7 days, cells were harvested and counted using a Neubauer hemocytometer. The same experiment was repeated twice.

Immunofluorescence analysis

The Hep-2 cell line or tumor stromal fibroblasts were grown in culture chambers (Nunc, Naperville, IL, USA) and, after 3 days, the chambers were carefully removed, and the slides with adherent cells were fixed in 4% paraformaldehyde and 0.5% glutaraldehyde, 0.1 mol/L sodium phosphate buffer, pH 7.4, for 2 hours at 4°C. The slides were washed in the same buffer and incubated with 0.1% albumin bovine and 3% normal serum in PBS (PBSA) to block nonspecific binding. The cells were immunostained with primary mouse monoclonal antibodies (Ab) anti-vimentin (NCL-VIM-V9, Novocastria, Benton Lane, Newcastle, UK) or anti-cytokeratin (M3515, antibodies to all types of cytokeratins; AE1-AE3; Dako, Carpinteria, CA, USA) diluted at 1:200 in 1% PBSA, followed by overnight incubation at 4°C. For negative controls, the cells were incubated with nonimmune mouse serum (1:200 working dilution; Sigma-Aldrich). After repeated washings in 1% PBS, a goat anti-mouse IgG (Fc fragment-specific, Dako, Glostrup, Denmark) antibody conjugated to FITC (1:50; British BioCell International, Cardiff, UK) was added, followed by 1 hour incubation at room temperature. Thus, the cells were washed thoroughly in PBS. Analysis was conducted using an Axioskop 2 light microscope (Zeiss, GR) equipped with a digital camera. Digital images were captured by using software AxioVision (Zeiss, GR).

Immunohistochemical analysis

Apoptosis was assayed using AnxA5 staining as described [45]. Fixed Hep-2 cell line or tumor stromal fibroblast in slides from culture chambers were incubated with the following reagents: 2.1% sodium citrate for 30 min at 96°C; 3% hydrogen peroxide for 15 min; 0.1% Tween 20 (Sigma-Aldrich) diluted in 0.4% PBS for 15 min; non-specific binding sites were blocked with 10% albumin bovine (BSA) diluted in TBS (20 mM Tris

buffer in 0.9% NaCl, pH 8.2) for 30 min. The slides were then incubated overnight with a rabbit polyclonal antibody anti-AnxA5 (sc8300, Santa Cruz Biotechnology, California, USA), diluted 1:200. After repeated washings in 1% PBSA, a goat anti-rabbit IgG (Fc fragment specific) antibody conjugated to 5 nm colloidal gold particles (N24916, Invitrogen) was added. Silver enhancing solution (L24919, Invitrogen) was used to augment gold particle staining. At the end of the reaction, cells were washed thoroughly in distilled water, counterstained with haematoxylin and examined using an Axioskop2 microscope (ZEISS, GR).

RNA extraction for Rapid Subtraction Hybridization (RaSH) and real time PCR experiments

Hep-2 cells and stromal fibroblasts were seeded at a density of 1×10^6 cells/mL per 75 cm² culture flasks in complete medium (controls) and in conditioned medium. Hep-2 cells and fibroblasts were cultured for 5 and 3 days, respectively, and harvested by addition of TRIzol Reagent, following treatment with DNase (Invitrogen). Total RNA from primary tumor samples was also extracted using TRIzol Reagent and treated with DNase. cDNA synthesis was performed using a High Capacity cDNA Archive kit (Applied Biosystems, Foster City, CA, USA) as described by the manufacturer.

RaSH

RaSH technique was performed as described by Jiang et al. (2000) [46]. Aliquots (20 µg) of total RNA from control cells (driver) or treated cells (tester) were used for double-stranded cDNA synthesis using standard protocols [47].

The cDNA was digested with MboI (Invitrogen) at 37°C for 3 h followed by phenol/chloroform extraction and ethanol precipitation. The digested cDNAs were mixed with the adaptors XPDN-14 5'-CTGATCACTC-GAGA and XPDN-12 5'-GATCTCTCGAGT (Sigma Chemical, final concentration 20 µM) in 30 µl of 1× ligation buffer (Gibco BRL), heated at 55°C for 1 min, and cooled down to 14°C within 1 h. After adding 3 µl of T4 DNA ligase (5 U/µl) (Gibco, BRL), ligation was carried out overnight at 14°C. After phenol/chloroform extraction and ethanol/glycogen precipitation, the mixtures were diluted to 100 µl with TE buffer (10 mM Tris/1 mM EDTA); 40 µl of the mixtures were used for PCR amplification.

The PCR mixtures were set up using 10 µM XPDN-18 5'-CTGATCACTCGAGAGATC, 0.4 mM dNTPs, 10 × PCR buffer, 1.5 mM MgCl₂ and 1U Taq DNA polymerase (Invitrogen). Thermocycler conditions were one cycle at 72°C for 5 min, followed by 25 cycles of 94°C for 1 min, 55°C for 1 min, 72°C for 1 min, ending in a final extension at 72°C for 3 min. Ten µg of purified

PCR product (tester) was digested with 20U XhoI (Invitrogen) followed by phenol/chloroform extraction and ethanol precipitation.

One-hundred nanograms of the tester cDNA were mixed with 5 µg of the driver cDNA in hybridization solution (0.5 M NaCl, 50 mM Tris/HCl, SDS2% and 40% formamide) and, after heating at 95°C, incubated at 42°C for 48 h. After extraction and precipitation, the hybridization mixture (1 µg) was ligated with XhoI-digested pZero plasmid and transformed into competent bacteria. Bacterial colonies were picked and used as DNA template for PCR. Clones were sequenced using an automated DNA sequencer and sequence homologies were searched using the BLAST program [48]. Gene ontology (GO) annotation was used for the functional classification of up- and down-regulated genes [49].

Quantitative PCR

For validation experiments, cells were seeded at a density of 1×10^6 cells/mL per 75 cm² culture flasks in two sets of quadruplicates. Twenty-four hours later, when cells had already adhered, Hep-2 culture replicas were treated with FCMs and fibroblast cultures were treated with HCMs. One replica in each set (control) was treated with self-conditioned medium. Hep-2 cells and fibroblasts were harvested after 5 and 3 days, respectively, and RNA was extracted as described above.

Nine differentially expressed genes were selected for validation by quantitative real time PCR experiments according to their direct or indirect involvement in tumorigenesis. Their expression was checked in treated samples relative to matched non-treated samples. One of these genes (*ARID4A*) was also selected for quantitative real time PCR validation in fresh tumor samples of 24 laryngeal SCC and in 23 oral tongue SCC relative to matched normal samples.

The primers were manually designed with: 19-23 bp length, 30-70% GC content and a short amplicon size (90-110 bp). Their sequences are available upon request. Real time PCR was performed in triplicate using a 7500 Fast Real-Time PCR System (Applied Biosystems). Reaction mixture consisted of a 20 µl volume solution containing 10 µl of Power SYBR Green PCR Master Mix (Applied Biosystems), 500 nM of each primer and 100 ng cDNA. The PCR conditions were 95°C for 10 min followed by 40 cycles of 95° for 15 s and 60° for 1 min. Melting curve analysis was performed for each gene to check the specificity and identity of the RT-PCR products.

For each primer set, the efficiency of the PCR reaction (linear equation: $y = \text{slope} + \text{intercept}$) was measured in triplicate on serial dilutions of the same cDNA sample. The PCR efficiency (E) was calculated by the formula $E = [10^{(-1/\text{slope})}]$ and ranged from 1.96 to 2.02 in the different assays.

Three control genes (*GAPDH*, *ACTB* and *TUBA6*) were used as internal standards. The relative expression ratio (fold change) of the target genes was calculated according to Pfaffl (2001) [50]. Statistical analysis was performed by a two-tailed unpaired *t* test using GraphPad prism software.

Proteomic analysis

Hep-2 cells and stromal fibroblasts were seeded at a density of 1×10^6 cells/mL per 75 cm² culture flasks in complete medium and in conditioned medium, as described for RASH experiments. Hep-2 cells and fibroblasts were cultured for 5 and 3 days, respectively, and harvested by centrifugation at 3200 rpm for 5 min at 4°C. Cells were disrupted by sonication, proteins were isolated and two-dimensional electrophoresis (2-DE) was performed, as described by de Marqui et al. (2006) [51]. Briefly, isoelectric focusing was carried out in a IPGphor (GE Healthcare) using 13-cm immobilized pH 3-10 L gradient strips. Vertical 12.5% SDS-PAGE was performed in a SE 600 Ruby electrophoresis unit (GE Healthcare) and proteins were detected by Coomassie Blue staining. Differentially expressed proteins were excised from gel, destained, dried and in-gel tryptic-digested. Negative and positive control digests were performed on gel slices that contained no protein and on slices cut from a band of the molecular weight marker, respectively.

Samples were analyzed using MALDI Q-TOF (Matrix Assisted Laser Desorption Ionization - Quadrupole Ion Filter - Time of Flight) Premier (Waters Corporation, Milford, MA, USA) mass spectrometer (MS/MS). Duplicate or triplicate runs of each sample were made to ensure an accurate analysis.

For protein identification, the resulting MS/MS data were interpreted by MASCOT software (MS/MS Ions Search) [52] and searched against the Mass Spectrometry Protein Sequence Database (MSDB). The UniProtKB/Swiss-Prot [53] database was used for the functional classification of up- and down- expressed proteins.

Data Handling and Statistical Analysis

Quantification of apoptotic cells was performed with a high magnification objective ($\times 40$) counting cells in 100 μm^2 areas and reported as mean \pm SEM per group. Densitometric analysis for the immunofluorescence staining used an arbitrary scale ranging from 0 to 255 units. Statistical differences between groups were determined by analysis of variance followed, if significant, by the Bonferroni test.

Results

Stromal fibroblasts: selection and immunofluorescence analysis

Fetal calf serum concentration and culture time provided a simple method of selecting fibroblasts from a

primary carcinoma of retromolar area. Fibroblast cultures at passage 78 still showed spindle-shaped cells, which displayed the typical fibroblast markers, weak cyokeratin and intense vimentin immunoreactivity in cytoplasm, after immunofluorescence analysis (Figure 1B, E). Staining was obtained with both antibodies (cyto-keratin and vimentin) in Hep-2 cells (Figure 1C, F). No labeling was detected in sections incubated with the control nonimmune mouse serum (Figure 1A, D).

Ultrastructural analysis showed that the stromal fibroblasts present large euchromatic nuclei, more granular endoplasmatic reticulum, mitochondria and nucleoli than normal fibroblasts (data not shown). Therefore, the spontaneously immortalized cell line of fibroblasts retained the characteristics of stromal cells and may correspond to cancer-associated fibroblasts (CAF).

Conditioned medium inhibits proliferation and induces apoptosis

Growth curves of Hep-2 cells treated with FCM showed decreased proliferation (Figure 2). Growth inhibition was observed as early as day 1 and was statistically significant ($P < 0.05$) at day 3 and day 5.

The immunohistochemistry reaction with AnxA5 antibody showed the presence of gold particles on the cytoplasm of the Hep-2 apoptotic cells (Figure 3). The AnxA5 immunoreactivity was found more in the apoptotic process of Hep-2 cells incubated in FCM (56%) than in cells without the treatment (24%). Apoptotic cells displayed distinctive morphology, a notable decrease in the nuclear size, irregular shape and cytoplasmic blebbing.

Genes identified using the RaSH approach

A total of 81 clones from the Hep-2 cell line and fibroblast libraries were sequenced. In the Hep-2 cell line, forty-one genes exhibited changes in expression levels in response to FCM treatment (33 down- and 8 up-regulated) and, in fibroblasts, 17 genes showed down-regulation in response to HCM treatment. These genes are involved in response to stimulus, apoptosis, cell proliferation and differentiation, signal transduction, transcription, translation and transport (Table 1 and 2).

Real-time PCR validation of differentially expressed genes

Nine genes displaying down- (*ARID4A*, *CALR*, *GNB2L1*, *GPNMB*, *RNF10*, *SQSTM1*, *USP9X*) or up-regulation (*DAP3*, *PRDX1*) in Hep-2 cells treated with FCM were selected and the expression data for six down-regulated genes (*ARID4A*, *CALR*, *GNB2L1*, *RNF10*, *SQSTM1*, *USP9X*) were confirmed by real time PCR (Figure 4A). Most results were, therefore, consistent with the RaSH data.

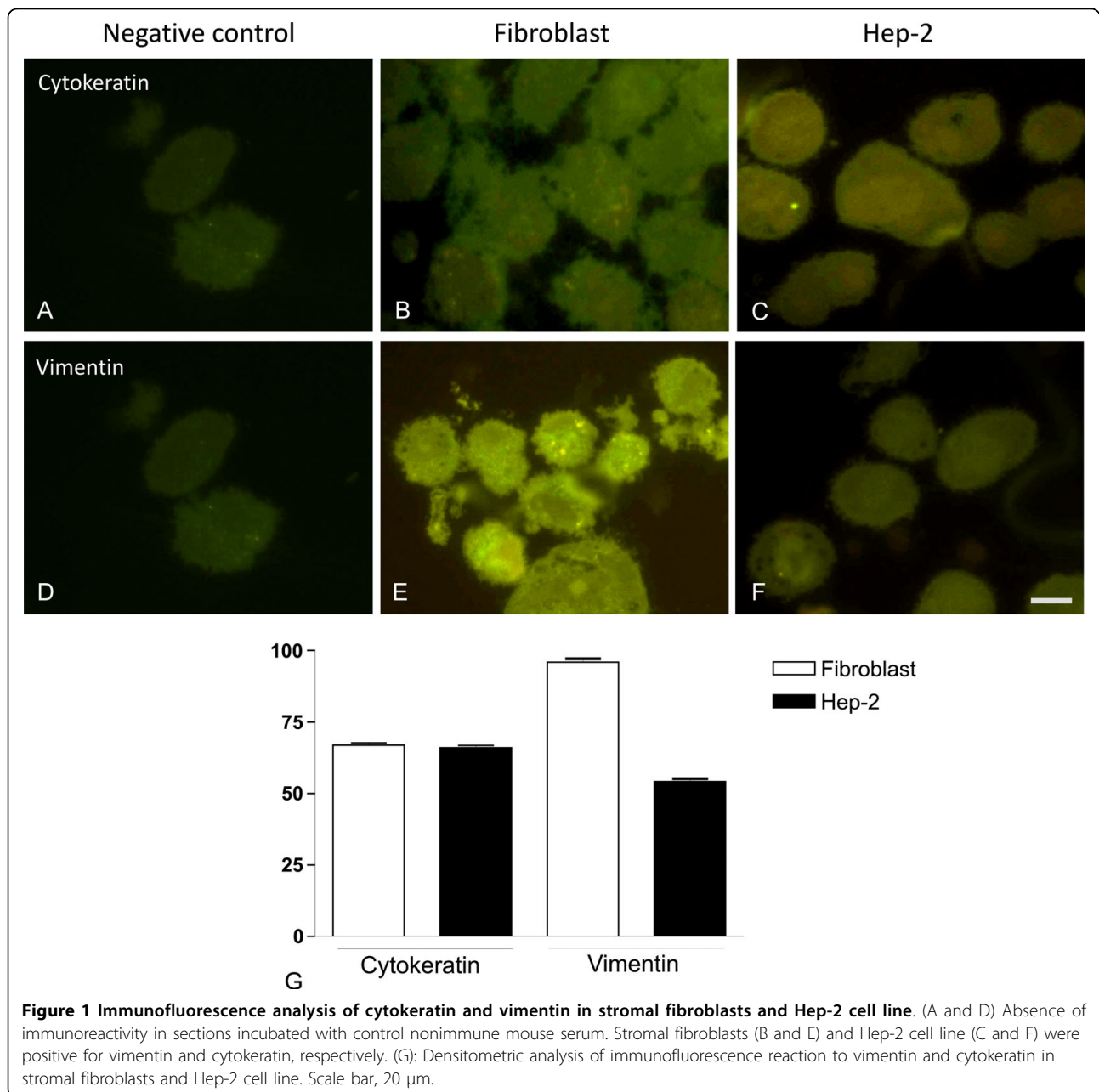


Figure 1 Immunofluorescence analysis of cytokeratin and vimentin in stromal fibroblasts and Hep-2 cell line. (A and D) Absence of immunoreactivity in sections incubated with control nonimmune mouse serum. Stromal fibroblasts (B and E) and Hep-2 cell line (C and F) were positive for vimentin and cytokeratin, respectively. (G): Densitometric analysis of immunofluorescence reaction to vimentin and cytokeratin in stromal fibroblasts and Hep-2 cell line. Scale bar, 20 μm.

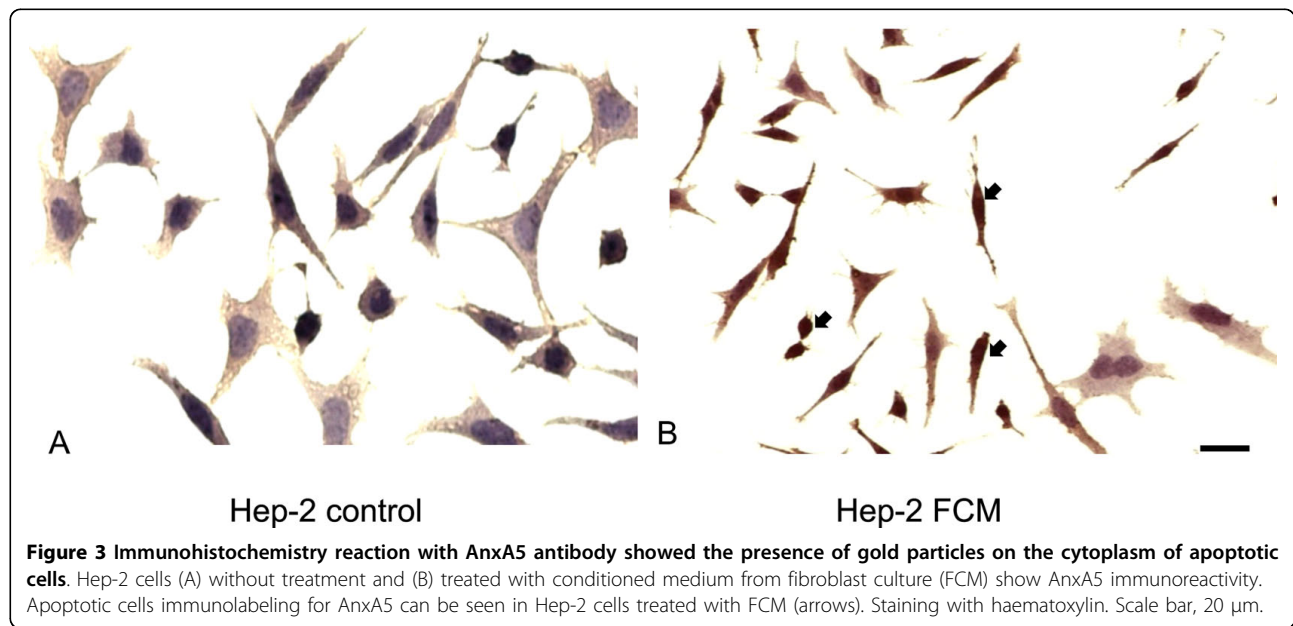
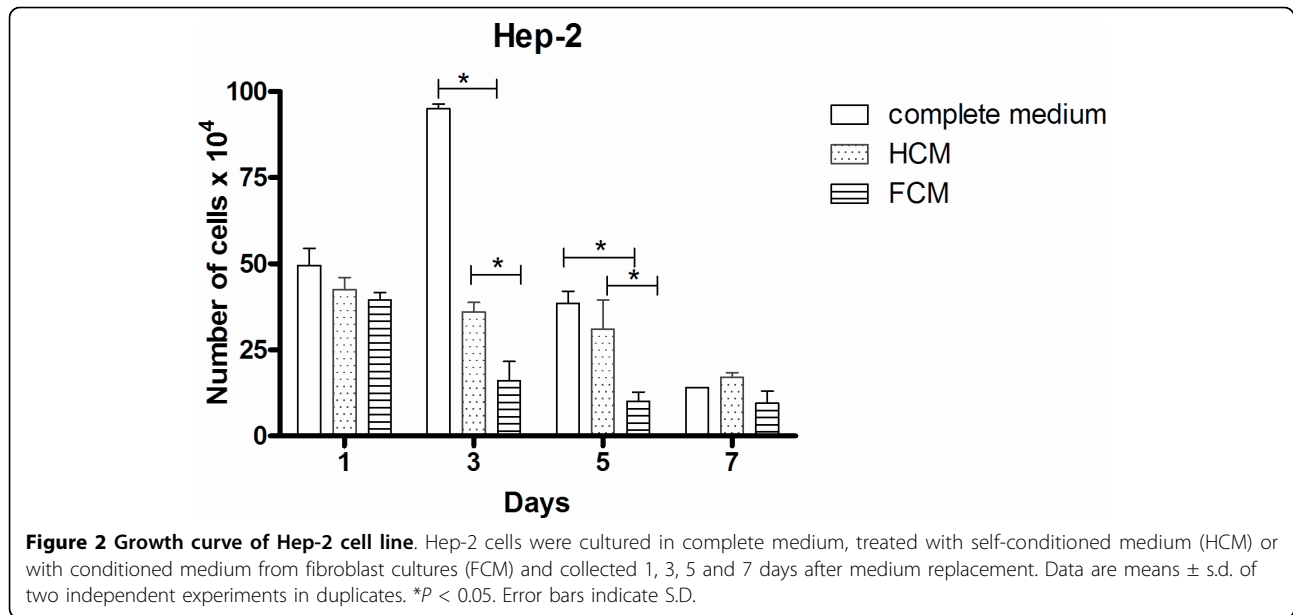
ARID4A expression was also analyzed in 24 pairs of tumor and matched normal tissues from laryngeal squamous cell carcinomas and in 23 pairs of tumor and matched normal tissues from oral tongue squamous cell carcinomas. *ARID4A* mRNA levels were decreased (≥ 2 -fold) in almost half of the squamous cell carcinomas samples (-1.04 to -6.9-fold change, 23 of 47 samples, i.e., 49%) and were increased in some of these samples (1.51 to 6.26-fold change, 7 of 47 samples, i.e., 15%) (Figure 4B). In contrast, no differences in transcript levels were observed between 17 of 47 samples (36%) and normal tissue. Therefore, similarly to the Hep-2 cell line, most

primary head and neck tumors (49%) showed down-regulation of *ARID4A* transcripts.

No differences were observed in respect to clinicopathological features between samples presenting up- and down-regulation of *ARID4A* transcripts (Additional file 1).

Proteomics approach

Comparison between 2-DE patterns from treated cells and controls revealed approximately 80 spots with significant differences in intensity. Seven proteins (Figure 5) showing expression level changes in response



to CM treatment were identified by MALDI-Q-TOF-MS mass spectrometry (Additional file 2). Five proteins (alpha enolase, heterogeneous nuclear ribonucleoprotein C C1/C2, aldolase A, tubulin beta and glyceraldehyde-3-phosphate dehydrogenase) were down-regulated in Hep-2 cell line treated with conditioned medium (FCM72) and two proteins (vimentin and actin) were underexpressed in fibroblasts treated with Hep-2 cell line conditioned medium (HCM72). These proteins are involved in transcription, growth control, response to stimulus, RNA processing, glycolysis, cell motion and membrane trafficking.

Discussion

The molecular crosstalk between neoplastic and the surrounding tissue induces several stromal changes, including neoangiogenesis and immune/inflammatory reaction, as well as new extracellular matrix formation and the activation of fibroblast-like cells, a process known as desmoplasia [54], [55]. Initially, the desmoplastic response was considered a barrier against tumor invasion, but there is growing evidence that desmoplasia is an unfavorable prognostic factor. For example, Sis et al. [56] suggested that desmoplasia is related to increased risks of regional metastases, poorly differentiated

Table 1 Information on biological processes based on Gene ontology

Biological Process	Down-regulated genes
Cell communication	
signal transduction	<i>FAS, SQSTM1, YWHAZ</i>
Transcription	<i>ARID4A, CALR, MYC, PARP1, RNF10, SQSTM1</i>
Translation	<i>AARS, RPLP0, RPS17, RPS23</i>
Apoptosis	<i>CALR</i>
induction	<i>FAS</i>
anti-apoptosis	<i>TPT1, YWHAZ</i>
Cell migration	<i>TMSB4X</i>
Cell cycle	<i>DYNC1H1, MYC, PSMC6</i>
Cell proliferation	
negative regulation	<i>GPNMB, LDOC1</i>
positive regulation	<i>MYC</i>
Developmental process	
epidermis development	<i>UGCG</i>
Response to stimulus	
defense response	
inflammatory response	<i>LTA4H</i>
response to stress	<i>EIF2AK1, SQSTM1</i>
response to oxidative stress	
response to external stimulus	<i>EIF2AK1</i>
Transport	<i>CALR, NDUFA4, SQSTM1</i>
Metabolic process	<i>COX7C, OLA1,</i>
protein metabolic process	<i>PARP1, SQSTM1, USP9X</i>
protein modification process	<i>GRPEL2, HSP90AB1, PPP2R2A, PRPF4B, USP48</i>
lipid metabolic process	<i>LTA4H, UGCG</i>
DNA repair	<i>PARP1</i>
RNA processing	<i>PRPF4B, SF3B1</i>
Cellular homeostasis	<i>CALR, MYC, RPS17</i>
No classification	<i>GNB2L1, RCN1</i>
	Up-regulated genes
Transcription	<i>ENO1</i>
Translation	<i>EIF1, TARS</i>
Apoptosis	<i>RTN3</i>
induction	<i>DAP3</i>
Cell proliferation	<i>PRDX1</i>
negative regulation	<i>ENO1</i>
Developmental process	
organ development	<i>PRDX1</i>
Response to stimulus	
response to stress	<i>EIF1, RTN3</i>
Metabolic process	<i>PRDX1</i>
protein metabolic process	
protein modification process	<i>P4HB</i>
nucleic acid metabolic process	
RNA processing	<i>USP39</i>

Top down- and up-regulated genes selected by RaSH in Hep-2 samples treated with FCM.

Table 2 Information on biological processes based on Gene Ontology

Biological Process	Down-regulated genes
Cell communication	
signal transduction	<i>S100A6, FN1</i>
Transcription	<i>FOSL1</i>
Translation	<i>RPL37A, RPL7, RPL19, RPL27A, RPLP0</i>
Apoptosis	<i>CTSB</i>
anti-apoptosis	<i>TPT1</i>
Cell adhesion	<i>FN1</i>
Cell proliferation	
positive regulation	<i>S100A6, FOSL1</i>
Developmental process	
organ development	
epidermis development	<i>COL1A1</i>
Response to stimulus	
defense response	<i>FOSL1</i>
response to stress	<i>FN1</i>
Transport	<i>ERGIC3, STX4</i>
Metabolic process	
protein metabolic process	<i>CTSB</i>
RNA processing	<i>PRPF3</i>
No classification	<i>CIZ1, POLE4</i>

Top down-regulated genes selected by RaSH in CAF samples treated with HCM.

primary tumors and lymphatic and venous invasion in colorectal carcinoma. Similar results were observed for head and neck squamous cell carcinomas, which show a high risk of neck recurrence in presence of a desmoplastic stromal pattern [57].

In the present study, we investigated the influence of soluble paracrine factors produced *in vitro* by stromal cells derived from an oral carcinoma and by a neoplastic epithelial cell line on proliferation and gene/protein expression. First, we noted that conditioned medium from stromal fibroblast cultures inhibited Hep-2 cell line proliferation and induced apoptosis, suggesting that factors secreted by fibroblasts include proteins that interfere in cell growth and death of neoplastic cells. In addition, using rapid subtraction hybridization and proteomic analysis, we identified gene products generated by stromal and neoplastic cells that may influence proliferation, differentiation and apoptosis, or drive response to stimulus.

Down-regulated genes in neoplastic cells treated with FCM are involved in signal transduction (*FAS, SQSTM1, YWHAZ*), transcription (*ARID4A, CALR, MYC, PARP1, RNF10, SQSTM1*), translation (*AARS, RPLP0, RPS17, RPS23*), apoptosis (*CALR, FAS, TPT1, YWHAZ*), cell migration (*TMSB4X, GNB2L1*), cell cycle and cell proliferation (*DYNC1H1, GPNMB, LDOC1, MYC, PSM*),

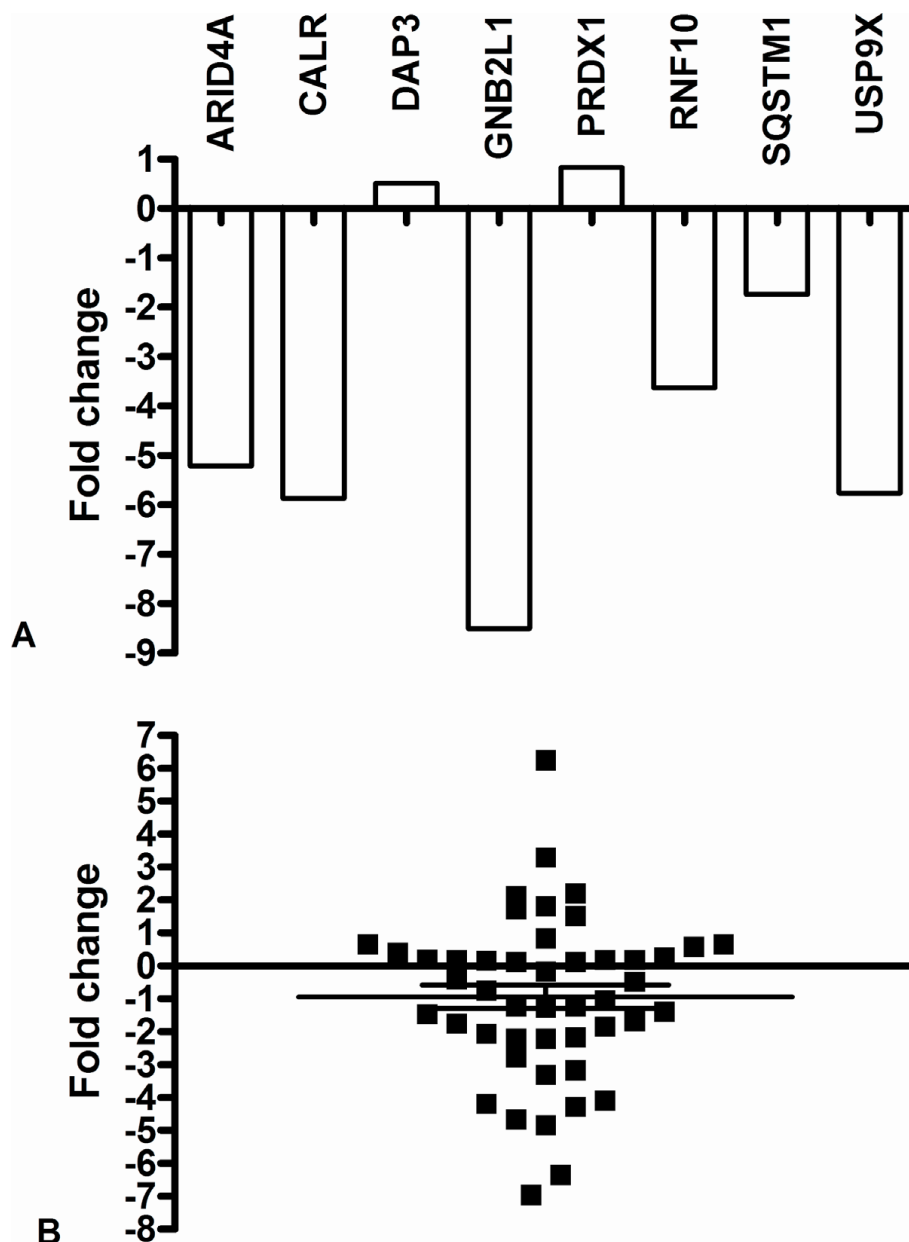


Figure 4 Real-time PCR gene expression in a conditioned medium-treated neoplastic cell line and in primary tumors. (A) Expression of *ARID4A*, *CALR*, *DAP3*, *GNB2L1*, *PRDX1*, *RNF10*, *SQSTM1* and *USP9X* genes in Hep-2 cells treated with conditioned medium from fibroblast cultures. (B). *ARID4A* gene expression in 47 laryngeal and oral tongue carcinomas. Relative quantitation of target gene expression for each sample was calculated according to Pfaffl [50]; *GAPDH* was used as the internal reference and control sample as the calibrator. Values were Log2 transformed (y-axis) so that all values below -1 indicate down-regulation in gene expression while values above 1 represent up-regulation in tumor samples compared to normal samples.

epidermis development (*UGCG*), response to stimulus (*EIF2AK1*, *LTA4H*, *SQSTM1*), transport (*CALR*, *NDUFA4*, *SQSTM1*) and different metabolic processes (*USP9X*). Up-regulated genes are also involved in transcription and translation (*ENO1*, *EIF1*, *TARS*), apoptosis (*DAP3*, *RTN3*), cell proliferation (*PRDX1*, *ENO1*), organ development (*PRDX1*), response to stress (*EIF1*, *RTN3*) and metabolic processes (*PRDX1*, *P4HB*, *USP39*).

In fibroblasts treated with HCM, the biological processes of down-regulated genes include signal transduction (*S100A6*, *FNI*), transcription and translation (*FOSL1*, *RPL37A*, *RPL7*, *RPL19*, *RPL27A*, *RPLP0*), apoptosis (*CTSB*, *TPT1*), cell proliferation (*S100A6*, *FOSL1*), epidermis development (*COL1A1*), response to stimulus (*FNI*, *FOSL1*), transport (*ERGIC3*, *STX4*) and protein and RNA metabolism (*CTSB*, *PRPF3*).

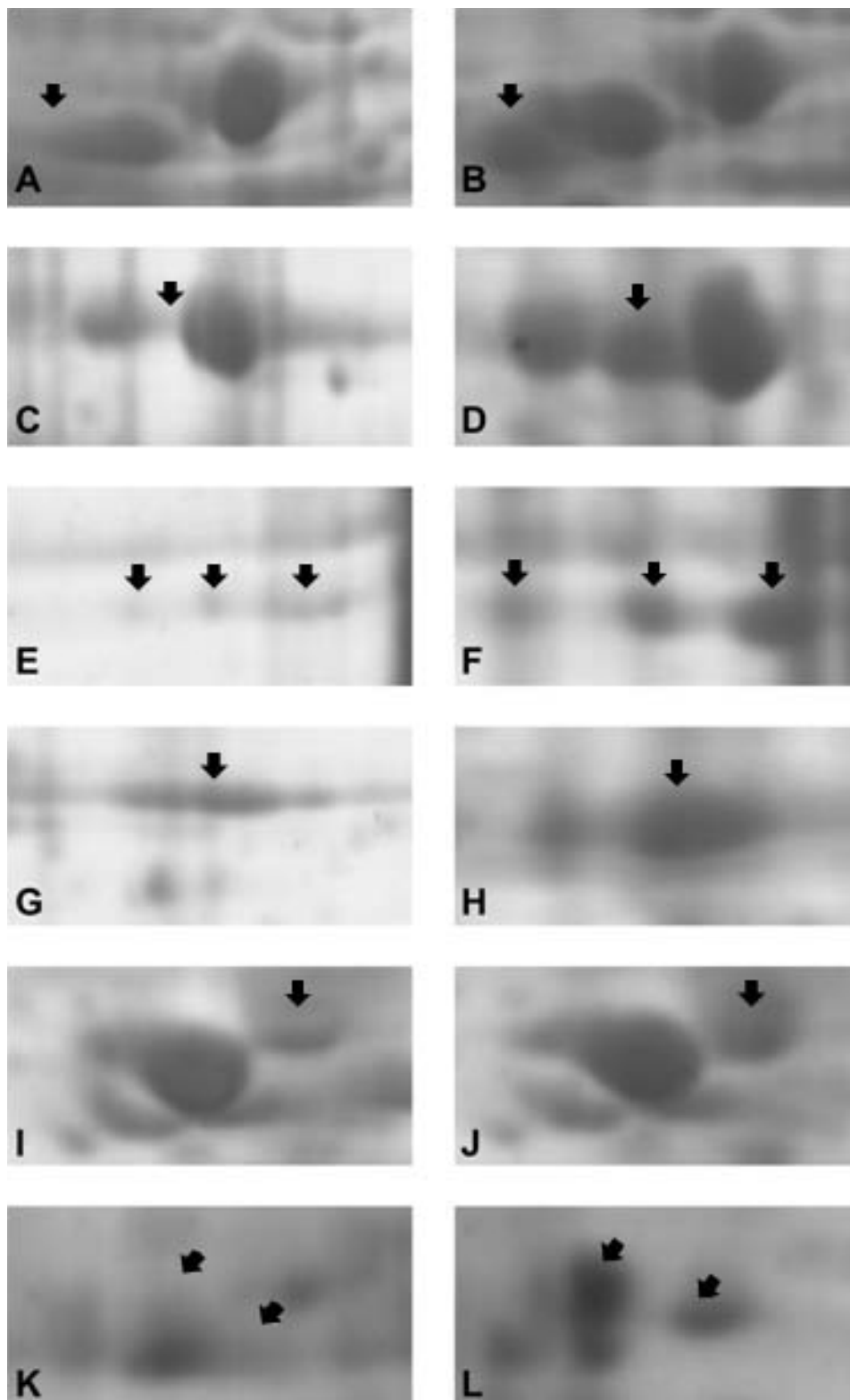


Figure 5 Enlarged 2-DE gels of proteins from conditioned medium-treated Hep-2 cells and stromal fibroblasts. Five proteins (arrows), tubulin beta (A-B), alpha enolase (C-D), aldolase A (E-F), glyceraldehyde-3-phosphate dehydrogenase (G-H) and heterogeneous nuclear ribonucleoprotein C (I-J) were down-regulated in Hep-2 cell line treated with fibroblast conditioned medium (A, C, E, G and I) and two proteins (K-L), vimentin (arrow on left) and actin (arrow on right), were underexpressed in fibroblasts treated with Hep-2 cell line conditioned medium (K).

Two genes exhibited similar patterns in both cells (*RPLP0*, *TPT1*), which may indicate that the transcript levels are affected by soluble paracrine factors produced by either fibroblasts or neoplastic cells or by other *in vitro* conditions. Therefore, they may not be specific to interactions between stroma and tumor.

After literature analysis, nine genes (*ARID4A*, *CALR*, *GNB2L1*, *GPNMB*, *RNF10*, *SQSTM1*, *USP9X*, *PRDX1* and *DAP3*) showing potential involvement in signaling cascades related to tumorigenesis and/or stromal/tumor cell interactions were selected for validation by real-time RT-PCR using treated and non-treated cell lines. For six genes (*ARID4A*, *CALR*, *GNB2L1*, *RNF10*, *SQSTM1*, *USP9X*), the results were consistent with the RASH data. In almost half of the primary tumors analyzed, *ARID4A* transcripts also showed down-regulation, although no correlation with clinicopathological features was detected. These findings in primary tumors should reflect the complex network of a multi-cellular tissue, a situation contrasting with that of a neoplastic cell line cultured in medium conditioned by fibroblasts.

The product of *ARID4A* - AT rich interactive domain 4A (RBP1-like) - also known as *RBP1* or *RBBP1* gene, interacts with the tumor suppressor retinoblastoma (pRB) and histone-modifying complexes, repressing promoters of specific genes [58]. Röhl et al. [59] detected several genes, including *ARID4A*, overexpressed in astrocytes treated with medium conditioned by activated microglia, which protected them against stress conditions. Recently, Wu et al. [60] showed that *Arid4a*-deficient mice exhibit down-regulation of several homeobox genes and of the forkhead box gene *Foxp3*, which codes a transcription factor involved in the development and function of regulatory T cells [61]. These mice also show bone marrow failure with myelofibrosis and higher frequencies of hematologic malignancies, providing evidence that *ARID4A* functions as a tumor suppressor gene and its absence is permissive for the proliferation of connective tissue elements. The study of Perez et al. [62] added data on the role of this gene in cancer. These authors detected increased mRNA levels of *ARID4A* and *RBI* in normal human epidermal keratinocytes treated with arsenic and benzo [a]pyrene *in vitro*. Since these chemicals alter proliferation and inhibit differentiation of keratinocytes [63-65], the findings may indicate that up-regulation of *ARID4A* is negatively related to epithelial differentiation. Therefore, the potential modulation of this gene by paracrine factors produced by stromal fibroblasts may represent an attempt to promote differentiation of neoplastic epithelial cells and, at the same time, their proliferation.

Calreticulin (coded by *CALR* or *CRT* gene) is a calcium-binding protein of the endoplasmic reticulum with intracellular and extracellular functions related to

cellular adhesion, migration, and phagocytosis [66]. Calreticulin can be observed on the surface of stressed cells and, when bound to the plasma membrane of apoptotic cells, drives the phagocytosis by macrophages and dendritic cells [67]. In absence of this protein, the cells are not efficiently removed by phagocytes [68]. Recently, Nanney et al. [69] showed that calreticulin stimulates both migration and proliferation of keratinocytes and fibroblasts and apparently attracts monocytes and macrophages, suggesting its involvement in inflammatory response. Otherwise, fibroblasts underexpressing *CALR* exhibit weak adhesion and spreading [70]. Accordingly, Kypreou et al. [71] detected a correlation between calreticulin up-regulation and progression of fibrosis and also that TGF-beta, a contributing factor in fibrotic processes, up-regulated calreticulin in cultured human epithelial cells. In light of the data, we speculate that the low levels of this protein observed in treated Hep-2 cells inhibit proliferation, or represent a protective response of neoplastic cells to phagocytosis and antitumor immune process.

Guanine nucleotide binding protein (G protein), beta polypeptide 2-like 1 or Rack1 (coded by *GNB2L1* gene) is a cytosolic protein homologous to the beta subunit of G proteins, and contains seven WD repeats, which act as sites for protein-protein interactions. Binding partners of *GNB2L1* include protein kinase C, Src family kinases, components of the ERK pathway, cytokine and interferon receptors, beta integrins and many others. Many of these interactions are consistent with the participation of Rack1 in cell adhesion, movement and growth [72-75].

Sequestosome 1 or ubiquitin-binding protein p62 (coded by *SQSTM1* or *p60* or *p62* gene) is a 62-kDa protein that binds to the Src homology 2 (SH2) domain of p56^{lck} kinase in a phosphotyrosine-independent manner [76]. It has been suggested that p62 is a signaling adaptor which links different signal transduction pathways related to cell proliferation, differentiation and death, including NF- κ B pathway [77-82]. *SQSTM1* abnormal expression has been observed in hepatocellular, prostate and breast cancers [83-85] and is associated with poor outcomes in breast cancer [86].

Another gene down-regulated by fibroblast-conditioned medium is *USP9X* (ubiquitin specific peptidase 9, X-linked), also known as *DDFRX*, *FAF* or *FAM*. This gene is a member of the peptidase C19 family and encodes a protein similar to ubiquitin-specific proteases (USPs). These proteases regulate the production and recycling of ubiquitin and are critically involved in the control of cell growth, differentiation, and apoptosis [87]. Alteration of USPs may play an important role in the pathogenesis of cancer [88] and may exert distinct growth regulatory activities by acting as oncoproteins or

tumor suppressor proteins. Overexpression of certain USPs correlates with progression towards a more malignant phenotype in carcinoma of lung, kidney, breast and prostate [89,90].

RNF10 (ring finger protein 10) is the least known gene selected for validation. The product contains a ring finger motif, which is involved in protein-protein interactions and has been described in proteins implicated in many cellular processes such as signal transduction, transcriptional regulation, ubiquitination, and apoptosis [91,92].

With respect to proteomic analysis, few differences (mostly quantitative) between treated and non-treated cells were detected. Among the proteins differentially expressed, alpha-enolase, heterogeneous nuclear ribonucleoprotein C C1/C2, aldolase A, tubulin beta and glyceraldehyde-3-phosphate dehydrogenase were down-regulated in neoplastic cells treated with FCM and vimentin and actin were down-regulated in fibroblasts treated with HCM. These proteins, produced by neoplastic cells or fibroblasts, may affect tumorigenesis. For example, the glycolytic enzyme alpha-enolase and its enzymatically inactive isoform MBP-1 (*c-myc* promoter binding protein 1) are negative regulators for *MYC* expression [93,94]. *MYC* is one of the most frequently de-regulated oncogenes in cancer [95] and, in the absence of both enzymes, may become activated and accelerate tumor growth. Contrary to RaSH results, alpha enolase protein was observed underexpressed by proteomic analysis in treated Hep-2 cells, which may indicate a nonspecific finding or a post-transcriptional/posttranslational regulation of the RNA/enzyme.

Conclusions

Fibroblasts, as other cells in tumor microenvironments, need to maintain close communication with cancer cells, promoting proliferation, recruitment of inflammatory cells and acquisition of invasive characteristics. Similarly, cancer cells may influence stromal cells to generate a favorable and supportive environment, which would supply them with nutrients and factors necessary for developing the tumor and spreading of metastasis. In the present study, we observed both positive and negative effects exerted by fibroblasts on Hep-2 cells, favoring or not the former. A significant and common denominator in the results was the potential induction of signaling changes associated with immune or inflammatory response in the absence of a specific protein. In fact, *ARID4A* down-regulation is related to low levels of the transcript factor Foxp3 [60], which in turn is linked to immune responsiveness by targeting NF- κ B and CREB pathways [96]. The final effect is the inhibition of the inflammatory response and the cost is a permissive sign for fibroblast proliferation [60]. Down-regulation of

CARL also blocks the inflammatory response but has negative effects on stroma growth [69]. In presence of low levels of Rack1, again a deficient or altered inflammatory response may occur since Rack1 underexpression has already been related to the deregulation of cytokine production [97]. Similar results have been observed in p62-deficient mice, which exhibit abnormal control of NF- κ B activation and reduced inflammation in experimental conditions [98]. The opposite effect is expected for osteoactivin underexpression because this protein has been observed as a negative regulator of macrophage inflammatory responses [99].

The complexity of the tumor microenvironment is immense and much information is still necessary for better understanding how the relationship between stroma and carcinoma cells can be used for diagnostic and prognostic evaluation and a target for therapy.

Additional file 1: Clinicopathological features of 24 patients with larynx SCC and of 23 patients with tongue SCC.

Additional file 2: Underexpressed proteins in Hep-2 cells and fibroblasts treated with conditioned medium from fibroblasts (FCM) and Hep-2 (HCM), respectively.

Acknowledgements

We acknowledge the financial support from Fundação de Amparo à Pesquisa do Estado de São Paulo/FAPESP (Grants 04/12054-9 and 06/60162-0), Rede Proteoma do Estado de São Paulo (Grant FAPESP 04/14846-0/FINEP 01.07.0290.00), The Ludwig Institute for Cancer Research, and the researcher fellowships from FAPESP (FCR-L) and Conselho Nacional de Pesquisas/CNPq (EHT, SMO).

The GENCAPO (Head and Neck Genome) Project authors are the following: Cury PM⁷, de Carvalho MB⁸, Dias-Neto E^{3,14}, Figueiredo DLA⁹, Fukuyama EE⁵, Góis-Filho JF⁵, Leopoldino AM¹⁵, Mamede RCM⁹, Michaluart-Junior P⁶, Moyses RA⁹, Nóbrega FG⁴, Nóbrega MP⁴, Nunes FD¹³, Ojopi EPB³, Serafini LN¹⁰, Severino P¹, Silva AMA⁸, Silva Jr WA¹¹, Silveira NJF¹⁶, Souza SCOM¹³, Tajara EH², Wünsch-Filho V¹², Amar A⁸, Bandeira CM⁴, Braconi MA⁴, Brandão LG⁶, Brandão RM¹¹, Canto AL⁴, Cerione M⁵, Cicco R⁵, Chagas RV⁴, Chedid H⁸, Costa A¹², Cunha BR², Curioni OA⁸, Fortes CS¹², Franzi SA⁸, Frizzera APZ⁷, Gazito D⁸, Guimarães PEM⁶, Kaneto CM¹¹, López RVM¹², Macarenco R⁴, Magalhães MR⁸, Meneses C⁴, Mercante AMC⁸, Pinheiro DG¹¹, Polachini GM², Rapoport A⁸, Rodini CO¹³, Rodrigues-Lisoni FC², Rodrigues RV⁴, Rossi L⁸, Santos ARD¹¹, Santos M⁸, Settani F⁵, Silva FAM¹⁵, Silva IT¹¹, Souza TB⁸, Stabenow E⁶, Takamori JT⁸, Valentim PJ⁵, Vidotto A², Xavier FCA¹³, Yamagushi F⁵, Cominato ML⁵, Correa PMS⁴, Mendes GS⁵, Paiva R⁵, Ramos O⁶, Silva C⁹, Silva MJ⁵, Tarlá MVC¹¹ (also presented in <http://ctc.fmrp.usp.br/clinicalgenomics/cp/group.asp>).

Affiliations: ¹Instituto de Ensino e Pesquisa Albert Einstein, São Paulo; ²Departamento de Biologia Molecular, Faculdade de Medicina de São José do Rio Preto; ³Departamento e Instituto de Psiquiatria, Faculdade de Medicina, Universidade de São Paulo (USP), São Paulo; ⁴Departamento de Biociências e Diagnóstico Bucal, Faculdade de Odontologia, Universidade Estadual Paulista, São José dos Campos, São Paulo; ⁵Serviço de Cirurgia de Cabeça e Pescoço, Instituto do Câncer Arnaldo Vieira de Carvalho, São Paulo; ⁶Departamento de Cirurgia de Cabeça e Pescoço, Faculdade de Medicina, USP, São Paulo; ⁷Departamento de Patologia, Faculdade de Medicina de São José do Rio Preto; ⁸Hospital Heliópolis, São Paulo; ⁹Serviço de Cirurgia de Cabeça e Pescoço, Faculdade de Medicina de Ribeirão Preto, USP; ¹⁰Departamento de Patologia, Faculdade de Medicina de Ribeirão Preto, USP; ¹¹Departamento de Genética, Faculdade de Medicina de Ribeirão Preto, USP; ¹²Departamento de Epidemiologia, Faculdade de Saúde Pública, USP, São Paulo; ¹³Departamento de Estomatologia, Faculdade de Odontologia da

USP, São Paulo; ¹⁴Centro de Pesquisas do Hospital AC Camargo. São Paulo, ¹⁵Departamento de Análises Clínicas, Toxicológicas e Bromatológicas, Faculdade de Ciências Farmacêuticas de Ribeirão Preto, USP; ¹⁶Departamento de Ciências Exatas, Universidade Federal de Alfenas, UNIFAL, MG; Brazil.

Author details

¹Department of Molecular Biology, School of Medicine (FAMERP), São José do Rio Preto, Brazil. ²Department of Biology, Instituto de Biociências, Letras e Ciências Exatas (IBILCE), São Paulo State University (UNESP), São José do Rio Preto, Brazil. ³Department of Otorhinolaryngology and Head and Neck Surgery, School of Medicine (FAMERP), São José do Rio Preto, Brazil. ⁴Department of Genetics and Evolutionary Biology, Institute of Biosciences, University of São Paulo (USP), São Paulo, Brazil. ⁵Department of Head and Neck Surgery, Arnaldo Vieira de Carvalho Hospital, São Paulo, Brazil. ⁶Division of Head and Neck Surgery, Department of Surgery, School of Medicine (USP), São Paulo, Brazil. ⁷Department of Head and Neck Surgery, Heliópolis Hospital, São Paulo, Brazil. ⁸Department of Biology and Zootechny, Faculty of Engineering of Ilha Solteira (UNESP), Ilha Solteira, Brazil. ⁹Author list and addresses presented in the Acknowledgements.

Authors' contributions

FCR-L participated in the design of the study and analysis of the data, carried out cell culture, RaSH experiments and drafted the manuscript. PPJR helped with RaSH experiments. AV and GMP carried out proteomics analysis. JVM was responsible for sample collection and processing. JC-R carried out cloning and sequencing of the samples. BRC carried out cell culture experiments. TH helped with manuscript preparation. CFS performed the real time PCR experiments. RAPT and SMO carried out immunofluorescence and immunohistochemical analysis. EEF and PMJR carried out clinical data analysis for sample selection. MBdC carried out clinical data analysis for sample selection and drafted the manuscript. GENCAPO team members were responsible for sample collection and initial on-site sample processing, provided the pathological analysis of the cases, obtained the informed consent and discussed the findings. EHT participated in the study design and coordination, carried out the analysis and interpretation of the data and drafted the manuscript. All authors read and approved the final manuscript.

Competing interests

The authors declare that they have no competing interests.

Received: 26 June 2009 Accepted: 4 May 2010 Published: 4 May 2010

References

1. Kumar V FN, Abbas A: *Robbins & Cotran: Pathologic Basis of Disease*. Philadelphia: Saunders 2004.
2. Dvorak HF: Tumors: wounds that do not heal. Similarities between tumor stroma generation and wound healing. *N Engl J Med* 1986, **315**(26):1650-1659.
3. Tlsty TD, Hein PW: Know thy neighbor: stromal cells can contribute oncogenic signals. *Curr Opin Genet Dev* 2001, **11**(1):54-59.
4. Li H, Fan X, Houghton J: Tumor microenvironment: the role of the tumor stroma in cancer. *J Cell Biochem* 2007, **101**(4):805-815.
5. Zhao H, Ramos CF, Brooks JD, Peehl DM: Distinctive gene expression of prostatic stromal cells cultured from diseased versus normal tissues. *J Cell Physiol* 2007, **210**(1):111-121.
6. Finak G, Bertos N, Pepin F, Sadokova S, Souleimanova M, Zhao H, Chen H, Omeroglu G, Meterissian S, Omeroglu A, et al: Stromal gene expression predicts clinical outcome in breast cancer. *Nat Med* 2008, **14**(5):518-527.
7. Ao M, Franco OE, Park D, Raman D, Williams K, Hayward SW: Cross-talk between paracrine-acting cytokine and chemokine pathways promotes malignancy in benign human prostatic epithelium. *Cancer Res* 2007, **67**(9):4244-4253.
8. Degen M, Brellier F, Kain R, Ruiz C, Terracciano L, Orend G, Chiquet-Ehrismann R: Tenascin-W is a novel marker for activated tumor stroma in low-grade human breast cancer and influences cell behavior. *Cancer Res* 2007, **67**(19):9169-9179.
9. Micke P, Ostman A: Tumour-stroma interaction: cancer-associated fibroblasts as novel targets in anti-cancer therapy? *Lung Cancer* 2004, **45**(Suppl 2):S163-175.
10. Zalatnai A: Molecular aspects of stromal-parenchymal interactions in malignant neoplasms. *Curr Mol Med* 2006, **6**(6):685-693.
11. Kobayashi R, Deavers M, Patten R, Rice-Stitt T, Halbe J, Gallardo S, Freedman RS: 14-3-3 zeta protein secreted by tumor associated monocytes/macrophages from ascites of epithelial ovarian cancer patients. *Cancer Immunol Immunother* 2009, **58**(2):247-258.
12. Pietras K, Pahler J, Bergers G, Hanahan D: Functions of paracrine PDGF signaling in the proangiogenic tumor stroma revealed by pharmacological targeting. *PLoS Med* 2008, **5**(1):e19.
13. Mueller MM, Fusenig NE: Friends or foes - bipolar effects of the tumour stroma in cancer. *Nat Rev Cancer* 2004, **4**(11):839-849.
14. Quemener C, Gabison EE, Naimi B, Lescaille G, Bougateg F, Podgorniak MP, Labarchede G, Lebbe C, Calvo F, Menashi S, et al: Extracellular matrix metalloproteinase inducer up-regulates the urokinase-type plasminogen activator system promoting tumor cell invasion. *Cancer Res* 2007, **67**(1):9-15.
15. Albini A, Sporn MB: The tumour microenvironment as a target for chemoprevention. *Nat Rev Cancer* 2007, **7**(2):139-147.
16. Maeda S, Omata M: Inflammation and cancer: role of nuclear factor-kappaB activation. *Cancer Sci* 2008, **99**(5):836-842.
17. Kuper H, Adami HO, Trichopoulos D: Infections as a major preventable cause of human cancer. *J Intern Med* 2000, **248**(3):171-183.
18. Rodrigues-Lisoni FC, Mehet DK, Peitl P Jr, John CD, da Silva Junior WA, Tajara E, Buckingham JC, Solitto E: In vitro and in vivo studies on CCR10 regulation by Annexin A1. *FEBS Lett* 2006, **580**(5):1431-1438.
19. Silitino-Souza R, Rodrigues-Lisoni FC, Cury PM, Maniglia JV, Raposo LS, Tajara EH, Christian HC, Oliani SM: Annexin 1: differential expression in tumor and mast cells in human larynx cancer. *Int J Cancer* 2007, **120**(12):2582-2589.
20. Alves VA, Nonogaki S, Cury PM, Wunsch-Filho V, de Carvalho MB, Michaluart-Junior P, Moyses RA, Curioni OA, Figueiredo DL, Scapulatempo-Neto C, et al: Annexin A1 subcellular expression in laryngeal squamous cell carcinoma. *Histopathology* 2008, **53**(6):715-727.
21. Allavena P, Garlanda C, Borrello MG, Sica A, Mantovani A: Pathways connecting inflammation and cancer. *Curr Opin Genet Dev* 2008, **18**(1):3-10.
22. Olumi AF, Grossfeld GD, Hayward SW, Carroll PR, Tlsty TD, Cunha GR: Carcinoma-associated fibroblasts direct tumor progression of initiated human prostatic epithelium. *Cancer Res* 1999, **59**(19):5002-5011.
23. Orimo A, Weinberg RA: Stromal fibroblasts in cancer: a novel tumor-promoting cell type. *Cell Cycle* 2006, **5**(15):1597-1601.
24. Elenbaas B, Weinberg RA: Heterotypic signaling between epithelial tumor cells and fibroblasts in carcinoma formation. *Exp Cell Res* 2001, **264**(1):169-184.
25. Hawsawi NM, Ghebeh H, Hendrayani SF, Tulbah A, Al-Eid M, Al-Tweigeri T, Ajarim D, Alaiya A, Dermime S, Aboussekhra A: Breast carcinoma-associated fibroblasts and their counterparts display neoplastic-specific changes. *Cancer Res* 2008, **68**(8):2717-2725.
26. Chang HY, Chi JT, Dudoit S, Bondre C, Rijn van de M, Botstein D, Brown PO: Diversity, topographic differentiation, and positional memory in human fibroblasts. *Proc Natl Acad Sci USA* 2002, **99**(20):12877-12882.
27. Kalluri R, Zeisberg M: Fibroblasts in cancer. *Nat Rev Cancer* 2006, **6**(5):392-401.
28. Eyden B: The myofibroblast: phenotypic characterization as a prerequisite to understanding its functions in translational medicine. *J Cell Mol Med* 2008, **12**(1):22-37.
29. Fukumura D, Xavier R, Sugiura T, Chen Y, Park EC, Lu N, Selig M, Nielsen G, Taksir T, Jain RK, et al: Tumor induction of VEGF promoter activity in stromal cells. *Cell* 1998, **94**(6):715-725.
30. Sternlicht MD, Lochter A, Sympon CJ, Huey B, Rougier JP, Gray JW, Pinkel D, Bissell MJ, Werb Z: The stromal proteinase MMP3/stromelysin-1 promotes mammary carcinogenesis. *Cell* 1999, **98**(2):137-146.
31. Mueller L, Goumas FA, Affeldt M, Sandtner S, Gehling UM, Brilloff S, Walter J, Karnatz N, Lamszus K, Rogiers X, et al: Stromal fibroblasts in colorectal liver metastases originate from resident fibroblasts and generate an inflammatory microenvironment. *Am J Pathol* 2007, **171**(5):1608-1618.
32. Bair EL, Massey CP, Tran NL, Borchers AH, Heimark RL, Cress AE, Bowden GT: Integrin- and cadherin-mediated induction of the matrix metalloproteinase matrilysin in cocultures of malignant oral squamous cell carcinoma cells and dermal fibroblasts. *Exp Cell Res* 2001, **270**(2):259-267.

33. Ikebe T, Nakayama H, Shinohara M, Shirasuna K: **NF-kappaB involvement in tumor-stroma interaction of squamous cell carcinoma.** *Oral Oncol* 2004, **40**(10):1048-1056.
34. Che ZM, Jung TH, Choi JH, Yoon do J, Jeong HJ, Lee EJ, Kim J: **Collagen-based co-culture for invasive study on cancer cells-fibroblasts interaction.** *Biochem Biophys Res Commun* 2006, **346**(1):268-275.
35. Zhang W, Matrisian LM, Holmbeck K, Vick CC, Rosenthal EL: **Fibroblast-derived MT1-MMP promotes tumor progression in vitro and in vivo.** *BMC Cancer* 2006, **6**:52.
36. Kenny PA, Lee GY, Bissell MJ: **Targeting the tumor microenvironment.** *Front Biosci* 2007, **12**:3468-3474.
37. Suresh S: **Biomechanics and biophysics of cancer cells.** *Acta Biomater* 2007, **3**(4):413-438.
38. Halsted KC, Bowen KB, Bond L, Luman SE, Jorczyk CL, Fyffe WE, Kronz JD, Oxford JT: **Collagen alpha1(XI) in normal and malignant breast tissue.** *Mod Pathol* 2008, **21**(10):1246-1254.
39. Gough MJ, Ruby CE, Redmond WL, Dhungel B, Brown A, Weinberg AD: **OX40 agonist therapy enhances CD8 infiltration and decreases immune suppression in the tumor.** *Cancer Res* 2008, **68**(13):5206-5215.
40. Schneider BP, Sledge GW Jr: **Drug insight: VEGF as a therapeutic target for breast cancer.** *Nat Clin Pract Oncol* 2007, **4**(3):181-189.
41. Gettinger S: **Targeted therapy in advanced non-small-cell lung cancer.** *Semin Respir Crit Care Med* 2008, **29**(3):291-301.
42. Aidinis V, Carninci P, Armaka M, Witke W, Harokopos V, Pavelka N, Koczan D, Argyropoulos C, Thwin MM, Moller S, et al: **Cytoskeletal rearrangements in synovial fibroblasts as a novel pathophysiological determinant of modeled rheumatoid arthritis.** *PLoS Genet* 2005, **1**(4):e48.
43. Chen TR, Shaw MW: **Stable chromosome changes in human malignant melanoma.** *Cancer Res* 1973, **33**(9):2042-2047.
44. Miyamoto M, Sugawa H, Mori T, Hase K, Kuma K, Imura H: **Epidermal growth factor receptors on cultured neoplastic human thyroid cells and effects of epidermal growth factor and thyroid-stimulating hormone on their growth.** *Cancer Res* 1988, **48**(13):3652-3656.
45. Solito E, Kamal A, Russo-Marie F, Buckingham JC, Marullo S, Perretti M: **A novel calcium-dependent proapoptotic effect of annexin 1 on human neutrophils.** *FASEB J* 2003, **17**(11):1544-1546.
46. Jiang H, Kang DC, Alexandre D, Fisher PB: **RaSH, a rapid subtraction hybridization approach for identifying and cloning differentially expressed genes.** *Proc Natl Acad Sci USA* 2000, **97**(23):12684-12689.
47. Sambrook J, Russel DW: *Molecular Cloning: a laboratory manual* Cold Spring Harbor, N.Y.: Cold Spring Harbor Laboratory Press, 3 2001.
48. BLAST. [<http://www.ncbi.nlm.nih.gov/BLAST/>].
49. GeneOntology. [<http://www.geneontology.org>].
50. Pfaffl MW: **A new mathematical model for relative quantification in real-time RT-PCR.** *Nucleic Acids Res* 2001, **29**(9):e45.
51. de Marqui AB, Vidotto A, Polachini GM, Bellato Cde M, Cabral H, Leopoldino AM, de Gois Filho JF, Fukuyama EE, Settanni FA, Cury PM, et al: **Solubilization of proteins from human lymph node tissue and two-dimensional gel storage.** *J Biochem Mol Biol* 2006, **39**(2):216-222.
52. MASCOT. [http://www.matrixscience.com/cgi/search_form.pl?FORMVER=2&SEARCH=MIS].
53. UniProtKB/Swiss-Prot. [<http://ca.expasy.org/sprot/>].
54. Ohtani H: **Pathophysiologic significance of host reactions in human cancer tissue: desmoplasia and tumor immunity.** *Tohoku J Exp Med* 1999, **187**(3):193-202.
55. De Wever O, Mareel M: **Role of tissue stroma in cancer cell invasion.** *J Pathol* 2003, **200**(4):429-447.
56. Sis B, Sarioglu S, Sokmen S, Sakar M, Kupelioglu A, Fuzun M: **Desmoplasia measured by computer assisted image analysis: an independent prognostic marker in colorectal carcinoma.** *J Clin Pathol* 2005, **58**(1):32-38.
57. Olsen KD, Caruso M, Foote RL, Stanley RJ, Lewis JE, Buskirk SJ, Frassica DA, DeSanto LW, O'Fallon WM, Hoverman VR: **Primary head and neck cancer. Histopathologic predictors of recurrence after neck dissection in patients with lymph node involvement.** *Arch Otolaryngol Head Neck Surg* 1994, **120**(12):1370-1374.
58. Hurst DR, Xie Y, Vaidya KS, Mehta A, Moore BP, Accavitti-Loper MA, Samant RS, Saxena R, Silveira AC, Welch DR: **Alterations of BRMS1-ARID4A interaction modify gene expression but still suppress metastasis in human breast cancer cells.** *J Biol Chem* 2008, **283**(12):7438-7444.
59. Rohl C, Armbrust E, Kolbe K, Lucius R, Maser E, Venz S, Gulden M: **Activated microglia modulate astroglial enzymes involved in oxidative and inflammatory stress and increase the resistance of astrocytes to oxidative stress in Vitro.** *Glia* 2008, **56**(10):1114-1126.
60. Wu MY, Eldin KW, Beaudet AL: **Identification of chromatin remodeling genes Arid4a and Arid4b as leukemia suppressor genes.** *J Natl Cancer Inst* 2008, **100**(17):1247-1259.
61. Zheng Y, Rudensky AY: **Foxp3 in control of the regulatory T cell lineage.** *Nat Immunol* 2007, **8**(5):457-462.
62. Perez DS, Handa RJ, Yang RS, Campain JA: **Gene expression changes associated with altered growth and differentiation in benzo[a]pyrene or arsenic exposed normal human epidermal keratinocytes.** *J Appl Toxicol* 2008, **28**(4):491-508.
63. Perez DS, Armstrong-Lea L, Fox MH, Yang RS, Campain JA: **Arsenic and benzo[a]pyrene differentially alter the capacity for differentiation and growth properties of primary human epidermal keratinocytes.** *Toxicol Sci* 2003, **76**(2):280-290.
64. Reznikova TV, Phillips MA, Rice RH: **Arsenite suppresses Notch1 signaling in human keratinocytes.** *J Invest Dermatol* 2009, **129**(1):155-161.
65. Tse WP, Cheng CH, Che CT, Lin ZX: **Arsenic trioxide, arsenic pentoxide, and arsenic iodide inhibit human keratinocyte proliferation through the induction of apoptosis.** *J Pharmacol Exp Ther* 2008, **326**(2):388-394.
66. Johnson S, Michalak M, Opas M, Eggleton P: **The ins and outs of calreticulin: from the ER lumen to the extracellular space.** *Trends Cell Biol* 2001, **11**(3):122-129.
67. Obeid M, Tesniere A, Ghiringhelli F, Fimia GM, Apetoh L, Perfettini JL, Castedo M, Mignot G, Panaretakis T, Casares N, et al: **Calreticulin exposure dictates the immunogenicity of cancer cell death.** *Nat Med* 2007, **13**(1):54-61.
68. Gardai SJ, Bratton DL, Ogden CA, Henson PM: **Recognition ligands on apoptotic cells: a perspective.** *J Leukoc Biol* 2006, **79**(5):896-903.
69. Nanney LB, Woodrell CD, Greives MR, Cardwell NL, Pollins AC, Bancroft TA, Chesser A, Michalak M, Rahman M, Siebert JW, et al: **Calreticulin enhances porcine wound repair by diverse biological effects.** *Am J Pathol* 2008, **173**(3):610-630.
70. Szabo E, Papp S, Opas M: **Differential calreticulin expression affects focal contacts via the calmodulin/CaMK II pathway.** *J Cell Physiol* 2007, **213**(1):269-277.
71. Kypreou KP, Kavvas P, Karamessinis P, Peroulis M, Alberti A, Sideras P, Psarras S, Capetanaki Y, Politis PK, Charonis AS: **Altered expression of calreticulin during the development of fibrosis.** *Proteomics* 2008, **8**(12):2407-2419.
72. Vomastek T, Iwanicki MP, Schaeffer HJ, Tarcsfalvi A, Parsons JT, Weber MJ: **RACK1 targets the extracellular signal-regulated kinase/mitogen-activated protein kinase pathway to link integrin engagement with focal adhesion disassembly and cell motility.** *Mol Cell Biol* 2007, **27**(23):8296-8305.
73. McCahill A, Warwicker J, Bolger GB, Houslay MD, Yarwood SJ: **The RACK1 scaffold protein: a dynamic cog in cell response mechanisms.** *Mol Pharmacol* 2002, **62**(6):1261-1273.
74. Doan AT, Huttenlocher A: **RACK1 regulates Src activity and modulates paxillin dynamics during cell migration.** *Exp Cell Res* 2007, **313**(12):2667-2679.
75. Mamidipudi V, Dhillon NK, Parman T, Miller LD, Lee KC, Cartwright CA: **RACK1 inhibits colonic cell growth by regulating Src activity at cell cycle checkpoints.** *Oncogene* 2007, **26**(20):2914-2924.
76. Joung I, Strominger JL, Shin J: **Molecular cloning of a phosphotyrosine-independent ligand of the p56lck SH2 domain.** *Proc Natl Acad Sci USA* 1996, **93**(12):5991-5995.
77. Duran A, Linares JF, Galvez AS, Wikenheiser K, Flores JM, Diaz-Meco MT, Moscat J: **The signaling adaptor p62 is an important NF-kappaB mediator in tumorigenesis.** *Cancer Cell* 2008, **13**(4):343-354.
78. Sanz L, Sanchez P, Lallena MJ, Diaz-Meco MT, Moscat J: **The interaction of p62 with RIP links the atypical PKCs to NF-kappaB activation.** *EMBO J* 1999, **18**(11):3044-3053.
79. Sanz L, Diaz-Meco MT, Nakano H, Moscat J: **The atypical PKC-interacting protein p62 channels NF-kappaB activation by the IL-1-TRAF6 pathway.** *EMBO J* 2000, **19**(7):1576-1586.
80. Wooten MW, Seibenhener ML, Mamidipudi V, Diaz-Meco MT, Barker PA, Moscat J: **The atypical protein kinase C-interacting protein p62 is a scaffold for NF-kappaB activation by nerve growth factor.** *J Biol Chem* 2001, **276**(11):7709-7712.

81. Mamidipudi V, Li X, Wooten MW: **Identification of interleukin 1 receptor-associated kinase as a conserved component in the p75-neurotrophin receptor activation of nuclear factor-kappa B.** *J Biol Chem* 2002, **277**(31):28010-28018.
82. Chang S, Kim JH, Shin J: **p62 forms a ternary complex with PKCzeta and PAR-4 and antagonizes PAR-4-induced PKCzeta inhibition.** *FEBS Lett* 2002, **510**(1-2):57-61.
83. Stumptner C, Heid H, Fuchsichler A, Hauser H, Mischinger HJ, Zatlouk K, Denk H: **Analysis of intracytoplasmic hyaline bodies in a hepatocellular carcinoma. Demonstration of p62 as major constituent.** *Am J Pathol* 1999, **154**(6):1701-1710.
84. Thompson HG, Harris JW, Wold BJ, Lin F, Brody JP: **p62 overexpression in breast tumors and regulation by prostate-derived Ets factor in breast cancer cells.** *Oncogene* 2003, **22**(15):2322-2333.
85. Kitamura H, Torigoe T, Asanuma H, Hisasue SI, Suzuki K, Tsukamoto T, Satoh M, Sato N: **Cytosolic overexpression of p62 sequestosome 1 in neoplastic prostate tissue.** *Histopathology* 2006, **48**(2):157-161.
86. Rolland P, Madjd Z, Durrant L, Ellis IO, Layfield R, Spendllove I: **The ubiquitin-binding protein p62 is expressed in breast cancers showing features of aggressive disease.** *Endocr Relat Cancer* 2007, **14**(1):73-80.
87. Rolen U, Kobzeva V, Gasparjan N, Ovaa H, Winberg G, Kisseljov F, Masucci MG: **Activity profiling of deubiquitinating enzymes in cervical carcinoma biopsies and cell lines.** *Mol Carcinog* 2006, **45**(4):260-269.
88. Dees EC, Orłowski RZ: **Targeting the ubiquitin-proteasome pathway in breast cancer therapy.** *Future Oncol* 2006, **2**(1):121-135.
89. Ovaa H, Kessler BM, Rolen U, Galardy PJ, Ploegh HL, Masucci MG: **Activity-based ubiquitin-specific protease (USP) profiling of virus-infected and malignant human cells.** *Proc Natl Acad Sci USA* 2004, **101**(8):2253-2258.
90. Deng S, Zhou H, Xiong R, Lu Y, Yan D, Xing T, Dong L, Tang E, Yang H: **Over-expression of genes and proteins of ubiquitin specific peptidases (USPs) and proteasome subunits (PSs) in breast cancer tissue observed by the methods of RFDD-PCR and proteomics.** *Breast Cancer Res Treat* 2007, **104**(1):21-30.
91. Borden KL: **RING domains: master builders of molecular scaffolds?** *J Mol Biol* 2000, **295**(5):1103-1112.
92. Freemont PS: **RING for destruction?** *Curr Biol* 2000, **10**(2):R84-87.
93. Spencer CA, Groudine M: **Control of c-myc regulation in normal and neoplastic cells.** *Adv Cancer Res* 1991, **56**:1-48.
94. Subramanian A, Miller DM: **Structural analysis of alpha-enolase. Mapping the functional domains involved in down-regulation of the c-myc protooncogene.** *J Biol Chem* 2000, **275**(8):5958-5965.
95. Prochownik EV: **c-Myc: linking transformation and genomic instability.** *Curr Mol Med* 2008, **8**(6):446-458.
96. Grant C, Oh U, Fugo K, Takenouchi N, Griffith C, Yao K, Newhook TE, Ratner L, Jacobson S: **Foxp3 represses retroviral transcription by targeting both NF-kappaB and CREB pathways.** *PLoS Pathog* 2006, **2**(4):e33.
97. Racchi M, Sinforiani E, Govoni S, Marinovich M, Galli CL, Corsini E: **RACK-1 expression and cytokine production in leukocytes obtained from AD patients.** *Aging Clin Exp Res* 2006, **18**(2):153-157.
98. Moscat J, Diaz-Meco MT, Wooten MW: **Signal integration and diversification through the p62 scaffold protein.** *Trends Biochem Sci* 2007, **32**(2):95-100.
99. Ripoll VM, Irvine KM, Ravasi T, Sweet MJ, Hume DA: **Gpnmb is induced in macrophages by IFN-gamma and lipopolysaccharide and acts as a feedback regulator of proinflammatory responses.** *J Immunol* 2007, **178**(10):6557-6566.

Pre-publication history

The pre-publication history for this paper can be accessed here:
<http://www.biomedcentral.com/1755-8794/3/14/prepub>

doi:10.1186/1755-8794-3-14

Cite this article as: Rodrigues-Lisoni et al.: Genomics and proteomics approaches to the study of cancer-stroma interactions. *BMC Medical Genomics* 2010 **3**:14.

Submit your next manuscript to BioMed Central and take full advantage of:

- Convenient online submission
- Thorough peer review
- No space constraints or color figure charges
- Immediate publication on acceptance
- Inclusion in PubMed, CAS, Scopus and Google Scholar
- Research which is freely available for redistribution

Submit your manuscript at
www.biomedcentral.com/submit



Protein profiles of polar TNM groups in oral carcinomas: non-aggressive large tumors and their small aggressive opponents

Giovana Mussi Polachini¹, Ana Maria da Cunha Mercante², Andréia Machado Leopoldino³, Tiago Henrique¹, Alessandra Vidotto¹, Andréia Cristina Kazue Kuramoto⁴, Edecio Cunha Neto^{4,5,6}, Jorge Kalil^{4,5,6}, Erica Erina Fukuyama⁷, José Francisco de Góis Filho⁷, Patrícia Maluf Cury⁸, Marcos Brasilino de Carvalho⁹, Fabio Daumas Nunes¹⁰, Pedro Michaluart Junior¹¹, Victor Wünsch Filho¹², Head and Neck Genome Project GENCAPO¹³, Adriana Madeira Alvares da Silva⁹ and Eloiza Helena Tajara^{1,14*}

¹Departments of Molecular Biology and ⁸Pathology, School of Medicine (FAMERP), São José do Rio Preto, SP, Brazil

²Laboratories of Pathologic Anatomy and ⁹Molecular Biology, Heliópolis Hospital, São Paulo, SP, Brazil

³Department of Clinical Analysis, Toxicology, Bromatology, Faculty of Pharmaceutical Sciences, University of São Paulo (USP), Ribeirão Preto, SP, Brazil

⁴Laboratory of Immunology, Heart Institute, University of São Paulo, São Paulo, SP, Brazil

⁵Division of Clinical Immunology and Allergy, Department of Medicine, School of Medicine, University of São Paulo, São Paulo, SP, Brazil

⁶Institute of Investigation in Immunology, São Paulo, SP, Brazil

⁷Service of Head and Neck Surgery, Arnaldo Vieira de Carvalho Hospital, São Paulo, SP, Brazil

¹⁰Department of Estomatology, School of Odontology, University of São Paulo, São Paulo, SP, Brazil

¹¹Division of Head and Neck Surgery, Department of Surgery, School of Medicine, University of São Paulo, São Paulo, SP, Brazil

¹²Department of Epidemiology, School of Public Health, University of São Paulo, São Paulo, SP, Brazil

¹³<http://ctc.fmrp.usp.br/clinicalgenomics/cp/group.asp> (complete author list and addresses presented in the Appendix)

¹⁴Department of Genetics and Evolutionary Biology, Institute of Biosciences, University of São Paulo, São Paulo, SP, Brazil

***Correspondence:** Eloiza Helena Tajara, PhD, Department of Molecular Biology, School of Medicine/FAMERP, Av. Brigadeiro Faria Lima, 5416, Vila São Pedro, CEP 15090-000, São José do Rio Preto, SP, Brazil. **E-mail:** tajara@famerp.br, **Phone:** +55 17 3201-5737, **Fax:** +55 17 3227 6201

Keywords:

Head and neck carcinoma / Immunohistochemistry / Oral cancer / Proteomics

Abbreviations: **IH**, immunohistochemistry; **LA**, “less-aggressive”; **MA**, “more-aggressive”; **OSCC**, oral squamous cell carcinoma; **TNM**, tumor-node-metastasis; **SAGE**, serial analysis of gene expression

Abstract

The prediction of tumor behavior for patients with oral squamous cell carcinomas (OSCCs) still represents a challenge for clinicians and researchers. The presence of regional lymph node metastasis is their most important prognostic factor but is limited in predicting local recidive or survival. In addition, early metastatic disease is often missed by clinical, histological and radiological analysis. This emphasizes the need for identifying biomarkers which may effectively contribute to early diagnosis and prediction of tumor progression.

In this study, we used one- and two-dimensional electrophoresis, fluorescent two-dimensional differential in-gel electrophoresis, mass spectrometry, Western blot and immunohistochemistry to analyze protein expression in OSCCs from different anatomic subsites and their matched adjacent normal mucosa. Firstly, we investigated the protein expression profile in the context of a known prognosticator, namely, the presence of neoplastic cells in regional lymph nodes. Using a refinement for classifying OSCCs in regard to prognosis, we also grouped small but already metastatic and large non-metastatic tumors.

Compared to the data obtained with the traditional classification, similar but not identical protein patterns were observed. The results indicate that tumor size is important to improve the distinction between polar TNM groups - aggressive and less-aggressive tumors - and some differences may have prognostic impact.

1 Introduction

Many recent advances in the area of cancer biology have occurred as a result of the use of high-throughput approaches. Large-scale analysis of transcripts and proteins has shed light on different aspects of tumorigenesis and provided exceptional opportunities for the identification of novel molecular targets for drug development. In this scenario, there is no doubt that DNA microarray, serial analysis of gene expression (SAGE), and more recently, deep-sequencing technologies have contributed with a huge amount of data on cancer gene expression. However, transcriptional profiling suffers from the susceptibility of RNA to degradation and from the lack of agreement between RNA and protein contents [1]. In fact, for valid conclusions on the functional meaning of a transcriptional pattern, data on the levels of the corresponding proteins are generally decisive. Moreover, post-translational modifications, protein-protein interaction, cellular trafficking and degradation, which modulate protein activity and function, are important information missed by mRNA expression analysis [2].

Global protein analysis is, therefore, crucial for defining the molecular profile of cancer. Two major technologies are well known in proteomics analysis, two-dimensional gel electrophoresis (2-DE) and mass spectrometry (MS), which are applied for protein separation and identification, respectively. In the last years, several technical advances have been incorporated into these methodologies improving their efficiency and accuracy. Fluorescent 2-D differential in-gel electrophoresis (2-D DIGE), for example, is a more recent high-throughput version of 2-DE and permits the analysis of two protein samples on the same gel, reducing gel-to-gel variation [3]. MS-based proteomics has also evolved (reviewed by [2]), using multidimensional protein fractionation to increase coverage [4], new tools to analyze posttranslational modifications (reviewed by [5]), affinity purification-MS to evaluate interactions between proteins [6], or combining liquid chromatography separation - tandem MS (LC-MS/MS) with quantitative and semi-quantitative methods to measure relative and absolute protein abundance [7, 8]. In addition, multiplexed immunoassays have been developed for simultaneously screening multiple protein biomarkers [9].

Although facing limitations in terms of proteome coverage and time-consuming tasks, proteomics analysis has been employed to study a wide variety of tumors (or body

fluids), such as breast [10-13], bladder [14-17], kidney [18-21], liver [22-25], lung [26-29], prostate [30-33], esophageal [34-36] and head and neck cancer [37-46].

In head and neck tumors, several proteomic data have suggested that protein profile may be of diagnostic and predictive value [43, 47-49], including in the early phases of the disease [46, 50, 51]. Early diagnostic and prognostic markers are especially important for these tumors, since, in their initial stages, the patients exhibit few symptoms. This fact, added to the lack of efficient screening methods, results in diagnosis delay and high mortality rates.

Head and neck carcinomas are heterogeneous with regard to anatomic sites, clinical presentations and outcomes [52, 53]. Among them, oral squamous cell carcinoma (OSCC) is one of the more common types, with approximately 270,000 new cases in the world per year [54, 55], most related to tobacco and alcohol use [56-58]. Recently, human papillomavirus has also been identified as a causal factor and this association is especially strong for oropharyngeal cancers and for non-smokers and non-drinkers but weakest for cancers of oral cavity and larynx [59, 60].

The presence of regional lymph node metastasis is still the most important prognostic factor in oral cancer, similar to other head and neck tumors [61]. However, early metastatic disease is often missed by clinical, histological and radiological analysis [62, 63]. This emphasizes the need for identifying early detection biomarkers, which may help to understand the tumor behavior and to increase survival rates.

In this study, we used one- and two-dimensional electrophoresis, fluorescent two-dimensional differential in-gel electrophoresis and mass spectrometry technologies to analyze protein expression in OSCCs from different anatomic subsites and their matched adjacent normal mucosa. Firstly, we investigated the protein expression profile in the context of a known prognosticator, namely, the presence of neoplastic cells in regional lymph nodes, independently of the tumor size as usually done for head and neck carcinomas. Using a refinement for classifying oral carcinomas in regard to prognosis, we also grouped small but already metastatic and large non-metastatic tumors. The rationale for this exploratory classification is the fact that standard criteria, as discussed for staging system by Patel and Shah [64], are limited in predicting local recidive or survival.

2 Materials and methods

2.1 Patients and specimens

Two hundred forty-five surgical specimens of primary OSCC and adjacent normal mucosa were obtained from a total of 141 patients with surgically resected carcinoma at Hospital do Câncer Arnaldo Vieira de Carvalho, Hospital das Clínicas and Hospital Heliópolis, São Paulo, SP, Brazil between 2000 and 2006. None of the patients had received preoperative radiation or chemotherapy. The samples were collected by the Head and Neck Genome Project (GENCAPO), a collaborative consortium with more than 50 researchers from 9 institutions in São Paulo State, Brazil, whose aim is to develop clinical, genetic and epidemiological analysis of head and neck squamous cell carcinomas.

Immediately after surgery, the specimen was cut in two, one part was snap-frozen and stored in liquid nitrogen and the other part was fixed in formalin for routine histopathological examination. Analysis of hematoxylin and eosin-stained sections indicated that each tumor sample contained at least 70% tumor cells and the surgical margins were “tumor-free”. The total set of samples was derived from six oral subsites (C01, C02, C03, C04, C05 and C06) according to the criteria established by the World Health Organization (WHO) (<http://apps.who.int/classifications/apps/icd/icd10online/>). The tumors were classified by the Tumor-Node-Metastases (TNM) system [65]. Using a refinement for classifying oral carcinomas in regard to prognosis, small but already metastatic tumors (T1-2N+) at diagnosis were considered potentially “more-aggressive” (MA), and larger but non-metastatic ones (T2-3N0) were considered “less-aggressive” (LA). In addition, T3-4N+ and T1,4N0 samples were also used for some analyses. A full description of the clinical data, including tumor stage, is provided in Supporting Table 1. Global survival was calculated from the date of the first treatment until the date of death or last known follow-up.

The study was approved by the ethics committees of enrolled institutions and by the National Committee of Ethics in Research (CONEP 1763/05, 18/05/2005). All patients gave their written consent to participate in the study after being informed about the research purposes. Pathological procedures were performed according to protocols approved by the Brazilian Society of Pathology [66].

2.2 Protein extraction

Proteins were extracted after RNA extraction by TRIzol® Reagent (Invitrogen Corp., Carlsbad, CA, USA). Briefly, the organic phase containing DNA and proteins was isolated, DNA was precipitated with ethanol and, subsequently, the proteins of supernatant fraction were precipitated with isopropyl alcohol. The samples were maintained for 10 min at 15 to 30°C and sedimented at 12,000 g for 10 min at 4°C. The pellets were washed three times with 0.3 M guanidine hydrochloride in 95% ethanol. During each wash step, the pellets were maintained in the washing solution for 20 min at room temperature and centrifuged at 7,500 g for 5 min at 4°C. After the last wash, the pellets were vortexed in ethanol, stored for 20 min at room temperature and centrifuged at 7,500 g for 5 min at 4°C. The samples were dried for 5 to 10 min and diluted in 1% SDS at 50°C overnight. After centrifugation at 10,000 g for 10 min at 4°C, the supernatants were recovered and protein quantitation was performed using the detergent-compatible BCA™ Protein Assay Kit (Pierce Biotechnology Inc., Rockford, IL, USA). Proteins from a small subgroup of 24 samples were extracted according to the protocol previously described by de Marqui et al. [67] and the protein concentration was determined by the Bradford method [68]. All protein samples were stored in aliquots at -80°C until analysis.

To minimize individual differences and to enable duplicate analysis of samples with limited amount of proteins, one- and two-dimensional electrophoresis experiments were performed using pooled samples grouped according to anatomic subsites and TNM system. In total, 74 individual samples from smoker patients older than 40 years were combined in pools of tumors or surgical margins. The pools were prepared by mixing equal amounts of protein from each sample, resulting in a total of 100 and 1500 µg per pool for 1-DE and 2-DE gels, respectively. A description of all the pools is presented in Supporting Table 2.

Differently of 2-DE, 2D-DIGE experiments were performed using individual C02 and C04 samples from tumors T1-2N+ and T3N0 (8 cases each, respectively). To overcome experimental variations, internal standards were created combining equal amounts of total protein from all 16 samples. The samples were also derived from smoker patients older than 40 years.

2.3 One-dimensional electrophoresis (1-DE)

One pool T1-2N+ and one pool T3N0 combining C02 and C04 tumors and one pool with matched surgical margins were separated by one-dimensional 12% resolving/5% stacking SDS polyacrylamide gel (PAGE). Under reducing conditions, the proteins were denatured at 98°C for 10 min in 5X loading buffer with DTT, and 100 µg of each pool were loaded into the wells. SDS-PAGE was carried out on a vertical polyacrylamide gel system (SE 400 Vertical Unit, GE Healthcare, Uppsala, Sweden) at 130 V. Molecular mass was estimated using low molecular weight standard proteins of 14.4–97 kDa (LMW Calibration Kit for SDS Electrophoresis, GE Healthcare). Proteins were detected by Coomassie Brilliant Blue staining, and the gels were scanned using an ImageScanner (GE Healthcare). Each gel lane (from about 10 to 45kD) was cut into 12 slices of approximately equal size. The slices were destained, dehydrated and digested with trypsin (Promega, Madison, WI, USA), as previously described by Højlund et al. [69], Lefort et al. [70] and Yi et al. [71].

2.4 Two-dimensional electrophoresis (2-DE)

One pool T1-2N+ and one pool T2-3N0 combining C02 and C04 tumors and two pools with matched surgical margins were analyzed by 2-DE according to the protocol previously described by de Marqui et al. [67], with modifications. In order to investigate the protein expression profile in the context of the presence or absence of lymph node metastases, independently of the tumor size, we also analyzed one pool T2-4N+ and one pool T2-4N0 (C02 and C04 tumors) and two pools of their surgical margins. In addition, one pool of tumors from another subsite (C01) was analyzed as well as their surgical margins (Supporting Table 2).

Proteins were cleaned using ice-cold acetone 100% and resuspended in rehydration solution (8 M urea, 2% w/v CHAPS, 0.3% w/v DTT, 0.5% v/v IPG buffer pH 3-10, bromophenol blue trace) to a final volume of 250 µL before loaded onto immobilized 13 cm linear pH gradient (IPG) strips (pH 3-10, GE Healthcare). Isoelectric focusing (IEF) was performed for a total of 26,500 Vh at 20°C and 50 µA/strip, using an Ettan IPGphor Isoelectric Focusing (GE Healthcare).

IPG strips were equilibrated for 15 min in equilibration solution [6 M urea, 50 mM Tris-HCl pH 8.8, 30% v/v glycerol (87% v/v), 2% w/v SDS, bromophenol blue trace]

containing 1% w/v DTT, followed by incubation for 15 min in the same solution containing 2.5% w/v iodoacetamide instead of DTT. IPG strips were sealed on top of 12.5% SDS-polyacrylamide gels using 0.5% w/v low-melting agarose in SDS running buffer with bromophenol blue. Electrophoresis was performed at 15 mA per gel for 30 min at room temperature, followed by 30 mA per gel for 3-5 h, in a Hoefer SE 600 Ruby system (GE Healthcare). All samples were run in duplicate or triplicate to guarantee reproducibility. The proteins were visualized by Coomassie Brilliant Blue staining. The LMW Calibration Kit (GE Healthcare) was used as a protein standard.

Gels were scanned using an ImageScanner (GE Healthcare) and the images were analyzed using the ImageMaster 2D Elite software (GE Healthcare) for spot detection, quantification, and comparative and statistical analysis. Basically, tumor and surgical margin groups were created and the gels were matched to a reference gel. Differences in protein expression levels were considered as significant when Student's *t* test gave a *p*-value < 0.05 and when spots showed visually different sizes and intensities.

2.5 Fluorescent two-dimensional differential in-gel electrophoresis (2-D DIGE)

For DIGE experiments, proteins were concentrated using ULTRAFREE® - 0.5 Centrifugal Filter Device (Biomax Membrane, 5 kDa; Millipore Inc., Billerica, MA, USA) and pH was adjusted to 8.5 by adding 50 mM NaOH or 50 mM HCl.

The samples were labeled with fluorescent cyanine dyes (Cy2, Cy3 or Cy5; GE Healthcare), following the manufacturer's recommended protocols. In brief, 1 µL of 400 µM CyDye was added to 50 µg of each unique protein sample. The mixture of sample and dye was vortexed, centrifuged and kept on ice in the dark for 30 min. The reaction was quenched by the addition of 10 mM lysine (1 µL). The solution was vortexed, centrifuged and left for 10 min on ice in the dark.

Eight T1-2N+ (MA) and eight T3N0 (LA) tumor samples were labeled with Cy3 or Cy5. An internal standard composed of equal amounts of total protein from all 16 samples was labeled with Cy2. Fifty µg of protein isolated from an individual tumor sample labeled with Cy3, 50 µg of protein isolated from another individual tumor sample labeled with Cy5, and 50 µg of protein from the internal standard labeled with Cy2 were mixed and subjected to 2-DE, according to the experimental design (Table 1). Two unlabeled pooled internal standards (each one with 250 µg) were also prepared.

DeStreak Rehydration Solution (plus 1% v/v IPG buffer pH 3-10; GE Healthcare) was added to each mix to a final volume of 150 μ L. After vortexed and kept for 15 min at room temperature, the samples were applied to an IPG strip (pH 3-10 L, 13 cm; GE Healthcare), previously rehydrated overnight with 250 μ L DeStreak Buffer (plus 1% v/v IPG buffer pH 3-10).

IEF was performed for a total of 31,000 Vh (at 20°C, 10 μ A/strip) using an Ettan IPGphor apparatus (GE Healthcare) and the second-dimension electrophoresis was conducted for 30 min at 2 W per gel and then for 3.5 h at 10 W per gel and 10°C, in an Ettan DALT six Electrophoresis System (GE Healthcare). The gels containing unlabeled internal standard were stained with Deep Purple Total Protein Stain (GE Healthcare), according to manufacturer's instructions.

DIGE gels were scanned on a Typhoon Trio™ Variable Mode Imager (GE Healthcare) at 100 μ m resolution. Images were normalized by adjusting the exposure times according to the average pixel values observed. Gel analysis was performed using DeCyder 2D Software, Version 6.5 (GE Healthcare). Changes detected by CyDye-stained gel analysis were aligned with Deep Purple-stained gel protein patterns. Spots that showed a significant change ($p < 0.01$) in abundance were picked from Deep Purple-stained gels using an Ettan Spot Picker (GE Healthcare) and identified by mass spectrometry.

2.6 Mass spectrometry (MS), protein identification and annotation

Slices from 1-DE gel and differentially expressed protein spots from 2-DE gels were excised manually and digested with trypsin, according to the protocol previously described by Cutillas et al. [72] and de Marqui et al. [67], respectively.

Digested samples from one-dimensional gel were directly analyzed using an ElectroSpray Ionization Quadrupole Time of Flight MS/MS system (Q-TOF Ultima API; Waters Corporation, Milford, MA, USA). Peptide digest from two-dimensional gels were mixed with matrix solution (10 mg/mL α -cyano-4-hydroxycinnamic acid, 0.1% v/v TFA in 50% v/v ACN) in a 1:1 (v:v) ratio, spotted on a stainless steel sample plate and air dried. Mass determinations were performed on a MALDI TOF-TOF (Matrix Assisted Laser Desorption Ionization - Time of Flight - Time of Flight) 4700 Proteomics Analyzer (Applied Biosystems Inc., Foster City, CA, USA) or a MALDI Q-

TOF (Matrix Assisted Laser Desorption Ionization - Quadrupole Ion Trap - Time of Flight) Premier (Waters Corporation). Each sample was run in triplicate.

For protein identification, the data were searched against MSDB (Mass Spectrometry Protein Sequence Database) or NCBI nr (National Center for Biotechnology Information non-redundant); database using Mascot Distiller version 2.2.1.0 and Mascot Daemon version 2.2.0 (Matrix Science Ltd., London, UK). The parameters for spectra acquisition were set up as follows: *Homo sapiens* taxonomy; trypsin enzyme; one missed cleavage site; carbamidomethylation of cysteine and oxidation of methionine as modifications; peptide tolerance of 1 or 0.1 Da; MS/MS tolerance of 0.1 or 0.8 Da; peptide charge of 1+ or 2+ and 3+; monoisotopic masses; Mascot Generic as data format and ESI-QUAD-TOF, MALDI-TOF-TOF or MALDI-QUAD-TOF instruments. The criteria for positive identification of proteins were: (1) individual ion scores at $p < 0.05$, and (2) molecular weights and isoelectric points matched to values obtained from image analysis.

Gene Ontology (GO) annotation (<http://www.geneontology.org/>) was used to assign biological process terms for differentially expressed proteins.

2.7 Immunodetection methods

One protein displaying down (keratin, type II cytoskeletal 4 or CK-4) was selected for validation using immunodetection methods.

For Western blotting, CK-4 expression was checked in individual samples (19 pairs of matched tumors and surgical margins plus 5 tumors and 7 surgical margins) from different oral subsites (Supporting Table 1). The antibodies used were mouse monoclonal antibody against CK-4 (6B10: sc-52321; Santa Cruz Biotechnology Inc., Santa Cruz, CA, USA) diluted 1:500, mouse monoclonal anti- α -tubulin (TU-02: sc-8035; Santa Cruz Biotechnology) diluted 1:500 and mouse monoclonal anti- β -actin (Sigma-Aldrich, Saint Louis, MO, USA) diluted 1:5000. Protein samples (9 μ g) were separated on SDS-PAGE (12% resolving gel with 5% stacking gel) at 130 V for 60 min (Mini-Protean 3 Cell; BioRad Inc., Hercules, CA, USA), in denaturing conditions. The molecular weight ladders used were the PageRuler™ Prestained Protein Ladder (SM0671; Fermentas Life Sciences, Burlington, Ontario, Canada) and the See Blue Plus2 Pre-Stained Standard (Invitrogen).

The proteins were transferred (325 mA for 70 min) to PVDF (Polyvinylidene Fluoride) membranes (Immobilon-P; Millipore) using transfer buffer (25 mM Tris, 0.2 M glycine, 20% v/v methanol) and the Mini-Protean 3 Cell electrophoresis system (BioRad). The membranes were submitted to chromogenic staining using the Western Breeze Kit (Invitrogen), according to the manufacturer's protocol. The blots were analyzed using Gel Logic HP 2200 imaging system (Carestream Health Inc/Kodak Health Group, Rochester, NY, USA) and the levels of CK-4 were normalized against α -tubulin and β -actin.

For immunohistochemistry analysis, a tissue microarray (TMA) with 73 primary OSCC samples and 66 tissue slides containing archival formalin-fixed, paraffin-embedded tissue (FFPE) sections of matched non-neoplastic mucosa were used (Supporting Table 1). In TMA, one representative tumor area was selected from a hematoxylin- and eosin-stained section of a donor block. Four cylinders per patient (diameter of 1 mm each) were punched out and arrayed in a recipient paraffin block using an arraying device (Beecher Instruments, Silver Spring, MD, USA). Therefore, the tissue microarrays contained 292 cores of tumor samples.

Cytokeratin-4 immunohistochemical analysis of oral tumor samples (Supporting Table 1) was performed by a pathologist using conventional protocols [73-77]. Briefly, after deparaffinization in xylene and rehydration in graded ethanol, antigen epitope retrieval was performed using 10 mM citrate buffer, pH 6.0 in a vapor cooker. Endogenous peroxidase activity was blocked with 3% hydrogen peroxide for 15 min. Primary mouse anti-CK-4 monoclonal antibody (sc-52321; Santa Cruz Biotechnology Inc.), diluted 1:200, was incubated overnight at 8°C followed by addition of the secondary antibody and streptavidin-biotin peroxidase (LSAB+, code k0690, Dako, CA, USA). Color of reaction product was developed by 3,3'-diaminobenzidine (DAB, Dako) and counterstaining was performed with Harris hematoxylin.

The primary antibody was omitted for negative controls and a normal prostate sample was used as positive control. Immunoexpression of CK-4 was graded subjectively as 0 (no evidence of staining), grades 1 (5-25% of positive cells), 2 (26-50%), 3 (51-75%) and 4 (>75% of positive cells). Intensity of immunoexpression was also evaluated semiquantitatively as follows: 0, none; 1, mild; 2, moderate; and 3,

intense. Cases in which 10% or more of the tumor cells were positively stained with anti-CK-4 antibody were considered to be CK-4- positive.

3 Results

3.1 Casuistic information

Of the 141 patients with oral carcinomas included in the present study, 118 (83.7%) were male and 23 (16.3%) female, most were older than 50 years (55.5 ± 10.1 years), smokers or former smokers (94.3%) and/or had a history of chronic alcohol (85.8%). Seventy-eight (55.3%) had metastatic (N+) and 63 (44.7%) had non-metastatic (N0) carcinomas: 24.8% (35/141) of tumors were classified as “more-aggressive” (T1-2N+), 35.5% (50/141) as “less-aggressive” (T2-3N0), and 30.5% (43/141), 3.5% (5/141) and 5.7% (8/141) of the cases were T3-4N+, T1N0 and T4N0, respectively.

Global survival for N+ and N0 patients ranged from less than 1 to 76 and 4 to 83 months, respectively. Considering T1-2N+ and T2-3N0 groups, the global survival ranged from 5 to 76 and 4 to 83 months, respectively.

3.2 Protein identification

With respect to protein profile, comparison of 2-DE between tumor and normal tissues and between metastatic/”more-aggressive” and non-metastatic/”less-aggressive” samples revealed spots with different expression. Thirty-one proteins were identified by mass spectrometry and database searching (Supporting Table 3). Observed and calculated molecular weight and pI showed a high correlation, reinforcing the validity of the results. Some proteins were present in train spots, suggesting distinctive posttranslational modifications or isoforms derived from alternative splicing.

Over- and under-expressed proteins were observed in tumor tissues compared with the surgical margins. Differences between subsites were also detected (Table 2). These proteins are involved in different biological processes including apoptosis, cell adhesion, motion and proliferation, cell signaling, cytokine production, cytoskeleton organization, epithelial cell differentiation, immune and inflammatory response, tissue, organ and system development, transcription, translation and transport. “More-aggressive” and “less-aggressive” groups exhibited similar but not identical patterns (Table 2).

Quantitative differences between these groups included higher expression of annexin A1, beta-globin, calgranulin-B, creatine kinase M-type, cofilin-1, galectin-7, HSP27, glutathione S-transferase P, myoglobin, serum albumin and superoxide dismutase [Cu-Zn] in “more-aggressive” ones. Enlarged and representative 2-DE gel images of paired protein samples are shown in Figure 1 and Supporting Figures 1, 2 and 3.

Few differences were also observed in DIGE experiments. Seventeen protein spots showed differential expression but only two proteins were identified: creatine kinase M-type and alpha-enolase, which were respectively over- and under-expressed in “more-aggressive” tumors compared to “less-aggressive” ones.

Besides the proteins detected by two-dimensional electrophoresis, ESI-Q-TOF-MS/MS analysis of pooled samples resolved by 1-DE identified 376 proteins for T1-2N+ and 418 for T3N0 tumors, and 284 for surgical margin samples (Supporting Tables 4, 5 and 6, respectively). Higher number of proteins involved in cell component biogenesis, anatomical structure formation and organelle organization were observed in more-aggressive samples. Otherwise, this group showed a low frequency of proteins involved in glycolysis. Normal tissues showed a lower number of proteins related to translational elongation and a higher frequency of genes involved in cell surface binding, as compared to tumor samples. Several uncharacterized proteins were detected.

3.3 Validation of downregulation of CK-4 by immunodetection assays

Confirming what was observed in 2-DE, CK-4 immunodetection experiments showed consistent differences in expression in cancer samples when compared with the normal tissues. In Western blottings, CK-4 showed low levels in 3/4 (75%) “more-aggressive” and 4/4 (100%) “less-aggressive” tumors compared to surgical margins or in 15/17 (88.2%) N+ and 5/7 (71.4%) N0 oral carcinomas (Figure 2). The immunohistochemical analysis revealed the complete absence of CK-4 expression in 73/73 tumors (Figure 3).

4 Discussion

In the last decades, many genetic and epigenetic events related to head and neck tumorigenesis were described, including inactivation of tumor suppressor p16-INK4a

and p53 proteins, and activation or overexpression of epidermal growth factor receptor, cyclin D and vascular endothelial growth factor. Several of these events have been shown to be associated with reduced survival or more-aggressive tumor behavior (reviewed by [78]). However, despite enormous efforts and progress over those years, relevant markers which may effectively contribute to early diagnosis, prediction of tumor progression or personal therapy are not yet available. In fact, traditional histopathological criteria, as presence of lymph node metastases, are limited in predicting local recidive or survival.

In the present study, we compared traditional and exploratory parameters for classifying oral carcinomas with regard to protein expression profile, using one- and two-dimensional electrophoresis, fluorescent two-dimensional differential in-gel electrophoresis/2D-DIGE, mass spectrometry, immunodetection techniques, and a large set of oral squamous cell carcinoma samples. Differential expression was evaluated using pools of small but already metastatic and larger but non-metastatic tumors and paired histological normal surgical margins. The patient group was homogeneous in relation to age (older than 40 years) and tobacco and alcohol use, therefore, potentially presenting similar etiologic factors. The data were also validated in samples from different head and neck subsites, independently of tumor size.

Comparing the protein pattern of oral carcinomas and surgical margins, a consistent finding was the absence of cytokeratin 4 in almost all tumor samples, confirming the results of previous studies [41, 79, 80]. CK-4 occurs as heterodimers in suprabasal layers of non-keratinized tissues such as buccal and soft palate [81]. Because it is a marker for squamous differentiation [82], the loss or substitution of CK-4 with another cytokeratin may be consequence of the tissue dedifferentiation during the oncogenic process. Chung et al. [83] suggested that downregulation of CK-4 in esophageal squamous cell carcinoma is an early event.

Underexpression of CK-4 in tumors may be of limited use in diagnosis but would be important if related to aggressiveness. In the present study, no significant differences were found between metastatic and non-metastatic tumors. Because CK-4 immunostaining was detected in two T1N0 tumor samples, it is possible that dysregulation of cytokeratins occurs later in tumorigenesis.

Protein patterns of carcinomas from base of tongue (C01) and from other and unspecified parts of tongue (C02) or floor of mouth (C04) were similar in spite that the former are typically aggressive whereas C02 and C04 exhibit better prognostic [84]. The more striking differences were downregulation of galectin-7 and calgranulin-B in C01 but not in C02/C04 and may be in part explained by the influences of micro-environmental factors.

No qualitative and few quantitative differences in protein expression were observed between “more-aggressive” and “less-aggressive” groups, suggesting that the boundaries of these groups are not well demarcated. “More-aggressive” tumors, although with lower levels than normal samples, exhibited higher expression of creatine kinase M-type (M-CK) and myoglobin than “less-aggressive” ones, which may be related to larger energy and oxygen demands. Higher levels of annexin A1, beta-globin, calgranulin-B, cofilin-1, galectin-7, HSP27, glutathione S-transferase P (GSTP1-1) and superoxide dismutase [Cu-Zn] were also observed in “more-aggressive” tumors. In this group, under-expression of alpha-enolase was detected only in DIGE experiments.

As noted by Koehn et al. [85], upregulation of M-CK, GSTP1-1 and HSP27 are linked to p53 pathway, which plays an important role in the regulation of the cell cycle and apoptosis [86], and is frequently mutated in oral squamous cell carcinomas [87]. The transcription of *CKM* and *GSTP1* genes appears to be controlled by the tumor protein p53 during muscle differentiation and stress conditions [88-90] and the chaperone HSP27 apparently participates in the regulation of cellular senescence by modulating the p53 pathway [91]. Therefore, higher levels of these proteins may be related to differentiation and apoptosis escape during oral carcinogenesis and provide evidence that p53 pathway is prominently involved in “more-aggressive” behavior.

Increased expression of GSTP1-1 was already observed in oral and other head and neck carcinomas [57, 92], specially in higher-grade lesions [93], and associated with shorter survival in lung cancer [94], leukemia [95], and lymphomas [96]. Recently, GSTP1 was recognized as a downstream target of the epidermal growth factor receptor (EGFR) [97], suggesting that the potential relation between higher levels of GSTP1-1 and aggressiveness may be consequence of the overexpression of EGFR, a marker associated with worst overall survival in head and neck carcinomas [98-100] and poor prognosis in several cancers [101, 102].

High levels of M-CK and HSP27 were also detected in oral carcinomas [37, 57, 58, 92, 103] but their association with tumor aggressiveness is not clear. In fact, both positive and negative correlations between HSP27 expression and survival rates have been reported for OSCC [104, 105] although, in other tumors, several studies have observed an association of high HSP27 levels with metastasis and short survival [29, 106-108].

A protein pattern favoring metastasis to lymph nodes should be present in the “more-aggressive” and shorter survival group defined by the present study. Besides GSTP1-1 and HSP27, other differential proteins, such as those acting on inflammation, may contribute to this behavior. For example, the inflammatory chemoattractant calgranulin B has been implicated in the metastatic process, facilitating the homing of tumour cells to pre-metastatic sites [109-111], and was shown to be upregulated in oral carcinomas [37]. Annexin A1 appears to be a functional antagonist of chemoattractants and inhibits cell migration [112]. This role in mediating antiinflammatory effects may be an answer to the influence of calgranulin and other factors on neoplastic cells. Otherwise, annexin A1, which is a substrate of EGFR and other coyness involved in tumor development [113], was identified as a metastasis-associated protein in a proteomic analysis of primary and metastatic cell lines of head and neck carcinomas derived from the same patient [114] and is downregulated by the breast cancer metastasis suppressor gene *BRMS1* [115].

The cofilin and its regulatory proteins have a central role in the actin filament remodeling and are other important factors directly involved in chemotaxis, cell migration and metastasis [116, 117]. Although already found upregulated in oral carcinomas and saliva from the patients [46, 85, 92, 103, 118], no data is available on the predictive role of cofilin regarding the metastatic potential of oral carcinomas.

Few data are also available on alpha enolase, galectin 7 and superoxide dismutase [Cu-Zn] in head and neck tumorigenesis [57, 92, 119], contrary to the most investigated galectin 1 and 3 and superoxide dismutase 2, which have been associated with worse disease-free survival and metastasis in these tumors [120-124]. Saussez et al. [125] observed high levels of galectin 7 in hypopharyngeal tumors showing rapid recurrence rates and dismal prognoses whereas Cada et al. [126] did not found an association of this protein expression with tumor size or metastasis in head and neck carcinomas from

different subsites. With respect to alpha enolase, a glycolytic enzyme which can bind to c-myc promoter and suppress transcription of c-myc oncogene [127], Chang et al. [128] observed that patients with lung tumors and reduced enolase-alpha expression had a significantly poorer overall survival.

The results of the present study reinforce the idea that it is not an individual protein but one or more pathways which are responsible for the aggressive phenotype. The next years will certainly bring new information to complete the picture on the determinants of the oral carcinoma behavior.

To our knowledge, this is the first proteomic study of oral carcinomas which compares a known prognosticator, namely, the presence of neoplastic cells in regional lymph nodes independently of the tumor size, and an exploratory classification using small but already metastatic and large non-metastatic tumors. Compared to the data obtained with the traditional classification, similar but not identical protein patterns were observed. The results indicate that tumor size is important to improve the distinction between polar TNM groups - aggressive and less-aggressive tumors - and some differences may have prognostic impact.

We acknowledge the financial support from “Fundação de Amparo à Pesquisa do Estado de São Paulo”/FAPESP (Grants 04/12054-9, 04/15630-0 and 06/60162-0), “Rede Proteoma do Estado de São Paulo” (“Auxílio FAPESP n° 04/14846-0/Convênio FINEP n° 01.07.0290.00”), The Ludwig Institute for Cancer Research, and the researcher fellowships from FAPESP (FCR-L) and Conselho Nacional de Pesquisa/CNPq (EHT).

The authors have declared no conflict of interest.

Appendix

The GENCAPO (Head and Neck Genome) Project authors are the following: Cury PM⁷, de Carvalho MB⁸, Dias-Neto E³, Figueiredo DLA⁹, Fukuyama EE⁵, Góis-Filho JF⁵, Leopoldino AM¹⁵, Mamede RCM⁹, Michaluart-Junior P⁶, Moreira-Filho CA¹, Moyses RA⁶, Nóbrega FG⁴, Nóbrega MP⁴, Nunes FD¹³, Ojopi EPB³, Okamoto OK¹⁴, Serafini LN¹⁰, Severino P¹, Silva AMA⁸, Silva Jr WA¹¹, Silveira NJF¹⁶, Souza SCOM¹³, Tajara EH², Wünsch-Filho V¹², Zago MA¹⁷, Amar A⁸, Arap SS⁶, Araújo NSS⁶, Araújo-

Filho V⁶, Barbieri RB⁸, Bandeira CM⁴, Braconi MA⁴, Brandão LG⁶, Brandão RM¹¹, Canto AL⁴, Carmona-Raphe J², Cerione M⁵, Cernea CR⁶, Cicco R⁵, Chagas MJ⁴, Chedid H⁸, Correia LA⁸, Costa A¹², Cunha BR², Curioni OA⁸, Dias THG³, Durazzo M⁶, Ferraz AR⁶, Figueiredo RO¹², Fortes CS¹², Franzi SA⁸, Frizzera APZ⁷, Gallo J⁶, Gazito D⁸, Guimarães PEM⁶, Inamine R¹², Kaneto CM¹¹, Lehn CN⁸, López RVM¹², Macarenco R⁴, Magalhães MR⁸, Magalhães RP⁶, Meneses C⁴, Mercante AMC⁸, Montenegro FLM⁶, Pinheiro DG¹¹, Polachini GM², Rapoport A⁸, Rodini CO¹³, Rodrigues AN¹², Rodrigues-Lisoni FC², Rodrigues RV², Rossi L⁸, Santos ARD¹¹, Santos M⁸, Settani F⁵, Silva FAM¹⁵, Silva IT¹¹, Silva-Filho GB⁶, Smith RB⁶, Souza TB⁸, Stabenow E⁶, Takamori JT⁸, Tavares MR⁶, Turcano R⁶, Valentim PJ⁵, Vidotto A², Volpi EM⁶, Xavier FCA¹³, Yamagushi F⁵, Cominato ML⁵, Correa PMS⁴, Mendes GS⁵, Paiva R⁵, Ramos O⁶, Silva C⁶, Silva MJ⁵, Tarlá MVC¹¹.

Affiliations: ¹Instituto de Ensino e Pesquisa Albert Einstein, São Paulo; ²Departamento de Biologia Molecular, Faculdade de Medicina de São José do Rio Preto; ³Departamento e Instituto de Psiquiatria, Faculdade de Medicina, Universidade de São Paulo (USP), São Paulo; ⁴Departamento de Biociências e Diagnóstico Bucal, Faculdade de Odontologia, Universidade Estadual Paulista, São José dos Campos, São Paulo, ⁵Serviço de Cirurgia de Cabeça e Pescoço, Instituto do Câncer Arnaldo Vieira de Carvalho, São Paulo; ⁶Departamento de Cirurgia de Cabeça e Pescoço, Faculdade de Medicina, USP, São Paulo; ⁷Departamento de Patologia, Faculdade de Medicina de São José do Rio Preto; ⁸Hospital Heliópolis, São Paulo; ⁹Serviço de Cirurgia de Cabeça e Pescoço, Faculdade de Medicina de Ribeirão Preto, USP; ¹⁰Departamento de Patologia, Faculdade de Medicina de Ribeirão Preto, USP; ¹¹Departamento de Genética, Faculdade de Medicina de Ribeirão Preto, USP; ¹²Departamento de Epidemiologia, Faculdade de Saúde Pública, USP, São Paulo; ¹³Departamento de Estomatologia, Faculdade de Odontologia da USP, São Paulo; ¹⁴Departamento de Neurologia/Neurocirurgia, UNIFESP, São Paulo; ¹⁵Departamento de Análises Clínicas, Toxicológicas e Bromatológicas, Faculdade de Ciências Farmacêuticas de Ribeirão Preto, USP; ¹⁶Instituto de Pesquisa e Desenvolvimento, UNIVAP, São José dos Campos; ¹⁷Departamento de Clínica Médica, Faculdade de Medicina de Ribeirão Preto, USP, SP, Brazil.

5 References

- [1] Han, M. H., Hwang, S. I., Roy, D. B., Lundgren, D. H., *et al.*, Proteomic analysis of active multiple sclerosis lesions reveals therapeutic targets. *Nature* 2008, *451*, 1076-1081.
- [2] Gstaiger, M., Aebersold, R., Applying mass spectrometry-based proteomics to genetics, genomics and network biology. *Nat Rev Genet* 2009, *10*, 617-627.
- [3] Unlu, M., Morgan, M. E., Minden, J. S., Difference gel electrophoresis: a single gel method for detecting changes in protein extracts. *Electrophoresis* 1997, *18*, 2071-2077.
- [4] Brunner, E., Ahrens, C. H., Mohanty, S., Baetschmann, H., *et al.*, A high-quality catalog of the *Drosophila melanogaster* proteome. *Nat Biotechnol* 2007, *25*, 576-583.

- [5] Jensen, O. N., Interpreting the protein language using proteomics. *Nat Rev Mol Cell Biol* 2006, 7, 391-403.
- [6] Wepf, A., Glatter, T., Schmidt, A., Aebersold, R., Gstaiger, M., Quantitative interaction proteomics using mass spectrometry. *Nat Methods* 2009, 6, 203-205.
- [7] Desiderio, D. M., Zhu, X., Quantitative analysis of methionine enkephalin and beta-endorphin in the pituitary by liquid secondary ion mass spectrometry and tandem mass spectrometry. *J Chromatogr A* 1998, 794, 85-96.
- [8] Callister, S. J., Barry, R. C., Adkins, J. N., Johnson, E. T., *et al.*, Normalization approaches for removing systematic biases associated with mass spectrometry and label-free proteomics. *J Proteome Res* 2006, 5, 277-286.
- [9] Kingsmore, S. F., Patel, D. D., Multiplexed protein profiling on antibody-based microarrays by rolling circle amplification. *Curr Opin Biotechnol* 2003, 14, 74-81.
- [10] Wulfschlegel, J. D., Sgroi, D. C., Krutzsch, H., McLean, K., *et al.*, Proteomics of human breast ductal carcinoma in situ. *Cancer Res* 2002, 62, 6740-6749.
- [11] Bouchal, P., Roumeliotis, T., Hrstka, R., Nenttil, R., *et al.*, Biomarker discovery in low-grade breast cancer using isobaric stable isotope tags and two-dimensional liquid chromatography-tandem mass spectrometry (iTRAQ-2DLC-MS/MS) based quantitative proteomic analysis. *J Proteome Res* 2009, 8, 362-373.
- [12] Hu, X., Zhang, Y., Zhang, A., Li, Y., *et al.*, Comparative serum proteome analysis of human lymph node negative/positive invasive ductal carcinoma of the breast and benign breast disease controls via label-free semiquantitative shotgun technology. *OMICS* 2009, 13, 291-300.
- [13] Umar, A., Kang, H., Timmermans, A. M., Look, M. P., *et al.*, Identification of a putative protein profile associated with tamoxifen therapy resistance in breast cancer. *Mol Cell Proteomics* 2009, 8, 1278-1294.
- [14] Celis, J. E., Celis, P., Ostergaard, M., Basse, B., *et al.*, Proteomics and immunohistochemistry define some of the steps involved in the squamous differentiation of the bladder transitional epithelium: a novel strategy for identifying metaplastic lesions. *Cancer Res* 1999, 59, 3003-3009.
- [15] Kreunin, P., Zhao, J., Rosser, C., Urquidi, V., *et al.*, Bladder cancer associated glycoprotein signatures revealed by urinary proteomic profiling. *J Proteome Res* 2007, 6, 2631-2639.

- [16] Schiffer, E., Vlahou, A., Petrolekas, A., Stravodimos, K., *et al.*, Prediction of muscle-invasive bladder cancer using urinary proteomics. *Clin Cancer Res* 2009, *15*, 4935-4943.
- [17] Issaq, H. J., Nativ, O., Waybright, T., Luke, B., *et al.*, Detection of bladder cancer in human urine by metabolomic profiling using high performance liquid chromatography/mass spectrometry. *J Urol* 2008, *179*, 2422-2426.
- [18] Klade, C. S., Voss, T., Krystek, E., Ahorn, H., *et al.*, Identification of tumor antigens in renal cell carcinoma by serological proteome analysis. *Proteomics* 2001, *1*, 890-898.
- [19] Okamura, N., Masuda, T., Gotoh, A., Shirakawa, T., *et al.*, Quantitative proteomic analysis to discover potential diagnostic markers and therapeutic targets in human renal cell carcinoma. *Proteomics* 2008, *8*, 3194-3203.
- [20] Perroud, B., Ishimaru, T., Borowsky, A. D., Weiss, R. H., Grade-dependent proteomics characterization of kidney cancer. *Mol Cell Proteomics* 2009, *8*, 971-985.
- [21] Seliger, B., Dressler, S. P., Wang, E., Kellner, R., *et al.*, Combined analysis of transcriptome and proteome data as a tool for the identification of candidate biomarkers in renal cell carcinoma. *Proteomics* 2009, *9*, 1567-1581.
- [22] Seow, T. K., Ong, S. E., Liang, R. C., Ren, E. C., *et al.*, Two-dimensional electrophoresis map of the human hepatocellular carcinoma cell line, HCC-M, and identification of the separated proteins by mass spectrometry. *Electrophoresis* 2000, *21*, 1787-1813.
- [23] Chaerkady, R., Harsha, H. C., Nalli, A., Gucek, M., *et al.*, A quantitative proteomic approach for identification of potential biomarkers in hepatocellular carcinoma. *J Proteome Res* 2008, *7*, 4289-4298.
- [24] Looi, K. S., Nakayasu, E. S., Diaz, R. A., Tan, E. M., *et al.*, Using proteomic approach to identify tumor-associated antigens as markers in hepatocellular carcinoma. *J Proteome Res* 2008, *7*, 4004-4012.
- [25] Orimo, T., Ojima, H., Hiraoka, N., Saito, S., *et al.*, Proteomic profiling reveals the prognostic value of adenomatous polyposis coli-end-binding protein 1 in hepatocellular carcinoma. *Hepatology* 2008, *48*, 1851-1863.

- [26] Brichory, F., Beer, D., Le Naour, F., Giordano, T., Hanash, S., Proteomics-based identification of protein gene product 9.5 as a tumor antigen that induces a humoral immune response in lung cancer. *Cancer Res* 2001, *61*, 7908-7912.
- [27] Park, H. J., Kim, B. G., Lee, S. J., Heo, S. H., *et al.*, Proteomic profiling of endothelial cells in human lung cancer. *J Proteome Res* 2008, *7*, 1138-1150.
- [28] Li, D. J., Deng, G., Xiao, Z. Q., Yao, H. X., *et al.*, Identifying 14-3-3 sigma as a lymph node metastasis-related protein in human lung squamous carcinoma. *Cancer Lett* 2009, *279*, 65-73.
- [29] Yao, H., Zhang, Z., Xiao, Z., Chen, Y., *et al.*, Identification of metastasis associated proteins in human lung squamous carcinoma using two-dimensional difference gel electrophoresis and laser capture microdissection. *Lung Cancer* 2009, *65*, 41-48.
- [30] Meehan, K. L., Holland, J. W., Dawkins, H. J., Proteomic analysis of normal and malignant prostate tissue to identify novel proteins lost in cancer. *Prostate* 2002, *50*, 54-63.
- [31] Fortin, T., Salvador, A., Charrier, J. P., Lenz, C., *et al.*, Clinical quantitation of prostate-specific antigen biomarker in the low nanogram/milliliter range by conventional bore liquid chromatography-tandem mass spectrometry (multiple reaction monitoring) coupling and correlation with ELISA tests. *Mol Cell Proteomics* 2009, *8*, 1006-1015.
- [32] Garbis, S. D., Tyritzis, S. I., Roumeliotis, T., Zerefos, P., *et al.*, Search for potential markers for prostate cancer diagnosis, prognosis and treatment in clinical tissue specimens using amine-specific isobaric tagging (iTRAQ) with two-dimensional liquid chromatography and tandem mass spectrometry. *J Proteome Res* 2008, *7*, 3146-3158.
- [33] Byrne, J. C., Downes, M. R., O'Donoghue, N., O'Keane, C., *et al.*, 2D-DIGE as a strategy to identify serum markers for the progression of prostate cancer. *J Proteome Res* 2009, *8*, 942-957.
- [34] Uemura, N., Nakanishi, Y., Kato, H., Saito, S., *et al.*, Transglutaminase 3 as a prognostic biomarker in esophageal cancer revealed by proteomics. *Int J Cancer* 2009, *124*, 2106-2115.

- [35] Zhou, G., Li, H., Gong, Y., Zhao, Y., *et al.*, Proteomic analysis of global alteration of protein expression in squamous cell carcinoma of the esophagus. *Proteomics* 2005, 5, 3814-3821.
- [36] Liu, W. L., Zhang, G., Wang, J. Y., Cao, J. Y., *et al.*, Proteomics-based identification of autoantibody against CDC25B as a novel serum marker in esophageal squamous cell carcinoma. *Biochem Biophys Res Commun* 2008, 375, 440-445.
- [37] He, Q. Y., Chen, J., Kung, H. F., Yuen, A. P., Chiu, J. F., Identification of tumor-associated proteins in oral tongue squamous cell carcinoma by proteomics. *Proteomics* 2004, 4, 271-278.
- [38] Lo, W. Y., Lai, C. C., Hua, C. H., Tsai, M. H., *et al.*, S100A8 is identified as a biomarker of HPV18-infected oral squamous cell carcinomas by suppression subtraction hybridization, clinical proteomics analysis, and immunohistochemistry staining. *J Proteome Res* 2007, 6, 2143-2151.
- [39] Roesch-Ely, M., Nees, M., Karsai, S., Ruess, A., *et al.*, Proteomic analysis reveals successive aberrations in protein expression from healthy mucosa to invasive head and neck cancer. *Oncogene* 2007, 26, 54-64.
- [40] Freed, G. L., Cazares, L. H., Fichandler, C. E., Fuller, T. W., *et al.*, Differential capture of serum proteins for expression profiling and biomarker discovery in pre- and posttreatment head and neck cancer samples. *Laryngoscope* 2008, 118, 61-68.
- [41] Patel, V., Hood, B. L., Molinolo, A. A., Lee, N. H., *et al.*, Proteomic analysis of laser-captured paraffin-embedded tissues: a molecular portrait of head and neck cancer progression. *Clin Cancer Res* 2008, 14, 1002-1014.
- [42] Chi, L. M., Lee, C. W., Chang, K. P., Hao, S. P., *et al.*, Enhanced interferon signaling pathway in oral cancer revealed by quantitative proteome analysis of microdissected specimens using 16O/18O labeling and integrated two-dimensional LC-ESI-MALDI tandem MS. *Mol Cell Proteomics* 2009, 8, 1453-1474.
- [43] Ralhan, R., Desouza, L. V., Matta, A., Chandra Tripathi, S., *et al.*, Discovery and verification of head-and-neck cancer biomarkers by differential protein expression analysis using iTRAQ labeling, multidimensional liquid chromatography, and tandem mass spectrometry. *Mol Cell Proteomics* 2008, 7, 1162-1173.

- [44] Wang, Z., Jiang, L., Huang, C., Li, Z., *et al.*, Comparative proteomics approach to screening of potential diagnostic and therapeutic targets for oral squamous cell carcinoma. *Mol Cell Proteomics* 2008, 7, 1639-1650.
- [45] Nagaraj, N. S., Evolving 'omics' technologies for diagnostics of head and neck cancer. *Brief Funct Genomic Proteomic* 2009, 8, 49-59.
- [46] Ralhan, R., Desouza, L. V., Matta, A., Chandra Tripathi, S., *et al.*, iTRAQ-multidimensional liquid chromatography and tandem mass spectrometry-based identification of potential biomarkers of oral epithelial dysplasia and novel networks between inflammation and premalignancy. *J Proteome Res* 2009, 8, 300-309.
- [47] Mlynarek, A. M., Balys, R. L., Su, J., Hier, M. P., *et al.*, A cell proteomic approach for the detection of secretable biomarkers of invasiveness in oral squamous cell carcinoma. *Arch Otolaryngol Head Neck Surg* 2007, 133, 910-918.
- [48] Bijian, K., Mlynarek, A. M., Balys, R. L., Jie, S., *et al.*, Serum proteomic approach for the identification of serum biomarkers contributed by oral squamous cell carcinoma and host tissue microenvironment. *J Proteome Res* 2009, 8, 2173-2185.
- [49] Matta, A., DeSouza, L. V., Shukla, N. K., Gupta, S. D., *et al.*, Prognostic significance of head-and-neck cancer biomarkers previously discovered and identified using iTRAQ-labeling and multidimensional liquid chromatography-tandem mass spectrometry. *J Proteome Res* 2008, 7, 2078-2087.
- [50] Linkov, F., Lisovich, A., Yurkovetsky, Z., Marrangoni, A., *et al.*, Early detection of head and neck cancer: development of a novel screening tool using multiplexed immunobead-based biomarker profiling. *Cancer Epidemiol Biomarkers Prev* 2007, 16, 102-107.
- [51] Matta, A., Tripathi, S. C., DeSouza, L. V., Grigull, J., *et al.*, Heterogeneous ribonucleoprotein K is a marker of oral leukoplakia and correlates with poor prognosis of squamous cell carcinoma. *Int J Cancer* 2009, 125, 1398-1406.
- [52] Dobrossy, L., Epidemiology of head and neck cancer: magnitude of the problem. *Cancer Metastasis Rev* 2005, 24, 9-17.
- [53] Ye, H., Yu, T., Temam, S., Ziober, B. L., *et al.*, Transcriptomic dissection of tongue squamous cell carcinoma. *BMC Genomics* 2008, 9, 69.
- [54] Parkin, D. M., Bray, F., Ferlay, J., Pisani, P., Estimating the world cancer burden: Globocan 2000. *Int J Cancer* 2001, 94, 153-156.

- [55] Parkin, D. M., Bray, F., Ferlay, J., Pisani, P., Global cancer statistics, 2002. *CA Cancer J Clin* 2005, 55, 74-108.
- [56] Ko, Y. C., Huang, Y. L., Lee, C. H., Chen, M. J., *et al.*, Betel quid chewing, cigarette smoking and alcohol consumption related to oral cancer in Taiwan. *J Oral Pathol Med* 1995, 24, 450-453.
- [57] Chen, J., He, Q. Y., Yuen, A. P., Chiu, J. F., Proteomics of buccal squamous cell carcinoma: the involvement of multiple pathways in tumorigenesis. *Proteomics* 2004, 4, 2465-2475.
- [58] Lo, W. Y., Tsai, M. H., Tsai, Y., Hua, C. H., *et al.*, Identification of over-expressed proteins in oral squamous cell carcinoma (OSCC) patients by clinical proteomic analysis. *Clin Chim Acta* 2007, 376, 101-107.
- [59] Hobbs, C. G., Sterne, J. A., Bailey, M., Heyderman, R. S., *et al.*, Human papillomavirus and head and neck cancer: a systematic review and meta-analysis. *Clin Otolaryngol* 2006, 31, 259-266.
- [60] D'Souza, G., Kreimer, A. R., Viscidi, R., Pawlita, M., *et al.*, Case-control study of human papillomavirus and oropharyngeal cancer. *N Engl J Med* 2007, 356, 1944-1956.
- [61] Layland, M. K., Sessions, D. G., Lenox, J., The influence of lymph node metastasis in the treatment of squamous cell carcinoma of the oral cavity, oropharynx, larynx, and hypopharynx: N0 versus N+. *Laryngoscope* 2005, 115, 629-639.
- [62] Woolgar, J. A., Pathology of the N0 neck. *Br J Oral Maxillofac Surg* 1999, 37, 205-209.
- [63] Barnes, L., Eveson, J.W., Reichart, P., Sidransky, D., editors., *Pathology and Genetics of Head and Neck Tumours*, IARC Press, Lyon 2005.
- [64] Patel, S. G., Shah, J. P., TNM staging of cancers of the head and neck: striving for uniformity among diversity. *CA Cancer J Clin* 2005, 55, 242-258; quiz 261-242, 264.
- [65] Sobin, L. H., Wittekind, C., editor, *TNM Classification of Malignant Tumors*, John Wiley & Sons, Hoboken, New Jersey 2002.
- [66] Bacchi, C. E. A. P., Franco, M.F., *Manual de Padronização de Laudos Histopatológicos*, Reichmann & Autores, São Paulo 2005.
- [67] de Marqui, A. B., Vidotto, A., Polachini, G. M., Bellato C de M., *et al.*, Solubilization of proteins from human lymph node tissue and two-dimensional gel storage. *J Biochem Mol Biol* 2006, 39, 216-222.

- [68] Bradford, M. M., A rapid and sensitive method for the quantitation of microgram quantities of protein utilizing the principle of protein-dye binding. *Anal Biochem* 1976, 72, 248-254.
- [69] Hojlund, K., Yi, Z., Hwang, H., Bowen, B., *et al.*, Characterization of the human skeletal muscle proteome by one-dimensional gel electrophoresis and HPLC-ESI-MS/MS. *Mol Cell Proteomics* 2008, 7, 257-267.
- [70] Lefort, N., Yi, Z., Bowen, B., Glancy, B., *et al.*, Proteome profile of functional mitochondria from human skeletal muscle using one-dimensional gel electrophoresis and HPLC-ESI-MS/MS. *J Proteomics* 2009, 72, 1046-1060.
- [71] Yi, Z., Bowen, B. P., Hwang, H., Jenkinson, C. P., *et al.*, Global relationship between the proteome and transcriptome of human skeletal muscle. *J Proteome Res* 2008, 7, 3230-3241.
- [72] Cutillas, P. R., Geering, B., Waterfield, M. D., Vanhaesebroeck, B., Quantification of gel-separated proteins and their phosphorylation sites by LC-MS using unlabeled internal standards: analysis of phosphoprotein dynamics in a B cell lymphoma cell line. *Mol Cell Proteomics* 2005, 4, 1038-1051.
- [73] Hsu, S. M., Raine, L., Fanger, H., The use of antiavidin antibody and avidin-biotin-peroxidase complex in immunoperoxidase technics. *Am J Clin Pathol* 1981, 75, 816-821.
- [74] Harlow, E., Lane, D., *Antibodies: A Laboratory Manual*, New York 1988.
- [75] Santos, R. T. M., Wakamatsu, A., Kanamura, C.T., Nonogaki, S., Pinto, G.A., editor, *Manual de imuno-histoquímica*, Sociedade Brasileira de Patologia, São Paulo 1999.
- [76] La Rosa, S., Uccella, S., Erba, S., Capella, C., Sessa, F., Immunohistochemical detection of fibroblast growth factor receptors in normal endocrine cells and related tumors of the digestive system. *Appl Immunohistochem Mol Morphol* 2001, 9, 319-328.
- [77] Hsu, F. D., Nielsen, T. O., Alkushi, A., Dupuis, B., *et al.*, Tissue microarrays are an effective quality assurance tool for diagnostic immunohistochemistry. *Mod Pathol* 2002, 15, 1374-1380.
- [78] Argiris, A., Karamouzis, M. V., Raben, D., Ferris, R. L., Head and neck cancer. *Lancet* 2008, 371, 1695-1709.

- [79] Kainuma, K., Katsuno, S., Hashimoto, S., Oguchi, T., *et al.*, Differences in the expression of genes between normal tissue and squamous cell carcinomas of head and neck using cancer-related gene cDNA microarray. *Acta Otolaryngol* 2006, *126*, 967-974.
- [80] Negishi, A., Masuda, M., Ono, M., Honda, K., *et al.*, Quantitative proteomics using formalin-fixed paraffin-embedded tissues of oral squamous cell carcinoma. *Cancer Sci* 2009, *100*, 1605-1611.
- [81] Presland, R. B., Jurevic, R. J., Making sense of the epithelial barrier: what molecular biology and genetics tell us about the functions of oral mucosal and epidermal tissues. *J Dent Educ* 2002, *66*, 564-574.
- [82] Moll, R., Franke, W. W., Schiller, D. L., Geiger, B., Krepler, R., The catalog of human cytokeratins: patterns of expression in normal epithelia, tumors and cultured cells. *Cell* 1982, *31*, 11-24.
- [83] Chung, J. Y., Braunschweig, T., Hu, N., Roth, M., *et al.*, A multiplex tissue immunoblotting assay for proteomic profiling: a pilot study of the normal to tumor transition of esophageal squamous cell carcinoma. *Cancer Epidemiol Biomarkers Prev* 2006, *15*, 1403-1408.
- [84] Timar, J., Csuka, O., Remenar, E., Repassy, G., Kasler, M., Progression of head and neck squamous cell cancer. *Cancer Metastasis Rev* 2005, *24*, 107-127.
- [85] Koehn, J., Krapfenbauer, K., Huber, S., Stein, E., *et al.*, Potential involvement of MYC- and p53-related pathways in tumorigenesis in human oral squamous cell carcinoma revealed by proteomic analysis. *J Proteome Res* 2008, *7*, 3818-3829.
- [86] Brown, C. J., Lain, S., Verma, C. S., Fersht, A. R., Lane, D. P., Awakening guardian angels: drugging the p53 pathway. *Nat Rev Cancer* 2009, *9*, 862-873.
- [87] Szymanska, K., Levi, J. E., Menezes, A., Wunsch-Filho, V., *et al.*, TP53 and EGFR mutations in combination with lifestyle risk factors in tumours of the upper aerodigestive tract from South America. *Carcinogenesis* 2009.
- [88] Tamir, Y., Bengal, E., p53 protein is activated during muscle differentiation and participates with MyoD in the transcription of muscle creatine kinase gene. *Oncogene* 1998, *17*, 347-356.
- [89] Lo, H. W., Stephenson, L., Cao, X., Milas, M., *et al.*, Identification and functional characterization of the human glutathione S-transferase P1 gene as a novel

transcriptional target of the p53 tumor suppressor gene. *Mol Cancer Res* 2008, 6, 843-850.

[90] Adler, V., Yin, Z., Fuchs, S. Y., Benezra, M., *et al.*, Regulation of JNK signaling by GSTp. *EMBO J* 1999, 18, 1321-1334.

[91] O'Callaghan-Sunol, C., Gabai, V. L., Sherman, M. Y., Hsp27 modulates p53 signaling and suppresses cellular senescence. *Cancer Res* 2007, 67, 11779-11788.

[92] Wang, Z., Feng, X., Liu, X., Jiang, L., *et al.*, Involvement of potential pathways in malignant transformation from oral leukoplakia to oral squamous cell carcinoma revealed by proteomic analysis. *BMC Genomics* 2009, 10, 383.

[93] Bentz, B. G., Haines, G. K., 3rd, Radosevich, J. A., Glutathione S-transferase pi in squamous cell carcinoma of the head and neck. *Laryngoscope* 2000, 110, 1642-1647.

[94] Vlachogeorgos, G. S., Manali, E. D., Blana, E., Legaki, S., *et al.*, Placental isoform glutathione S-transferase and P-glycoprotein expression in advanced nonsmall cell lung cancer: association with response to treatment and survival. *Cancer* 2008, 114, 519-526.

[95] Tidefelt, U., Elmhorn-Rosenborg, A., Paul, C., Hao, X. Y., *et al.*, Expression of glutathione transferase pi as a predictor for treatment results at different stages of acute nonlymphoblastic leukemia. *Cancer Res* 1992, 52, 3281-3285.

[96] Thieblemont, C., Rolland, D., Baseggio, L., Felman, P., *et al.*, Comprehensive analysis of GST-pi expression in B-cell lymphomas: Correlation with histological subtypes and survival. *Leuk Lymphoma* 2008, 49, 1403-1406.

[97] Okamura, T., Singh, S., Buolamwini, J., Haystead, T., *et al.*, Tyrosine phosphorylation of the human glutathione S-transferase P1 by epidermal growth factor receptor. *J Biol Chem* 2009, 284, 16979-16989.

[98] Ang, K. K., Berkey, B. A., Tu, X., Zhang, H. Z., *et al.*, Impact of epidermal growth factor receptor expression on survival and pattern of relapse in patients with advanced head and neck carcinoma. *Cancer Res* 2002, 62, 7350-7356.

[99] Chen, I. H., Chang, J. T., Liao, C. T., Wang, H. M., *et al.*, Prognostic significance of EGFR and Her-2 in oral cavity cancer in betel quid prevalent area cancer prognosis. *Br J Cancer* 2003, 89, 681-686.

[100] Agra, I. M., Carvalho, A. L., Pinto, C. A., Martins, E. P., *et al.*, Biological markers and prognosis in recurrent oral cancer after salvage surgery. *Arch Otolaryngol Head Neck Surg* 2008, 134, 743-749.

- [101] Rusch, V., Klimstra, D., Venkatraman, E., Pisters, P. W., *et al.*, Overexpression of the epidermal growth factor receptor and its ligand transforming growth factor alpha is frequent in resectable non-small cell lung cancer but does not predict tumor progression. *Clin Cancer Res* 1997, 3, 515-522.
- [102] Herbst, R. S., Review of epidermal growth factor receptor biology. *Int J Radiat Oncol Biol Phys* 2004, 59, 21-26.
- [103] Turhani, D., Krapfenbauer, K., Thurnher, D., Langen, H., Fountoulakis, M., Identification of differentially expressed, tumor-associated proteins in oral squamous cell carcinoma by proteomic analysis. *Electrophoresis* 2006, 27, 1417-1423.
- [104] Wang, A., Liu, X., Sheng, S., Ye, H., *et al.*, Dysregulation of heat shock protein 27 expression in oral tongue squamous cell carcinoma. *BMC Cancer* 2009, 9, 167.
- [105] Mese, H., Sasaki, A., Nakayama, S., Yoshioka, N., *et al.*, Prognostic significance of heat shock protein 27 (HSP27) in patients with oral squamous cell carcinoma. *Oncol Rep* 2002, 9, 341-344.
- [106] Xu, L., Chen, S., Bergan, R. C., MAPKAPK2 and HSP27 are downstream effectors of p38 MAP kinase-mediated matrix metalloproteinase type 2 activation and cell invasion in human prostate cancer. *Oncogene* 2006, 25, 2987-2998.
- [107] Lemieux, P., Oesterreich, S., Lawrence, J. A., Steeg, P. S., *et al.*, The small heat shock protein hsp27 increases invasiveness but decreases motility of breast cancer cells. *Invasion Metastasis* 1997, 17, 113-123.
- [108] Elpek, G. O., Karaveli, S., Simsek, T., Keles, N., Aksoy, N. H., Expression of heat-shock proteins hsp27, hsp70 and hsp90 in malignant epithelial tumour of the ovaries. *APMIS* 2003, 111, 523-530.
- [109] Yong, H. Y., Moon, A., Roles of calcium-binding proteins, S100A8 and S100A9, in invasive phenotype of human gastric cancer cells. *Arch Pharm Res* 2007, 30, 75-81.
- [110] Moon, A., Yong, H. Y., Song, J. I., Cukovic, D., *et al.*, Global gene expression profiling unveils S100A8/A9 as candidate markers in H-ras-mediated human breast epithelial cell invasion. *Mol Cancer Res* 2008, 6, 1544-1553.
- [111] Hiratsuka, S., Watanabe, A., Aburatani, H., Maru, Y., Tumour-mediated upregulation of chemoattractants and recruitment of myeloid cells predetermines lung metastasis. *Nat Cell Biol* 2006, 8, 1369-1375.

- [112] Walther, A., Riehemann, K., Gerke, V., A novel ligand of the formyl peptide receptor: annexin I regulates neutrophil extravasation by interacting with the FPR. *Mol Cell* 2000, 5, 831-840.
- [113] Gerke, V., Moss, S. E., Annexins: from structure to function. *Physiol Rev* 2002, 82, 331-371.
- [114] Wu, W., Tang, X., Hu, W., Lotan, R., *et al.*, Identification and validation of metastasis-associated proteins in head and neck cancer cell lines by two-dimensional electrophoresis and mass spectrometry. *Clin Exp Metastasis* 2002, 19, 319-326.
- [115] Cicek, M., Samant, R. S., Kinter, M., Welch, D. R., Casey, G., Identification of metastasis-associated proteins through protein analysis of metastatic MDA-MB-435 and metastasis-suppressed BRMS1 transfected-MDA-MB-435 cells. *Clin Exp Metastasis* 2004, 21, 149-157.
- [116] Wang, W., Mouneimne, G., Sidani, M., Wyckoff, J., *et al.*, The activity status of cofilin is directly related to invasion, intravasation, and metastasis of mammary tumors. *J Cell Biol* 2006, 173, 395-404.
- [117] Wang, W., Eddy, R., Condeelis, J., The cofilin pathway in breast cancer invasion and metastasis. *Nat Rev Cancer* 2007, 7, 429-440.
- [118] Dowling, P., Wormald, R., Meleady, P., Henry, M., *et al.*, Analysis of the saliva proteome from patients with head and neck squamous cell carcinoma reveals differences in abundance levels of proteins associated with tumour progression and metastasis. *J Proteomics* 2008, 71, 168-175.
- [119] Ito, S., Honma, T., Ishida, K., Wada, N., *et al.*, Differential expression of the human alpha-enolase gene in oral epithelium and squamous cell carcinoma. *Cancer Sci* 2007, 98, 499-505.
- [120] Honjo, Y., Inohara, H., Akahani, S., Yoshii, T., *et al.*, Expression of cytoplasmic galectin-3 as a prognostic marker in tongue carcinoma. *Clin Cancer Res* 2000, 6, 4635-4640.
- [121] Plzak, J., Betka, J., Smetana, K., Jr., Chovanec, M., *et al.*, Galectin-3 - an emerging prognostic indicator in advanced head and neck carcinoma. *Eur J Cancer* 2004, 40, 2324-2330.

- [122] Chiang, W. F., Liu, S. Y., Fang, L. Y., Lin, C. N., *et al.*, Overexpression of galectin-1 at the tumor invasion front is associated with poor prognosis in early-stage oral squamous cell carcinoma. *Oral Oncol* 2008, *44*, 325-334.
- [123] Ye, H., Wang, A., Lee, B. S., Yu, T., *et al.*, Proteomic based identification of manganese superoxide dismutase 2 (SOD2) as a metastasis marker for oral squamous cell carcinoma. *Cancer Genomics Proteomics* 2008, *5*, 85-94.
- [124] Wu, M. H., Hong, T. M., Cheng, H. W., Pan, S. H., *et al.*, Galectin-1-mediated tumor invasion and metastasis, up-regulated matrix metalloproteinase expression, and reorganized actin cytoskeletons. *Mol Cancer Res* 2009, *7*, 311-318.
- [125] Saussez, S., Cucu, D. R., Decaestecker, C., Chevalier, D., *et al.*, Galectin 7 (p53-induced gene 1): a new prognostic predictor of recurrence and survival in stage IV hypopharyngeal cancer. *Ann Surg Oncol* 2006, *13*, 999-1009.
- [126] Cada, Z., Chovanec, M., Smetana, K., Betka, J., *et al.*, Galectin-7: will the lectin's activity establish clinical correlations in head and neck squamous cell and basal cell carcinomas? *Histol Histopathol* 2009, *24*, 41-48.
- [127] Feo, S., Arcuri, D., Piddini, E., Passantino, R., Giallongo, A., ENO1 gene product binds to the c-myc promoter and acts as a transcriptional repressor: relationship with Myc promoter-binding protein 1 (MBP-1). *FEBS Lett* 2000, *473*, 47-52.
- [128] Chang, Y. S., Wu, W., Walsh, G., Hong, W. K., Mao, L., Enolase-alpha is frequently down-regulated in non-small cell lung cancer and predicts aggressive biological behavior. *Clin Cancer Res* 2003, *9*, 3641-3644.

Figure legends

Figure 1. Detailed alteration patterns of proteins in OSCC tumors identified by 2-DE and mass spectrometry: annexin A1 (ANXA1); beta-globin (HBB); creatine kinase M-type (M-CK); myoglobin (MB); cofilin-1 (CFL1); galectin-7 (Gal-7); glutathione S-transferase P (GSTP1-1); heat shock 27 kDa (HSP 27); calgranulin-B (S100-A9); superoxide dismutase (SOD1); tropomyosin-4 (TPM4). Tumor samples from tongue (C02) and floor of mouth (C04). T1-2N+ = “more-aggressive” tumors; T2-3N0 = “less-aggressive” tumors; N+ = metastatic tumors; N0 = non-metastatic tumors.

Figure 2. Analysis of CK-4 protein. Representative Western blots illustrating CK-4 expression in a subset of (A,B) eight oral squamous cell carcinomas and five non-neoplastic surgical margins by using anti-CK-4. A, Tumour samples (lanes 1, 3, 5, 7) and matched margins (lanes 2, 4, 6, 8) from patients with T1N0, T4N2, T4N1 and T4N1 carcinomas, respectively. B, Surgical margin (lane 1) and tumour samples (lanes 2, 3, 4, 5) from patients with T4N2, T4N2, T4N2, T1N0 and T2N2, respectively. β -actin was used as an internal control. MW, PageRuler™ Prestained Protein Ladder.

Figure 3. Immunohistochemical analysis of CK-4 expression in OSCC. In panels (A,B), complete absence of CK-4 expression is observed in tumor tissues, whereas in clear contrast, in panels (C,D), CK-4 is significantly overexpressed in normal surgical margins. Slides were photographed at 400X (A, B, D) and 100X (C) magnifications.

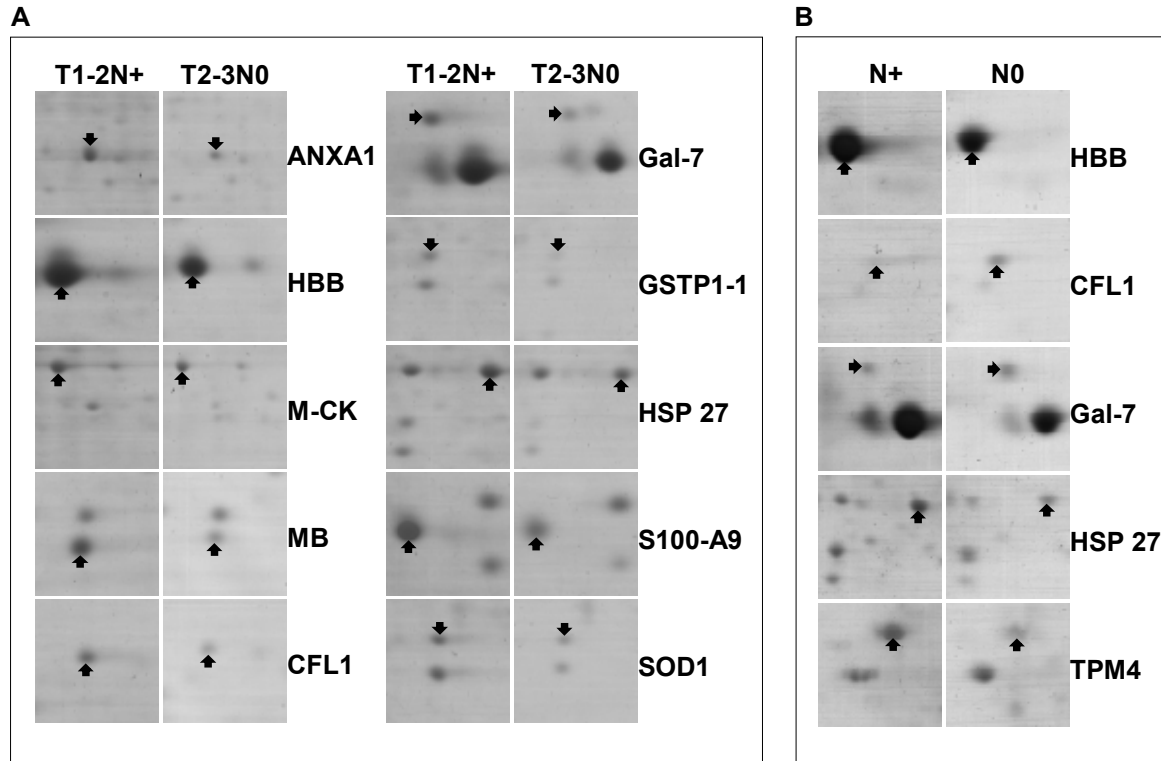


Figure 1

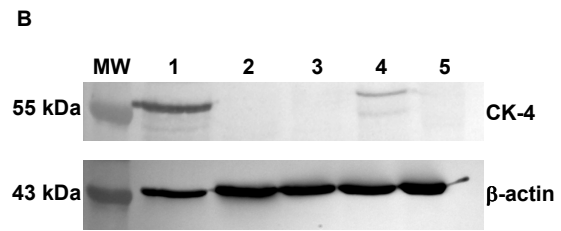
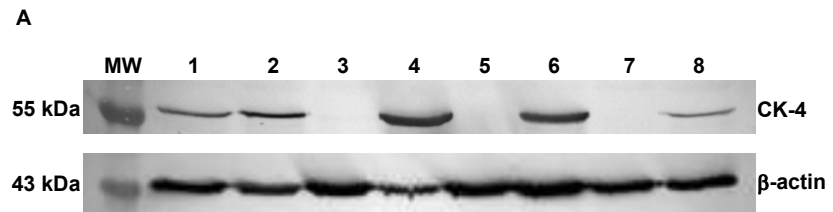


Figure 2

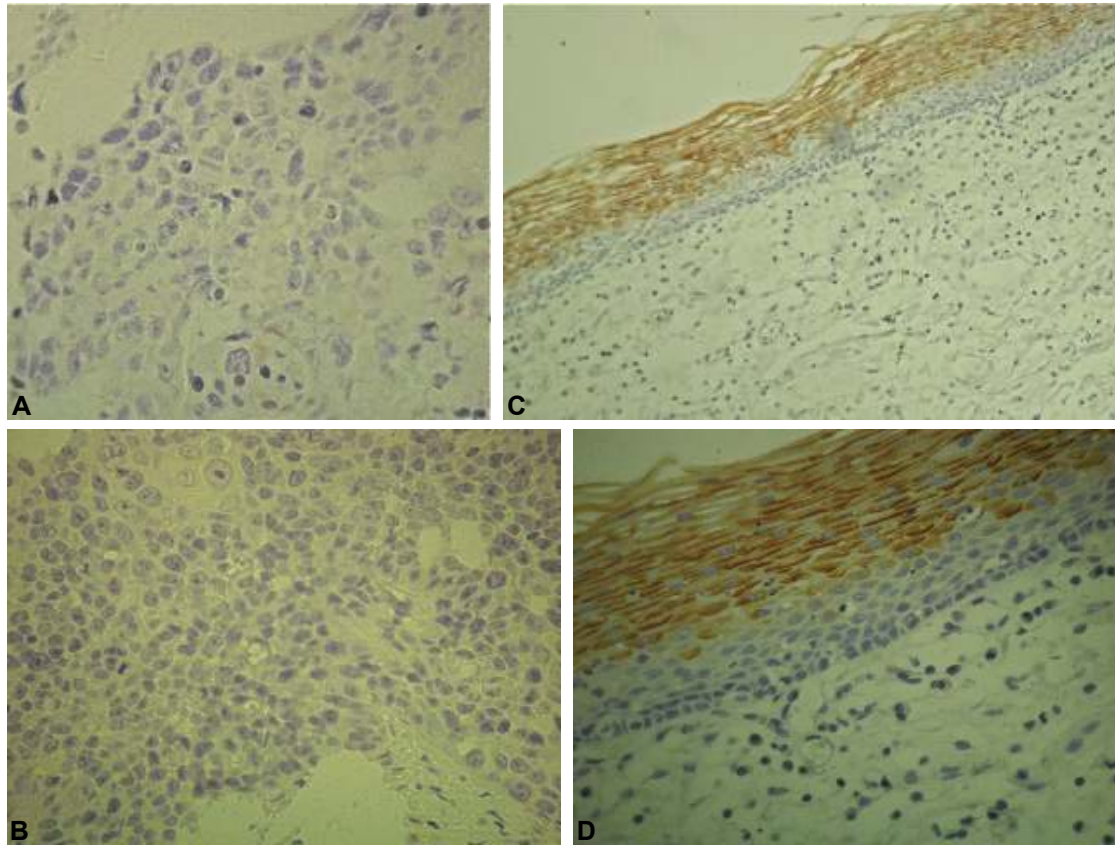


Figure 3

Table 1. Experimental design for 2-D DIGE

Gel	Dye			-
	Cy3	Cy5	Cy2	
	<i>T1-2N+ samples</i>	<i>T3N0 samples</i>		
1	CP3/0049	CP3/0103	Internal standard	
2	CP3/0012	CP2/0088	Internal standard	
3	CP3/0087	CP1/0021	Internal standard	
4	CP3/0050	CP1/0200	Internal standard	
	<i>T3N0 samples</i>	<i>T1-2N+ samples</i>		
5	CP3/0033	CP3/0193	Internal standard	
6	CP2/1012	CP1/0094	Internal standard	
7	CP1/0191	CP2/0120	Internal standard	
8	CP1/0075	CP3/0046	Internal standard	
9				unlabeled internal standard
10				unlabeled internal standard

CP1=Arnaldo Vieira de Carvalho Hospital; CP2=Heliópolis Hospital; CP3=Hospital of Clinics, SP, Brazil

Table 2. Differentially expressed proteins in oral squamous cell carcinomas identified by 2-DE and MS/MS. Lower (↓) and higher (↑) expression in T1-2N+ tumors versus T2-3N0 tumors (A) and in T2-4N+ tumors versus T2-4N0 tumors (D); lower (↓) and higher (↑) expression in tumors in relation to normal tissues (B, C, E, F, G); lower (↓) and higher (↑) expression in T1-2N+ tumors from C02/C04 sites (H) versus T1-2N+ tumors from C01 site (I). C01=Malignant neoplasm of base of tongue; C02=Higher parts of tongue; C03=Malignant neoplasm of other and unspecified parts of tongue; C04=Malignant neoplasm of floor of mouth

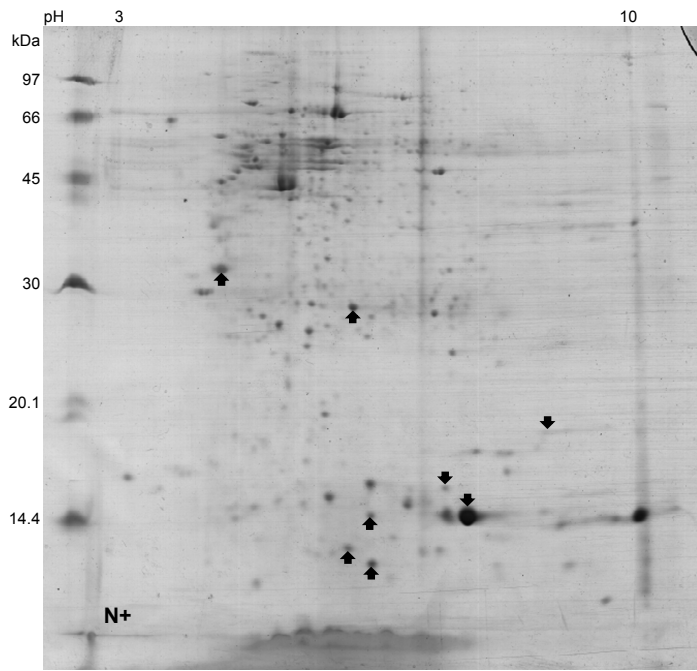
Protein identified	C02/C04										C01		C02/C04 ^H	
	T1-2N+ X T2-3N0 tumors ^A	T1-2N+ tumors X normal tissues ^B	T2-3N0 tumors X normal tissues ^C	T2-4N+ X T2-4N0 tumors ^D	T2-4N+ tumors X normal tissues ^E	T2-4N0 tumors X normal tissues ^F	T1-2N+ tumors X T1-2N+ ^H	T1-2N+ tumors X normal tissues ^G	T1-2N+ X C01 ^I	T1-2N+ X T1-2N+ ^I	T1-2N+ X T1-2N+ ^I	T1-2N+ X T1-2N+ ^I	T1-2N+ X T1-2N+ ^I	
Myosin light chain 1/3, skeletal muscle isoform		↓	↓		↓	↓						↑		
Annexin A1	↑		↓		↓	↓								
Annexin A2					↓	↓								
Beta-globin	↑	↓		↑										
Carbonic anhydrase 3		↓	↓		↓	↓			↓					
Creatine kinase M-type	↑	↓	↓		↓	↓			↓			↑		
Cytokeratin-13					↓	↓			↓					
Cytokeratin-4		↓			↓	↓			↓			↓		
Gamma-actin		↓	↓		↓	↓			↓			↓		
Myoglobin	↑	↓	↓		↓	↓			↓			↑		
Myosin light chain 3		↓	↓		↓	↓			↓			↑		
Myosin regulatory light chain 2, skeletal muscle isoform		↓	↓		↓	↓			↓			↑		
Myosin regulatory light chain 2, ventricular/cardiac muscle isoform		↓	↓		↓	↓			↓			↑		
Tropomyosin-1		↓	↓		↓	↓			↓			↑		
Tropomyosin-2		↓	↓		↓	↓			↓			↑		
Tropomyosin-3		↓	↓		↓	↓			↓			↑		
Troponin T, slow skeletal muscle		↑	↑		↑	↑			↑			↑		
Alpha-enolase		↑	↑		↑	↑			↑			↑		
Cofilin-1	↑	↑	↑	↓					↑			↑		
Cyclophilin A		↑	↑			↑			↑			↑		
Cytokeratin-16									↑			↑		
Cytokeratin-19		↑	↑						↑			↑		
Galectin-7	↑	↑	↑	↓	↑	↑			↑			↑		
Glutathione S-transferase P	↑	↑	↑		↑	↑			↑			↑		
Heat shock 27 kDa protein		↑	↑	↑	↑	↑			↑			↑		
Protein S100-A9 (Calgranulin-B)	↑	↑	↓		↑	↑			↓			↑		
Serum albumin	↑	↑	↑		↑	↑			↑			↑		
Stratifin (14-3-3 protein sigma)		↑	↑		↑	↑			↑			↑		
Superoxide dismutase [Cu-Zn]	↑	↑	↑	↑	↑	↑			↑			↑		
Tropomyosin-4		↑	↑	↑	↑	↑			↑			↑		
Vimentin		↑	↑		↑	↑			↑			↑		

Additional Files

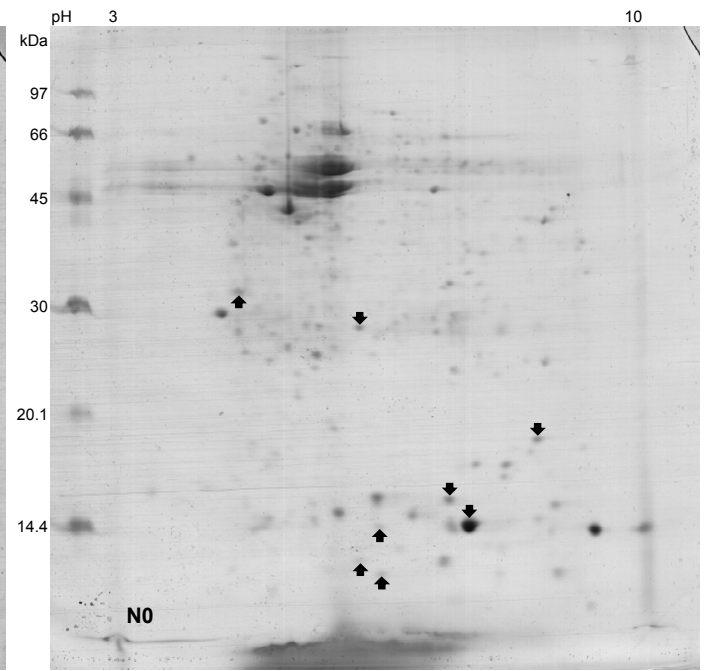
Supporting Figure 1. 2-DE maps of tumor pools from OSCC patients. Pools of N+ (A), N0 (B), T1-2N+ (C), and T2-3N0 (D) tumors. Differentially expressed proteins between A and B and between C and D are highlighted by arrows.

Supporting Figure 2. Detailed alteration patterns of proteins in OSCC tumors and surgical margins identified by 2-DE and mass spectrometry: myosin light chain 1/3, skeletal muscle isoform (MLC1/MLC3); beta-globin (HBB); carbonic anhydrase 3 (CA-III); creatine kinase M-type (M-CK); cytokeratin-4 (CK-4); gamma-actin (ACTG); myoglobin (MB); myosin light chain 3 (MYL3); myosin regulatory light chain 2, skeletal muscle isoform (MLC2B); myosin regulatory light chain 2, ventricular/cardiac muscle isoform (MLC-2v); tropomyosin-1 (TPM1); tropomyosin-2 (TPM2); tropomyosin-3 (TPM3); alpha-enolase (ENO1); cofilin-1 (CFL1); cyclophilin A (PPIase A); cytokeratin-19 (CK-19); glutathione S-transferase P (GSTP1-1); heat shock 27 kDa (HSP 27); calgranulin-B (S100-A9); serum albumin (ALB); stratifin (SFN); superoxide dismutase [Cu-Zn] (SOD1); tropomyosin-4 (TPM4); vimentin (VIM). T1-2N+ tumors and matched surgical margins from tongue (C02) and floor of mouth (C04).

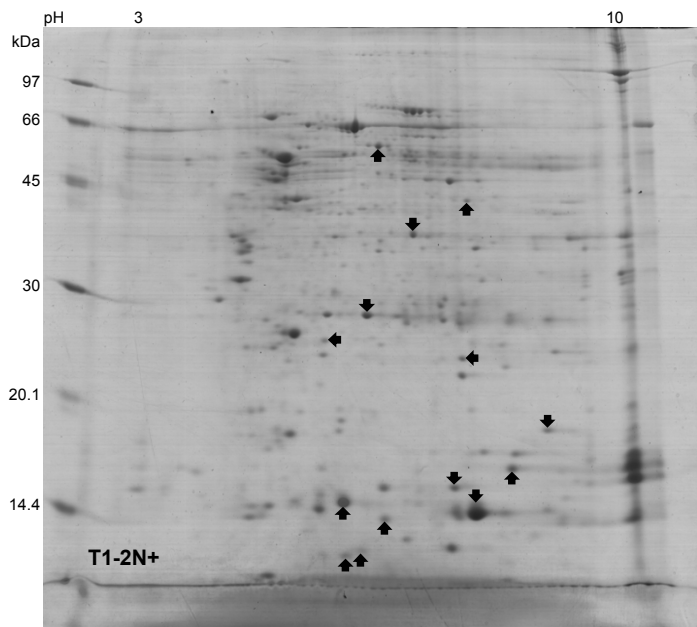
Supporting Figure 3. Detailed alteration patterns of proteins in OSCC tumors and surgical margins identified by 2-DE and mass spectrometry: myosin light chain 1/3, skeletal muscle isoform (MLC1/MLC3); annexin A1 (ANXA1); carbonic anhydrase 3 (CA-III); creatine kinase M-type (M-CK); gamma-actin (ACTG); myoglobin (MB); myosin light chain 3 (MYL3); myosin regulatory light chain 2, skeletal muscle isoform (MLC2B); myosin regulatory light chain 2, ventricular/cardiac muscle isoform (MLC-2v); tropomyosin-1 (TPM1); tropomyosin-2 (TPM2); tropomyosin-3 (TPM3); troponin T, slow skeletal muscle (TnTs); alpha-enolase (ENO1); cofilin-1 (CFL1); cyclophilin A (PPIase A); cytokeratin-19 (CK-19); galectin-7 (Gal-7); heat shock 27 kDa (HSP 27); serum albumin (ALB); stratifin (SFN); tropomyosin-4 (TPM4). T2-3N0 tumors and matched surgical margins from tongue (C02) and floor of mouth (C04).



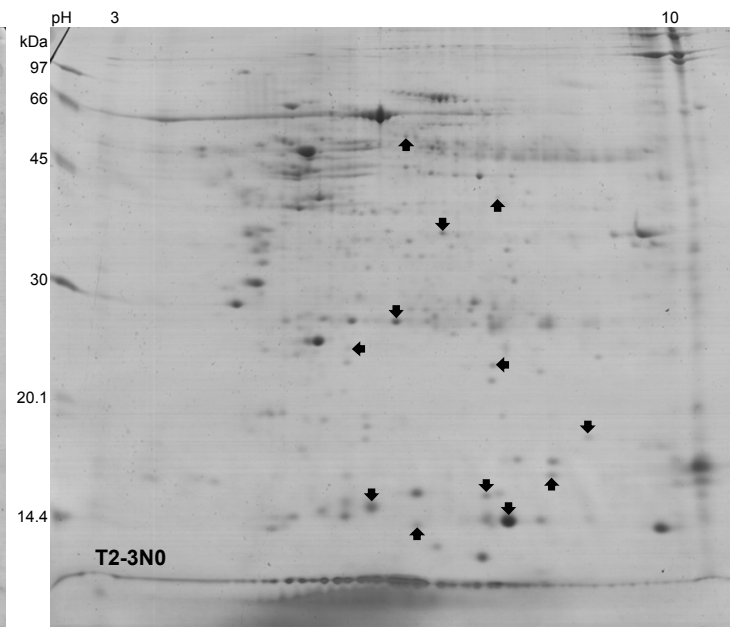
A



B

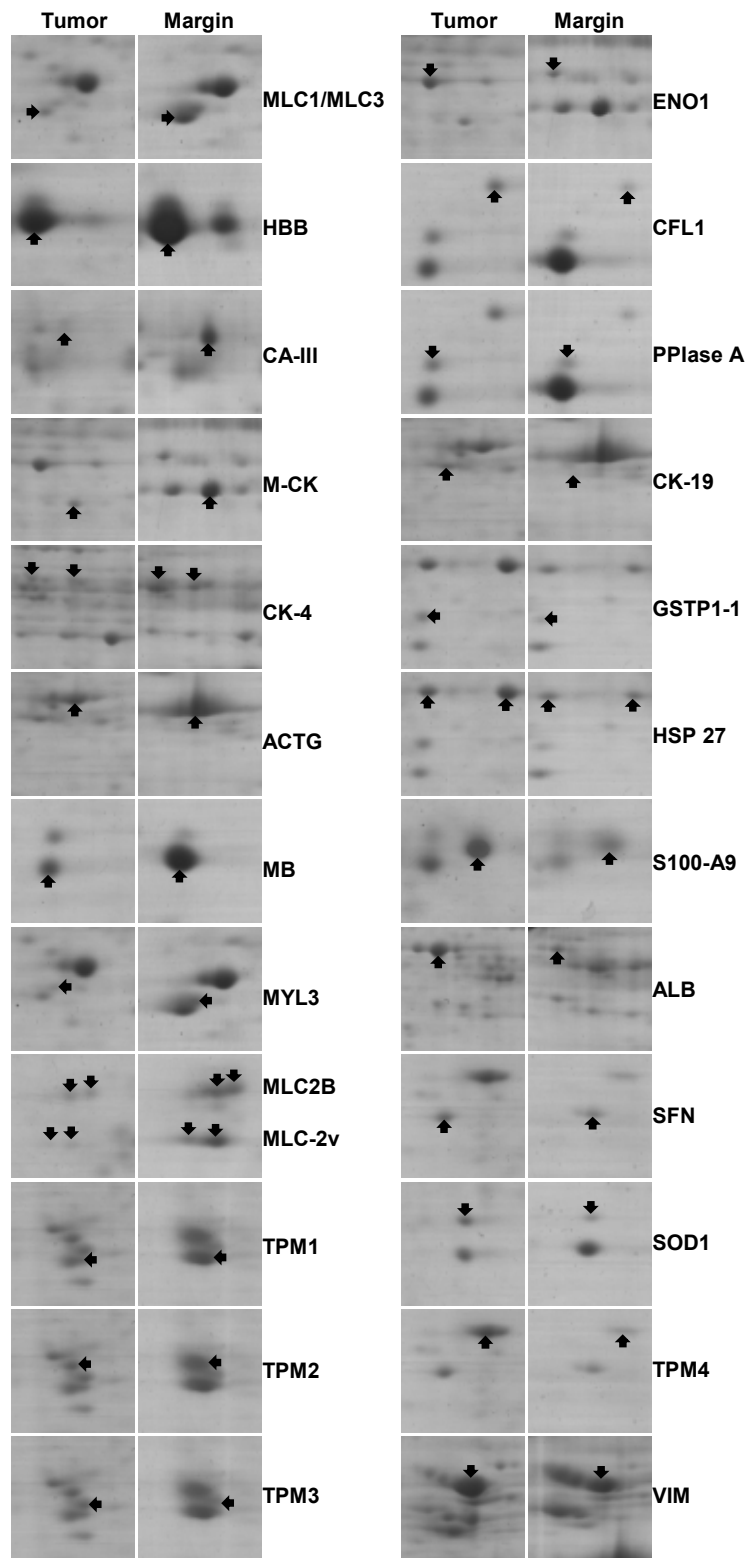


C

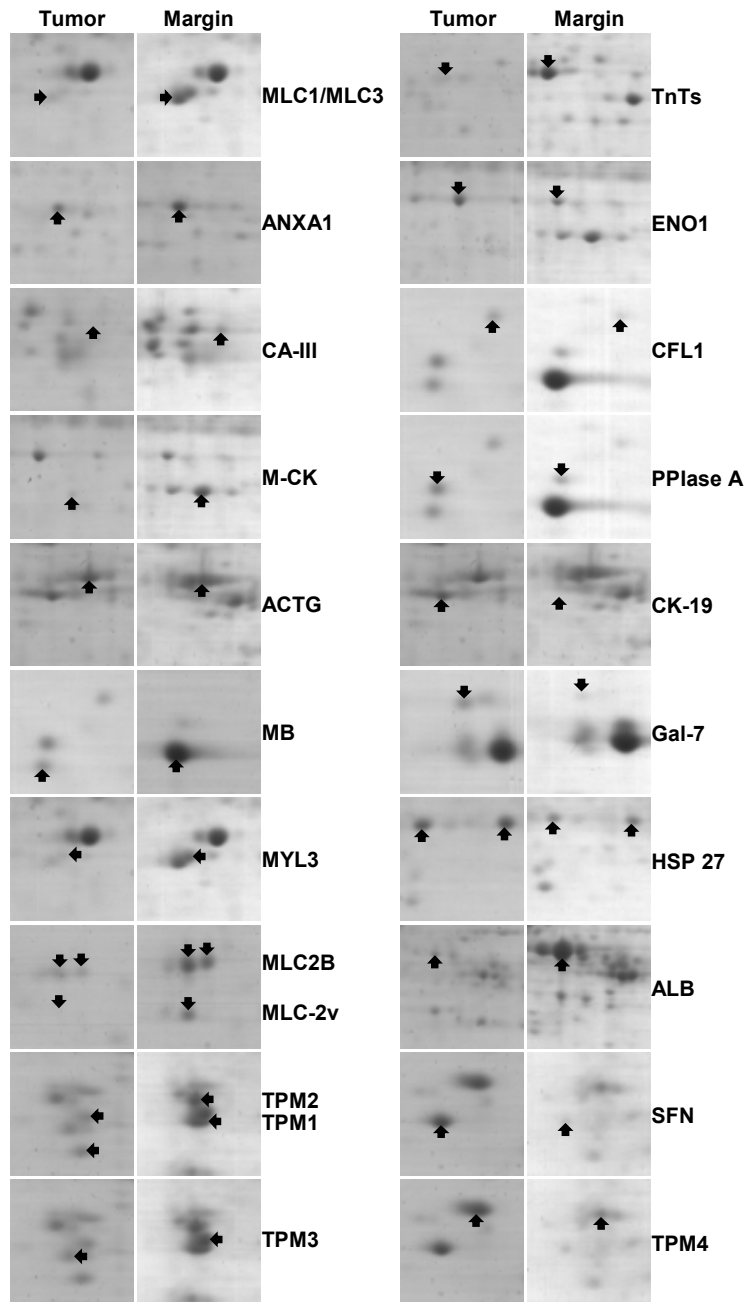


D

Supporting Figure 1



Supporting Figure 2



Supporting Figure 3

Supporting Table 1. Clinicopathological features of patients in this study

Supporting Table 2. Composition of pools used for 1-DE and 2-DE experiments

Supporting Table 3. Differentially expressed proteins identified by 2-DE and mass spectrometry in oral squamous cell carcinomas

Supporting Table 4. Proteins expressed in “more-aggressive” (T1-2N+) tumors. Proteins from about 10 to 45kD separated by 1-DE and identified by ESI-Q-TOF-MS/MS analysis

Supporting Table 5. Proteins expressed in “less-aggressive” (T3N0) tumors. Proteins from about 10 to 45kD separated by 1-DE and identified by ESI-Q-TOF-MS/MS analysis

Supporting Table 6. Proteins expressed in normal surgical margins. Proteins from about 10 to 45kD separated by 1-DE and identified by ESI-Q-TOF-MS/MS analysis

Supporting Table 1. Clinicopathological features of patients in this study

Case	Type of sample	Site ^{a)}	Gender /Age (ys)	AJCC ^{b)} pathologic stage	Histological differentiation	Lifetime smoking (yrs)	Lifetime alcohol consumption (yrs)	Patient status	Survival months	Vascular infiltration	Lymphatic infiltration	Perineural invasion	Techniques
264713	T/M	C06	F/54	T4N2bM0	-	P	P	-	-	-	-	-	WB
272020	T/M	C04	F/67	T3N2bM0	-	P	N	alive	24	-	-	-	WB
278241	T/M	C04	M/53	T4N1M0	-	P	P	alive	10	-	-	-	2-DE/WB
278980	T/M	C04	F/75	T4N2BM0	-	P	N	-	-	-	-	-	2-DE/WB
279088	T/M	C04	M/58	T2N2cMX	-	P	N	-	-	-	-	-	2-DE/WB
279131	T/M	C04	M/51	T2N0M0	-	P	P	alive/d	11	-	-	-	2-DE/WB
279627	T/M	C02	M/45	T4N1M0	-	P	P	alive	7	-	-	-	2-DE/WB
280334	T/M	C02	M/51	T2N2AM1	-	P	P	alive	7	-	-	-	2-DE/WB
275629	T	C04	M/54	T4N0M0	-	P	P	alive	13	-	-	-	2-DE/WB
277479	M	C04	M/55	T4N3M0	-	P	P	alive	10	-	-	-	WB
277855	M	C02	M/52	T3N1M0	-	P	P	alive	11	-	-	-	WB
279930	M	C04	M/66	T2N0MX	-	-	-	-	-	-	-	-	2-DE/WB
279958	M	C02	M/62	T4N0M0	-	P	N	alive	4	-	-	-	2-DE/WB
281581	M	C02	F/65	T2N0MX	-	P	P	-	-	-	-	-	2-DE
277243	M	C01	M/73	T4N1M0	-	P	N	-	-	-	-	-	WB
278354	M	C02	M/66	T2N0M0	-	P	P	-	-	-	-	-	WB
CP1/0094	T/M	C04	M/44	T2N2BM0	Well	27	27	dd	31	No	No	No	2-DE/2-D DIGE
CP2/0120	T/M	C02	F/41	T2N1M0	Moderate	24	N	dd	16	No	Yes	No	2-DE/2-D DIGE/IH
CP3/0012	T/M	C04	M/50	T1N1M0	Well	13	18	alive	74	No	No	No	2-DE/2-D DIGE
CP3/0046	T	C02	F/75	T2N2bM0	Moderate	23	67	dd	27	No	No	No	2-DE/2-D DIGE
CP3/0049	T/M	C02	M/62	T2N2bM0	Moderate	34	37	alive	23	No	No	Yes	2-DE/2-D DIGE
CP3/0050	T/M	C02	F/44	T2N1M0	Well	26	17	dd	20	No	No	Yes	2-DE/2-D DIGE
CP3/0083	T/M	C02	F/55	T1N1M0	Moderate	46	40	alive	47	No	Yes	No	2-DE
CP3/0087	T/M	C02	M/52	T2N2cM0	Moderate	40	37	d	46	No	No	Yes	2-DE/2-D DIGE
CP3/0139	T	C02	M/50	T2N2aM0	Moderate	37	37	alive	64	Yes	Yes	Yes	1-DE/2-DE
CP3/0193	T	C02	M/49	T2N1M0	Well	10	15	alive	56	No	No	No	2-DE/2-D DIGE
CP2/0175	M	C04	M/61	T2N2bM0	Moderate	43	41	dd	7	No	No	No	2-DE
CP1/0017	T/M	C02	M/55	T2N0M0	Moderate	45	29	alive	62	No	No	No	2-DE

Supporting Table 2. Composition of pools used for 1-DE and 2-DE experiments

Pool	Sites ^{a)}	Cases	Type of sample	Groups ^{b)}	Technique
1	C02/C04	CP2/0051 CP2/0132 CP3/0139 CP3/0280 CP3/0292	Tumors	T1-2N+	1-DE
2	C02/C04	CP1/0031 CP1/0151 CP1/0191 CP1/0277 CP1/0283	Tumors	T3N0	1-DE
3	C02/C04	CP1/0151 CP1/0262 CP1/0277 CP2/0051 CP3/0280 CP3/0292	Normal Surgical Margins	T1-2N+/ T3N0	1-DE
4	C02/C04	CP1/0094 CP2/0120 CP3/0012 CP3/0046 CP3/0049 CP3/0050 CP3/0083 CP3/0087 CP3/0139 CP3/0193	Tumors	T1-2N+	2-DE
5	C02/C04	CP1/0094 CP2/0120 CP2/0175 CP3/0012 CP3/0049 CP3/0050 CP3/0083 CP3/0087	Normal Surgical Margins	T1-2N+	2-DE
6	C02/C04	CP1/0017 CP1/0075 CP1/0080 CP1/0083 CP2/0093 CP3/0101 CP3/0138 CP3/0004 CP3/0120	Tumors	T2-3N0	2-DE
7	C02/C04	CP1/0017 CP1/0051 CP1/0075 CP1/0080 CP1/0083 CP2/0185 CP2/1004 CP3/0101 CP3/0120	Normal Surgical Margins	T2-3N0	2-DE
8	C02/C04	279088 279627 280334	Tumors	T2-4N+	2-DE
9	C02/C04	278241 278980	Normal Surgical Margins	T2-4N+	2-DE

Supporting Table 3. Differentially expressed proteins identified by 2-DE and mass spectrometry in oral squamous cell carcinomas

Protein	Accession no.	Theoretical mol. mass/pI	No. matched peptides	Mascot score^A	GO term – Process
Alpha-enolase (ENO1)	P06733	47.037/ 6.99	3	187	Negative regulation of cell growth Negative regulation of transcription
Annexin A1 (ANXA1)	P04083	38.583/ 6.64	3	131	Anti-apoptosis Cell motion Signal transduction Inflammatory response Keratinocyte differentiation Lipid metabolic process Protein modification process
Annexin A2 (ANXA2)	P07355	38.472/ 7.56	12	119	System development
Beta-globin (HBB)	P68871	15.867/ 6.81	4	211	Transport
Carbonic anhydrase 3 (CA-III)	P07451	29.426/ 6.94	2	74	Metabolic process Response to oxidative stress
Cofilin-1 (CFL1)	P23528	18.371/ 8.26	2	163	Rho protein signal transduction Anti-apoptosis
Creatine kinase M-type (M-CK)	P06732	43.101/ 6.77	5	215	Metabolic process
Cyclophilin A (PPIase A)	P62937	17.881/ 7.82	1	107	Protein folding Viral genome replication
Cytokeratin-13 (CK-13)	P13646	49.588/ 4.91	5	195	Epidermis development
Cytokeratin-16 (CK-16)	P08779	51.136/ 4.98	5	298	Cell proliferation Epidermis development
Cytokeratin-19 (CK-19)	P08727	44.091/ 5.05	3	101	Response to estrogen stimulus Cytoskeleton organization
Cytokeratin-4 (CK-4)	P19013	57.285/ 6.25	4	177	Epithelial cell differentiation Negative regulation of epithelial cell proliferation
Galectin-7 (Gal-7)	P47929	14.943/7.00	4	274	Cell adhesion
Gamma-actin (ACTG)	P63261	41.792/ 5.31	4	123	Cell motion
Glutathione S-transferase P (GSTP1-1)	P09211	23.224/ 5.44	3	225	Anti-apoptosis System development
Heat shock 27 kDa protein (HSP 27)	P04792	22.782/ 5.98	4	233	Anti-apoptosis Cell motion Translation

Supporting Table 4. Proteins expressed in “more-aggressive” (T1-2N+) tumors. Proteins from about 10 to 45kD separated by 1-DE and identified by ESI-Q-TOF-MS/MS analysis

Code of gene	Protein
gi 338043	[Human pre-mRNA splicing factor SF2p32, complete sequence.], gene product
gi 5726310	14-3-3 gamma protein [Homo sapiens]
gi 437363	14-3-3n
gi 1041969	17 kda cyclophilin A {internal fragment} [human, first trimester decidual and placental tissue, Pep
gi 693933	2-phosphopyruvate-hydratase alpha-enolase; carbonate dehydratase [Homo sapiens]
gi 5453880	acidic (leucine-rich) nuclear phosphoprotein 32 family, member A [Homo sapiens]
gi 178067	actin prepeptide [Homo sapiens]
gi 5031599	actin related protein 2/3 complex subunit 2 [Homo sapiens]
gi 5031593	actin related protein 2/3 complex subunit 5 [Homo sapiens]
gi 63055057	actin, beta-like 2 [Homo sapiens]
gi 4501887	actin, gamma 1 propeptide [Homo sapiens]
gi 62420949	actin-like protein [Homo sapiens]
gi 4502211	ADP-ribosylation factor 6 [Homo sapiens]
gi 28614	aldolase A [Homo sapiens]
gi 3098514	aldose reductase-related protein [Homo sapiens]
gi 30030	alpha-1 collagen VI (AA 574-1009) [Homo sapiens]
gi 178027	alpha-actin [Homo sapiens]
gi 183801	alpha-globin [Homo sapiens]
gi 37492	alpha-tubulin [Homo sapiens]
gi 179074	alternative
gi 4757756	annexin A2 isoform 2 [Homo sapiens]
gi 4502101	annexin I [Homo sapiens]
gi 58222648	anti-tetanus toxoid immunoglobulin light chain variable region [Homo sapiens]
gi 28918	antithrombin III [Homo sapiens]
gi 178855	apolipoprotein J precursor [Homo sapiens]
gi 284164	arginine-rich protein - human
gi 13625797	asporin precursor [Homo sapiens]
gi 3334899	autoantigen p542 [Homo sapiens]
gi 825671	B23 nucleophosmin (280 AA) [Homo sapiens]
gi 29383	BBC1 [Homo sapiens]
gi 1673514	B-cell receptor associated protein [Homo sapiens]

gi|4501885 beta actin [Homo sapiens]
gi|2654381 beta chain HLA-DQ molecule [Homo sapiens]
gi|193244897 beta globin [Homo sapiens]
gi|66473265 beta globin chain [Homo sapiens]
gi|6573280 beta tropomyosin [Homo sapiens]
gi|13562114 beta tubulin 1, class VI [Homo sapiens]
gi|179409 beta-globin
gi|21591225 BIA2 protein [Homo sapiens]
gi|179433 biglycan [Homo sapiens]
gi|306875 C protein [Homo sapiens]
gi|4885111 calmodulin-like 3 [Homo sapiens]
gi|7673316 calmodulin-like skin protein [Homo sapiens]
gi|5453599 capping protein (actin filament) muscle Z-line, alpha 2 [Homo sapiens]
gi|433308 capping protein alpha [Homo sapiens]
gi|4502517 carbonic anhydrase I [Homo sapiens]
gi|4557395 carbonic anhydrase II [Homo sapiens]
gi|4502599 carbonyl reductase 1 [Homo sapiens]
gi|2460249 cardiac ventricular troponin C [Homo sapiens]
gi|951338 CAS
gi|4503143 cathepsin D preproprotein [Homo sapiens]
gi|4929769 CGI-150 protein [Homo sapiens]
gi|4139784 Chain A, Canine Gdp-Ran Q69I Mutant
gi|75766275 Chain A, Crystal Structure Of Human Cypa Mutant K131a
gi|3891470 Chain A, Crystal Structure Of Human Galectin-7 In Complex With Galactosamine
gi|186972783 Chain A, Crystal Structure Of Iodinated Human Saposin D In Space Group C2221
gi|90108664 Chain A, Crystal Structure Of Lipid-Free Human Apolipoprotein A-I
gi|999892 Chain A, Crystal Structure Of Recombinant Human Triosephosphate Isomerase At 2.8 Angstroms Resoluti
gi|10835792 Chain A, Crystal Structure Of The Fab Fragment Of A Human Monoclonal Igm Cold Agglutinin
gi|1633054 Chain A, Cyclophilin A Complexed With Dipeptide Gly-Pro
gi|3318841 Chain A, Horf6 A Novel Human Peroxidase Enzyme
gi|1065361 Chain A, Human Adp-Ribosylation Factor 1 Complexed With Gdp, Full Length Non-Myristoylated
gi|4699695 Chain A, Human Beta-Tryptase: A Ring-Like Tetramer With Active Sites Facing A Central Pore
gi|3891975 Chain A, Human Cathepsin G
gi|15825659 Chain A, Human Factor Viii C2 Domain Complexed To Human Monoclonal Bo2c11 Fab

gi 1942609	Chain A, Human Rap1a, Residues 1-167, Double Mutant (E30d,K31e) Complexed With Gppnhp And The Ras-B
gi 157830361	Chain A, Human Serum Albumin In A Complex With Myristic Acid And Tri- Iodobenzoic Acid
gi 2981801	Chain A, Human Transcriptional Coactivator Pc4 C-Terminal Domain
gi 3114508	Chain A, R State Human Hemoglobin [alpha V96w], Carbonmonoxy
gi 159162145	Chain A, Rotamer Strain As A Determinant Of Protein Structural Specificity
gi 16974825	Chain A, Solution Structure Of Calcium-Calmodulin N-Terminal Domain
gi 31615803	Chain A, Synthetic Ubiquitin With Fluoro-Leu At 50 And 67
gi 809185	Chain A, The Effect Of Metal Binding On The Structure Of Annexin V And Implications For Membrane Bi
gi 494066	Chain A, Three-Dimensional Structure Of Class Pi Glutathione S- Transferase From Human Placenta In
gi 190613401	Chain A, Unusual Twinning In Crystals Of The Cits Binding Antibody Fab Fragment F3p4
gi 229597861	Chain A, X-Ray Crystal Structure Of Coil 1a Of Human Vimentin
gi 1421609	Chain A, X-Ray Structure Of Nm23 Human Nucleoside Diphosphate Kinase B Complexed With Gdp At 2 Angs
gi 3660434	Chain B, Crystal Structure Of Deoxy-Human Hemoglobin Beta6 Glu->trp
gi 166007160	Chain C, Solution Structure Of Human Immunoglobulin M
gi 161760892	Chain D, Neutron Structure Analysis Of Deoxy Human Hemoglobin
gi 349905	Chain F, Atomic Structures Of Wild-Type And Thermostable Mutant Recombinant Human Cu, Zn Superoxide
gi 493869	Chain L, Crystal Structure Of A Chimeric Fab' Fragment Of An Antibody Binding Tumour Cells
gi 66360499	Chain O, Crystal Structure Of Anthrax Edema Factor (Ef) In Complex With Calmodulin In The Presence
gi 230867	Chain R, Twinning In Crystals Of Human Skeletal Muscle D- Glyceraldehyde-3-Phosphate Dehydrogenase
gi 180663	c-myc binding protein [Homo sapiens]
gi 5031635	cofilin 1 (non-muscle) [Homo sapiens]
gi 3127926	collagen type VI, alpha 3 chain [Homo sapiens]
gi 30130	colligin [Homo sapiens]
gi 4503057	crystallin, alpha B [Homo sapiens]
gi 181250	cyclophilin
gi 4758086	cysteine and glycine-rich protein 1 isoform 1 [Homo sapiens]
gi 4502981	cytochrome c oxidase subunit IV isoform 1 precursor [Homo sapiens]
gi 30311	cytokeratin 18 (424 AA) [Homo sapiens]
gi 34073	cytokeratin 4 (408 AA) [Homo sapiens]
gi 181400	cytokeratin 8
gi 311614	dermatopontin [Homo sapiens]
gi 181540	desmin [Homo sapiens]
gi 1066080	DNA-binding protein [Homo sapiens]
gi 9802306	DNA-binding protein TAXREB107 [Homo sapiens]

gi 4557553	emerin [Homo sapiens]
gi 31179	enolase [Homo sapiens]
gi 119610782	enolase 3 (beta, muscle), isoform CRA_b [Homo sapiens]
gi 187302	epithelial cell marker protein 1
gi 4503475	eukaryotic translation elongation factor 1 alpha 2 [Homo sapiens]
gi 4503477	eukaryotic translation elongation factor 1 beta 2 [Homo sapiens]
gi 23345100	extracellular matrix protein periostin-bm [Homo sapiens]
gi 5453597	F-actin capping protein alpha-1 subunit [Homo sapiens]
gi 4557581	fatty acid binding protein 5 (psoriasis-associated) [Homo sapiens]
gi 182516	ferritin light subunit [Homo sapiens]
gi 4504981	galectin-1 [Homo sapiens]
gi 178045	gamma-actin [Homo sapiens]
gi 2282013	GAPDH-2 like [Homo sapiens]
gi 4758438	glucagon-like peptide 2 receptor precursor [Homo sapiens]
gi 31645	glyceraldehyde-3-phosphate dehydrogenase [Homo sapiens]
gi 996057	gp25l2 [Homo sapiens]
gi 386758	GRP78 precursor
gi 5174447	guanine nucleotide binding protein (G protein), beta polypeptide 2-like 1 [Homo sapiens]
gi 4885371	H1 histone family, member 0 [Homo sapiens]
gi 5174449	H1 histone family, member X [Homo sapiens]
gi 4504253	H2A histone family, member X [Homo sapiens]
gi 4504255	H2A histone family, member Z [Homo sapiens]
gi 223976	haptoglobin Hp2
gi 119613177	hCG1643544 [Homo sapiens]
gi 119612018	hCG1808204 [Homo sapiens]
gi 119630082	hCG2007439 [Homo sapiens]
gi 119612312	hCG2008737 [Homo sapiens]
gi 119617765	hCG26523, isoform CRA_a [Homo sapiens]
gi 5729877	heat shock 70kDa protein 8 isoform 1 [Homo sapiens]
gi 662841	heat shock protein 27 [Homo sapiens]
gi 229149	hemoglobin beta
gi 23268683	hemoglobin beta chain variant Hb.Sinai-Bel Air [Homo sapiens]
gi 4758516	hepatoma-derived growth factor isoform a [Homo sapiens]
gi 4504447	heterogeneous nuclear ribonucleoprotein A2/B1 isoform A2 [Homo sapiens]

gi 14043072	heterogeneous nuclear ribonucleoprotein A2/B1 isoform B1 [Homo sapiens]
gi 34740329	heterogeneous nuclear ribonucleoprotein A3 [Homo sapiens]
gi 4826760	heterogeneous nuclear ribonucleoprotein F [Homo sapiens]
gi 4885381	histone cluster 1, H1b [Homo sapiens]
gi 4885375	histone cluster 1, H1c [Homo sapiens]
gi 4885377	histone cluster 1, H1d [Homo sapiens]
gi 4504239	histone cluster 1, H2ai [Homo sapiens]
gi 24586679	histone cluster 1, H2ba [Homo sapiens]
gi 4504263	histone cluster 1, H2bm [Homo sapiens]
gi 45219796	Histone cluster 1, H3i [Homo sapiens]
gi 28195394	histone cluster 2, H2ab [Homo sapiens]
gi 56203471	histone cluster 2, H3, pseudogene 2 [Homo sapiens]
gi 356168	histone H1b
gi 31979	histone H2A.2 [Homo sapiens]
gi 184086	histone H2B.1
gi 386772	histone H3 [Homo sapiens]
gi 32177	HLA-B27 [Homo sapiens]
gi 7739447	hnRNP 2H9D [Homo sapiens]
gi 33877030	HNRPCL1 protein [Homo sapiens]
gi 306549	homology to rat ribosomal protein L23
gi 1040689	Human Diff6,H5,CDC10 homologue [Homo sapiens]
gi 38522	human elongation factor-1-delta [Homo sapiens]
gi 51476390	hypothetical protein [Homo sapiens]
gi 117938314	hypothetical protein LOC51237 [Homo sapiens]
gi 229536	Ig A L
gi 229585	Ig A1 Bur
gi 7438711	Ig kappa chain NIG26 precursor - human
gi 106586	Ig kappa chain V-III (KAU cold agglutinin) - human
gi 58476682	IGL@ protein [Homo sapiens]
gi 46254000	immunoglobulin heavy chain [Homo sapiens]
gi 39938240	immunoglobulin heavy chain variable region [Homo sapiens]
gi 306958	immunoglobulin kappa chain [Homo sapiens]
gi 33700	immunoglobulin lambda light chain [Homo sapiens]
gi 21669601	immunoglobulin lambda light chain VLJ region [Homo sapiens]

gi 218783334	immunoglobulin light chain [Homo sapiens]
gi 51103395	immunoglobulin variable region VL kappa domain [Homo sapiens]
gi 386848	keratin [Homo sapiens]
gi 4557699	keratin 12 [Homo sapiens]
gi 131412225	keratin 13 isoform a [Homo sapiens]
gi 4557701	keratin 17 [Homo sapiens]
gi 42760012	keratin 3 [Homo sapiens]
gi 9739163	keratin 5 [Homo sapiens]
gi 28173564	keratin 73 [Homo sapiens]
gi 386850	keratin K5
gi 386849	keratin type II [Homo sapiens]
gi 12698073	KIAA1764 protein [Homo sapiens]
gi 619788	L21 ribosomal protein [Homo sapiens]
gi 34234	laminin-binding protein [Homo sapiens]
gi 40254924	leucine rich repeat containing 59 [Homo sapiens]
gi 5031857	L-lactate dehydrogenase A isoform 1 [Homo sapiens]
gi 4557032	L-lactate dehydrogenase B [Homo sapiens]
gi 34709	manganese superoxide dismutase (MnSOD) [Homo sapiens]
gi 453369	maspin
gi 32189394	mitochondrial ATP synthase beta subunit precursor [Homo sapiens]
gi 28336	mutant beta-actin (beta'-actin) [Homo sapiens]
gi 190613770	mutant beta-globin [Homo sapiens]
gi 229361	myoglobin
gi 1220346	myosin light chain 2
gi 2605594	myosin regulatory light chain [Homo sapiens]
gi 5453740	myosin, light chain 12A, regulatory, non-sarcomeric [Homo sapiens]
gi 17986258	myosin, light chain 6, alkali, smooth muscle and non-muscle isoform 1 [Homo sapiens]
gi 4502281	Na ⁺ /K ⁺ -ATPase beta 3 subunit [Homo sapiens]
gi 553254	NADH cytochrome b5 reductase (EC 1.6.2.2) [Homo sapiens]
gi 5031931	nascent polypeptide-associated complex alpha subunit isoform b [Homo sapiens]
gi 930063	neurone-specific enolase [Homo sapiens]
gi 913159	neuropolypeptide h3 [human, brain, Peptide, 186 aa]
gi 393317	osteoblast specific factor 2 [Homo sapiens]
gi 7661704	osteoglycin preproprotein [Homo sapiens]

gi|2209347 p21-Arc [Homo sapiens]
gi|895845 p64 CLCP [Homo sapiens]
gi|30102944 peptidylprolyl isomerase A-like 4A [Homo sapiens]
gi|4505591 peroxiredoxin 1 [Homo sapiens]
gi|1498227 PHAPI2b protein [Homo sapiens]
gi|189868 phosphoglycerate mutase [Homo sapiens]
gi|2627129 polyubiquitin [Homo sapiens]
gi|190200 porin
gi|238427 Porin 3 IHM [human, skeletal muscle membranes, Peptide, 282 aa]
gi|145309046 POTE-2 alpha-actin [Homo sapiens]
gi|219978 prealbumin [Homo sapiens]
gi|239753333 PREDICTED: actin, beta-like 3 [Homo sapiens]
gi|169171114 PREDICTED: hypothetical protein [Homo sapiens]
gi|88988289 PREDICTED: hypothetical protein LOC648000 isoform 3 [Homo sapiens]
gi|109122155 PREDICTED: similar to 60S ribosomal protein L17 (L23) isoform 1 [Macaca mulatta]
gi|169213772 PREDICTED: similar to actin alpha 1 skeletal muscle protein [Homo sapiens]
gi|51464364 PREDICTED: similar to myosin regulatory light chain MRCL2 [Homo sapiens]
gi|73961071 PREDICTED: similar to tropomyosin 3 isoform 2 isoform 5 [Canis familiaris]
gi|12408675 prefoldin subunit 2 [Homo sapiens]
gi|337758 pre-serum amyloid P component [Homo sapiens]
gi|14189972 PRO2290 [Homo sapiens]
gi|4826898 profilin 1 [Homo sapiens]
gi|4505773 prohibitin [Homo sapiens]
gi|190447 prosomal protein P30-33K
gi|5453990 proteasome activator subunit 1 isoform 1 [Homo sapiens]
gi|1710248 protein disulfide isomerase-related protein 5 [Homo sapiens]
gi|134133226 protein expressed in prostate, ovary, testis, and placenta 2 [Homo sapiens]
gi|189617 protein PP4-X
gi|229526 protein Rei,Bence-Jones
gi|190668 psoriasin
gi|13786129 RAB33B, member RAS oncogene family [Homo sapiens]
gi|1491714 rab-related GTP-binding protein [Homo sapiens]
gi|29468353 RALY-like protein isoform 1 [Homo sapiens]
gi|182640 rapamycin-binding protein

gi 6912638	ras suppressor protein 1 isoform 1 [Homo sapiens]
gi 234746	RAS-related protein MEL [Homo sapiens]
gi 83674986	rcTPM3 [Homo sapiens]
gi 112877	RecName: Full=Alpha-1-acid glycoprotein 1; Short=AGP 1; AltName: Full=Orosomucoid-1; Short=OMD 1; F
gi 123510	RecName: Full=Haptoglobin-related protein; Flags: Precursor
gi 133254	RecName: Full=Heterogeneous nuclear ribonucleoprotein A1; Short=hnRNP core protein A1; AltName: Ful
gi 122224	RecName: Full=HLA class II histocompatibility antigen, DQ(1) beta chain; AltName: Full=DC-3 beta ch
gi 27734452	RecName: Full=Ras-related protein Rab-15
gi 267108	RecName: Full=Tetranectin; Short=TN; AltName: Full=C-type lectin domain family 3 member B; AltName:
gi 36038	rho GDP dissociation inhibitor (GDI) [Homo sapiens]
gi 306553	ribosomal protein small subunit
gi 337518	ribosomal protein
gi 495126	ribosomal protein L11 [Homo sapiens]
gi 4506597	ribosomal protein L12 [Homo sapiens]
gi 4506617	ribosomal protein L17 [Homo sapiens]
gi 4506607	ribosomal protein L18 [Homo sapiens]
gi 4506609	ribosomal protein L19 [Homo sapiens]
gi 4506613	ribosomal protein L22 proprotein [Homo sapiens]
gi 4506619	ribosomal protein L24 [Homo sapiens]
gi 292435	ribosomal protein L26
gi 4506623	ribosomal protein L27 [Homo sapiens]
gi 4432754	ribosomal protein L27a [Homo sapiens]
gi 550019	ribosomal protein L28
gi 793843	ribosomal protein L29 [Homo sapiens]
gi 1655596	ribosomal protein L31 [Homo sapiens]
gi 1008856	ribosomal protein L34
gi 6005860	ribosomal protein L35 [Homo sapiens]
gi 14591909	ribosomal protein L5 [Homo sapiens]
gi 36138	ribosomal protein L6 [Homo sapiens]
gi 55958183	ribosomal protein L7a [Homo sapiens]
gi 4506663	ribosomal protein L8 [Homo sapiens]
gi 4506667	ribosomal protein P0 [Homo sapiens]
gi 4506669	ribosomal protein P1 isoform 1 [Homo sapiens]
gi 4506671	ribosomal protein P2 [Homo sapiens]

gi 4506679	ribosomal protein S10 [Homo sapiens]
gi 4506681	ribosomal protein S11 [Homo sapiens]
gi 4506685	ribosomal protein S13 [Homo sapiens]
gi 5032051	ribosomal protein S14 [Homo sapiens]
gi 4506691	ribosomal protein S16 [Homo sapiens]
gi 6755368	ribosomal protein S18 [Mus musculus]
gi 4506695	ribosomal protein S19 [Homo sapiens]
gi 3088342	ribosomal protein S23 [Homo sapiens]
gi 4506707	ribosomal protein S25 [Homo sapiens]
gi 4432748	ribosomal protein S27 [Homo sapiens]
gi 4506715	ribosomal protein S28 [Homo sapiens]
gi 550021	ribosomal protein S5
gi 337514	ribosomal protein S6 [Homo sapiens]
gi 4506743	ribosomal protein S8 [Homo sapiens]
gi 14141193	ribosomal protein S9 [Homo sapiens]
gi 14424542	RPL14 protein [Homo sapiens]
gi 37046660	RPL7L1 protein [Homo sapiens]
gi 5174661	S100 calcium binding protein A2 [Homo sapiens]
gi 7657532	S100 calcium-binding protein A6 [Homo sapiens]
gi 4506773	S100 calcium-binding protein A9 [Homo sapiens]
gi 49660012	sarcomeric tropomyosin kappa; TPM1-kappa [Homo sapiens]
gi 337930	scar protein
gi 1478503	SCG10 [Homo sapiens]
gi 407421	SEB4B [Homo sapiens]
gi 14149696	SEC31 homolog B [Homo sapiens]
gi 338039	set
gi 339958	skeletal muscle tropomyosin [Homo sapiens]
gi 4759158	small nuclear ribonucleoprotein D2 isoform 1 [Homo sapiens]
gi 177175	smooth muscle protein
gi 1770517	SMT3A protein [Homo sapiens]
gi 4506901	splicing factor, arginine/serine-rich 3 [Homo sapiens]
gi 72534660	splicing factor, arginine/serine-rich 7 [Homo sapiens]
gi 551638	SSR alpha subunit [Homo sapiens]
gi 5031851	stathmin 1 isoform a [Homo sapiens]

gi|16307067 SUB1 homolog (*S. cerevisiae*) [Homo sapiens]
gi|914044 surface-associated sulphhydryl protein, SASP=thioredoxin homolog [human, THP-1 monocytes, Peptide Pa
gi|438069 thiol-specific antioxidant protein [Homo sapiens]
gi|5803187 transaldolase 1 [Homo sapiens]
gi|2896146 transcriptional coactivator ALY [Homo sapiens]
gi|460789 transformation upregulated nuclear protein [Homo sapiens]
gi|48255905 transgelin [Homo sapiens]
gi|4507357 transgelin 2 [Homo sapiens]
gi|13129092 transmembrane protein 109 [Homo sapiens]
gi|12275860 tripartite motif protein TRIM31 alpha [Homo sapiens]
gi|27597085 tropomyosin 1 alpha chain isoform 5 [Homo sapiens]
gi|42476296 tropomyosin 2 (beta) isoform 1 [Homo sapiens]
gi|47519616 tropomyosin 2 (beta) isoform 2 [Homo sapiens]
gi|58652133 tropomyosin 3 [*Bos taurus*]
gi|24119203 tropomyosin 3 isoform 2 [Homo sapiens]
gi|223555975 tropomyosin 4 isoform 1 [Homo sapiens]
gi|4507651 tropomyosin 4 isoform 2 [Homo sapiens]
gi|119604930 tropomyosin 4, isoform CRA_c [Homo sapiens]
gi|49660014 tropomyosin alpha striated muscle isoform; TPM1-alpha [Homo sapiens]
gi|5803203 troponin T3, skeletal, fast isoform 1 [Homo sapiens]
gi|35959 tubulin 5-beta [Homo sapiens]
gi|7106439 tubulin, beta 5 [*Mus musculus*]
gi|1195531 type I keratin 16; K16 [Homo sapiens]
gi|5803225 tyrosine 3/tryptophan 5 -monooxygenase activation protein, epsilon polypeptide [Homo sapiens]
gi|4507953 tyrosine 3/tryptophan 5 -monooxygenase activation protein, zeta polypeptide [Homo sapiens]
gi|4507949 tyrosine 3-monooxygenase/tryptophan 5-monooxygenase activation protein, beta polypeptide [Homo sapi
gi|4507951 tyrosine 3-monooxygenase/tryptophan 5-monooxygenase activation protein, eta polypeptide [Homo sapie
gi|229532 ubiquitin
gi|34039 unnamed protein product [Homo sapiens]
gi|34071 unnamed protein product [Homo sapiens]
gi|34526448 unnamed protein product [Homo sapiens]
gi|21751806 unnamed protein product [Homo sapiens]
gi|28940 unnamed protein product [Homo sapiens]
gi|31092 unnamed protein product [Homo sapiens]

gi 34039	unnamed protein product [Homo sapiens]
gi 31092	unnamed protein product [Homo sapiens]
gi 7022475	unnamed protein product [Homo sapiens]
gi 194375299	unnamed protein product [Homo sapiens]
gi 32132	unnamed protein product [Homo sapiens]
gi 32486	unnamed protein product [Homo sapiens]
gi 34527363	unnamed protein product [Homo sapiens]
gi 34069	unnamed protein product [Homo sapiens]
gi 16554039	unnamed protein product [Homo sapiens]
gi 194376242	unnamed protein product [Homo sapiens]
gi 34039	unnamed protein product [Homo sapiens]
gi 32486	unnamed protein product [Homo sapiens]
gi 194374397	unnamed protein product [Homo sapiens]
gi 194388338	unnamed protein product [Homo sapiens]
gi 31170	unnamed protein product [Homo sapiens]
gi 32111	unnamed protein product [Homo sapiens]
gi 194375299	unnamed protein product [Homo sapiens]
gi 31092	unnamed protein product [Homo sapiens]
gi 34039	unnamed protein product [Homo sapiens]
gi 32111	unnamed protein product [Homo sapiens]
gi 34866	unnamed protein product [Homo sapiens]
gi 34687	unnamed protein product [Homo sapiens]
gi 31077	unnamed protein product [Homo sapiens]
gi 32111	unnamed protein product [Homo sapiens]
gi 36535	unnamed protein product [Homo sapiens]
gi 31077	unnamed protein product [Homo sapiens]
gi 32111	unnamed protein product [Homo sapiens]
gi 29446	unnamed protein product [Homo sapiens]
gi 29446	unnamed protein product [Homo sapiens]
gi 32097	unnamed protein product [Homo sapiens]
gi 158258947	unnamed protein product [Homo sapiens]
gi 4803698	unnamed protein product [Homo sapiens]
gi 32097	unnamed protein product [Homo sapiens]
gi 29888	unnamed protein product [Homo sapiens]

gi 29446	unnamed protein product [Homo sapiens]
gi 32111	unnamed protein product [Homo sapiens]
gi 10434878	unnamed protein product [Homo sapiens]
gi 340219	vimentin [Homo sapiens]
gi 25188179	voltage-dependent anion channel 3 isoform b [Homo sapiens]

Myoglobin (MB)	P02144	17.052/ 7.29	2	187	Cell differentiation Organ development Transport Response stimulus
Myosin light chain 1/3, skeletal muscle isoform (MLC1/MLC3)	P05976	21.013/ 4.97	4	222	Organ development
Myosin regulatory light chain 2, skeletal muscle isoform (MLC2B)	Q96A32	18.883/ 4.91	3	86	Tissue development
Myosin regulatory light chain 2, ventricular/cardiac muscle isoform (MLC-2v)	P10916	18.658/ 4.92	2	56	Negative regulation of cell growth Muscle contraction Tissue morphogenesis
Myosin light chain 3 (MYL3)	P08590	21.800/ 5.03	5	174	Muscle contraction Tissue morphogenesis Regulation of catalytic activity
S100-A9 (Calgranulin-B)	P06702	13.110/ 5.71	2	156	Cell-cell signaling Inflammatory response
Serum albumin (ALB)	P02768	66.472/ 5.67	2	80	Cellular response to extracellular stimulus Maintenance of location Negative regulation of apoptosis Transport
Stratifin (14-3-3 protein sigma) (SFN)	P31947	27.774/ 4.68	7	66	Regulation of apoptosis Negative regulation of kinase activity Signal transduction
Superoxide dismutase [Cu-Zn] (SOD1)	P00441	15.804/ 5.70	2	102	Cell aging Muscle contraction Cellular biosynthetic process Regulation of catalytic activity Cellular homeostasis Regulation of kinase activity Response to oxidative stress Cytokine production
Tropomyosin-4 (TPM4)	P67936	28.390/ 4.67	3	107	Cell motion
Tropomyosin-1 (TPM1)	P09493	32.708/ 4.69	2	38	Regulation of muscle contraction Cell motion Response to oxidative stress Cytoskeleton organization Organelle organization

					Tissue morphogenesis
Tropomyosin-2 (TPM2)	P07951	32.850/ 4.66	3	146	Regulation of ATPase activity
Tropomyosin-3 (TPM3)	P06753	32.818/4.68	4	165	Cell motion
Troponin T, slow skeletal muscle (TnTs)	P13805	32.816/ 5.86	3	127	Muscle contraction
Vimentin (VIM)	P08670	53.520/ 5.06	4	150	Cell motion

A - Total MASCOT score: sum of individual matched peptide scores

		279088 279627 280334			
10	C02/C04	275629 279131	Tumors	T2-4N0	2-DE
11	C02/C04	279131 279930 279958 281581	Normal Surgical Margins	T2-4N0	2-DE
12	C01	CP1/0249 CP3/0109 CP3/0132 CP3/0142 CP3/0310	Tumors	T1-2N+	2-DE
13	C01	CP1/0249 CP3/0109 CP3/0132	Normal Surgical Margins	T1-2N+	2-DE

1=sites according to ICD-10 (International Statistical Classification of Diseases and Related Health Problems, 10th Revision). C01=Base of tongue; C02=Tongue; C04=Floor of mouth

CP1=Arnaldo Vieira de Carvalho Hospital; CP2=Heliópolis Hospital; CP3=Hospital of Clinics, SP, Brazil

2=groups of cases according to AJCC (American Joint Committee on Cancer) pathologic stage. T (size of tumor); N+ (metastatic lymph nodes); N0 (non-metastatic lymph nodes)

1-DE=one-dimensional electrophoresis; 2-DE=two-dimensional electrophoresis

CP1/0051	M	C04	M/62	T2N0M0	Moderate	47	44	alive	69	No	No	No	2-DE
CP1/0075	T/M	C04	M/54	T3N0M0	Moderate	33	33	alive/d	65	No	No	No	2-DE/2-D DIGE
CP1/0080	T/M	C04	M/67	T3N0M0	Well	52	49	alive	54	No	No	No	2-DE
CP1/0083	T/M	C04	M/72	T2N0M0	Well	36	34	alive	54	No	No	No	2-DE
CP2/0093	T/M	C04	M/55	T2N0M0	Well	37	37	dd	68	No	Yes	Yes	2-DE/IH
CP2/0185	T/M	C02	M/64	T2N0M0	Moderate	35	45	alive	19	No	Yes	Yes	2-DE/IH
CP2/1004	M	C04	F/44	T2N0M0	Well	20	6	alive	54	No	No	No	2-DE
CP3/0004	T	C04	M/60	T2N0M0	Well	26	32	alive	83	No	No	No	2-DE
CP3/0101	T/M	C04	M/62	T3N0M0	Moderate	52	30	alive	69	No	No	No	2-DE
CP3/0120	T/M	C04	F/46	T2N0M0	Well	31	31	dd	32	No	No	No	2-DE
CP3/0138	T	C04	M/75	T2N0M0	Moderate	53	45	alive	67	No	No	No	2-DE
CP1/0249	T/M	C01	M/44	T2N2BM0	Moderate	27	27	dd	33	No	Yes	Yes	2-DE
CP3/0109	T/M	C01	M/55	T2N3M0	Moderate	30	37	dd	7	Yes	Yes	Yes	2-DE
CP3/0132	T/M	C01	M/48	T2N2cM0	Moderate	29	24	alive	67	No	No	No	2-DE
CP3/0142	T	C01	M/47	T2N3M0	Moderate	26	16	alive	37	No	No	No	2-DE
CP3/0310	T	C01	M/58	T2N2bMx	Moderate	40	28	alive/d	5	-	-	Yes	2-DE
CP2/0088	T	C04	M/48	T3N0M0	Well	28	N	dd	70	No	No	No	2-D DIGE
CP1/0021	T	C02	M/43	T3N0M0	Moderate	31	29	alive	74	Yes	Yes	No	2-D DIGE
CP3/0103	T	C02	M/45	T3N0M0	Well	30	25	alive	66	No	No	Yes	2-D DIGE
CP1/0200	T	C02	M/55	T3N0M0	Moderate	40	33	alive	43	No	Yes	Yes	2-D DIGE
CP2/1012	T/M	C02	M/55	T3N0M0	Well	38	30	alive/d	49	No	Yes	No	2-D DIGE/IH
CP1/0191	T	C04	M/63	T3N0M0	Moderate	47	47	alive	53	No	No	Yes	1-DE/2-D DIGE
CP3/0033	T	C04	M/51	T3N0M0	Moderate	38	32	alive	79	No	No	Yes	2-D DIGE
CP1/0024	T/M	C04	F/48	T1N0M0	Moderate	34	N	alive	43	No	No	No	WB
CP1/0032	T/M	C04	M/64	T4N2CM0	Poor	49	45	dd	39	No	Yes	Yes	WB
CP1/0039	M	C02	M/44	T4N2BM0	Moderate	34	32	dd	11	No	No	No	WB
CP1/0055	T/M	C04	M/56	T4N2BM0	Well	36	31	dd	18	No	No	No	WB
CP1/0057	T/M	C02	M/57	T4N2BM0	Moderate	49	46	d	2	No	No	Yes	WB
CP1/0171	T/M	C04	M/70	T2N1M0	Well	N	59	alive	26	No	Yes	No	WB
CP1/0213	T/M	C04	M/68	T4N1M0	Well	54	46	alive	56	No	Yes	No	WB
CP1/0233	T/M	C04	F/39	T4N2CM0	Poor	N	N	dd	5	No	Yes	Yes	WB
CP3/0034	T	C02	F/51	T2N2aM0	Moderate	N	N	alive	76	No	No	Yes	WB
CP3/0056	T	C02	M/70	T1N0M0	-	52	52	d	25	No	Yes	No	WB

CP3/0082	T/M	C02/C04	M/59	T4N1M0	Well	37	39	alive	67	No	No	No	WB
CP3/0114	T	C02	M/72	T4N2cM0	Poor	50	34	dd	3	Yes	Yes	Yes	WB
CP3/0121	T	C02	M/50	T4N2bM0	Well	34	32	alive	68	No	Yes	Yes	WB
CP2/0003	T/M	C03	F/79	T2N1M0	Moderate	72	N	alive	74	No	Yes	No	IH
CP2/0008	T/M	C02	M/54	T2N0M0	Moderate	26	24	alive	75	No	Yes	Yes	IH
CP2/0010	T/M	C06	M/55	T3N0Mx	Well	38	P	dd	15	No	Yes	Yes	IH
CP2/0019	T/M	C04	M/63	T3N2M0	Moderate	45	43	dd	11	No	Yes	No	IH
CP2/0023	T/M	C02	M/54	T3N0M0	Moderate	41	34	alive	57	No	Yes	No	IH
CP2/0028	T/M	C05	M/43	T3N1M0	Well	31	20	alive	73	No	No	No	IH
CP2/0029	T	C04	M/70	T2N0M0	Moderate	56	54	alive	39	Yes	Yes	No	IH
CP2/0036	T/M	C06	M/55	T4N2b M0	Well	39	39	dd	54	No	Yes	Yes	IH
CP2/0039	T	C02	M/56	T2N0M0	Well	38	35	d	39	No	Yes	Yes	IH
CP2/0040	T/M	C02	M/41	T1N2bM0	Poor	N	N	alive	63	No	Yes	Yes	IH
CP2/0071	T/M	C04	M/49	T4N2bM0	Well	36	34	dd	19	No	Yes	No	IH
CP2/0074	T	C04	M/40	T4N0M0	Well	32	30	alive	27	No	No	Yes	IH
CP2/0081	T	C03	F/62	T4N0M0	Poor	26	N	dc	4	No	No	No	IH
CP2/0087	T/M	C03	M/69	T4N2bM0	Poor	27	52	dd	41	No	Yes	Yes	IH
CP2/0094	T/M	C02	M/47	T3N1M0	Poor	30	30	dd	18	No	Yes	Yes	IH
CP2/0109	T/M	C04	M/63	T3N0M0	Well	15	45	alive/d	54	No	Yes	Yes	IH
CP2/0113	T/M	C05	M/59	T3N0M0	Moderate	N	50	d	6	Yes	Yes	No	IH
CP2/0114	T/M	C04	M/51	T4N2M0	Moderate	22	41	d	8	Yes	Yes	Yes	IH
CP2/0115	T/M	C06	M/63	T4N0M0	Well	43	28	alive/d	47	No	Yes	Yes	IH
CP2/0116	T/M	C04	F/81	T2N0M0	Well	5	N	dd	44	No	No	No	IH
CP2/0117	T/M	C02	M/35	T2N2bM0	Moderate	28	17	dd	9	No	Yes	Yes	IH
CP2/0118	T/M	C02	M/45	T2N1M0	Well	23	12	d	51	No	Yes	Yes	IH
CP2/0122	T/M	C04	M/56	T2N2bM0	Well	40	40	dd	21	No	Yes	No	IH
CP2/0125	T/M	C03	M/53	T4N0M0	Well	41	41	dd	10	No	Yes	Yes	IH
CP2/0130	T/M	C03	M/49	T2N0M0	-	31	29	alive	61	-	Yes	-	IH
CP2/0132	T/M	C02	M/48	T2N1M0	Moderate	33	31	alive	61	No	Yes	No	1-DE/IH
CP2/0133	T/M	C02	M/46	T4N1M0	Moderate	32	28	alive	65	No	Yes	Yes	IH
CP2/0144	T/M	C06	M/65	T2N0M0	Moderate	43	43	alive	64	No	Yes	Yes	IH
CP2/0147	T/M	C05	M/74	T2N1M0	Moderate	64	51	alive	57	No	Yes	Yes	IH
CP2/0149	T/M	C04	M/58	T4N1M0	Moderate	50	40	d	7	No	Yes	No	IH

CP2/0152	T/M	C02	M/46	T4N2bM0	Moderate	33	33	alive	57	No	No	No	IH
CP2/0166	T	C03	F/62	T4N2bM0	Well	2	N	dd	7	No	No	Yes	IH
CP2/0168	T/M	C04	F/70	T2N0M0	Well	4	N	d	31	No	No	No	IH
CP2/0169	T/M	C04	M/42	T2N2bM0	Moderate	32	14	alive	62	No	Yes	Yes	IH
CP2/0170	T/M	C04	M/34	T4N2bM0	Moderate	20	20	dd	6	No	No	No	IH
CP2/0177	T/M	C02	M/45	T3N0M0	Well	N	25	alive	58	No	Yes	No	IH
CP2/0181	T/M	C04	M/62	T4N1M0	Well	55	45	alive	51	No	Yes	No	IH
CP2/0182	T/M	C06	M/38	T4N0M0	Moderate	14	14	alive	40	No	Yes	Yes	IH
CP2/0188	T/M	C02	M/41	T4N2bM0	Poor	27	27	dc	14	No	Yes	Yes	IH
CP2/0195	T/M	C04	M/47	T1N1M0	Moderate	33	27	alive	55	No	No	No	IH
CP2/0196	T/M	C04	M/69	T4N2cM0	Well	52	41	dd	< 1	No	Yes	Yes	IH
CP2/1002	T/M	C02	M/59	T2N2CM0	Well	34	41	dd	10	No	No	No	IH
CP2/1003	T/M	C03	F/59	T2N0Mx	Well	20	N	alive	57	No	No	No	IH
CP2/1006	T/M	C05	M/53	T1N0M0	Well	40	41	alive	57	No	No	No	IH
CP2/1008	T/M	C03	F/68	T4N1M0	Moderate	18	18	alive	40	No	No	No	IH
CP2/1010	T/M	C02	M/58	T1N0M0	Moderate	40	20	alive	52	No	No	No	IH
CP2/1019	T/M	C04	M/37	T4N2CM0	Well	21	21	dd	15	No	No	Yes	IH
CP2/1021	T	C03	M/67	T4N1M0	Well	57	50	dd	20	No	Yes	Yes	IH
CP2/1022	T/M	C02	M/44	T3N0M0	Well	30	26	alive/d	13	No	Yes	No	IH
CP2/1032	T/M	C03	F/57	T4N0M0	Moderate	N	N	alive	53	No	No	Yes	IH
CP2/1033	T/M	C05	M/62	T2N0M0	Well	16	41	alive	37	No	No	No	IH
CP2/1036	T/M	C02	M/57	T4N1M0	Moderate	32	32	dd	25	No	Yes	Yes	IH
CP2/1041	T	C04	M/42	T4N2cM0	Moderate	33	33	alive	39	No	Yes	Yes	IH
CP2/1043	T/M	C03	M/69	T4N2bM0	Well	50	46	dd	< 1	No	Yes	Yes	IH
CP2/1044	T/M	C02	F/51	T2N2AM0	Well	31	1	dd	24	No	Yes	Yes	IH
CP2/1051	T/M	C06	M/56	T3N2bM0	Well	43	30	alive	49	No	No	No	IH
CP2/1065	T/M	C02	M/59	T2N0M0	Moderate	43	39	dd	15	No	No	Yes	IH
CP2/1069	T/M	C02	M/46	T2N0M0	Moderate	31	24	alive	48	No	Yes	No	IH
CP2/1071	T/M	C02	M/44	T4N2CM0	Moderate	29	21	alive	48	No	No	Yes	IH
CP2/1073	T/M	C02	M/58	T2N0M0	Moderate	43	43	alive/d	32	Yes	Yes	Yes	IH
CP2/1074	T/M	C02	M/78	T3N0M0	Well	50	50	d	17	No	No	No	IH
CP2/1080	T/M	C04	M/64	T2N0M0	Well	53	40	alive	28	No	No	No	IH
CP2/1099	T/M	C04	M/56	T4N2bM0	Well	39	34	dd	22	No	Yes	Yes	IH

CP2/1104	T/M	C02	M/67	T3N2bM0	Well	52	52	dd	10	No	No	No	IH
CP2/1109	T/M	C04	M/52	T2N0M0	Moderate	36	18	alive	41	No	No	Yes	IH
CP2/1111	T/M	C03	M/42	T3N1M0	Moderate	27	27	dd	9	Yes	Yes	No	IH
CP2/1113	T/M	C04	F/53	T1N0M0	Moderate	35	N	alive	38	No	Yes	Yes	IH
CP2/1114	T/M	C03	M/58	T2N1M0	Moderate	45	40	alive/d	32	No	Yes	No	IH
CP2/1120	T/M	C04	M/47	T3N0M0	Well	33	30	alive	41	No	Yes	No	IH
CP3/0292	T/M	C04	M/50	T2N2c	Moderate	34	25	dd	8	No	No	Yes	1-DE
CP2/0051	T/M	C04	M/46	T2N2bM0	Well	33	10	dd	14	No	No	No	1-DE
CP3/0280	T/M	C04	M/52	T1N2b	Moderate	38	27	alive	44	No	No	Yes	1-DE
CP1/0031	T/M	C04	M/50	T3N0M0	Well	30	30	d	4	No	Yes	Yes	1-DE/WB
CP1/0283	T/M	C04	M/49	T3N0M0	Well	21	15	alive	36	No	No	Yes	1-DE/WB
CP1/0151	T/M	C02	M/47	T3N0M0	Moderate	33	33	dd	19	No	No	Yes	1-DE
CP1/0277	T/M	C02	M/66	T3N0M0	Moderate	45	35	alive	41	No	No	Yes	1-DE/WB
CP1/0262	M	C02	M/62	T3N0M0	Moderate	34	44	alive	32	No	No	Yes	1-DE

CP1=Arnaldo Vieira de Carvalho Hospital; CP2=Heliópolis Hospital; CP3=Hospital of Clinics, SP, Brazil

T=tumor; M=normal surgical margin

a) sites according to ICD (International Statistical Classification of Diseases and Related Health Problems, 10th Revision, Version 2007). C01=Malignant neoplasm of base of tongue; C02=Malignant neoplasm of other and unspecified parts of tongue; C03=Malignant neoplasm of gum; C04=Malignant neoplasm of floor of mouth; C05=Malignant neoplasm of palate; C06=Malignant neoplasm of other and unspecified parts of mouth

F=female; M=male

b) American Joint Committee on Cancer

P or N=positive or negative exposition to tobacco or alcohol, respectively, but consumption time is indeterminate

alive=alive without disease evidence; alive/d=alive with the disease (alive with a second primary tumor or tumoral recidive or metastasis); dd=dead by disease; dc=dead by commorbidity; d=dead by another cause

- =no available information

1-DE=one-dimensional electrophoresis; 2-DE=two-dimensional electrophoresis; 2-D DIGE=fluorescent two-dimensional differential in-gel electrophoresis; WB=western blot; IH=immunohistochemistry

Supporting Table 5. Proteins expressed in “less-aggressive” (T3N0) tumors. Proteins from about 10 to 45kD separated by 1-DE and identified by ESI-Q-TOF-MS/MS analysis

Code of gene	Protein
gi 338043	[Human pre-mRNA splicing factor SF2p32, complete sequence.], gene product
gi 437363	14-3-3n
gi 1041969	17 kda cyclophilin A {internal fragment} [human, first trimester decidual and placental tissue, Pep
gi 693933	2-phosphopyruvate-hydratase alpha-enolase; carbonate dehydratase [Homo sapiens]
gi 306891	90kDa heat shock protein
gi 5453880	acidic (leucine-rich) nuclear phosphoprotein 32 family, member A [Homo sapiens]
gi 13569879	acidic (leucine-rich) nuclear phosphoprotein 32 family, member E isoform 1 [Homo sapiens]
gi 5031599	actin related protein 2/3 complex subunit 2 [Homo sapiens]
gi 5031593	actin related protein 2/3 complex subunit 5 [Homo sapiens]
gi 4501881	actin, alpha 1, skeletal muscle [Homo sapiens]
gi 63055057	actin, beta-like 2 [Homo sapiens]
gi 62421158	actin-like protein [Homo sapiens]
gi 4502211	ADP-ribosylation factor 6 [Homo sapiens]
gi 54303910	aging-associated gene 9 protein [Homo sapiens]
gi 28595	aldolase A protein [Homo sapiens]
gi 3098514	aldose reductase-related protein [Homo sapiens]
gi 30054	alpha1 (III) collagen [Homo sapiens]
gi 30030	alpha-1 collagen VI (AA 574-1009) [Homo sapiens]
gi 182424	alpha-fibrinogen precursor [Homo sapiens]
gi 37492	alpha-tubulin [Homo sapiens]
gi 179074	alternative
gi 4757756	annexin A2 isoform 2 [Homo sapiens]
gi 4826643	annexin A3 [Homo sapiens]
gi 4502101	annexin I [Homo sapiens]
gi 11275302	anti TNF-alpha antibody light-chain Fab fragment [Homo sapiens]
gi 30258347	antibody light chain [Homo sapiens]
gi 21311323	anti-pneumococcal antibody 1A2 light chain variable region [Homo sapiens]
gi 58222968	anti-tetanus toxoid immunoglobulin light chain variable region [Homo sapiens]
gi 178855	apolipoprotein J precursor [Homo sapiens]
gi 284164	arginine-rich protein - human
gi 13625797	asporin precursor [Homo sapiens]

gi 119574400	ATP-binding cassette, sub-family F (GCN20), member 2, isoform CRA_c [Homo sapiens]
gi 3334899	autoantigen p542 [Homo sapiens]
gi 29383	BBC1 [Homo sapiens]
gi 4501885	beta actin [Homo sapiens]
gi 193244897	beta globin [Homo sapiens]
gi 66473265	beta globin chain [Homo sapiens]
gi 6573280	beta tropomyosin [Homo sapiens]
gi 34616	beta-2 microglobulin [Homo sapiens]
gi 179409	beta-globin
gi 179433	biglycan [Homo sapiens]
gi 306875	C protein [Homo sapiens]
gi 4885111	calmodulin-like 3 [Homo sapiens]
gi 433308	capping protein alpha [Homo sapiens]
gi 4502517	carbonic anhydrase I [Homo sapiens]
gi 29727	cardiac beta myosin heavy chain [Homo sapiens]
gi 951338	CAS
gi 4503143	cathepsin D preproprotein [Homo sapiens]
gi 337760	cerebroside sulfate activator protein
gi 157835338	Chain A, Changes In Conformational Stability Of A Series Of Mutant Human Lysozymes At Constant Posi
gi 157835340	Chain A, Contribution Of Hydrophobic Effect To The Conformational Stability Of Human Lysozyme
gi 75766275	Chain A, Crystal Structure Of Human Cypa Mutant K131a
gi 3891470	Chain A, Crystal Structure Of Human Galectin-7 In Complex With Galactosamine
gi 90108664	Chain A, Crystal Structure Of Lipid-Free Human Apolipoprotein A-I
gi 999892	Chain A, Crystal Structure Of Recombinant Human Triosephosphate Isomerase At 2.8 Angstroms Resoluti
gi 1633054	Chain A, Cyclophilin A Complexed With Dipeptide Gly-Pro
gi 1065111	Chain A, High Resolution Solution Nmr Structure Of Mixed Disulfide Intermediate Between Mutant Huma
gi 1065361	Chain A, Human Adp-Ribosylation Factor 1 Complexed With Gdp, Full Length Non-Myristoylated
gi 3891975	Chain A, Human Cathepsin G
gi 15825659	Chain A, Human Factor Viii C2 Domain Complexed To Human Monoclonal Bo2c11 Fab
gi 157830361	Chain A, Human Serum Albumin In A Complex With Myristic Acid And Tri- Iodobenzoic Acid
gi 640248	Chain A, Initial Crystallographic Analyses Of A Recombinant Interleukin-1 Receptor Antagonist Prote
gi 4929993	Chain A, Module-Substituted Chimera Hemoglobin Beta-Alpha (F133v)
gi 159162145	Chain A, Rotamer Strain As A Determinant Of Protein Structural Specificity
gi 16974825	Chain A, Solution Structure Of Calcium-Calmodulin N-Terminal Domain

gi 229751	Chain A, Structure Of Haemoglobin In The Deoxy Quaternary State With Ligand Bound At The Alpha Haem
gi 31615803	Chain A, Synthetic Ubiquitin With Fluoro-Leu At 50 And 67
gi 809185	Chain A, The Effect Of Metal Binding On The Structure Of Annexin V And Implications For Membrane Bi
gi 494066	Chain A, Three-Dimensional Structure Of Class Pi Glutathione S- Transferase From Human Placenta In
gi 61679690	Chain A, T-To-Thigh Quaternary Transitions In Human Hemoglobin: Alpha191a Deoxy Low-Salt
gi 190613401	Chain A, Unusual Twinning In Crystals Of The Cits Binding Antibody Fab Fragment F3p4
gi 229597861	Chain A, X-Ray Crystal Structure Of Coil 1a Of Human Vimentin
gi 1421609	Chain A, X-Ray Structure Of Nm23 Human Nucleoside Diphosphate Kinase B Complexed With Gdp At 2 Angs
gi 1431650	Chain B, Analysis Of The Crystal Structure, Molecular Modeling And Infrared Spectroscopy Of The Dis
gi 3660434	Chain B, Crystal Structure Of Deoxy-Human Hemoglobin Beta6 Glu->trp
gi 42543653	Chain B, Crystal Structure Of Human Anti-Hiv-1 Gp120 Reactive Antibody 412d
gi 208435643	Chain B, Crystal Structure Of K63-Specific Fab Apu.3a8 Bound To K63- Linked Di-Ubiquitin
gi 442850	Chain B, High-Resolution X-Ray Study Of Deoxy Recombinant Human Hemoglobins Synthesized From Beta-G
gi 229959	Chain B, Refined Crystal Structure Of Deoxyhemoglobin S. I. Restrained Least-Squares Refinement At
gi 229752	Chain B, Structure Of Haemoglobin In The Deoxy Quaternary State With Ligand Bound At The Alpha Haem
gi 55669799	Chain B, Three Dimensional Structure Of A Humanized Anti-Ifn-Gamma Fab In C2 Space Group
gi 166007160	Chain C, Solution Structure Of Human Immunoglobulin M
gi 161760892	Chain D, Neutron Structure Analysis Of Deoxy Human Hemoglobin
gi 349905	Chain F, Atomic Structures Of Wild-Type And Thermostable Mutant Recombinant Human Cu, Zn Superoxide
gi 5542067	Chain H, Comparison Of The Three-Dimensional Structures Of A Humanized And A Chimeric Fab Of An Ant
gi 160286046	Chain H, Crystal Structure Of A Recombinant Ige Fab Fragment In Complex With Bovine Beta-Lactoglobu
gi 17942616	Chain H, The Hapten Complexed Germline Precursor To Sulfide Oxidase Catalytic Antibody 28b4
gi 2914165	Chain H, Three-Dimensional Structure Of A Human Fab With High Affinity For Tetanus Toxoid
gi 494619	Chain I, The Refined 2.4 Angstroms X-Ray Crystal Structure Of Recombinant Human Stefin B In Complex
gi 46015316	Chain L, Crystal Structure Analysis Of Anti-Hiv-1 Fab 447-52d In Complex With V3 Peptide
gi 493869	Chain L, Crystal Structure Of A Chimeric Fab' Fragment Of An Antibody Binding Tumour Cells
gi 99031801	Chain L, Crystal Structure Of A Glycosylated Fab From An Igm Cryoglobulin With Properties Of A Natu
gi 1827928	Chain L, Igg Fab (Human Igg1, Kappa) Chimeric Fragment (Cbr96) Complexed With Lewis Y Nonoate Methy
gi 2194044	Chain L, Igg Fab Fragment (Cd25-Binding)
gi 230162	Chain M, Three-Dimensional Structure Of A Hybrid Light Chain Dimer. Protein Engineering Of A Bindin
gi 230867	Chain R, Twinning In Crystals Of Human Skeletal Muscle D- Glyceraldehyde-3-Phosphate Dehydrogenase
gi 4008131	chaperonin 10 [Homo sapiens]
gi 4502899	clathrin, light polypeptide A isoform a [Homo sapiens]
gi 180663	c-myc binding protein [Homo sapiens]

gi 5031635	cofilin 1 (non-muscle) [Homo sapiens]
gi 1915902	collagen (VI) alpha-1 chain [Homo sapiens]
gi 3127926	collagen type VI, alpha 3 chain [Homo sapiens]
gi 13938619	Creatine kinase, muscle [Homo sapiens]
gi 181250	cyclophilin
gi 4885165	cystatin A [Homo sapiens]
gi 30377	cytokeratin 13 [Homo sapiens]
gi 34073	cytokeratin 4 (408 AA) [Homo sapiens]
gi 4504351	delta globin [Homo sapiens]
gi 311614	dermatopontin [Homo sapiens]
gi 181540	desmin [Homo sapiens]
gi 9802306	DNA-binding protein TAXREB107 [Homo sapiens]
gi 1220311	elongation factor-1 alpha
gi 153267427	enolase 3 [Homo sapiens]
gi 181402	epidermal cytokeratin 2 [Homo sapiens]
gi 187302	epithelial cell marker protein 1
gi 4503475	eukaryotic translation elongation factor 1 alpha 2 [Homo sapiens]
gi 4503477	eukaryotic translation elongation factor 1 beta 2 [Homo sapiens]
gi 5453597	F-actin capping protein alpha-1 subunit [Homo sapiens]
gi 4557581	fatty acid binding protein 5 (psoriasis-associated) [Homo sapiens]
gi 182516	ferritin light subunit [Homo sapiens]
gi 182439	fibrinogen gamma chain [Homo sapiens]
gi 4504981	galectin-1 [Homo sapiens]
gi 2282013	GAPDH-2 like [Homo sapiens]
gi 12653507	Glutamic-oxaloacetic transaminase 2, mitochondrial (aspartate aminotransferase 2) [Homo sapiens]
gi 31645	glyceraldehyde-3-phosphate dehydrogenase [Homo sapiens]
gi 386758	GRP78 precursor
gi 5174447	guanine nucleotide binding protein (G protein), beta polypeptide 2-like 1 [Homo sapiens]
gi 4885371	H1 histone family, member 0 [Homo sapiens]
gi 5174449	H1 histone family, member X [Homo sapiens]
gi 4504255	H2A histone family, member Z [Homo sapiens]
gi 306882	haptoglobin precursor [Homo sapiens]
gi 183855	hbbm fused globin protein [Homo sapiens]
gi 119590486	hCG1640974, isoform CRA_a [Homo sapiens]

gi 119612018	hCG1808204 [Homo sapiens]
gi 119630082	hCG2007439 [Homo sapiens]
gi 119612312	hCG2008737 [Homo sapiens]
gi 119578813	hCG2011101 [Homo sapiens]
gi 119617765	hCG26523, isoform CRA_a [Homo sapiens]
gi 119614777	hCG95695, isoform CRA_a [Homo sapiens]
gi 662841	heat shock protein 27 [Homo sapiens]
gi 229149	hemoglobin beta
gi 47679341	hemoglobin beta [Homo sapiens]
gi 23268683	hemoglobin beta chain variant Hb.Sinai-Bel Air [Homo sapiens]
gi 239718	hemoglobin beta chain; beta-globin [Homo sapiens]
gi 51594277	hemoglobin Lepore-Baltimore [Homo sapiens]
gi 4504447	heterogeneous nuclear ribonucleoprotein A2/B1 isoform A2 [Homo sapiens]
gi 14043072	heterogeneous nuclear ribonucleoprotein A2/B1 isoform B1 [Homo sapiens]
gi 11321591	high-mobility group box 2 [Homo sapiens]
gi 4885381	histone cluster 1, H1b [Homo sapiens]
gi 4885375	histone cluster 1, H1c [Homo sapiens]
gi 4885377	histone cluster 1, H1d [Homo sapiens]
gi 4504239	histone cluster 1, H2ai [Homo sapiens]
gi 24586679	histone cluster 1, H2ba [Homo sapiens]
gi 45219796	Histone cluster 1, H3i [Homo sapiens]
gi 56203471	histone cluster 2, H3, pseudogene 2 [Homo sapiens]
gi 4504299	histone cluster 3, H3 [Homo sapiens]
gi 356168	histone H1b
gi 31979	histone H2A.2 [Homo sapiens]
gi 1568551	histone H2B [Homo sapiens]
gi 386772	histone H3 [Homo sapiens]
gi 7739447	hnRNP 2H9D [Homo sapiens]
gi 33877030	HNRPC1 protein [Homo sapiens]
gi 306549	homology to rat ribosomal protein L23
gi 23271312	HSPA2 protein [Homo sapiens]
gi 38522	human elongation factor-1-delta [Homo sapiens]
gi 51476390	hypothetical protein [Homo sapiens]
gi 117938314	hypothetical protein LOC51237 [Homo sapiens]

gi|912776 iduronate-2-sulfatase, IDS {EC 3.1.6.13} [human, Hunter syndrome patient severe phenotype, Peptide Mutant, 550 aa]
gi|229536 Ig A L
gi|229585 Ig A1 Bur
gi|229601 Ig G1 H Nie
gi|106482 Ig heavy chain V-III region (ART) - human (fragments)
gi|106586 Ig kappa chain V-III (KAU cold agglutinin) - human
gi|223815 Ig lambda C
gi|106643 Ig lambda chain - human
gi|4176418 IgG kappa chain [Homo sapiens]
gi|58476682 IGL@ protein [Homo sapiens]
gi|133778664 immunoglobulin G1 Fab heavy chain variable region [Homo sapiens]
gi|567156 immunoglobulin gamma-chain, V region [Homo sapiens]
gi|46254000 immunoglobulin heavy chain [Homo sapiens]
gi|5679468 immunoglobulin heavy chain variable region [Homo sapiens]
gi|306962 immunoglobulin kappa chain [Homo sapiens]
gi|416336 immunoglobulin kappa chain V region [Homo sapiens]
gi|9968499 immunoglobulin kappa chain variable region [Homo sapiens]
gi|3169770 immunoglobulin kappa light chain [Homo sapiens]
gi|17226640 immunoglobulin kappa light chain variable region [Homo sapiens]
gi|21669317 immunoglobulin kappa light chain VLJ region [Homo sapiens]
gi|170684534 immunoglobulin lambda 2 light chain [Homo sapiens]
gi|21669601 immunoglobulin lambda light chain VLJ region [Homo sapiens]
gi|306999 immunoglobulin light chain
gi|186152 immunoglobulin light chain [Homo sapiens]
gi|186133 immunoglobulin light chain constant region [Homo sapiens]
gi|51103395 immunoglobulin variable region VL kappa domain [Homo sapiens]
gi|386848 keratin [Homo sapiens]
gi|7331218 keratin 1 [Homo sapiens]
gi|119581150 keratin 14 (epidermolysis bullosa simplex, Dowling-Meara, Koebner), isoform CRA_b [Homo sapiens]
gi|4557701 keratin 17 [Homo sapiens]
gi|42760012 keratin 3 [Homo sapiens]
gi|18999435 Keratin 5 [Homo sapiens]
gi|5031839 keratin 6A [Homo sapiens]
gi|84040267 Keratin 6C [Homo sapiens]

gi|28173564 keratin 73 [Homo sapiens]
gi|386850 keratin K5
gi|186685 keratin type 16
gi|386849 keratin type II [Homo sapiens]
gi|71891729 KIAA1503 protein [Homo sapiens]
gi|619788 L21 ribosomal protein [Homo sapiens]
gi|40254924 leucine rich repeat containing 59 [Homo sapiens]
gi|5031857 L-lactate dehydrogenase A isoform 1 [Homo sapiens]
gi|4557032 L-lactate dehydrogenase B [Homo sapiens]
gi|307141 lysozyme precursor (EC 3.2.1.17)
gi|187181 macrophage migration inhibitory factor
gi|2906146 malate dehydrogenase precursor [Homo sapiens]
gi|34709 manganese superoxide dismutase (MnSOD) [Homo sapiens]
gi|28336 mutant beta-actin (beta'-actin) [Homo sapiens]
gi|188586 myosin light chain 2 [Homo sapiens]
gi|188590 myosin light chain 3 [Homo sapiens]
gi|5453740 myosin, light chain 12A, regulatory, non-sarcomeric [Homo sapiens]
gi|17986258 myosin, light chain 6, alkali, smooth muscle and non-muscle isoform 1 [Homo sapiens]
gi|5031931 nascent polypeptide-associated complex alpha subunit isoform b [Homo sapiens]
gi|930063 neurone-specific enolase [Homo sapiens]
gi|913159 neuropolypeptide h3 [human, brain, Peptide, 186 aa]
gi|300181 neutrophil gelatinase-associated lipocalin, NGAL [human, neutrophils, Peptide, 178 aa]
gi|228797 neutrophil granule peptide HP1
gi|35068 Nm23 protein [Homo sapiens]
gi|478813 nonhistone chromosomal protein HMG-1 - human
gi|190238 nucleolar phosphoprotein B23
gi|7661704 osteoglycin preproprotein [Homo sapiens]
gi|895845 p64 CLCP [Homo sapiens]
gi|30102944 peptidylprolyl isomerase A-like 4A [Homo sapiens]
gi|189034 perinatal myosin heavy chain [Homo sapiens]
gi|4505591 peroxiredoxin 1 [Homo sapiens]
gi|1498227 PHAPI2b protein [Homo sapiens]
gi|2076751 phosphatidylinositol 3-kinase delta catalytic subunit
gi|189868 phosphoglycerate mutase [Homo sapiens]

gi|2627129 polyubiquitin [Homo sapiens]
 gi|190200 porin
 gi|238427 Porin 31HM [human, skeletal muscle membranes, Peptide, 282 aa]
 gi|145309046 POTE-2 alpha-actin [Homo sapiens]
 gi|219978 prealbumin [Homo sapiens]
 gi|169171114 PREDICTED: hypothetical protein [Homo sapiens]
 gi|88988289 PREDICTED: hypothetical protein LOC648000 isoform 3 [Homo sapiens]
 gi|169213772 PREDICTED: similar to actin alpha 1 skeletal muscle protein [Homo sapiens]
 gi|88942898 PREDICTED: similar to beta-actin [Homo sapiens]
 gi|89038414 PREDICTED: similar to diazepam binding inhibitor [Homo sapiens]
 gi|169163387 PREDICTED: similar to TRIM5/CypA fusion protein [Homo sapiens]
 gi|5690431 prefoldin subunit 2 [Homo sapiens]
 gi|337758 pre-serum amyloid P component [Homo sapiens]
 gi|4826898 profilin 1 [Homo sapiens]
 gi|190447 prosomal protein P30-33K
 gi|5453990 proteasome activator subunit 1 isoform 1 [Homo sapiens]
 gi|4506185 proteasome alpha 4 subunit isoform 1 [Homo sapiens]
 gi|596140 proteasome subunit LMP7
 gi|190283 protective protein precursor
 gi|1710248 protein disulfide isomerase-related protein 5 [Homo sapiens]
 gi|134133226 protein expressed in prostate, ovary, testis, and placenta 2 [Homo sapiens]
 gi|229528 protein Len,Bence-Jones
 gi|189617 protein PP4-X
 gi|190668 psoriasin
 gi|29468353 RALY-like protein isoform 1 [Homo sapiens]
 gi|4506413 RAP1A, member of RAS oncogene family [Homo sapiens]
 gi|6912638 ras suppressor protein 1 isoform 1 [Homo sapiens]
 gi|83674986 rcTPM3 [Homo sapiens]
 gi|20531983 RecName: Full=Aldo-keto reductase family 1 member B10; AltName: Full=Aldose reductase-like; AltName
 gi|112877 RecName: Full=Alpha-1-acid glycoprotein 1; Short=AGP 1; AltName: Full=Orosomucoid-1; Short=OMD 1; F
 gi|123510 RecName: Full=Haptoglobin-related protein; Flags: Precursor
 gi|133254 RecName: Full=Heterogeneous nuclear ribonucleoprotein A1; Short=hnRNP core protein A1; AltName: Ful
 gi|121039 RecName: Full=Ig gamma-1 chain C region
 gi|125799 RecName: Full=Ig kappa chain V-III region NG9; Flags: Precursor

gi|74744045 RecName: Full=Protein S100-A7-like 2; AltName: Full=S100 calcium-binding protein A7-like 2
gi|267108 RecName: Full=Tetranectin; Short=TN; AltName: Full=C-type lectin domain family 3 member B; AltName:
gi|136066 RecName: Full=Triosephosphate isomerase; Short=TIM; AltName: Full=Triose-phosphate isomerase
gi|9857759 recombinant IgG4 heavy chain [Homo sapiens]
gi|36038 rho GDP dissociation inhibitor (GDI) [Homo sapiens]
gi|306553 ribosomal protein small subunit
gi|337518 ribosomal protein
gi|495126 ribosomal protein L11 [Homo sapiens]
gi|4506597 ribosomal protein L12 [Homo sapiens]
gi|4506617 ribosomal protein L17 [Homo sapiens]
gi|4506607 ribosomal protein L18 [Homo sapiens]
gi|119572748 ribosomal protein L18, isoform CRA_e [Homo sapiens]
gi|4506609 ribosomal protein L19 [Homo sapiens]
gi|4506613 ribosomal protein L22 proprotein [Homo sapiens]
gi|4506605 ribosomal protein L23 [Homo sapiens]
gi|4506619 ribosomal protein L24 [Homo sapiens]
gi|292435 ribosomal protein L26
gi|4506623 ribosomal protein L27 [Homo sapiens]
gi|4432754 ribosomal protein L27a [Homo sapiens]
gi|13904866 ribosomal protein L28 isoform 2 [Homo sapiens]
gi|793843 ribosomal protein L29 [Homo sapiens]
gi|1655596 ribosomal protein L31 [Homo sapiens]
gi|6005860 ribosomal protein L35 [Homo sapiens]
gi|14591909 ribosomal protein L5 [Homo sapiens]
gi|55958183 ribosomal protein L7a [Homo sapiens]
gi|119608470 ribosomal protein L7a, isoform CRA_d [Homo sapiens]
gi|4506663 ribosomal protein L8 [Homo sapiens]
gi|4506667 ribosomal protein P0 [Homo sapiens]
gi|4506669 ribosomal protein P1 isoform 1 [Homo sapiens]
gi|4506671 ribosomal protein P2 [Homo sapiens]
gi|4506679 ribosomal protein S10 [Homo sapiens]
gi|4506681 ribosomal protein S11 [Homo sapiens]
gi|553640 ribosomal protein S13 [Homo sapiens]
gi|5032051 ribosomal protein S14 [Homo sapiens]

gi 4506691	ribosomal protein S16 [Homo sapiens]
gi 4506693	ribosomal protein S17 [Homo sapiens]
gi 6755368	ribosomal protein S18 [Mus musculus]
gi 4506695	ribosomal protein S19 [Homo sapiens]
gi 15055539	ribosomal protein S2 [Homo sapiens]
gi 4506701	ribosomal protein S23 [Homo sapiens]
gi 4506707	ribosomal protein S25 [Homo sapiens]
gi 296452	ribosomal protein S26 [Homo sapiens]
gi 4506715	ribosomal protein S28 [Homo sapiens]
gi 550021	ribosomal protein S5
gi 337514	ribosomal protein S6 [Homo sapiens]
gi 4506743	ribosomal protein S8 [Homo sapiens]
gi 550023	ribosomal protein S9
gi 119592618	ribosomal protein S9, isoform CRA_c [Homo sapiens]
gi 36059	RING12 [Homo sapiens]
gi 37046660	RPL7L1 protein [Homo sapiens]
gi 71297264	RPS27A protein [Homo sapiens]
gi 5032057	S100 calcium binding protein A11 [Homo sapiens]
gi 7657532	S100 calcium-binding protein A6 [Homo sapiens]
gi 4506773	S100 calcium-binding protein A9 [Homo sapiens]
gi 49660012	sarcomeric tropomyosin kappa; TPM1-kappa [Homo sapiens]
gi 337930	scar protein
gi 407421	SEB4B [Homo sapiens]
gi 338039	set
gi 4506925	SH3 domain binding glutamic acid-rich protein like [Homo sapiens]
gi 11345462	signal peptidase complex subunit 3 [Homo sapiens]
gi 5454090	signal sequence receptor, delta [Homo sapiens]
gi 339956	skeletal muscle tropomyosin [Homo sapiens]
gi 1770517	SMT3A protein [Homo sapiens]
gi 4506901	splicing factor, arginine/serine-rich 3 [Homo sapiens]
gi 72534660	splicing factor, arginine/serine-rich 7 [Homo sapiens]
gi 685073	SPRC=small proline-rich protein [human, odontogenic keratocysts, Peptide Partial, 161 aa]
gi 551638	SSR alpha subunit [Homo sapiens]
gi 5031851	stathmin 1 isoform a [Homo sapiens]

gi|16307067 SUB1 homolog (*S. cerevisiae*) [Homo sapiens]
gi|845536 This CDS feature is included to show the translation of the corresponding V_region. Presently translation qualifiers on V_region features are illegal
gi|339683 Thy-1
gi|19072649 TPMsk3 [Homo sapiens]
gi|5803187 transaldolase 1 [Homo sapiens]
gi|553788 transferrin
gi|460789 transformation upregulated nuclear protein [Homo sapiens]
gi|48255905 transgelin [Homo sapiens]
gi|4507357 transgelin 2 [Homo sapiens]
gi|27597085 tropomyosin 1 alpha chain isoform 5 [Homo sapiens]
gi|47519616 tropomyosin 2 (beta) isoform 2 [Homo sapiens]
gi|58652133 tropomyosin 3 [*Bos taurus*]
gi|4507651 tropomyosin 4 isoform 2 [Homo sapiens]
gi|223486 tubulin beta
gi|7106439 tubulin, beta 5 [*Mus musculus*]
gi|5803225 tyrosine 3/tryptophan 5 -monooxygenase activation protein, epsilon polypeptide [Homo sapiens]
gi|5803227 tyrosine 3/tryptophan 5 -monooxygenase activation protein, theta polypeptide [Homo sapiens]
gi|4507953 tyrosine 3/tryptophan 5 -monooxygenase activation protein, zeta polypeptide [Homo sapiens]
gi|4507949 tyrosine 3-monooxygenase/tryptophan 5-monooxygenase activation protein, beta polypeptide [Homo sapiens]
gi|9507245 tyrosine 3-monooxygenase/tryptophan 5-monooxygenase activation protein, gamma polypeptide [*Rattus norvegicus*]
gi|5803207 U2 small nuclear RNA auxiliary factor 1 isoform a [Homo sapiens]
gi|229532 ubiquitin
gi|4507797 ubiquitin-conjugating enzyme E2v2 [Homo sapiens]
gi|16306948 Unknown (protein for IMAGE:3897065) [Homo sapiens]
gi|194384240 unnamed protein product [Homo sapiens]
gi|34039 unnamed protein product [Homo sapiens]
gi|29446 unnamed protein product [Homo sapiens]
gi|194376438 unnamed protein product [Homo sapiens]
gi|7022475 unnamed protein product [Homo sapiens]
gi|31092 unnamed protein product [Homo sapiens]
gi|28940 unnamed protein product [Homo sapiens]
gi|32486 unnamed protein product [Homo sapiens]
gi|34527413 unnamed protein product [Homo sapiens]
gi|34081 unnamed protein product [Homo sapiens]

gi 194377108	unnamed protein product [Homo sapiens]
gi 37403	unnamed protein product [Homo sapiens]
gi 16554039	unnamed protein product [Homo sapiens]
gi 37403	unnamed protein product [Homo sapiens]
gi 32486	unnamed protein product [Homo sapiens]
gi 32111	unnamed protein product [Homo sapiens]
gi 31092	unnamed protein product [Homo sapiens]
gi 29446	unnamed protein product [Homo sapiens]
gi 34039	unnamed protein product [Homo sapiens]
gi 47077184	unnamed protein product [Homo sapiens]
gi 16554039	unnamed protein product [Homo sapiens]
gi 36535	unnamed protein product [Homo sapiens]
gi 29446	unnamed protein product [Homo sapiens]
gi 194384240	unnamed protein product [Homo sapiens]
gi 32111	unnamed protein product [Homo sapiens]
gi 32488	unnamed protein product [Homo sapiens]
gi 34526424	unnamed protein product [Homo sapiens]
gi 16554039	unnamed protein product [Homo sapiens]
gi 34081	unnamed protein product [Homo sapiens]
gi 31092	unnamed protein product [Homo sapiens]
gi 194375974	unnamed protein product [Homo sapiens]
gi 32111	unnamed protein product [Homo sapiens]
gi 32488	unnamed protein product [Homo sapiens]
gi 28375485	unnamed protein product [Homo sapiens]
gi 34069	unnamed protein product [Homo sapiens]
gi 28435	unnamed protein product [Homo sapiens]
gi 29446	unnamed protein product [Homo sapiens]
gi 32111	unnamed protein product [Homo sapiens]
gi 29446	unnamed protein product [Homo sapiens]
gi 31092	unnamed protein product [Homo sapiens]
gi 29446	unnamed protein product [Homo sapiens]
gi 32097	unnamed protein product [Homo sapiens]
gi 31092	unnamed protein product [Homo sapiens]
gi 34201	unnamed protein product [Homo sapiens]

gi 29446	unnamed protein product [Homo sapiens]
gi 29888	unnamed protein product [Homo sapiens]
gi 32097	unnamed protein product [Homo sapiens]
gi 32111	unnamed protein product [Homo sapiens]
gi 31092	unnamed protein product [Homo sapiens]
gi 194376310	unnamed protein product [Homo sapiens]
gi 34071	unnamed protein product [Homo sapiens]
gi 29446	unnamed protein product [Homo sapiens]
gi 34039	unnamed protein product [Homo sapiens]
gi 194376438	unnamed protein product [Homo sapiens]
gi 36573	unnamed protein product [Homo sapiens]
gi 340219	vimentin [Homo sapiens]
gi 25188179	voltage-dependent anion channel 3 isoform b [Homo sapiens]

Supporting Table 6. Proteins expressed in normal surgical margins. Proteins from about 10 to 45kD separated by 1-DE and identified by ESI-Q-TOF-MS/MS analysis

Code of gene	Protein
gi 437363	14-3-3n
gi 119612724	actin, alpha, cardiac muscle, isoform CRA_c [Homo sapiens]
gi 63055057	actin, beta-like 2 [Homo sapiens]
gi 62421158	actin-like protein [Homo sapiens]
gi 28595	aldolase A protein [Homo sapiens]
gi 30030	alpha-1 collagen VI (AA 574-1009) [Homo sapiens]
gi 179711	alpha-2 collagen type VI-a'
gi 178027	alpha-actin [Homo sapiens]
gi 182424	alpha-fibrinogen precursor [Homo sapiens]
gi 183801	alpha-globin [Homo sapiens]
gi 37492	alpha-tubulin [Homo sapiens]
gi 4757756	annexin A2 isoform 2 [Homo sapiens]
gi 4502101	annexin I [Homo sapiens]
gi 30258347	antibody light chain [Homo sapiens]
gi 5360679	anti-Entamoeba histolytica immunoglobulin kappa light chain [Homo sapiens]
gi 212675141	anti-HIV-1 V3 immunoglobulin heavy chain [Homo sapiens]
gi 58222835	anti-tetanus toxoid immunoglobulin light chain variable region [Homo sapiens]
gi 178855	apolipoprotein J precursor [Homo sapiens]
gi 13625797	asporin precursor [Homo sapiens]
gi 4501885	beta actin [Homo sapiens]
gi 193244897	beta globin [Homo sapiens]
gi 66473265	beta globin chain [Homo sapiens]
gi 179409	beta-globin
gi 21591225	BIA2 protein [Homo sapiens]
gi 306875	C protein [Homo sapiens]
gi 688292	calmitine; calsequestrine [Homo sapiens]
gi 4502517	carbonic anhydrase I [Homo sapiens]
gi 4557395	carbonic anhydrase II [Homo sapiens]
gi 2460249	cardiac ventricular troponin C [Homo sapiens]
gi 951338	CAS
gi 4503143	cathepsin D preproprotein [Homo sapiens]

gi|5901922 cell division cycle 37 protein [Homo sapiens]
 gi|3891470 Chain A, Crystal Structure Of Human Galectin-7 In Complex With Galactosamine
 gi|90108664 Chain A, Crystal Structure Of Lipid-Free Human Apolipoprotein A-I
 gi|46015515 Chain A, Crystal Structure Of The Broadly Hiv-1 Neutralizing Fab X5 At 1.90 Angstrom Resolution
 gi|1633054 Chain A, Cyclophilin A Complexed With Dipeptide Gly-Pro
 gi|1065111 Chain A, High Resolution Solution Nmr Structure Of Mixed Disulfide Intermediate Between Mutant Huma
 gi|4699695 Chain A, Human Beta-Tryptase: A Ring-Like Tetramer With Active Sites Facing A Central Pore
 gi|15825659 Chain A, Human Factor Viii C2 Domain Complexed To Human Monoclonal Bo2c11 Fab
 gi|157830361 Chain A, Human Serum Albumin In A Complex With Myristic Acid And Tri- Iodobenzoic Acid
 gi|4929993 Chain A, Module-Substituted Chimera Hemoglobin Beta-Alpha (F133v)
 gi|3114508 Chain A, R State Human Hemoglobin [alpha V96w], Carbonmonoxy
 gi|16974825 Chain A, Solution Structure Of Calcium-Calmodulin N-Terminal Domain
 gi|229751 Chain A, Structure Of Haemoglobin In The Deoxy Quaternary State With Ligand Bound At The Alpha Haem
 gi|31615803 Chain A, Synthetic Ubiquitin With Fluoro-Leu At 50 And 67
 gi|809185 Chain A, The Effect Of Metal Binding On The Structure Of Annexin V And Implications For Membrane Bi
 gi|576259 Chain A, The Structure Of Pentameric Human Serum Amyloid P Component
 gi|190613401 Chain A, Unusual Twinning In Crystals Of The Cits Binding Antibody Fab Fragment F3p4
 gi|157835363 Chain A, X-Ray Crystal Structure Of A Recombinant Human Myoglobin Mutant At 2.8 Angstroms Resolutio
 gi|229597861 Chain A, X-Ray Crystal Structure Of Coil 1a Of Human Vimentin
 gi|3660434 Chain B, Crystal Structure Of Deoxy-Human Hemoglobin Beta6 Glu->trp
 gi|27574248 Chain B, Deoxy Hemoglobin (A,C:v1m,V62l; B,D:v1m,V67l)
 gi|442850 Chain B, High-Resolution X-Ray Study Of Deoxy Recombinant Human Hemoglobins Synthesized From Beta-G
 gi|218681905 Chain C, Crystal Structure Of Mj5 Fab, A Germline Antibody Variant Of Anti-Human Cytomegalovirus An
 gi|166007160 Chain C, Solution Structure Of Human Immunoglobulin M
 gi|161760892 Chain D, Neutron Structure Analysis Of Deoxy Human Hemoglobin
 gi|349905 Chain F, Atomic Structures Of Wild-Type And Thermostable Mutant Recombinant Human Cu, Zn Superoxide
 gi|46015317 Chain H, Crystal Structure Analysis Of Anti-Hiv-1 Fab 447-52d In Complex With V3 Peptide
 gi|2914165 Chain H, Three-Dimensional Structure Of A Human Fab With High Affinity For Tetanus Toxoid
 gi|494619 Chain I, The Refined 2.4 Angstroms X-Ray Crystal Structure Of Recombinant Human Stefin B In Complex
 gi|493869 Chain L, Crystal Structure Of A Chimeric Fab' Fragment Of An Antibody Binding Tumour Cells
 gi|99031801 Chain L, Crystal Structure Of A Glycosylated Fab From An Igm Cryoglobulin With Properties Of A Natu
 gi|33358191 Chain L, Crystal Structure Of Fab' From The Hiv-1 Neutralizing Antibody 2f5 In Complex With Its Gp4
 gi|1827928 Chain L, Igg Fab (Human Igg1, Kappa) Chimeric Fragment (Cbr96) Complexed With Lewis Y Nonoate Methy
 gi|160877748 Chain L, Neuropilin-1 B1 Domain In Complex With A Vegf-Blocking Fab

gi|230162 Chain M, Three-Dimensional Structure Of A Hybrid Light Chain Dimer. Protein Engineering Of A Bindin
gi|230867 Chain R, Twinning In Crystals Of Human Skeletal Muscle D- Glyceraldehyde-3-Phosphate Dehydrogenase
gi|5031635 cofilin 1 (non-muscle) [Homo sapiens]
gi|223373 complex-forming glycoprotein HC
gi|553231 creatine kinase M (EC 2.7.3.2) [Homo sapiens]
gi|13938619 Creatine kinase, muscle [Homo sapiens]
gi|4503057 crystallin, alpha B [Homo sapiens]
gi|181250 cyclophilin
gi|30377 cytokeratin 13 [Homo sapiens]
gi|34073 cytokeratin 4 (408 AA) [Homo sapiens]
gi|6457378 cytovillin 2 [Homo sapiens]
gi|311614 dermatopontin [Homo sapiens]
gi|181540 desmin [Homo sapiens]
gi|1220311 elongation factor-1 alpha
gi|153267427 enolase 3 [Homo sapiens]
gi|187302 epithelial cell marker protein 1
gi|4503475 eukaryotic translation elongation factor 1 alpha 2 [Homo sapiens]
gi|5453597 F-actin capping protein alpha-1 subunit [Homo sapiens]
gi|182439 fibrinogen gamma chain [Homo sapiens]
gi|4758438 glucagon-like peptide 2 receptor precursor [Homo sapiens]
gi|31645 glyceraldehyde-3-phosphate dehydrogenase [Homo sapiens]
gi|4885371 H1 histone family, member 0 [Homo sapiens]
gi|223976 haptoglobin Hp2
gi|306882 haptoglobin precursor [Homo sapiens]
gi|119572463 hCG1744641, isoform CRA_b [Homo sapiens]
gi|119630082 hCG2007439 [Homo sapiens]
gi|662841 heat shock protein 27 [Homo sapiens]
gi|61104911 heat shock protein 90Bb [Homo sapiens]
gi|229149 hemoglobin beta
gi|47679341 hemoglobin beta [Homo sapiens]
gi|23268683 hemoglobin beta chain variant Hb.Sinai-Bel Air [Homo sapiens]
gi|239718 hemoglobin beta chain; beta-globin [Homo sapiens]
gi|229172 hemoglobin delta
gi|4885397 hemoglobin, zeta [Homo sapiens]

gi 226337	hemopexin
gi 4504447	heterogeneous nuclear ribonucleoprotein A2/B1 isoform A2 [Homo sapiens]
gi 45767731	HIST1H4I protein [Homo sapiens]
gi 4885381	histone cluster 1, H1b [Homo sapiens]
gi 4885375	histone cluster 1, H1c [Homo sapiens]
gi 4885377	histone cluster 1, H1d [Homo sapiens]
gi 4504239	histone cluster 1, H2ai [Homo sapiens]
gi 24586679	histone cluster 1, H2ba [Homo sapiens]
gi 4504263	histone cluster 1, H2bm [Homo sapiens]
gi 56203471	histone cluster 2, H3, pseudogene 2 [Homo sapiens]
gi 31979	histone H2A.2 [Homo sapiens]
gi 1568551	histone H2B [Homo sapiens]
gi 184086	histone H2B.1
gi 386772	histone H3 [Homo sapiens]
gi 306549	homology to rat ribosomal protein L23
gi 51476390	hypothetical protein [Homo sapiens]
gi 229536	Ig A L
gi 229585	Ig A1 Bur
gi 229601	Ig G1 H Nie
gi 7438712	Ig kappa chain NIG93 precursor - human
gi 106586	Ig kappa chain V-III (KAU cold agglutinin) - human
gi 106600	Ig kappa chain V-III region (Jh) - human (fragment)
gi 223815	Ig lambda C
gi 106643	Ig lambda chain - human
gi 4176418	IgG kappa chain [Homo sapiens]
gi 49256427	IGH@ protein [Homo sapiens]
gi 130381795	immunoglobulin G1 Fab light chain variable region [Homo sapiens]
gi 8918518	immunoglobulin gamma heavy chain [Homo sapiens]
gi 1710419	immunoglobulin H23 light chain kappa variable region [Homo sapiens]
gi 16505713	immunoglobulin heavy chain [Homo sapiens]
gi 39937979	immunoglobulin heavy chain variable region [Homo sapiens]
gi 553426	immunoglobulin heavy chain VDJC region
gi 170684422	immunoglobulin kappa 1 light chain [Homo sapiens]
gi 306962	immunoglobulin kappa chain [Homo sapiens]

gi 416336	immunoglobulin kappa chain V region [Homo sapiens]
gi 9968499	immunoglobulin kappa chain variable region [Homo sapiens]
gi 3169770	immunoglobulin kappa light chain [Homo sapiens]
gi 21669317	immunoglobulin kappa light chain VLJ region [Homo sapiens]
gi 170684526	immunoglobulin lambda 2 light chain [Homo sapiens]
gi 21669555	immunoglobulin lambda light chain VLJ region [Homo sapiens]
gi 15149823	immunoglobulin lambda-3 surrogate light chain [Homo sapiens]
gi 185364	immunoglobulin lambda-chain
gi 306999	immunoglobulin light chain
gi 218783334	immunoglobulin light chain [Homo sapiens]
gi 186133	immunoglobulin light chain constant region [Homo sapiens]
gi 51103531	immunoglobulin variable region VL kappa domain [Homo sapiens]
gi 4557699	keratin 12 [Homo sapiens]
gi 18999435	Keratin 5 [Homo sapiens]
gi 28173564	keratin 73 [Homo sapiens]
gi 39795269	Keratin 79 [Homo sapiens]
gi 12314174	keratin 8 pseudogene 11 [Homo sapiens]
gi 386850	keratin K5
gi 186685	keratin type 16
gi 386849	keratin type II [Homo sapiens]
gi 4240195	KIAA0853 protein [Homo sapiens]
gi 5031857	L-lactate dehydrogenase A isoform 1 [Homo sapiens]
gi 4557032	L-lactate dehydrogenase B [Homo sapiens]
gi 2460037	m6A methyltransferase [Homo sapiens]
gi 2906146	malate dehydrogenase precursor [Homo sapiens]
gi 34707	Manganese superoxide dismutase [Homo sapiens]
gi 14589909	mitogen-activated protein kinase kinase kinase 5 [Homo sapiens]
gi 28336	mutant beta-actin (beta'-actin) [Homo sapiens]
gi 1220346	myosin light chain 2
gi 5453740	myosin, light chain 12A, regulatory, non-sarcomeric [Homo sapiens]
gi 10864053	myozenin 1 [Homo sapiens]
gi 5031931	nascent polypeptide-associated complex alpha subunit isoform b [Homo sapiens]
gi 913159	neuropolypeptide h3 [human, brain, Peptide, 186 aa]
gi 190238	nucleolar phosphoprotein B23

gi 7661704	osteoglycin preproprotein [Homo sapiens]
gi 4505591	peroxiredoxin 1 [Homo sapiens]
gi 189868	phosphoglycerate mutase [Homo sapiens]
gi 2627129	polyubiquitin [Homo sapiens]
gi 219978	prealbumin [Homo sapiens]
gi 169171114	PREDICTED: hypothetical protein [Homo sapiens]
gi 239751152	PREDICTED: hypothetical protein XP_002347737 [Homo sapiens]
gi 169213772	PREDICTED: similar to actin alpha 1 skeletal muscle protein [Homo sapiens]
gi 239752604	PREDICTED: similar to immunoglobulin lambda-like polypeptide 1 [Homo sapiens]
gi 182607	prepro-C3b/C4B inactivator [Homo sapiens]
gi 134133226	protein expressed in prostate, ovary, testis, and placenta 2 [Homo sapiens]
gi 189617	protein PP4-X
gi 83674986	rcTPM3 [Homo sapiens]
gi 112877	RecName: Full=Alpha-1-acid glycoprotein 1; Short=AGP 1; AltName: Full=Orosomucoid-1; Short=OMD 1; F
gi 123510	RecName: Full=Haptoglobin-related protein; Flags: Precursor
gi 121039	RecName: Full=Ig gamma-1 chain C region
gi 115887	RecName: Full=Mast cell carboxypeptidase A; Short=MC-CPA; AltName: Full=Carboxypeptidase A3; Flags:
gi 136066	RecName: Full=Triosephosphate isomerase; Short=TIM; AltName: Full=Triose-phosphate isomerase
gi 36038	rho GDP dissociation inhibitor (GDI) [Homo sapiens]
gi 495126	ribosomal protein L11 [Homo sapiens]
gi 4506613	ribosomal protein L22 proprotein [Homo sapiens]
gi 4506619	ribosomal protein L24 [Homo sapiens]
gi 4432754	ribosomal protein L27a [Homo sapiens]
gi 793843	ribosomal protein L29 [Homo sapiens]
gi 1655596	ribosomal protein L31 [Homo sapiens]
gi 6005860	ribosomal protein L35 [Homo sapiens]
gi 35903	ribosomal protein L7 [Homo sapiens]
gi 4506661	ribosomal protein L7a [Homo sapiens]
gi 4506669	ribosomal protein P1 isoform 1 [Homo sapiens]
gi 4506671	ribosomal protein P2 [Homo sapiens]
gi 5032051	ribosomal protein S14 [Homo sapiens]
gi 4506691	ribosomal protein S16 [Homo sapiens]
gi 3088342	ribosomal protein S23 [Homo sapiens]
gi 4506707	ribosomal protein S25 [Homo sapiens]

gi 337514	ribosomal protein S6 [Homo sapiens]
gi 7657532	S100 calcium-binding protein A6 [Homo sapiens]
gi 4506773	S100 calcium-binding protein A9 [Homo sapiens]
gi 49660012	sarcomeric tropomyosin kappa; TPM1-kappa [Homo sapiens]
gi 337930	scar protein
gi 28592	serum albumin [Homo sapiens]
gi 21620053	Similar to collagen, type VI, alpha 3 [Homo sapiens]
gi 1381814	skeletal muscle LIM-protein SLIM
gi 339781	slow skeletal muscle troponin T [Homo sapiens]
gi 467828	smooth muscle myosin alkali light chain
gi 1770517	SMT3A protein [Homo sapiens]
gi 685073	SPRC=small proline-rich protein [human, odontogenic keratocysts, Peptide Partial, 161 aa]
gi 914044	surface-associated sulphhydryl protein, SASP=thioredoxin homolog [human, THP-1 monocytes, Peptide Pa
gi 561696	This CDS feature is included to show the translation of the corresponding V_region. Presently trans
gi 19072649	TPMsk3 [Homo sapiens]
gi 4325109	transcriptional intermediary factor 1 gamma; TIF1gamma [Homo sapiens]
gi 339469	transferrin [Homo sapiens]
gi 27597085	tropomyosin 1 alpha chain isoform 5 [Homo sapiens]
gi 42476296	tropomyosin 2 (beta) isoform 1 [Homo sapiens]
gi 58652133	tropomyosin 3 [Bos taurus]
gi 223555975	tropomyosin 4 isoform 1 [Homo sapiens]
gi 4507651	tropomyosin 4 isoform 2 [Homo sapiens]
gi 49660014	tropomyosin alpha striated muscle isoform; TPM1-alpha [Homo sapiens]
gi 5803203	troponin T3, skeletal, fast isoform 1 [Homo sapiens]
gi 5803225	tyrosine 3/tryptophan 5 -monooxygenase activation protein, epsilon polypeptide [Homo sapiens]
gi 4507953	tyrosine 3/tryptophan 5 -monooxygenase activation protein, zeta polypeptide [Homo sapiens]
gi 339715	tyrosine kinase (FER) [Homo sapiens]
gi 229532	ubiquitin
gi 194376310	unnamed protein product [Homo sapiens]
gi 34039	unnamed protein product [Homo sapiens]
gi 194376438	unnamed protein product [Homo sapiens]
gi 29446	unnamed protein product [Homo sapiens]
gi 21751806	unnamed protein product [Homo sapiens]
gi 194388338	unnamed protein product [Homo sapiens]

gi 34069	unnamed protein product [Homo sapiens]
gi 158261511	unnamed protein product [Homo sapiens]
gi 34527235	unnamed protein product [Homo sapiens]
gi 31092	unnamed protein product [Homo sapiens]
gi 29446	unnamed protein product [Homo sapiens]
gi 28940	unnamed protein product [Homo sapiens]
gi 7022475	unnamed protein product [Homo sapiens]
gi 189053924	unnamed protein product [Homo sapiens]
gi 194376438	unnamed protein product [Homo sapiens]
gi 194376242	unnamed protein product [Homo sapiens]
gi 37403	unnamed protein product [Homo sapiens]
gi 34071	unnamed protein product [Homo sapiens]
gi 29446	unnamed protein product [Homo sapiens]
gi 16554039	unnamed protein product [Homo sapiens]
gi 21757066	unnamed protein product [Homo sapiens]
gi 21757073	unnamed protein product [Homo sapiens]
gi 194376242	unnamed protein product [Homo sapiens]
gi 34069	unnamed protein product [Homo sapiens]
gi 194384438	unnamed protein product [Homo sapiens]
gi 10434878	unnamed protein product [Homo sapiens]
gi 34526424	unnamed protein product [Homo sapiens]
gi 16554039	unnamed protein product [Homo sapiens]
gi 4803698	unnamed protein product [Homo sapiens]
gi 29446	unnamed protein product [Homo sapiens]
gi 32111	unnamed protein product [Homo sapiens]
gi 34866	unnamed protein product [Homo sapiens]
gi 21754605	unnamed protein product [Homo sapiens]
gi 34069	unnamed protein product [Homo sapiens]
gi 194375974	unnamed protein product [Homo sapiens]
gi 29446	unnamed protein product [Homo sapiens]
gi 32111	unnamed protein product [Homo sapiens]
gi 4803698	unnamed protein product [Homo sapiens]
gi 34687	unnamed protein product [Homo sapiens]
gi 29446	unnamed protein product [Homo sapiens]

gi 34687	unnamed protein product [Homo sapiens]
gi 32111	unnamed protein product [Homo sapiens]
gi 32111	unnamed protein product [Homo sapiens]
gi 29446	unnamed protein product [Homo sapiens]
gi 4803698	unnamed protein product [Homo sapiens]
gi 21751704	unnamed protein product [Homo sapiens]
gi 29446	unnamed protein product [Homo sapiens]
gi 32097	unnamed protein product [Homo sapiens]
gi 4803698	unnamed protein product [Homo sapiens]
gi 29446	unnamed protein product [Homo sapiens]
gi 29888	unnamed protein product [Homo sapiens]
gi 32097	unnamed protein product [Homo sapiens]
gi 340219	vimentin [Homo sapiens]
gi 62896523	vimentin variant [Homo sapiens]
gi 5441367	ZASP protein [Homo sapiens]

3. CONCLUSÕES

3. CONCLUSÕES

Para o nosso conhecimento, este é o primeiro estudo de carcinoma epidermóide de cavidade oral que compara um prognosticador conhecido, a presença de células neoplásicas em linfonodos regionais (independentemente do tamanho do tumor), com uma classificação exploratória que separa os tumores pequenos metastáticos e os grandes não-metastáticos em dois grupos. Em comparação com os dados obtidos com o parâmetro tradicional, semelhantes, mas não idênticos padrões de expressão protéica foram observados. Os resultados indicam que o tamanho do tumor é importante para melhorar a distinção entre grupos TNM polares.

As principais conclusões do presente trabalho são:

1. A etapa de extração é crítica para a obtenção de elevada e representativa quantidade de proteínas de tecidos biológicos e de alta resolução protéica nos géis de eletroforese bidimensional;
2. Os perfis protéicos do carcinoma epidermóide oral com fenótipo invasivo, do não-invasivo, dos tumores pequenos metastáticos, dos grandes não-metastáticos e dos tecidos normais mostram padrões similares entre si, porém com diferenças consistentes na expressão de algumas proteínas;
3. O tamanho tumoral é importante para melhorar a distinção entre grupos TNM polares – tumores agressivos e menos agressivos – e algumas diferenças podem ter impacto no prognóstico;

4. A citoqueratina-4 é um biomarcador potencial para o carcinoma epidermóide de cavidade oral;
5. A anexina A1 apresenta expressão reduzida em células neoplásicas de cabeça e pescoço, um fato que pode estar relacionado à inflamação, à proliferação de células epiteliais e à carcinogênese;
6. Os fibroblastos do estroma tumoral mantêm estreita comunicação com as células cancerosas, estimulando a proliferação, o recrutamento de células inflamatórias e a aquisição de características invasivas;
7. As células tumorais influenciam a expressão gênica das células estromais com aparente efeito sobre a indução e a inibição de respostas inflamatórias ou imunes.

4. REFERÊNCIAS BIBLIOGRÁFICAS

4. REFERÊNCIAS BIBLIOGRÁFICAS

1. Han MH, Hwang SI, Roy DB, Lundgren DH, Price JV, Ousman SS, et al. Proteomic analysis of active multiple sclerosis lesions reveals therapeutic targets. *Nature*. 2008 Feb 28;451(7182):1076-81.
2. Gstaiger M, Aebersold R. Applying mass spectrometry-based proteomics to genetics, genomics and network biology. *Nat Rev Genet*. 2009 Sep;10(9):617-27.
3. Unlu M, Morgan ME, Minden JS. Difference gel electrophoresis: a single gel method for detecting changes in protein extracts. *Electrophoresis*. 1997 Oct;18(11):2071-7.
4. Brunner E, Ahrens CH, Mohanty S, Baetschmann H, Loevenich S, Potthast F, et al. A high-quality catalog of the *Drosophila melanogaster* proteome. *Nat Biotechnol*. 2007 May;25(5):576-83.
5. Jensen ON. Interpreting the protein language using proteomics. *Nat Rev Mol Cell Biol*. 2006 Jun;7(6):391-403.
6. Wepf A, Glatter T, Schmidt A, Aebersold R, Gstaiger M. Quantitative interaction proteomics using mass spectrometry. *Nat Methods*. 2009 Mar;6(3):203-5.
7. Desiderio DM, Zhu X. Quantitative analysis of methionine enkephalin and beta-endorphin in the pituitary by liquid secondary ion mass spectrometry and tandem mass spectrometry. *J Chromatogr A*. 1998 Jan 23;794(1-2):85-96.
8. Callister SJ, Barry RC, Adkins JN, Johnson ET, Qian WJ, Webb-Robertson BJ, et al. Normalization approaches for removing systematic biases associated with mass spectrometry and label-free proteomics. *J Proteome Res*. 2006 Feb;5(2):277-86.

9. Kingsmore SF, Patel DD. Multiplexed protein profiling on antibody-based microarrays by rolling circle amplification. *Curr Opin Biotechnol.* 2003 Feb;14(1):74-81.
10. Wulfschlegel JD, Sgroi DC, Krutzsch H, McLean K, McGarvey K, Knowlton M, et al. Proteomics of human breast ductal carcinoma in situ. *Cancer Res.* 2002 Nov 15;62(22):6740-9.
11. Bouchal P, Roumeliotis T, Hrstka R, Nenutil R, Vojtesek B, Garbis SD. Biomarker discovery in low-grade breast cancer using isobaric stable isotope tags and two-dimensional liquid chromatography-tandem mass spectrometry (iTRAQ-2DLC-MS/MS) based quantitative proteomic analysis. *J Proteome Res.* 2009 Jan;8(1):362-73.
12. Hu X, Zhang Y, Zhang A, Li Y, Zhu Z, Shao Z, et al. Comparative serum proteome analysis of human lymph node negative/positive invasive ductal carcinoma of the breast and benign breast disease controls via label-free semiquantitative shotgun technology. *OMICS.* 2009 Aug;13(4):291-300.
13. Umar A, Kang H, Timmermans AM, Look MP, Meijer-van Gelder ME, den Bakker MA, et al. Identification of a putative protein profile associated with tamoxifen therapy resistance in breast cancer. *Mol Cell Proteomics.* 2009 Jun;8(6):1278-94.
14. Celis JE, Celis P, Ostergaard M, Basse B, Lauridsen JB, Ratz G, et al. Proteomics and immunohistochemistry define some of the steps involved in the squamous differentiation of the bladder transitional epithelium: a novel strategy for identifying metaplastic lesions. *Cancer Res.* 1999 Jun 15;59(12):3003-9.
15. Kreunin P, Zhao J, Rosser C, Urquidi V, Lubman DM, Goodison S. Bladder cancer associated glycoprotein signatures revealed by urinary proteomic profiling. *J Proteome Res.* 2007 Jul;6(7):2631-9.

16. Schiffer E, Vlahou A, Petrolekas A, Stravodimos K, Tauber R, Geschwend JE, et al. Prediction of muscle-invasive bladder cancer using urinary proteomics. *Clin Cancer Res.* 2009 Aug 1;15(15):4935-43.
17. Issaq HJ, Nativ O, Waybright T, Luke B, Veenstra TD, Issaq EJ, et al. Detection of bladder cancer in human urine by metabolomic profiling using high performance liquid chromatography/mass spectrometry. *J Urol.* 2008 Jun;179(6):2422-6.
18. Klade CS, Voss T, Krystek E, Ahorn H, Zatloukal K, Pummer K, et al. Identification of tumor antigens in renal cell carcinoma by serological proteome analysis. *Proteomics.* 2001 Jul;1(7):890-8.
19. Okamura N, Masuda T, Gotoh A, Shirakawa T, Terao S, Kaneko N, et al. Quantitative proteomic analysis to discover potential diagnostic markers and therapeutic targets in human renal cell carcinoma. *Proteomics.* 2008 Aug;8(15):3194-203.
20. Perroud B, Ishimaru T, Borowsky AD, Weiss RH. Grade-dependent proteomics characterization of kidney cancer. *Mol Cell Proteomics.* 2009 May;8(5):971-85.
21. Seliger B, Dressler SP, Wang E, Kellner R, Recktenwald CV, Lottspeich F, et al. Combined analysis of transcriptome and proteome data as a tool for the identification of candidate biomarkers in renal cell carcinoma. *Proteomics.* 2009 Mar;9(6):1567-81.
22. Seow TK, Ong SE, Liang RC, Ren EC, Chan L, Ou K, et al. Two-dimensional electrophoresis map of the human hepatocellular carcinoma cell line, HCC-M, and identification of the separated proteins by mass spectrometry. *Electrophoresis.* 2000 May;21(9):1787-813.
23. Chaerkady R, Harsha HC, Nalli A, Gucek M, Vivekanandan P, Akhtar J, et al. A quantitative proteomic approach for identification of potential biomarkers in hepatocellular carcinoma. *J Proteome Res.* 2008 Oct;7(10):4289-98.

24. Looi KS, Nakayasu ES, Diaz RA, Tan EM, Almeida IC, Zhang JY. Using proteomic approach to identify tumor-associated antigens as markers in hepatocellular carcinoma. *J Proteome Res.* 2008 Sep;7(9):4004-12.
25. Orimo T, Ojima H, Hiraoka N, Saito S, Kosuge T, Kakisaka T, et al. Proteomic profiling reveals the prognostic value of adenomatous polyposis coli-end-binding protein 1 in hepatocellular carcinoma. *Hepatology.* 2008 Dec;48(6):1851-63.
26. Brichory F, Beer D, Le Naour F, Giordano T, Hanash S. Proteomics-based identification of protein gene product 9.5 as a tumor antigen that induces a humoral immune response in lung cancer. *Cancer Res.* 2001 Nov 1;61(21):7908-12.
27. Park HJ, Kim BG, Lee SJ, Heo SH, Kim JY, Kwon TH, et al. Proteomic profiling of endothelial cells in human lung cancer. *J Proteome Res.* 2008 Mar;7(3):1138-50.
28. Li DJ, Deng G, Xiao ZQ, Yao HX, Li C, Peng F, et al. Identifying 14-3-3 sigma as a lymph node metastasis-related protein in human lung squamous carcinoma. *Cancer Lett.* 2009 Jun 28;279(1):65-73.
29. Yao H, Zhang Z, Xiao Z, Chen Y, Li C, Zhang P, et al. Identification of metastasis associated proteins in human lung squamous carcinoma using two-dimensional difference gel electrophoresis and laser capture microdissection. *Lung Cancer.* 2009 Jul;65(1):41-8.
30. Meehan KL, Holland JW, Dawkins HJ. Proteomic analysis of normal and malignant prostate tissue to identify novel proteins lost in cancer. *Prostate.* 2002 Jan 1;50(1):54-63.
31. Fortin T, Salvador A, Charrier JP, Lenz C, Lacoux X, Morla A, et al. Clinical quantitation of prostate-specific antigen biomarker in the low nanogram/milliliter range

by conventional bore liquid chromatography-tandem mass spectrometry (multiple reaction monitoring) coupling and correlation with ELISA tests. *Mol Cell Proteomics*. 2009 May;8(5):1006-15.

32. Garbis SD, Tyrirtzis SI, Roumeliotis T, Zerefos P, Giannopoulou EG, Vlahou A, et al. Search for potential markers for prostate cancer diagnosis, prognosis and treatment in clinical tissue specimens using amine-specific isobaric tagging (iTRAQ) with two-dimensional liquid chromatography and tandem mass spectrometry. *J Proteome Res*. 2008 Aug;7(8):3146-58.

33. Byrne JC, Downes MR, O'Donoghue N, O'Keane C, O'Neill A, Fan Y, et al. 2D-DIGE as a strategy to identify serum markers for the progression of prostate cancer. *J Proteome Res*. 2009 Feb;8(2):942-57.

34. Zhou G, Li H, Gong Y, Zhao Y, Cheng J, Lee P. Proteomic analysis of global alteration of protein expression in squamous cell carcinoma of the esophagus. *Proteomics*. 2005 Sep;5(14):3814-21.

35. Liu WL, Zhang G, Wang JY, Cao JY, Guo XZ, Xu LH, et al. Proteomics-based identification of autoantibody against CDC25B as a novel serum marker in esophageal squamous cell carcinoma. *Biochem Biophys Res Commun*. 2008 Oct 24;375(3):440-5.

36. Uemura N, Nakanishi Y, Kato H, Saito S, Nagino M, Hirohashi S, et al. Transglutaminase 3 as a prognostic biomarker in esophageal cancer revealed by proteomics. *Int J Cancer*. 2009 May 1;124(9):2106-15.

37. He QY, Chen J, Kung HF, Yuen AP, Chiu JF. Identification of tumor-associated proteins in oral tongue squamous cell carcinoma by proteomics. *Proteomics*. 2004 Jan;4(1):271-8.

38. Lo WY, Lai CC, Hua CH, Tsai MH, Huang SY, Tsai CH, et al. S100A8 is identified as a biomarker of HPV18-infected oral squamous cell carcinomas by suppression subtraction hybridization, clinical proteomics analysis, and immunohistochemistry staining. *J Proteome Res.* 2007 Jun;6(6):2143-51.
39. Roesch-Ely M, Nees M, Karsai S, Ruess A, Bogumil R, Warnken U, et al. Proteomic analysis reveals successive aberrations in protein expression from healthy mucosa to invasive head and neck cancer. *Oncogene.* 2007 Jan 4;26(1):54-64.
40. Freed GL, Cazares LH, Fichandler CE, Fuller TW, Sawyer CA, Stack BC, Jr., et al. Differential capture of serum proteins for expression profiling and biomarker discovery in pre- and posttreatment head and neck cancer samples. *Laryngoscope.* 2008 Jan;118(1):61-8.
41. Patel V, Hood BL, Molinolo AA, Lee NH, Conrads TP, Braisted JC, et al. Proteomic analysis of laser-captured paraffin-embedded tissues: a molecular portrait of head and neck cancer progression. *Clin Cancer Res.* 2008 Feb 15;14(4):1002-14.
42. Chi LM, Lee CW, Chang KP, Hao SP, Lee HM, Liang Y, et al. Enhanced interferon signaling pathway in oral cancer revealed by quantitative proteome analysis of microdissected specimens using ¹⁶O/¹⁸O labeling and integrated two-dimensional LC-ESI-MALDI tandem MS. *Mol Cell Proteomics.* 2009 Jul;8(7):1453-74.
43. Ralhan R, Desouza LV, Matta A, Chandra Tripathi S, Ghanny S, Datta Gupta S, et al. Discovery and verification of head-and-neck cancer biomarkers by differential protein expression analysis using iTRAQ labeling, multidimensional liquid chromatography, and tandem mass spectrometry. *Mol Cell Proteomics.* 2008 Jun;7(6):1162-73.

44. Wang Z, Jiang L, Huang C, Li Z, Chen L, Gou L, et al. Comparative proteomics approach to screening of potential diagnostic and therapeutic targets for oral squamous cell carcinoma. *Mol Cell Proteomics*. 2008 Sep;7(9):1639-50.
45. Nagaraj NS. Evolving 'omics' technologies for diagnostics of head and neck cancer. *Brief Funct Genomic Proteomic*. 2009 Jan;8(1):49-59.
46. Ralhan R, Desouza LV, Matta A, Chandra Tripathi S, Ghanny S, Dattagupta S, et al. iTRAQ-multidimensional liquid chromatography and tandem mass spectrometry-based identification of potential biomarkers of oral epithelial dysplasia and novel networks between inflammation and premalignancy. *J Proteome Res*. 2009 Jan;8(1):300-9.
47. Mlynarek AM, Balys RL, Su J, Hier MP, Black MJ, Alaoui-Jamali MA. A cell proteomic approach for the detection of secretable biomarkers of invasiveness in oral squamous cell carcinoma. *Arch Otolaryngol Head Neck Surg*. 2007 Sep;133(9):910-8.
48. Bijian K, Mlynarek AM, Balys RL, Jie S, Xu Y, Hier MP, et al. Serum proteomic approach for the identification of serum biomarkers contributed by oral squamous cell carcinoma and host tissue microenvironment. *J Proteome Res*. 2009 May;8(5):2173-85.
49. Matta A, DeSouza LV, Shukla NK, Gupta SD, Ralhan R, Siu KW. Prognostic significance of head-and-neck cancer biomarkers previously discovered and identified using iTRAQ-labeling and multidimensional liquid chromatography-tandem mass spectrometry. *J Proteome Res*. 2008 May;7(5):2078-87.
50. Linkov F, Lisovich A, Yurkovetsky Z, Marrangoni A, Velikokhatnaya L, Nolen B, et al. Early detection of head and neck cancer: development of a novel screening tool

using multiplexed immunobead-based biomarker profiling. *Cancer Epidemiol Biomarkers Prev.* 2007 Jan;16(1):102-7.

51. Matta A, Tripathi SC, DeSouza LV, Grigull J, Kaur J, Chauhan SS, et al. Heterogeneous ribonucleoprotein K is a marker of oral leukoplakia and correlates with poor prognosis of squamous cell carcinoma. *Int J Cancer.* 2009 Sep 15;125(6):1398-406.

52. Dobrossy L. Epidemiology of head and neck cancer: magnitude of the problem. *Cancer Metastasis Rev.* 2005 Jan;24(1):9-17.

53. Ye H, Yu T, Temam S, Ziober BL, Wang J, Schwartz JL, et al. Transcriptomic dissection of tongue squamous cell carcinoma. *BMC Genomics.* 2008;9:69.

54. Parkin DM, Bray F, Ferlay J, Pisani P. Estimating the world cancer burden: Globocan 2000. *Int J Cancer.* 2001 Oct 15;94(2):153-6.

55. Parkin DM, Bray F, Ferlay J, Pisani P. Global cancer statistics, 2002. *CA Cancer J Clin.* 2005 Mar-Apr;55(2):74-108.

56. Ko YC, Huang YL, Lee CH, Chen MJ, Lin LM, Tsai CC. Betel quid chewing, cigarette smoking and alcohol consumption related to oral cancer in Taiwan. *J Oral Pathol Med.* 1995 Nov;24(10):450-3.

57. Chen J, He QY, Yuen AP, Chiu JF. Proteomics of buccal squamous cell carcinoma: the involvement of multiple pathways in tumorigenesis. *Proteomics.* 2004 Aug;4(8):2465-75.

58. Lo WY, Tsai MH, Tsai Y, Hua CH, Tsai FJ, Huang SY, et al. Identification of over-expressed proteins in oral squamous cell carcinoma (OSCC) patients by clinical proteomic analysis. *Clin Chim Acta.* 2007 Feb;376(1-2):101-7.

59. Hobbs CG, Sterne JA, Bailey M, Heyderman RS, Birchall MA, Thomas SJ. Human papillomavirus and head and neck cancer: a systematic review and meta-analysis. *Clin Otolaryngol*. 2006 Aug;31(4):259-66.
60. D'Souza G, Kreimer AR, Viscidi R, Pawlita M, Fakhry C, Koch WM, et al. Case-control study of human papillomavirus and oropharyngeal cancer. *N Engl J Med*. 2007 May 10;356(19):1944-56.
61. Layland MK, Sessions DG, Lenox J. The influence of lymph node metastasis in the treatment of squamous cell carcinoma of the oral cavity, oropharynx, larynx, and hypopharynx: N0 versus N+. *Laryngoscope*. 2005 Apr;115(4):629-39.
62. Woolgar JA. Pathology of the N0 neck. *Br J Oral Maxillofac Surg*. 1999 Jun;37(3):205-9.
63. Barnes L, Eveson, J.W., Reichart, P., Sidransky, D., editors. *Pathology and Genetics of Head and Neck Tumours*. Barnes L EJ, Reichart P, Sidransky D, editors., editor. Lyon: IARC Press; 2005.
64. Patel SG, Shah JP. TNM staging of cancers of the head and neck: striving for uniformity among diversity. *CA Cancer J Clin*. 2005 Jul-Aug;55(4):242-58; quiz 61-2, 64.